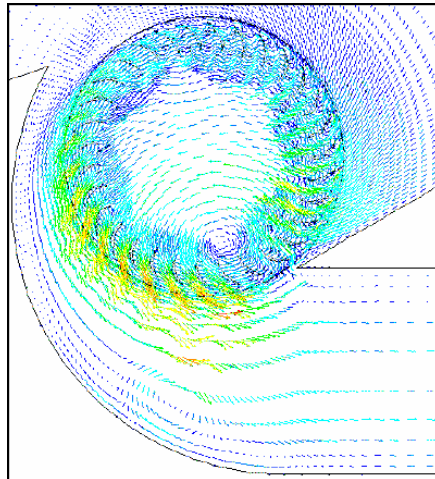
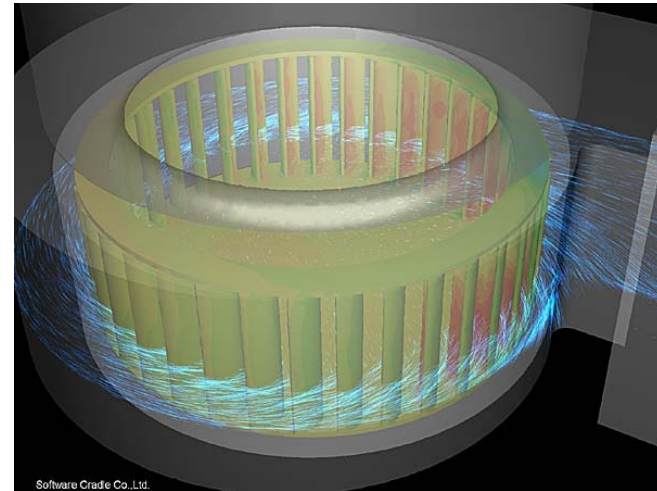
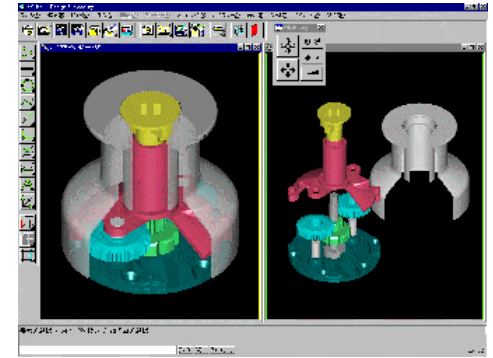


流體機械設計

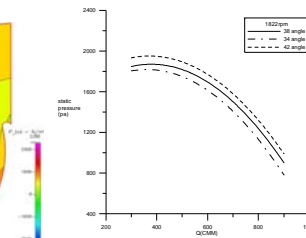
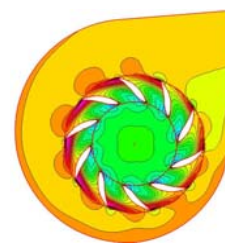
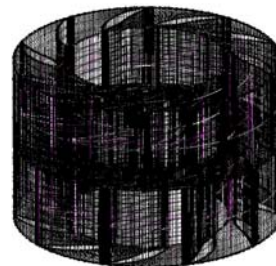
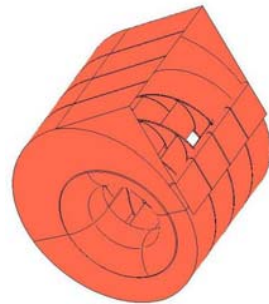
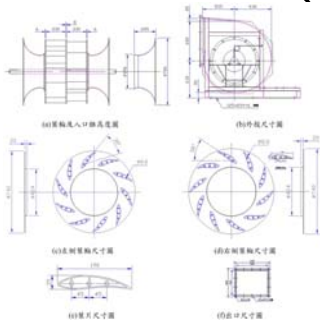
(Design of Turbomachinery)



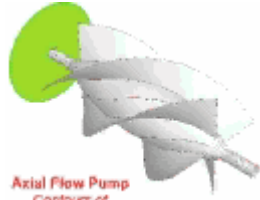
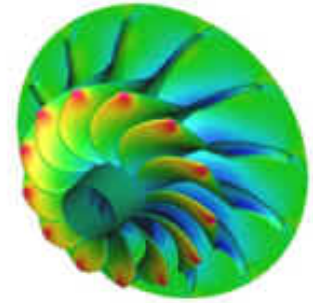
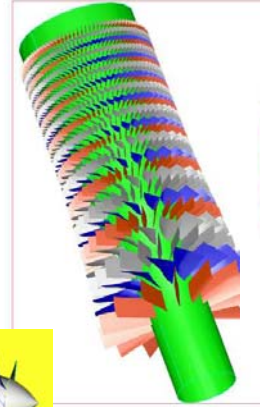
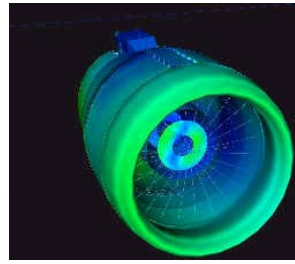
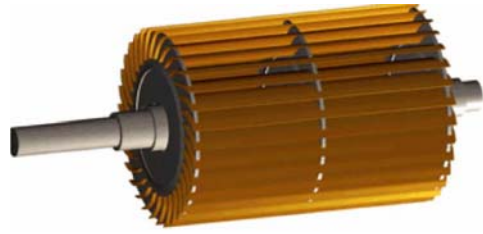
高等流體機械設計



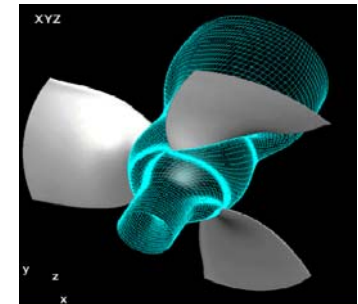
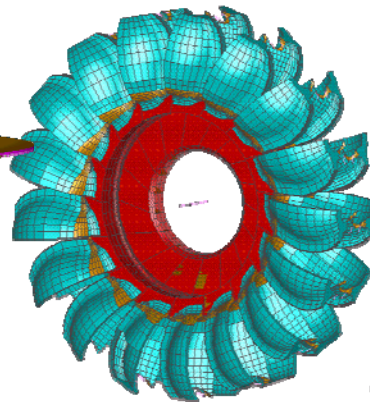
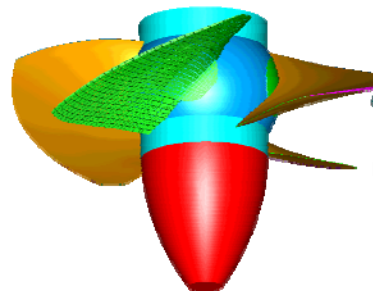
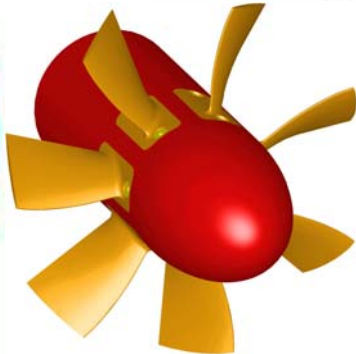
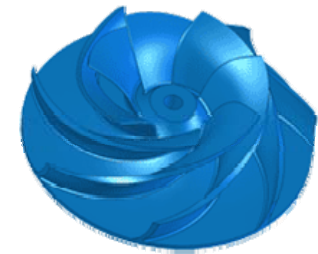
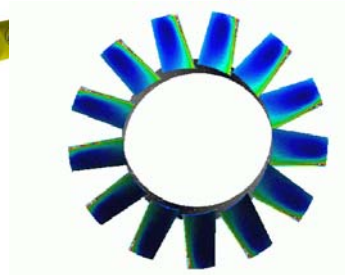
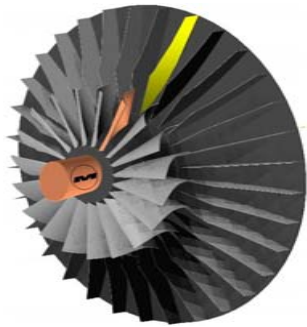
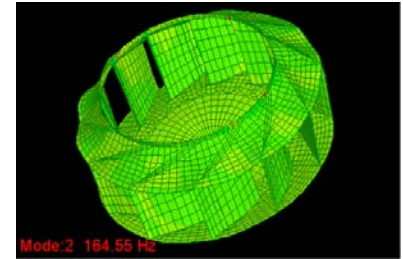
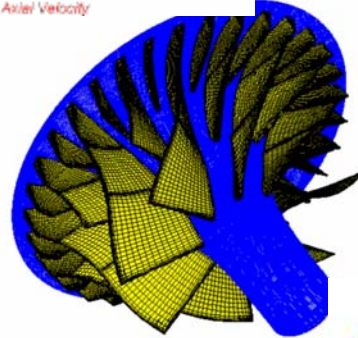
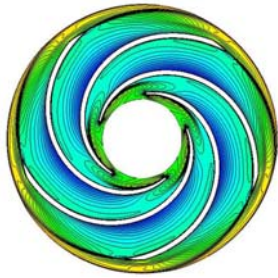
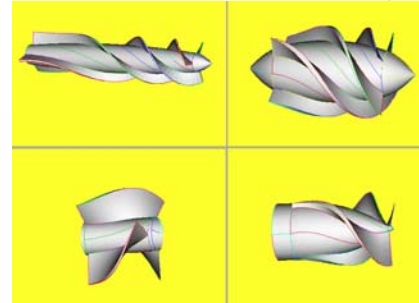
=流體機械(Turbomachinery)設計
+CAD(Computer-Aided Design)
+CAD(computer-Aided Drafting)
+CFD(Computational Fluid Dynamics)
+CAM(Computer-Aided Manufacture)
=CAE(Computational-Aided Engineering)

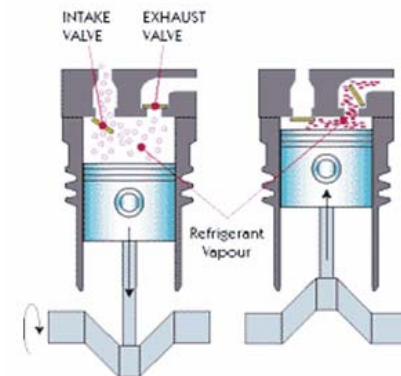
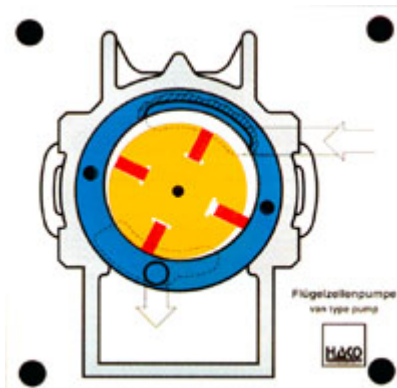
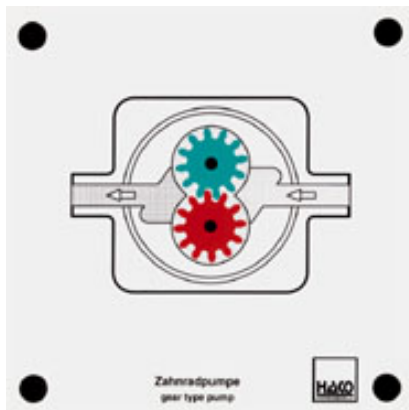
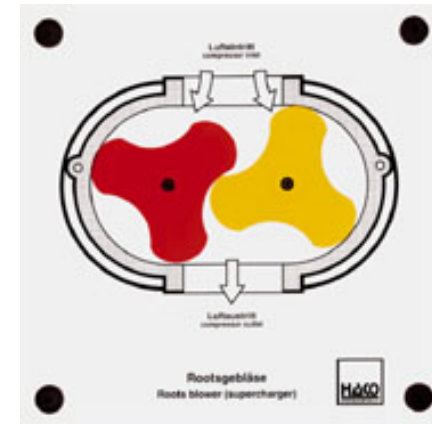
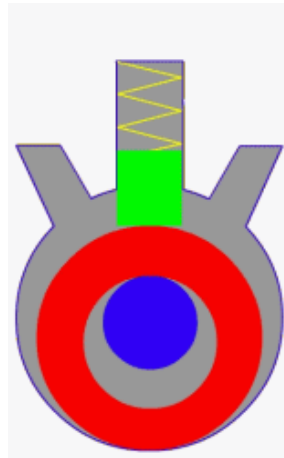
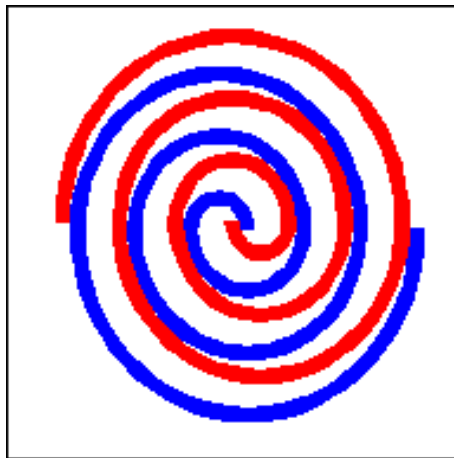
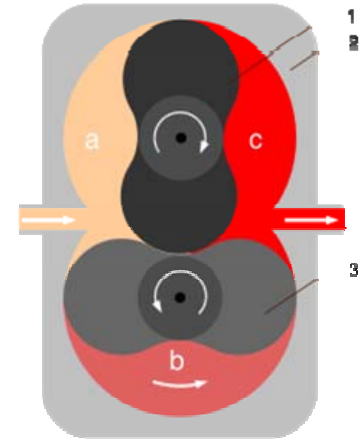
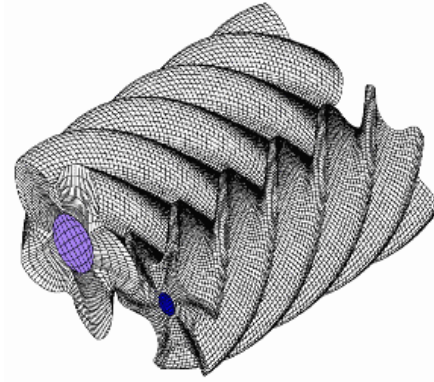
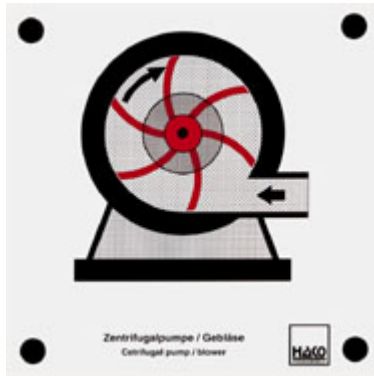


輪機機械



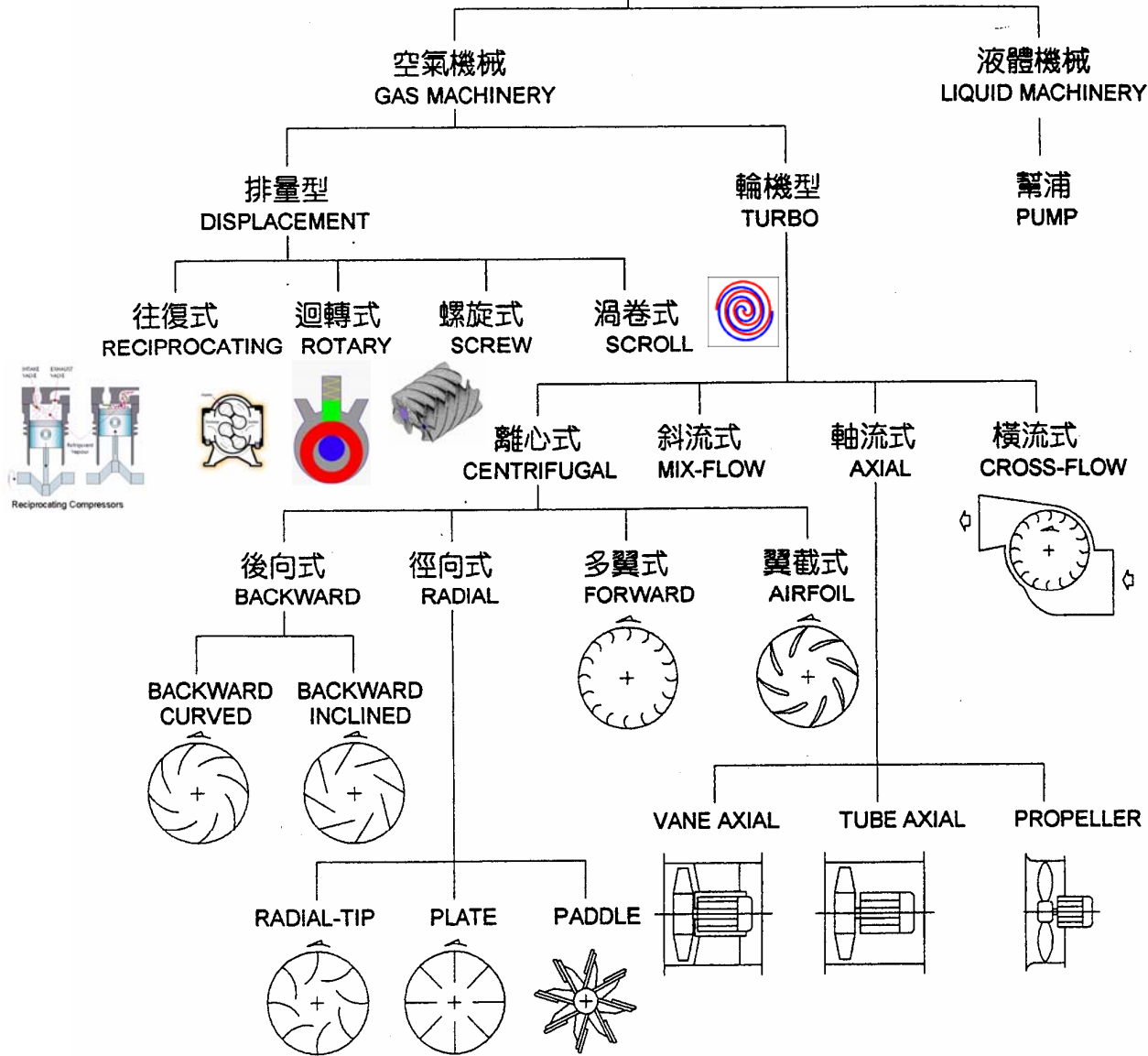
Axial Flow Pump
Contours of Axial Velocity





Reciprocating Compressors

流體機械
(對流體作功)



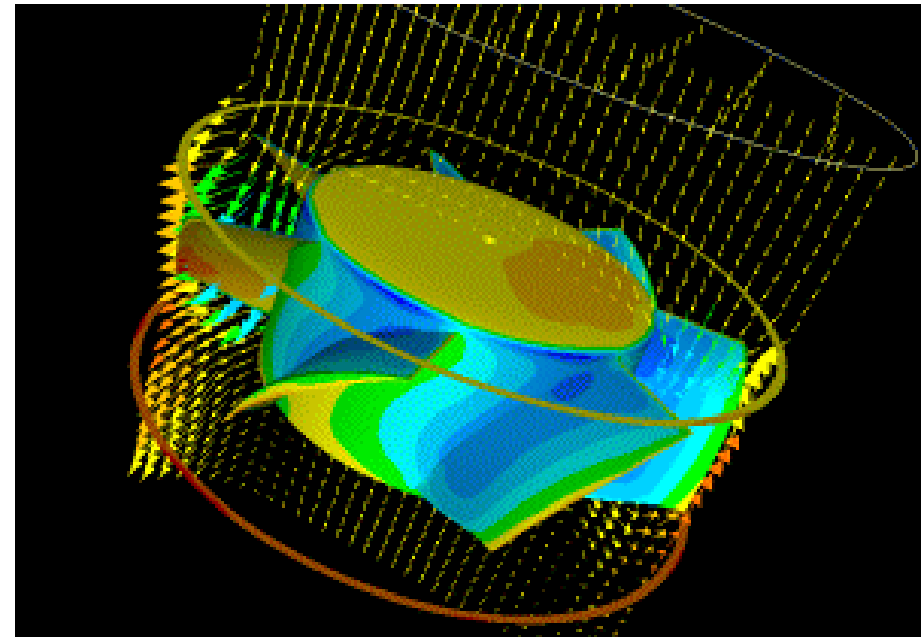
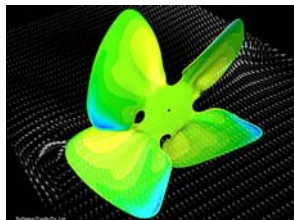
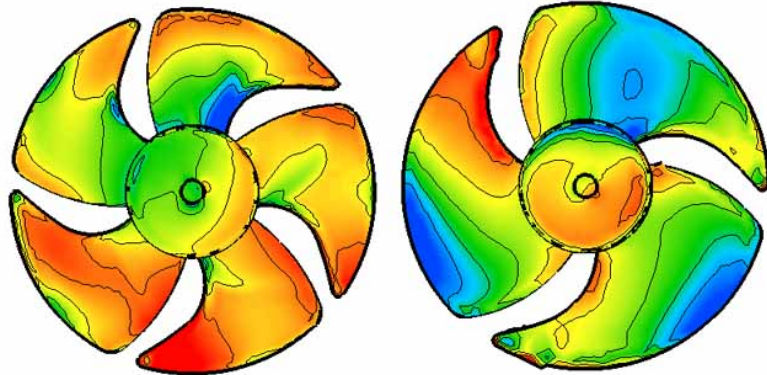
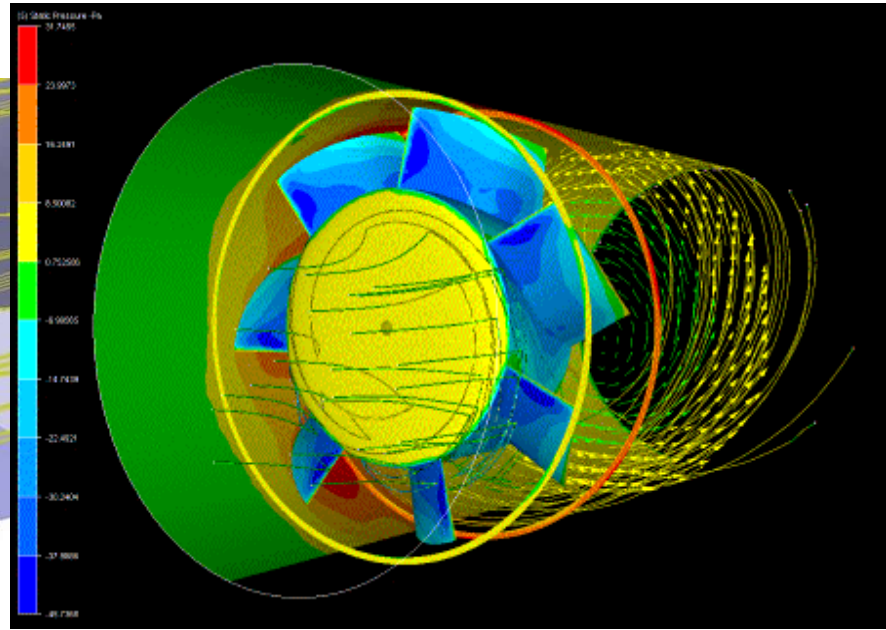
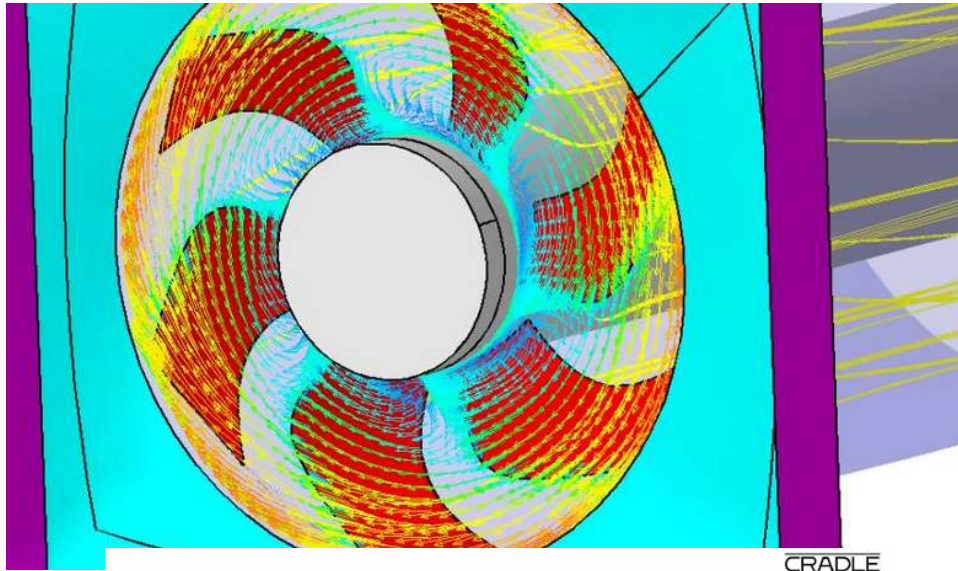
衝動式輪機
(impulse turbine) { 帕爾登水輪機 (Pelton turbine)
橫流水輪機 (cross-flow turbine)

適用於高落差的水源，其動作原理是以噴嘴將水之位能轉變為動能而衝擊水輪機之輪葉，使之產生旋轉的機械能

反動式輪機
(reaction turbine) { 混流式 (mixed-flow)
——法式水輪機 (Francis turbine)
斜流式 (diagonal-flow)
——達里斯水輪機 (Deriaz turbine)
軸流式 (axial-flow)
——卡普蘭水輪機 (Kaplan turbine)
旋葉水輪機 (propeller turbine)
泵水輪機 (pump turbine)

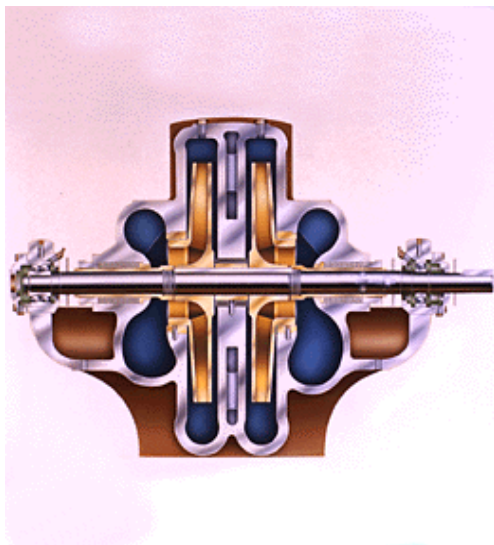
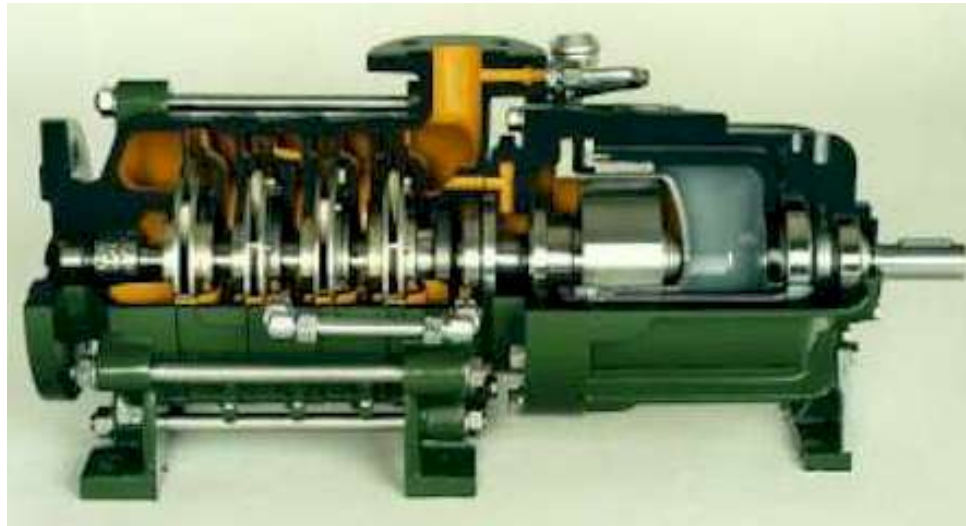
適用於中、低落差的水源，其動作原理係將水壓入輪機內，再流過輪葉，將壓力能轉變為動能而使轉輪旋轉

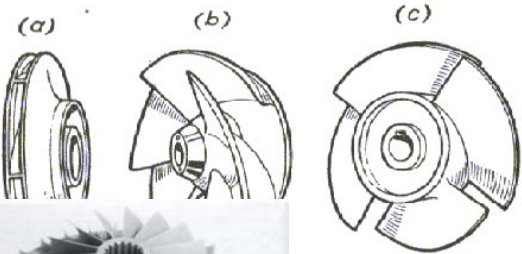
CFD



Pressure Distribution and Velocity on Impeller

Pump





pumps: (a) radial-flow for d-flow; (c) axial-flow

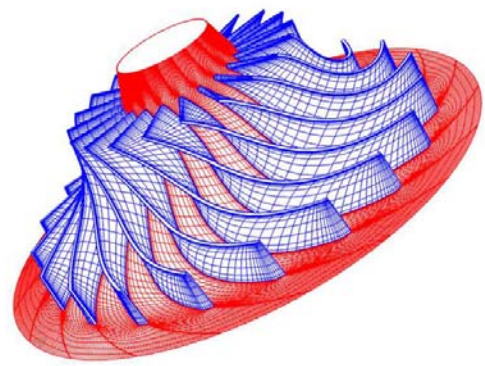
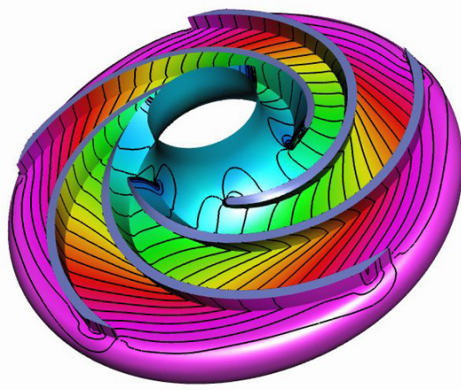
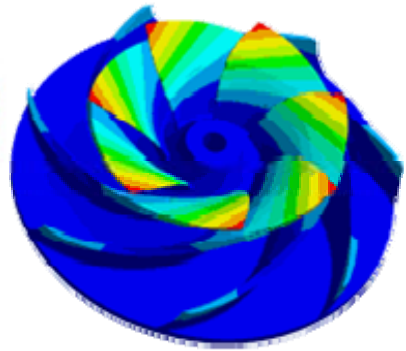
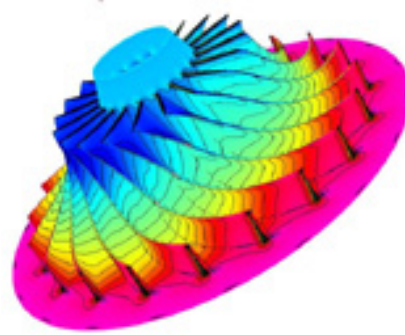
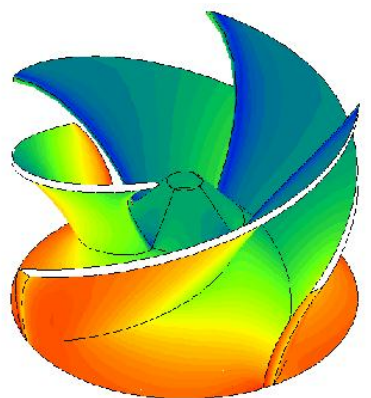
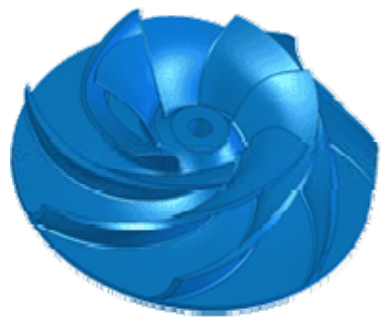
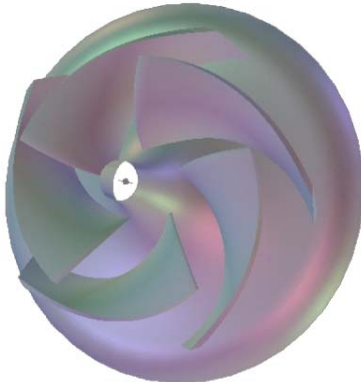
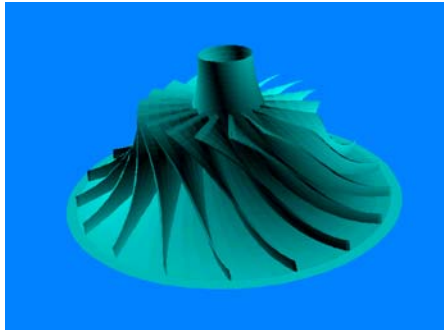


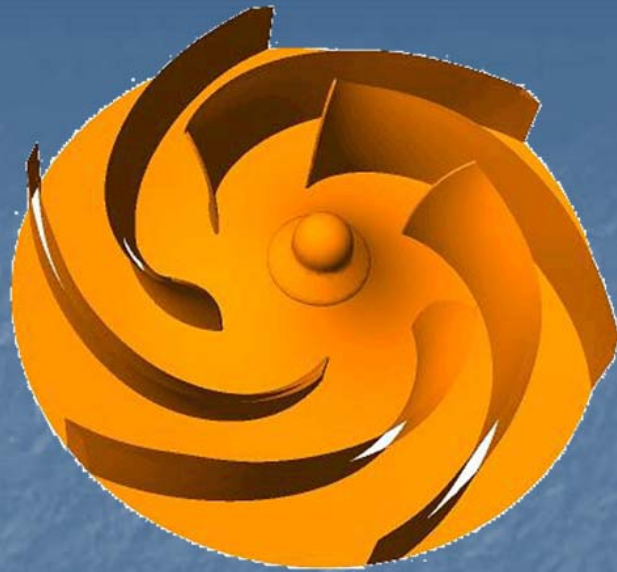
Impellor of centrifugal compressor

Source: Jones and Vanderholm.

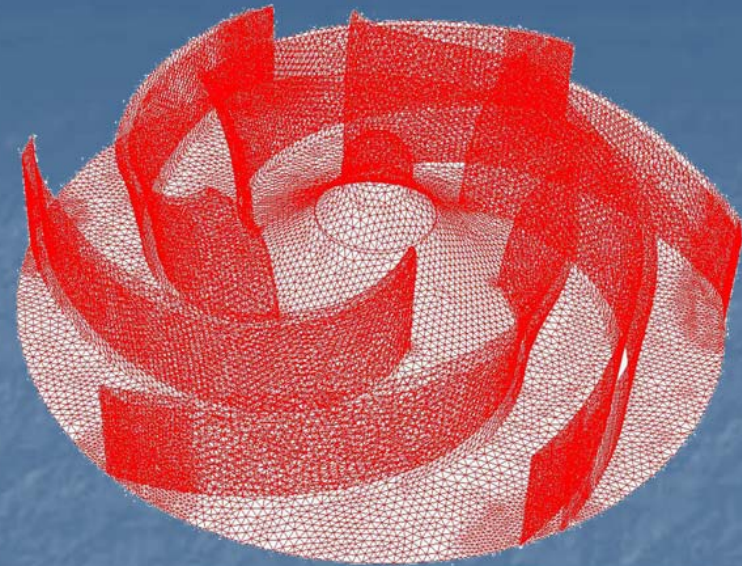


mi-op
centr





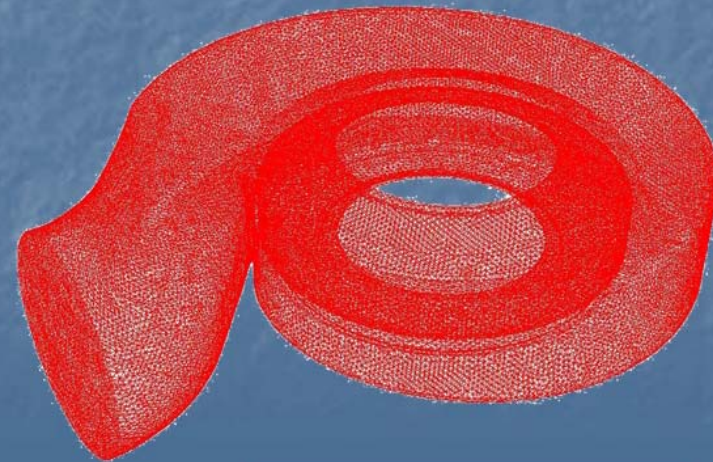
Impeller CAD Geometry



Meshed Impeller Model

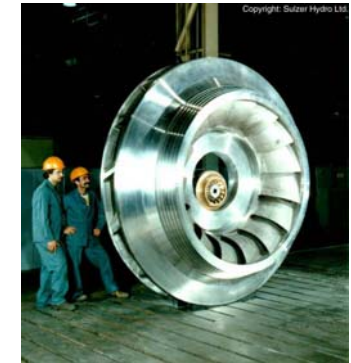


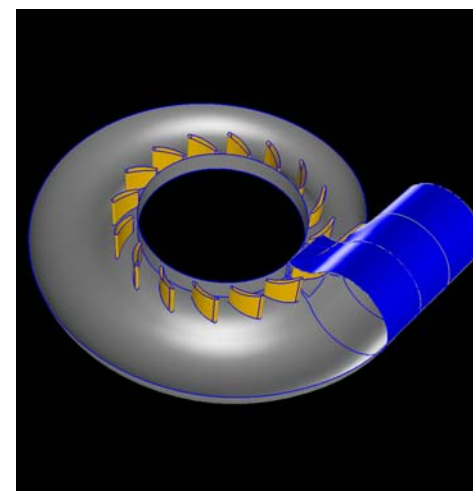
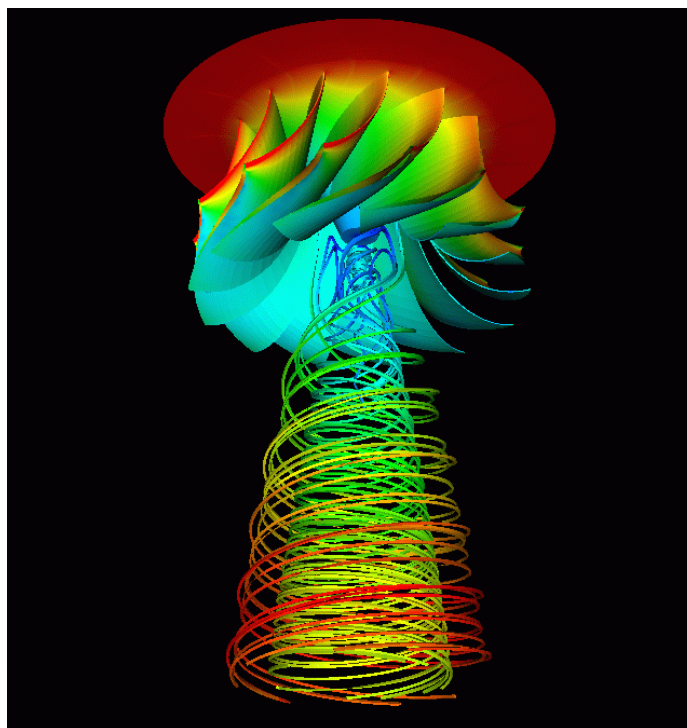
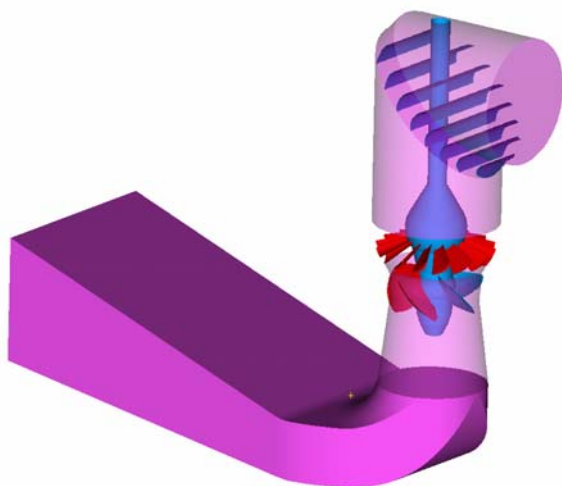
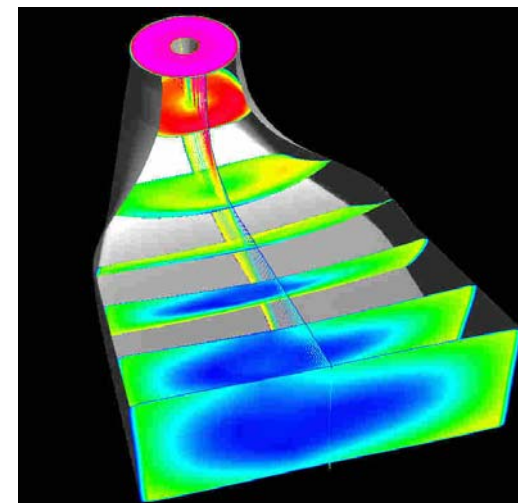
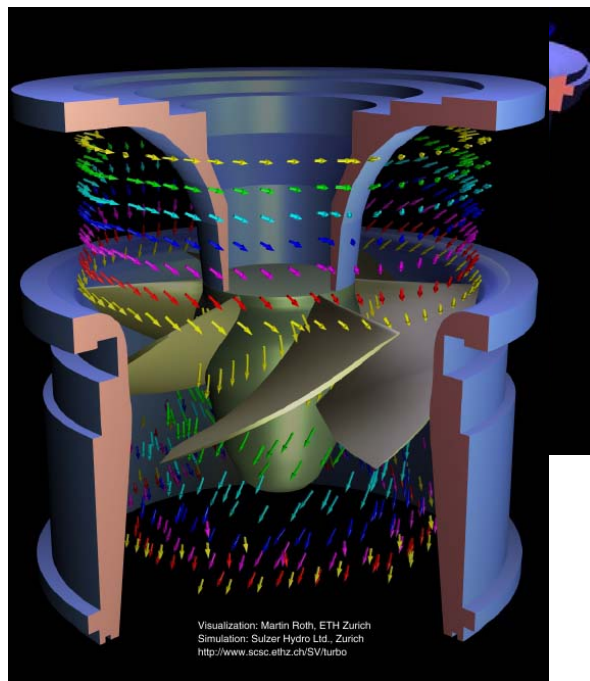
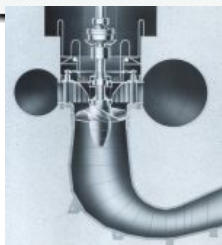
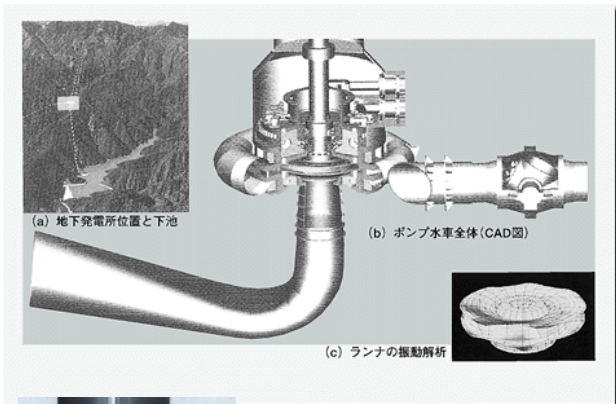
Volute CAD Geometry

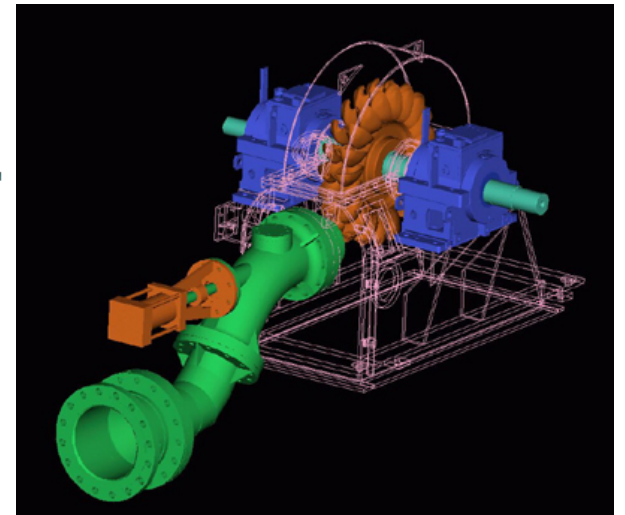
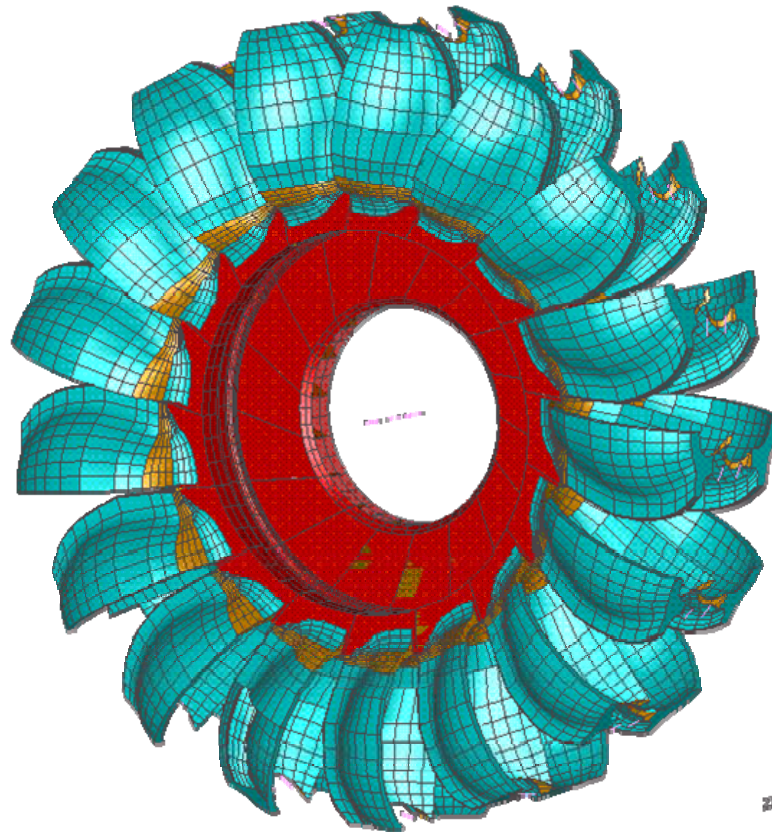
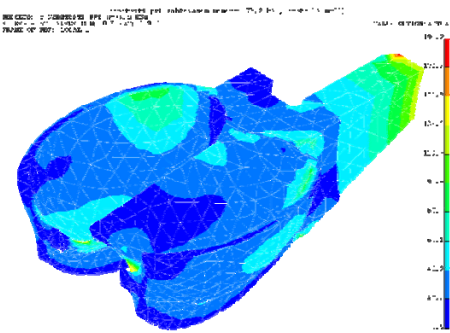
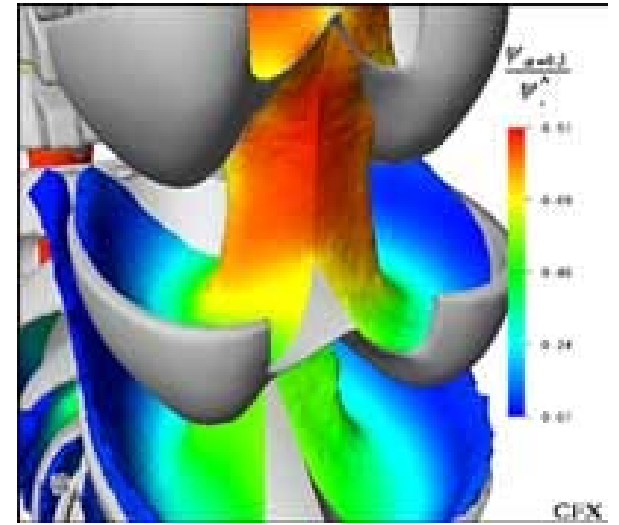
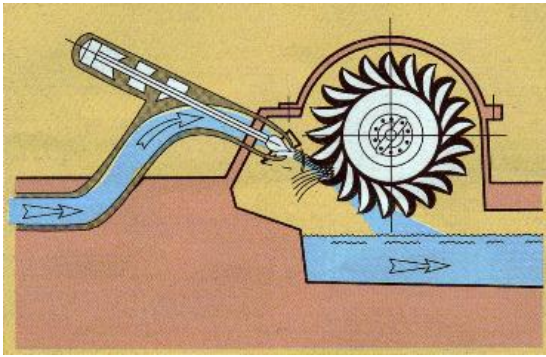


Meshed Volute Model

Water turbine

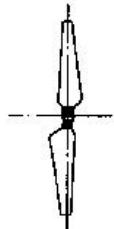




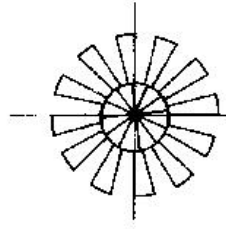


Wind Turbine

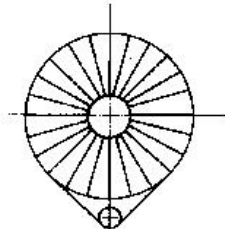
HORIZONTAL AXIS LIFT FORCES



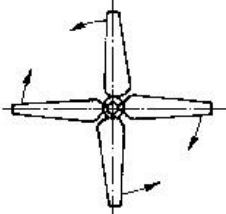
*High speed
single/double/three-bladed*



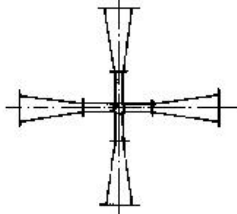
*low speed
multi-bladed*



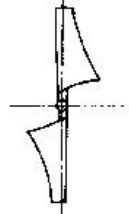
bicycle typ



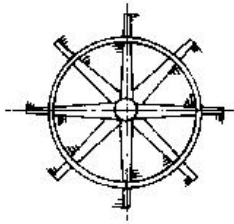
*contra rotating
double rotor*



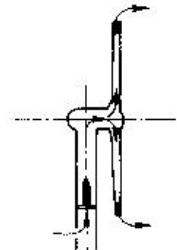
Flettner



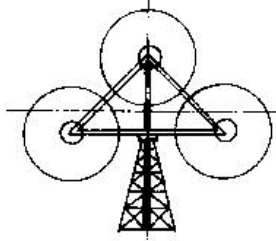
sail wing



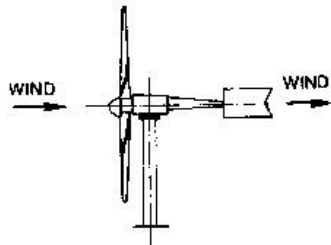
ring generator



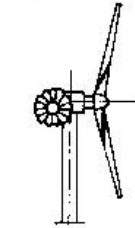
*pneumatic gear
Enfield-Andreau*



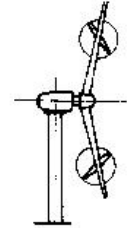
multrotor



upwind vane

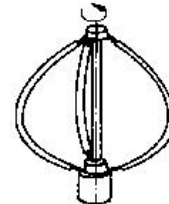


*downwind
sidewheel*

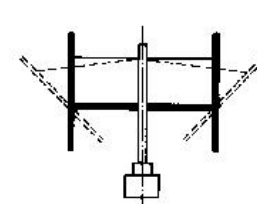


towing rotors

VERTICAL AXIS LIFT FORCES



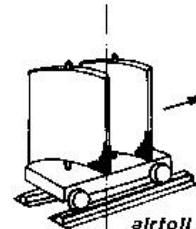
Darrieus



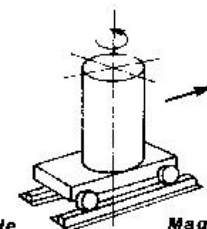
H/V-Darrieus



giromill

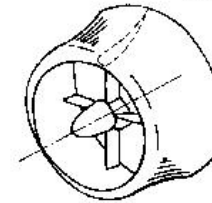


airfoil vehicle

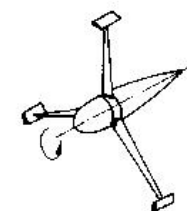


Magnus/Flettner vehicle

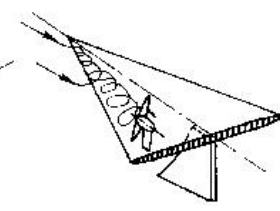
CONCENTRATING DEVICES



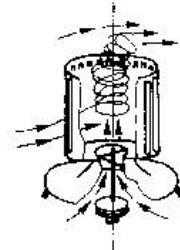
shrouded rotor



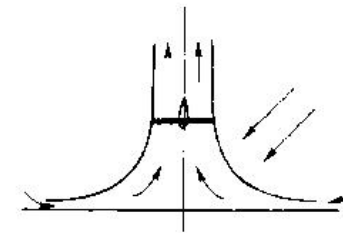
wing tips



unconfined vortex

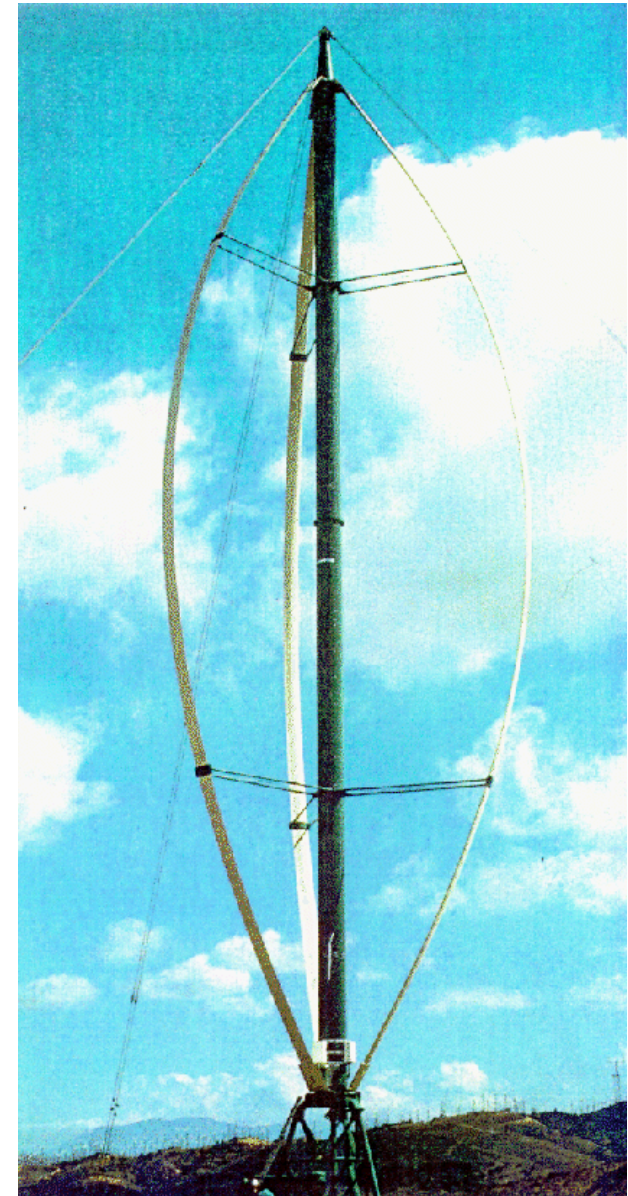
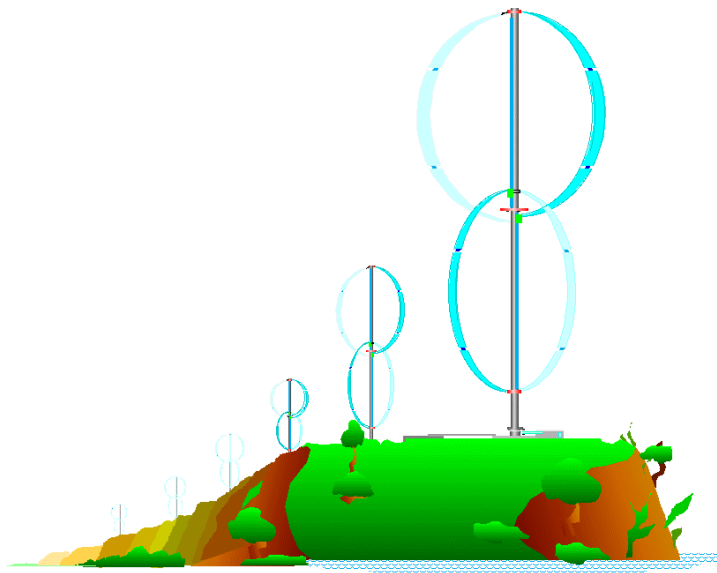


*confined vortex
tornado typ*

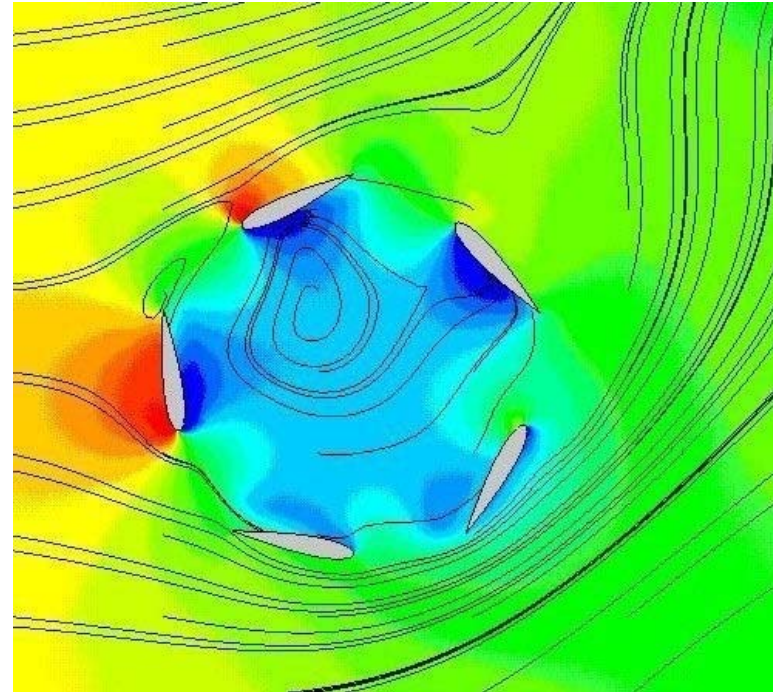
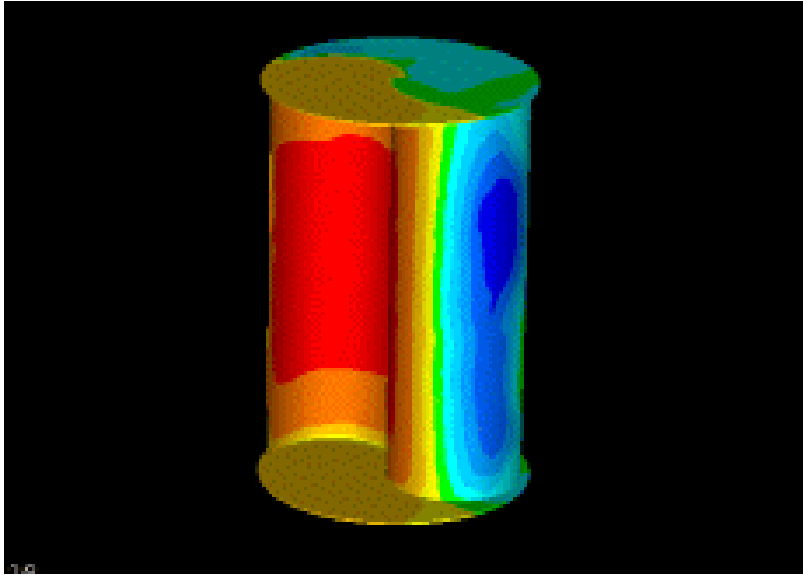


sunlight thermal tower

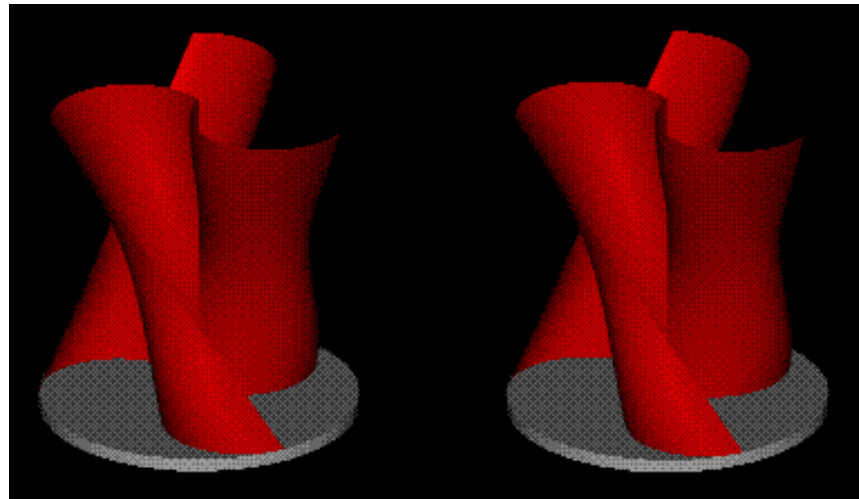
Wind Turbine

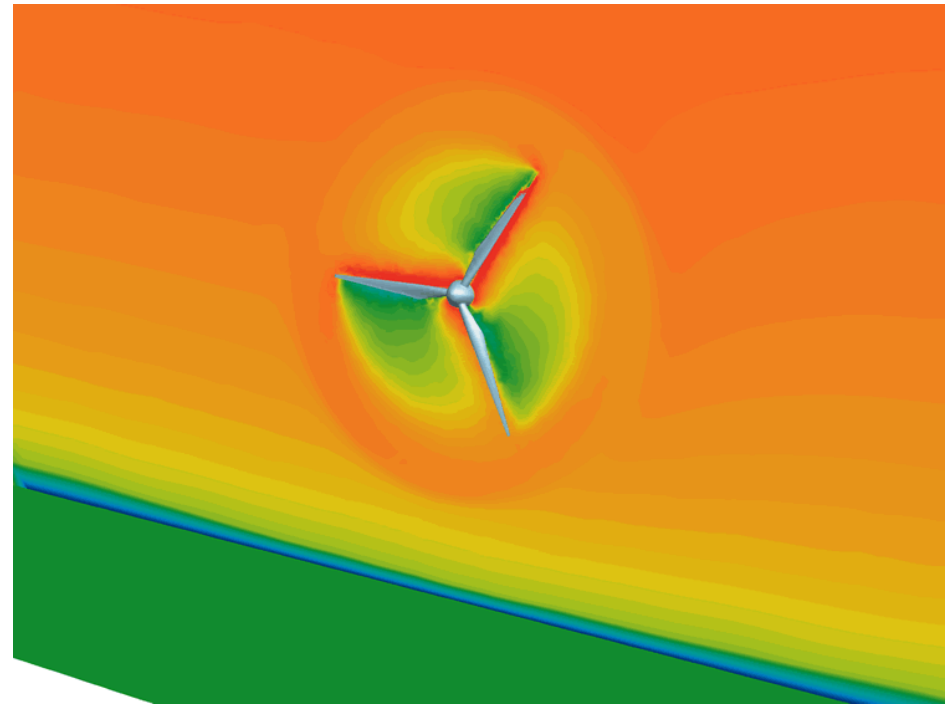
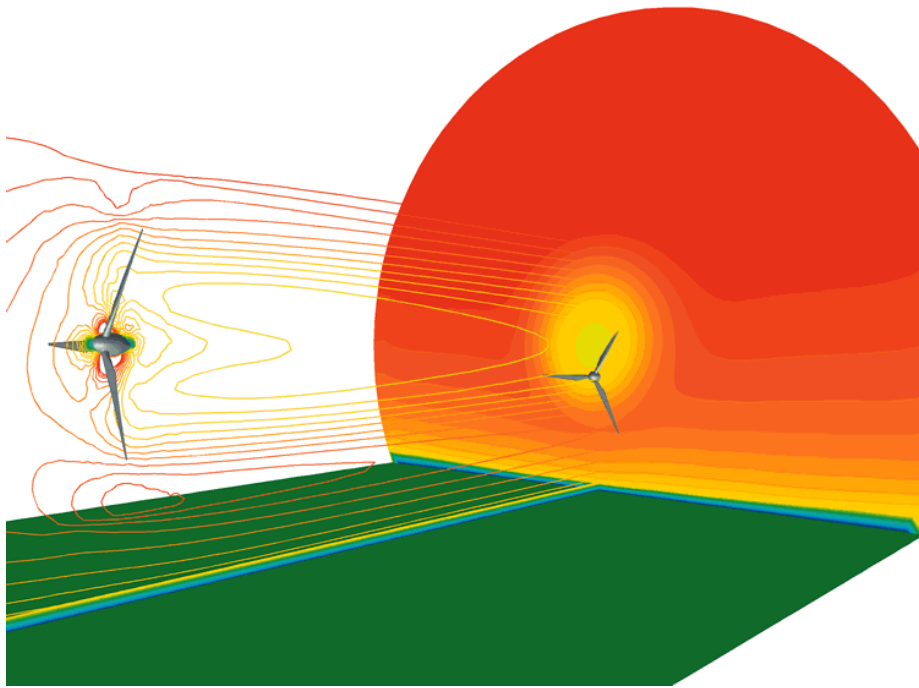


ADVANCED WIND TURBINE FOR MULTI-MEGAWATT POWER GENERATION



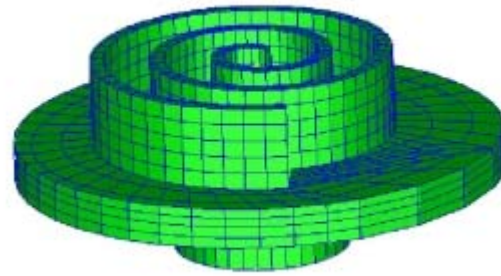
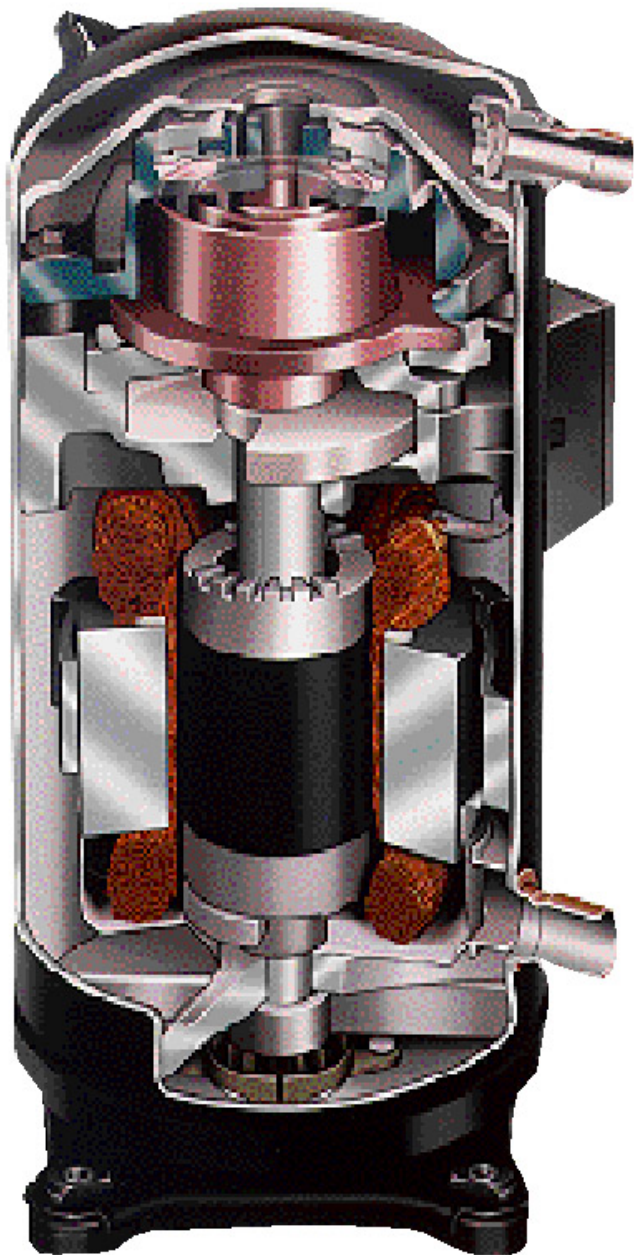
Wind Turbine CFD Simulation Analysis



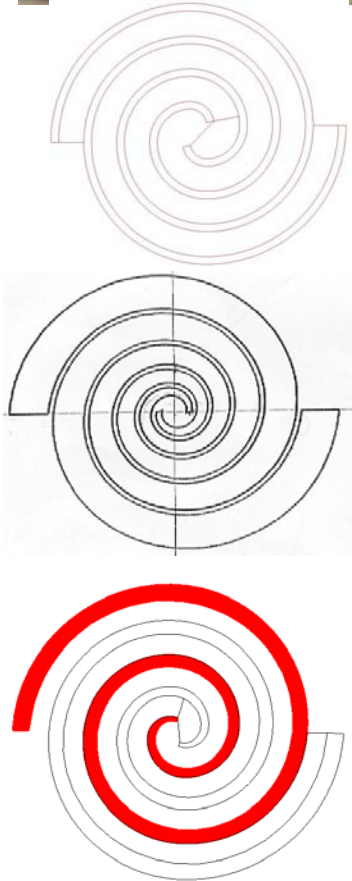
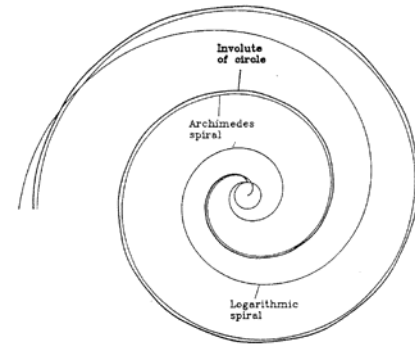
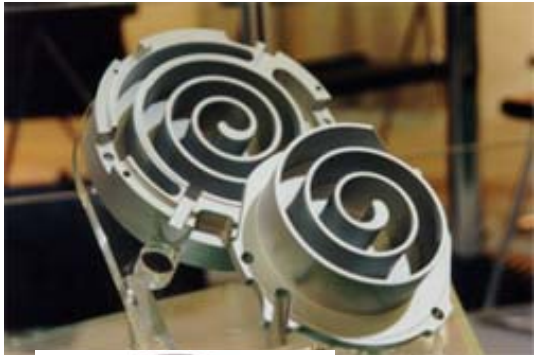


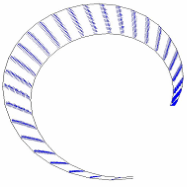
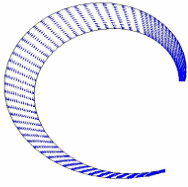
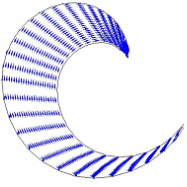
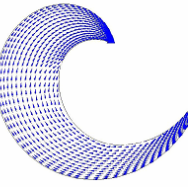
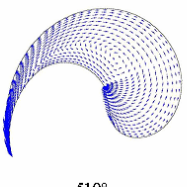
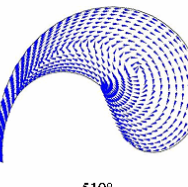
Velocity contours behind one turbine show the wake effect on a second, smaller turbine

Scroll Compressor



14. 渦卷式冷媒壓縮機壓縮室熱流場特性之數值模擬分析



漸開線型	對數螺旋線型
 60°	 60°
 210°	 210°
 510°	 510°

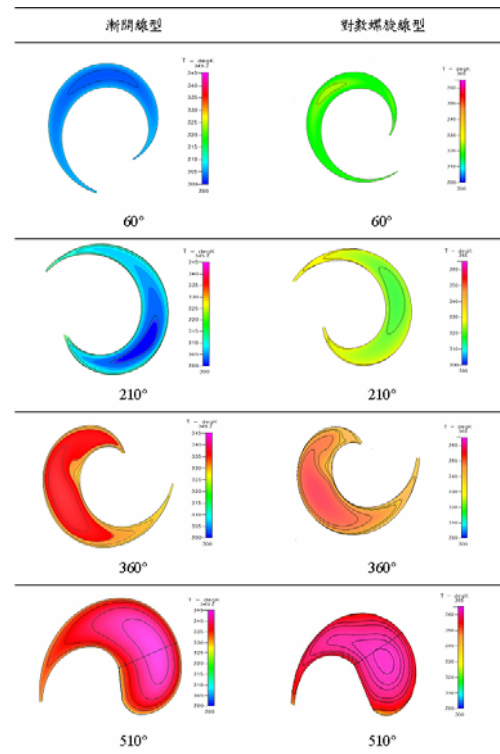
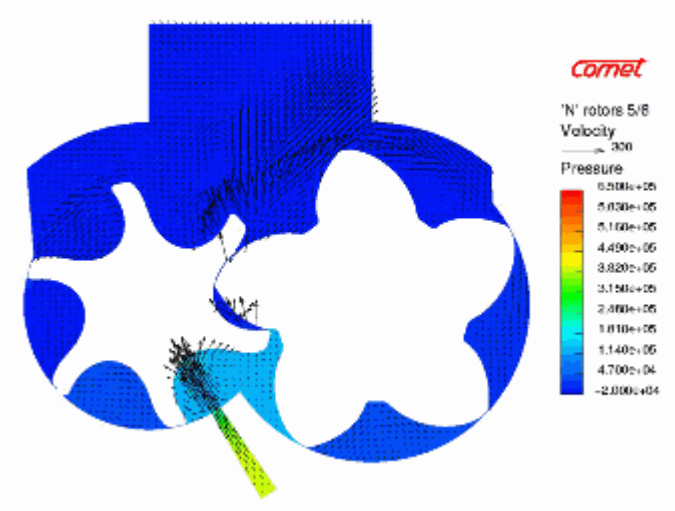
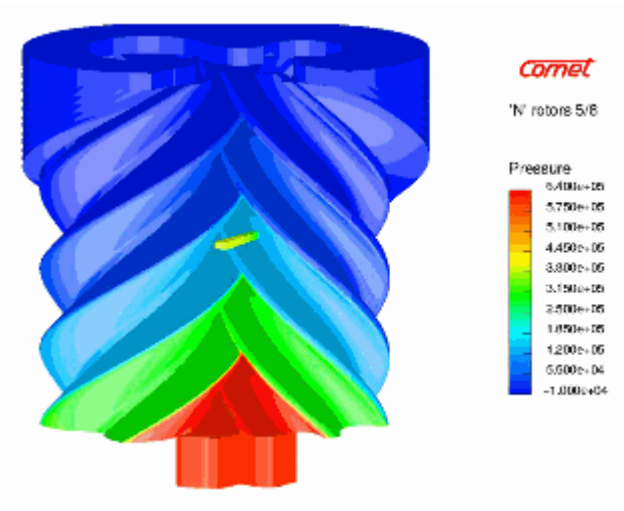
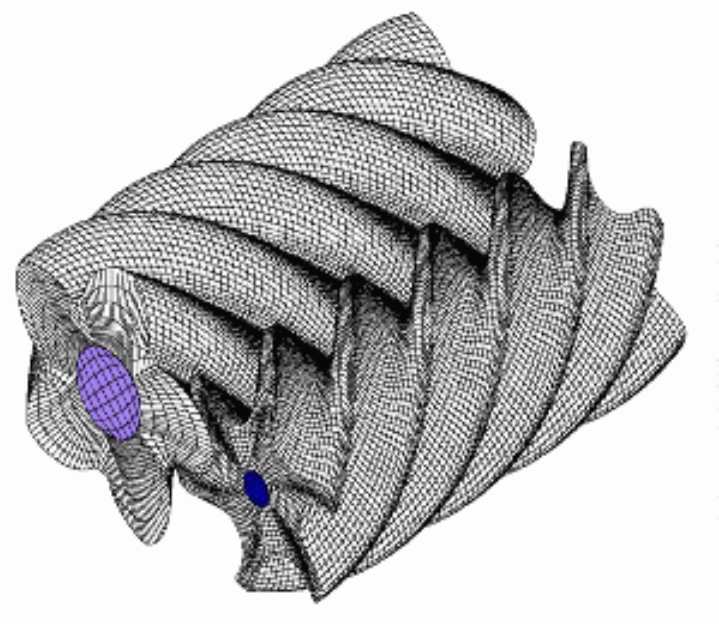


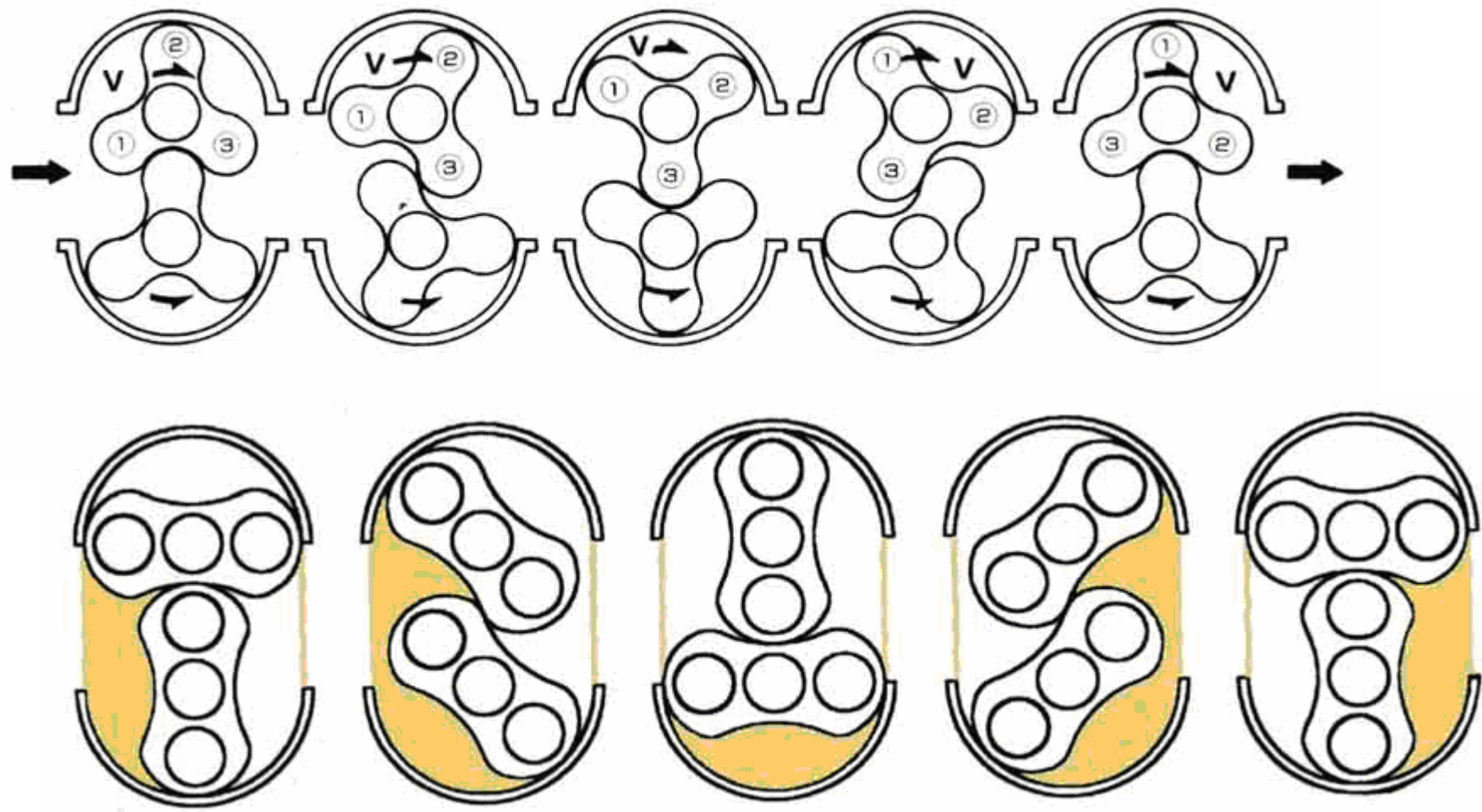
圖 4.33 案例 3 之壓縮室溫度場分析

CFD in Rotary Screw Compressor



魯氏鼓風機之動作原理

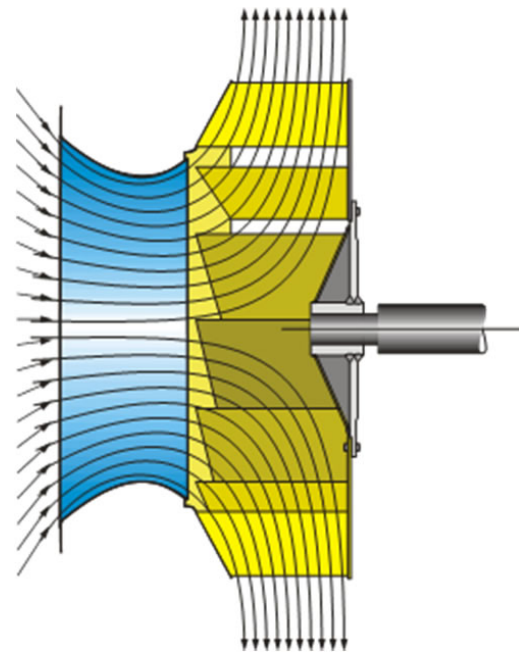
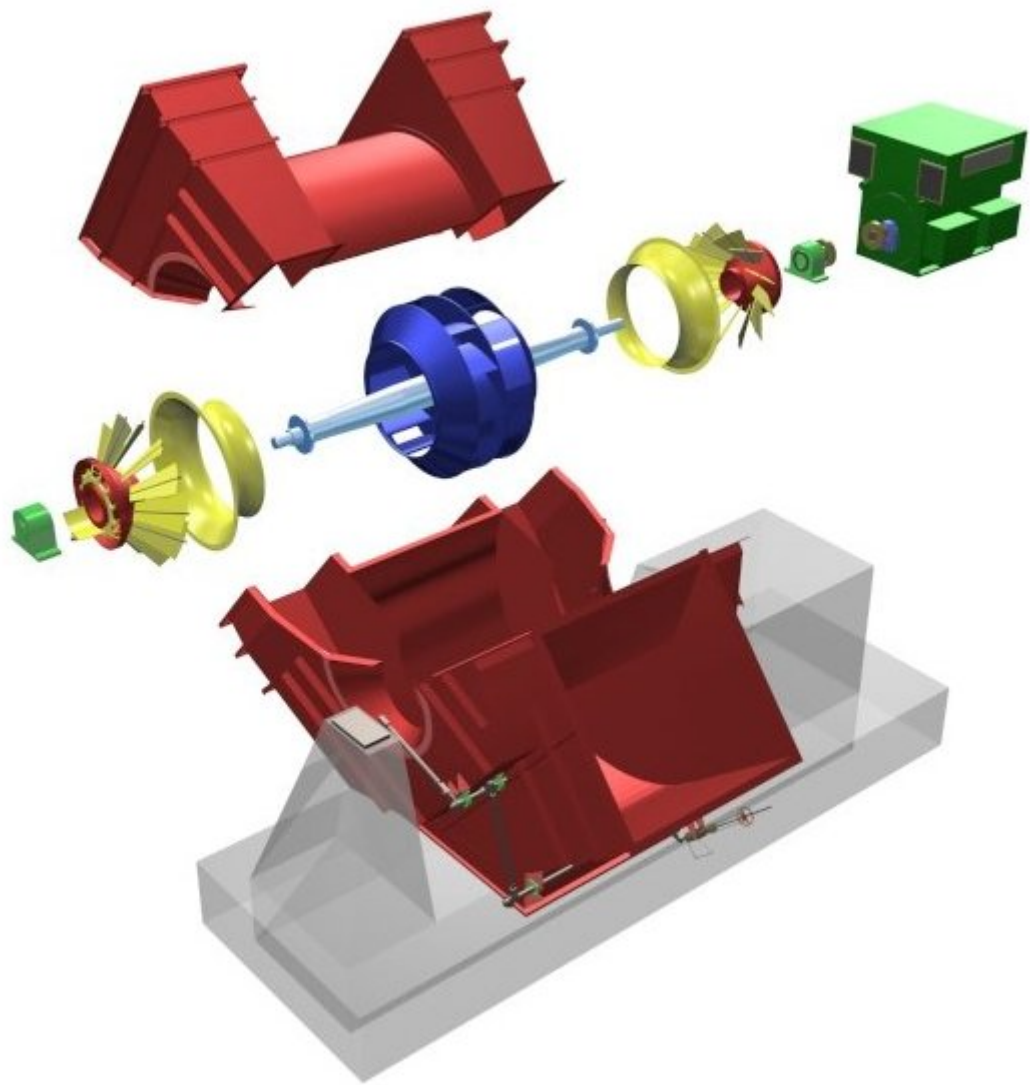
THE PRINCIPLES OPERATION OF ROOTS BLOWER

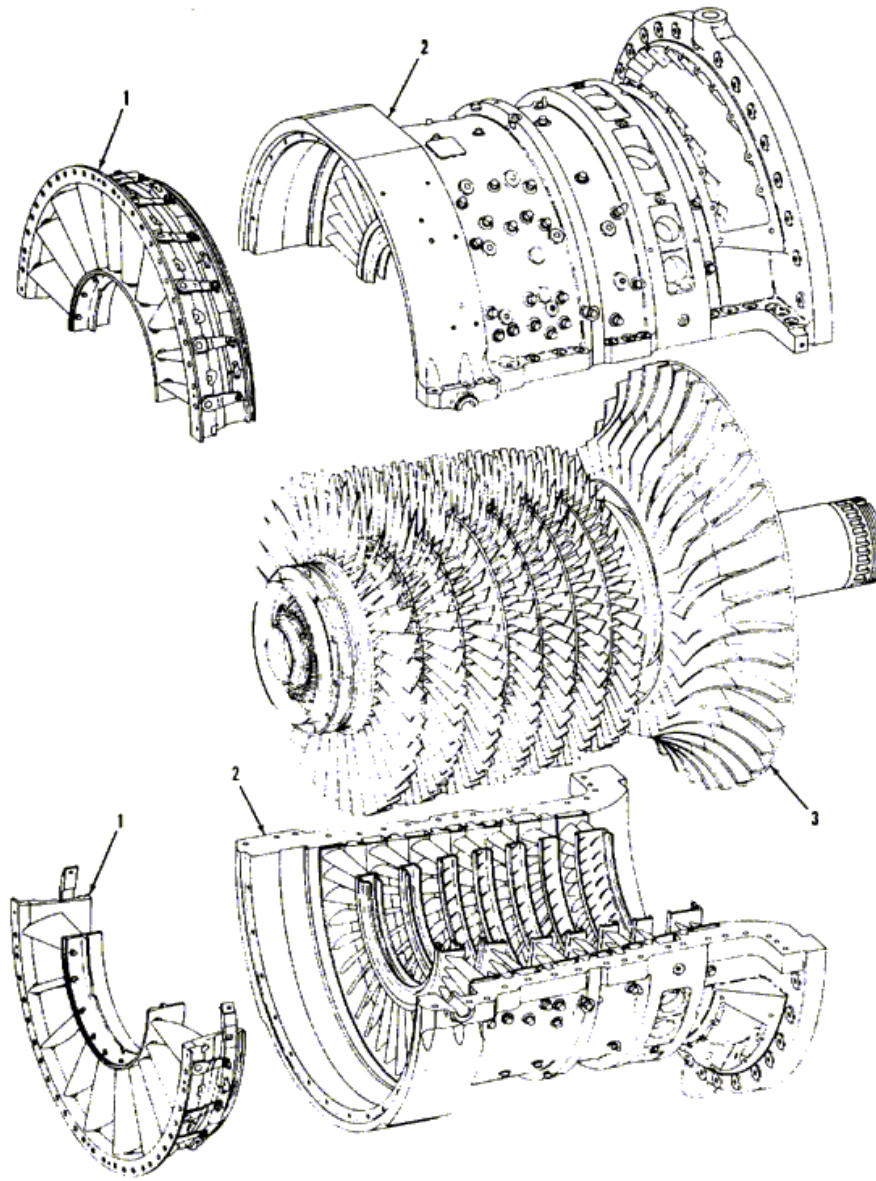


在殼體內部設置有2組，互朝相反方向迴轉之轉子，轉子與轉子，及轉子與殼體間僅留有極小的餘隙，如此狀態下迴轉之。當其中一轉子葉端經過吸入口時，其與殼體之間所捕捉之一定量空氣，自吸入側移送至吐出側，壓向高壓側，以吸入之狀態吐出之。

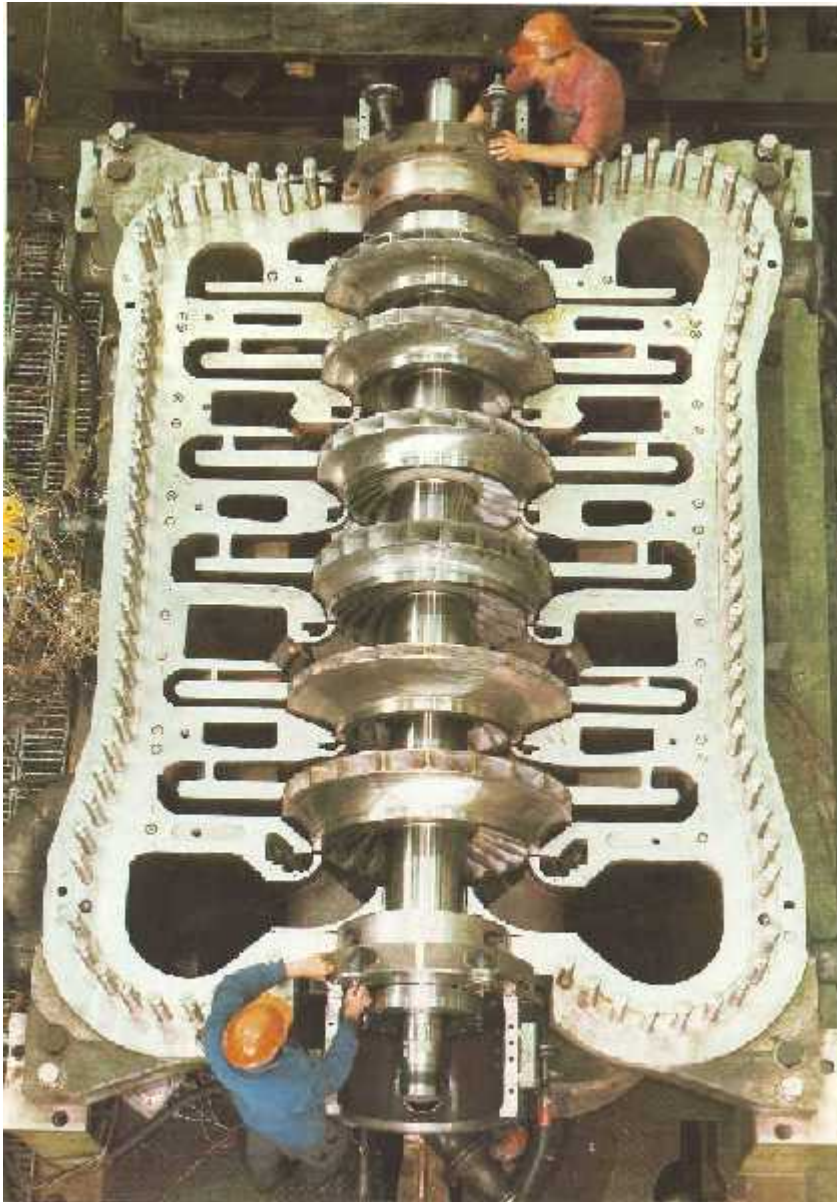
吸入側之空氣，如圖一～圖二所示，其乃至葉端 1、2 與殼體間捕捉移送，被捕捉移送之體積為V經由圖三、圖四步驟，被移送至吐出口開口處，在圖五之狀態下吐出之。

就三葉轉子之情形而言，此一動作，每一迴轉反覆進行六次，因而得以送出與迴轉數次一定比例之定量空氣。

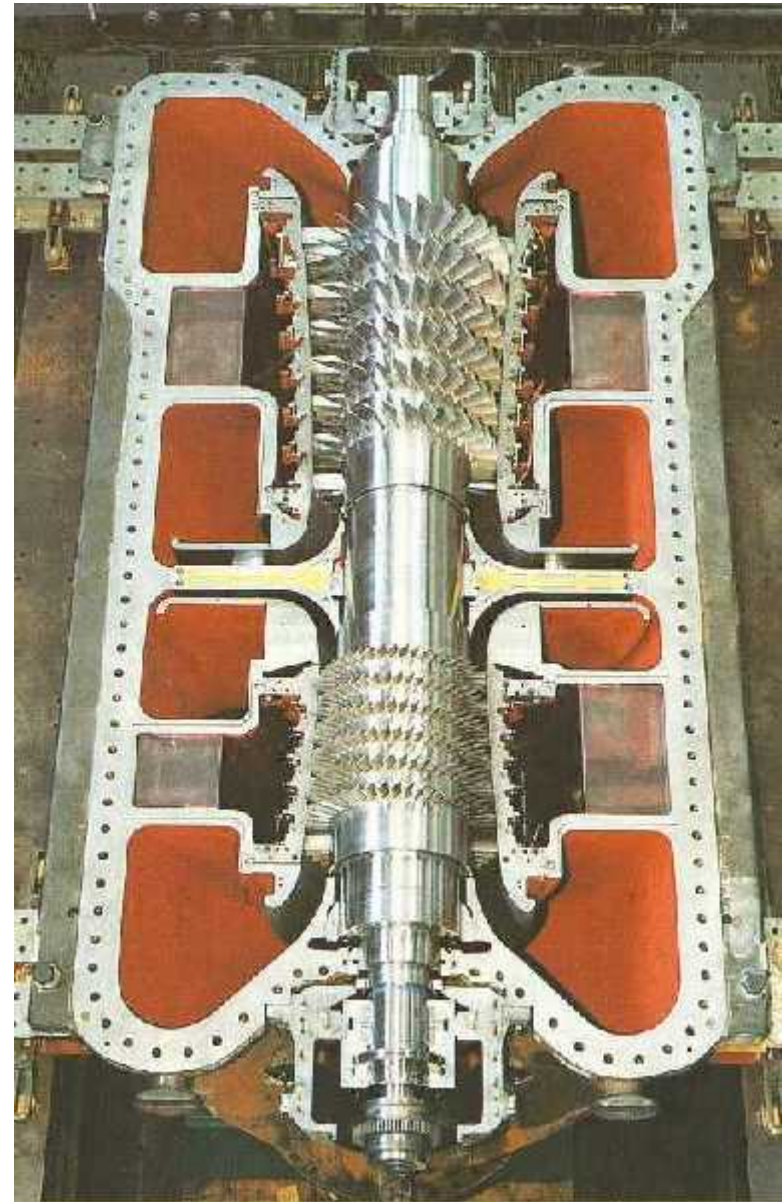




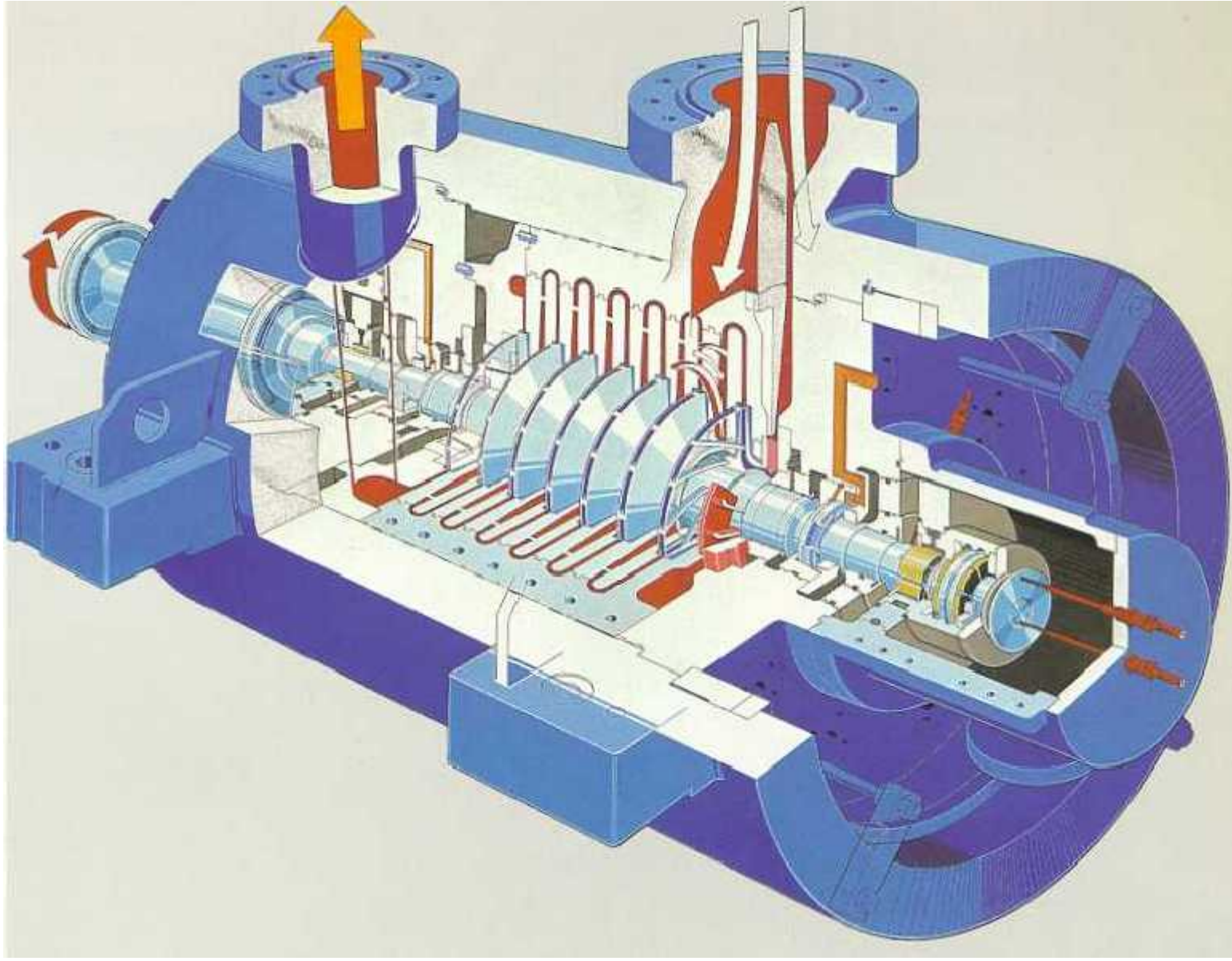
Axial-Centrifugal-Flow Compressor



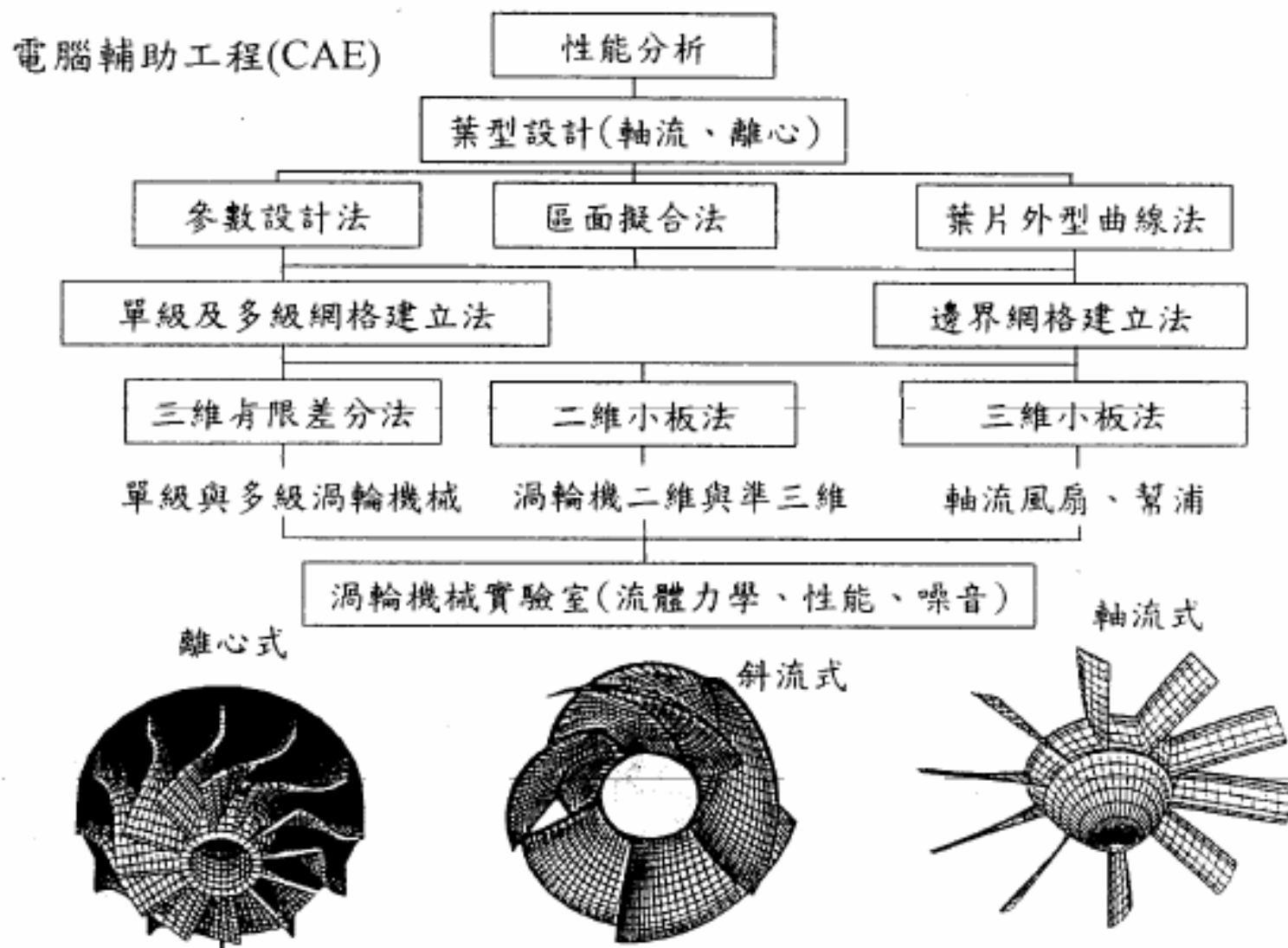
Centrifugal compressors for large refrigeration circuits



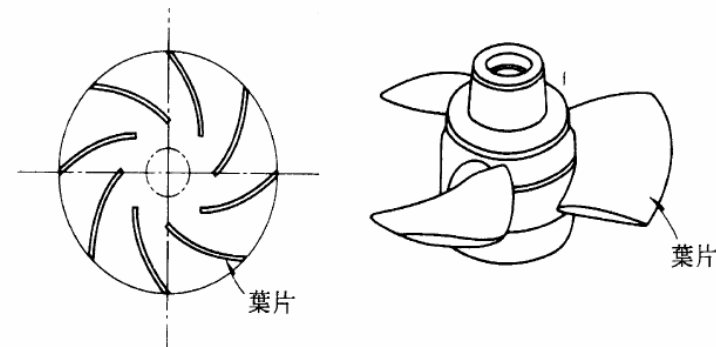
Axial compressor for air separation



電腦輔助設計架構：



輪機機械 (turbomachinery) 係指利用於一平板圓周或一圓筒面上安裝呈輻射狀排列之葉片 (vane) 所形成之葉輪 (如圖 2.1 所示) , 使葉輪旋轉且使流體流經其間而達成能量傳送之機械 , 如水輪機 (water turbine) 、 泵 (pump) 、 送風機 (壓縮機) (blower , compressor) 、 蒸汽輪機 (steam turbine) 、 與氣輪機 (gas turbine) 等。水輪機係將流體之位能轉換成機械功之機械 ; 而泵與送風機 (壓縮機) 係將機械功轉換成流體壓力能之機械。蒸汽輪機與氣輪機則均係將流體所具有之能量 (主要為熱能) 轉換成機械功 , 不屬於一般所謂的流體機械之範圍 , 另有專門書籍討論 ; 本書係針對通稱之流體機械 (包括水輪機、泵、送風機) 作詳細說明 ,



(a) 葉片排列圓周上之葉輪 (b) 葉片排列於圓筒面上之葉輪

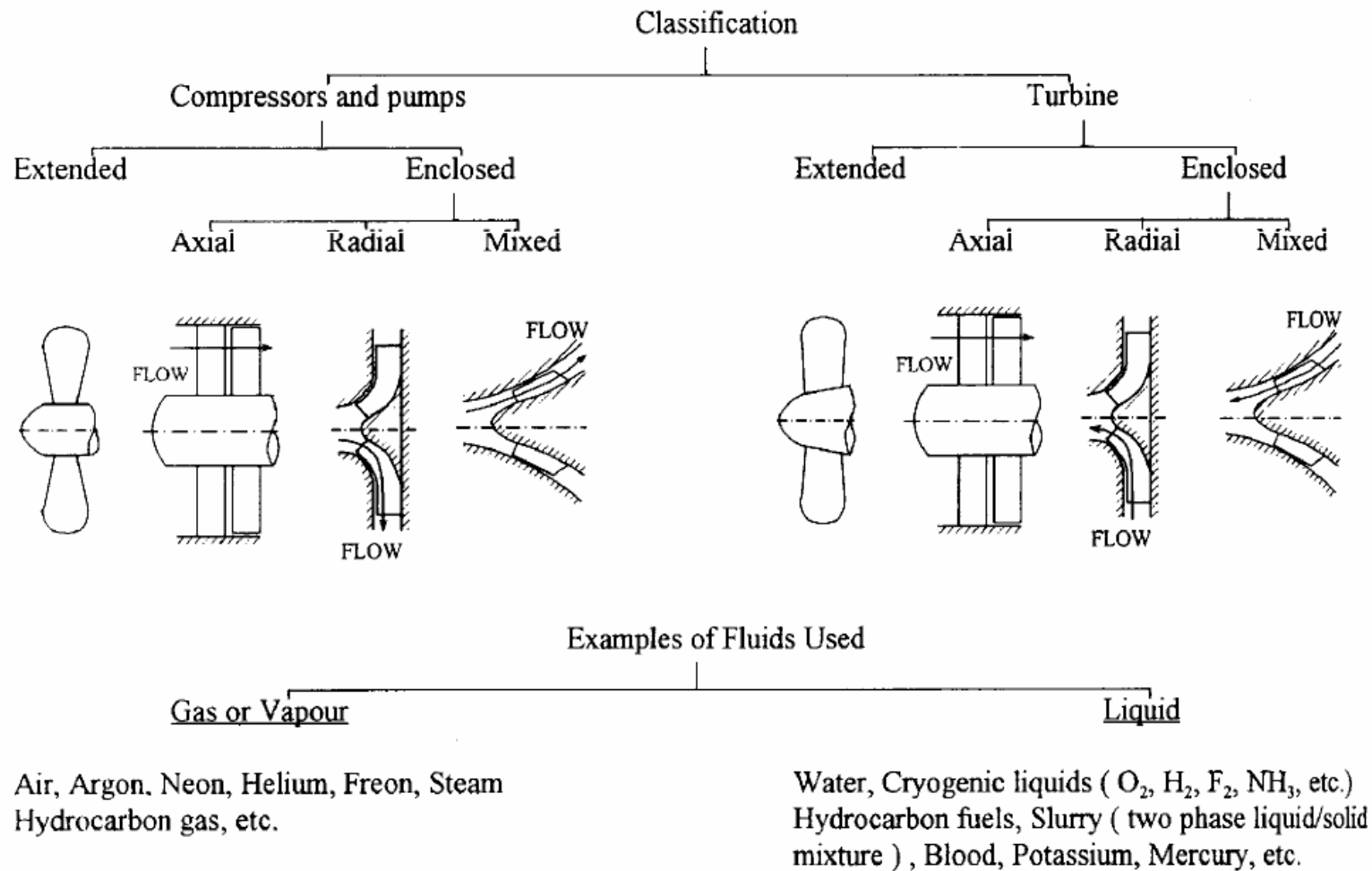
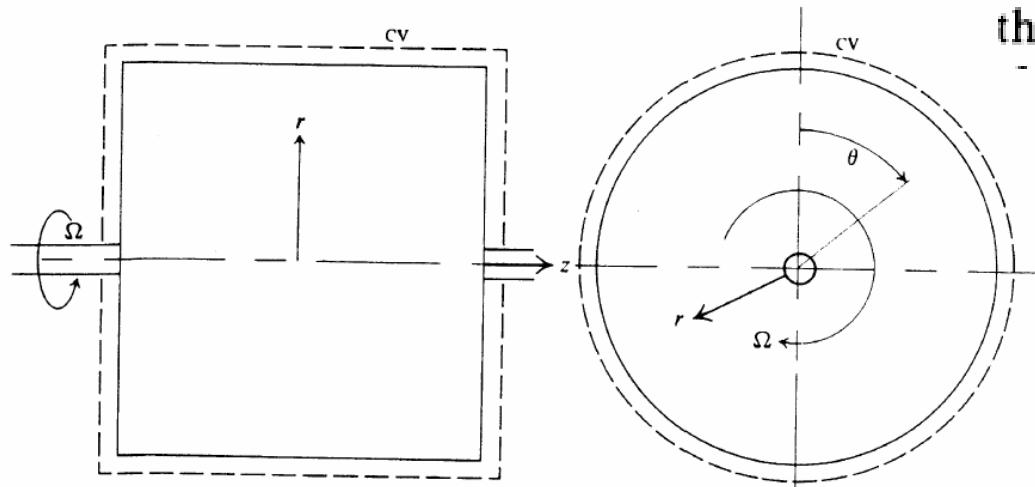


Figure 1.1 Classification of turbomachinery.

GENERAL RELATIONS FOR TURBOMACHINES

Euler's Turbomachinery Equation



$$\sum M_{cv_z} = \oint_{CS} \rho (\mathbf{r} \times \mathbf{V})_z (\mathbf{V} \cdot d\mathbf{A})$$

the angular-momentum term $(\mathbf{r} \times \mathbf{V})_z$

$$\mathbf{V} = \mathbf{i}_r v_r + \mathbf{i}_\theta v_\theta + \mathbf{i}_z v_z$$

$$\mathbf{r} = \mathbf{i}_r r$$

$$(\mathbf{r} \times \mathbf{V})_z = r v_\theta$$

Control volume for a turbomachine.

$$\mathcal{T}_{\text{shaft}} = - \iint_{\text{inlet}} \rho r v_\theta d\dot{Q} + \iint_{\text{outlet}} \rho r v_\theta d\dot{Q}$$

$$\mathcal{T}_{\text{shaft}} = -(\rho r v_\theta)_1 \iint_{\text{inlet}} d\dot{Q} + (\rho r v_\theta)_2 \iint_{\text{outlet}} d\dot{Q}$$

Euler's turbomachinery equation

valid for compressible flow

$$\mathcal{T}_{\text{shaft}} = (\rho r v_{\theta})_2 \dot{Q}_{\text{outlet}} - (\rho r v_{\theta})_1 \dot{Q}_{\text{inlet}}$$

Integrating the flow rates over the inlet and outlet,

$$\dot{m} = \rho_1 \dot{Q}_{\text{inlet}} = \rho_2 \dot{Q}_{\text{outlet}}$$

$$\mathcal{T}_{\text{shaft}} = \dot{m}[(r v_{\theta})_2 - (r v_{\theta})_1]$$

The shaft power $\mathcal{P}_{\text{shaft}}$ is

$$\mathcal{P}_{\text{shaft}} = \mathcal{T}_{\text{shaft}} \Omega = \dot{m} \Omega [(r v_{\theta})_2 - (r v_{\theta})_1]$$

where Ω is the angular velocity of the turbomachine. Positive power means that the angular momentum of the flow has been increased, $(r v_{\theta})_2 > (r v_{\theta})_1$. A pump increases the angular momentum of the flow passing through it. A turbine decreases the angular momentum of the flow, and the shaft power is negative.

$P > 0$ for pump

$P < 0$ for turbine

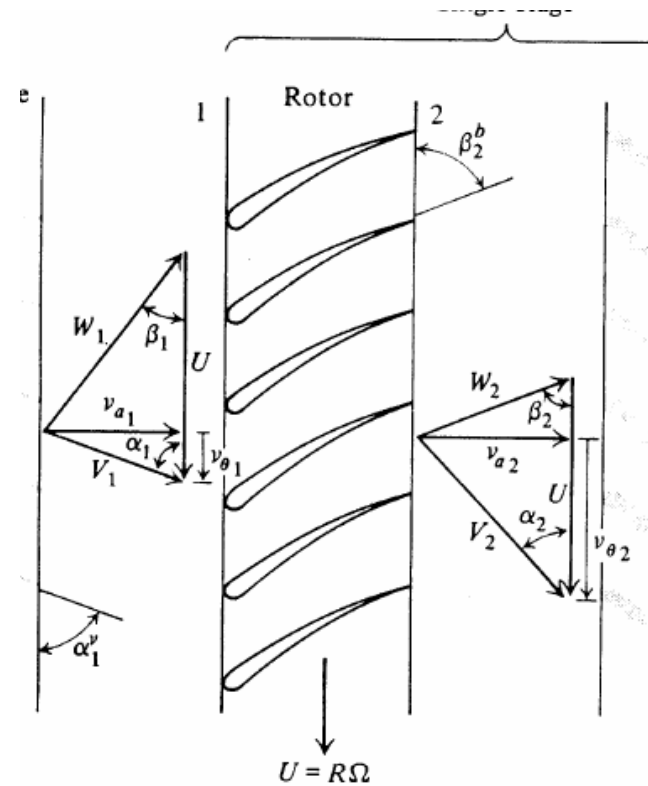
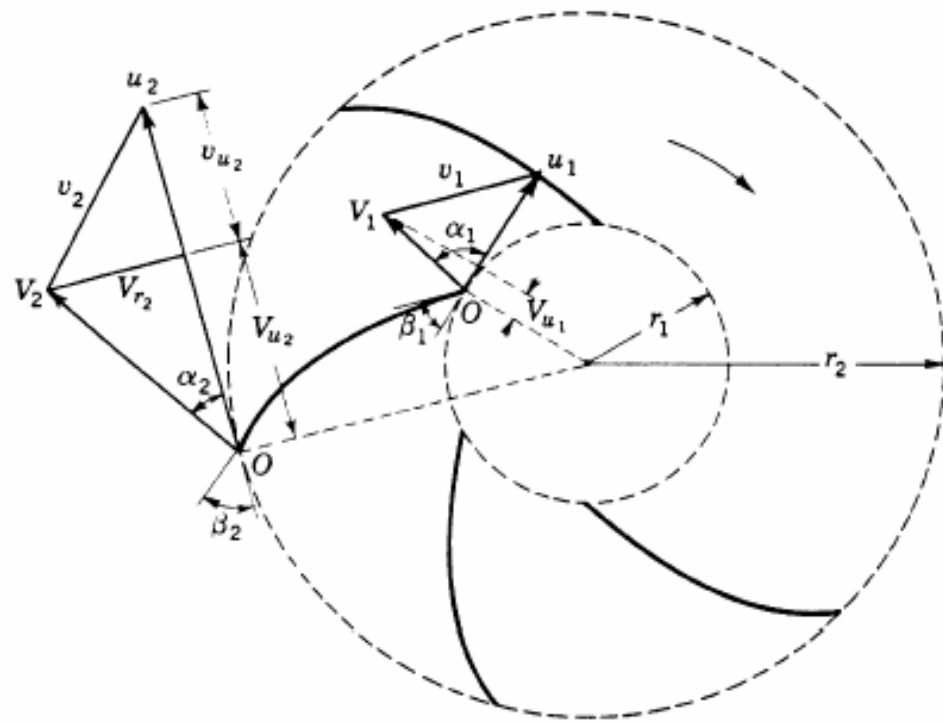
The ideal total head change of the flow, i.e., neglecting any mechanical energy losses due to friction, is

$$(\Delta h_t)_{1 \rightarrow 2} = \frac{\mathcal{P}_{\text{shaft}}}{\dot{m}g} = \frac{\Omega}{g} [(rv_\theta)_2 - (rv_\theta)_1]$$

$$= \frac{U_2 v_{\theta 2} - U_1 v_{\theta 1}}{g}$$

the speed of the rotating surface U at any radial location r

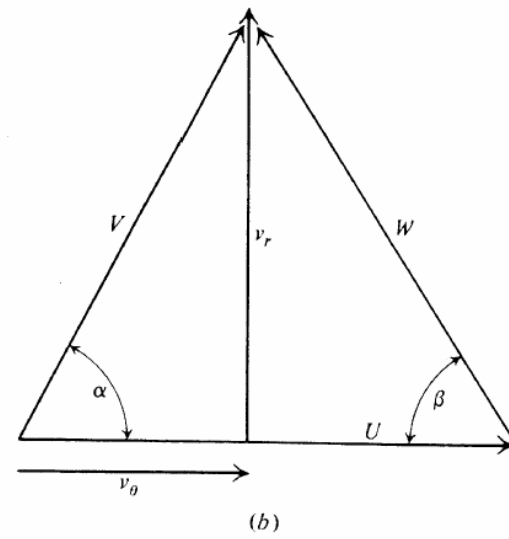
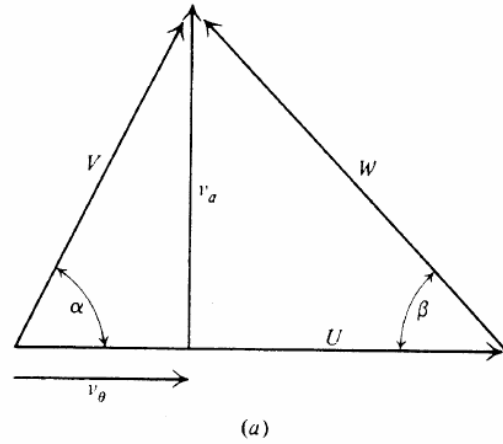
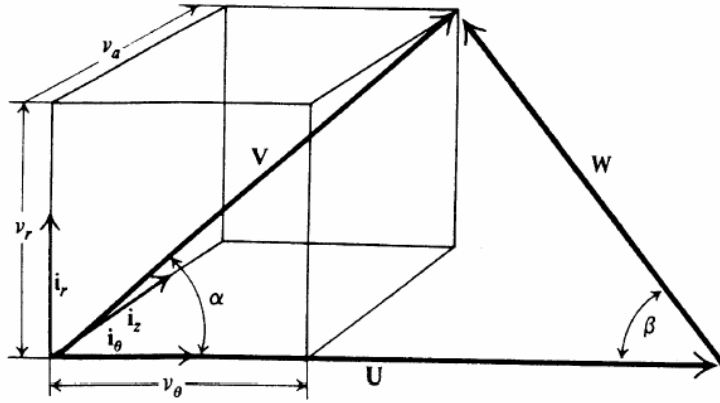
$$U = r\Omega$$



Velocity relations for flow through a centrifugal-pump impeller and Axial-flow compressor.

Velocity Triangles

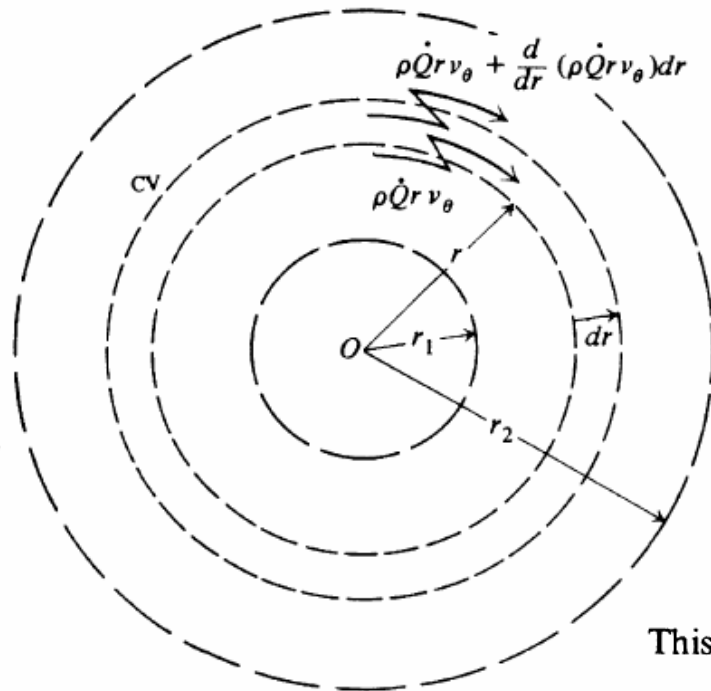
$$\mathbf{V} = \mathbf{U} + \mathbf{W}$$



Free-Vortex Flow

Some turbomachines have regions which contain no surfaces but in which the flow changes radius. Even though there are no surfaces to exert torques on the flow and change its tangential velocity, the change in radius, by itself, causes the tangential velocity to change.

$$\mathcal{T}_{\text{shaft}} = \sum M_{\text{CV}_z} = \oint_{\text{CS}} \rho(\mathbf{r} \times \mathbf{V})_z (\mathbf{V} \cdot d\mathbf{A}) = 0$$



$$-\rho \dot{Q}(rv_\theta) + \rho \dot{Q}(rv_\theta) + \frac{d}{dr} [\rho \dot{Q}(rv_\theta)] dr = 0$$

$$\frac{d}{dr} (rv_\theta) = 0 \quad \text{or} \quad rv_\theta = \text{const}$$

$$v_\theta \propto 1/r$$

This tangential velocity variation with radius is called *free-vortex flow*.

Control volume for free-vortex flow.

Bernoulli Equation for a Turbomachine

be used to obtain the ideal static-pressure change in a turbomachine.

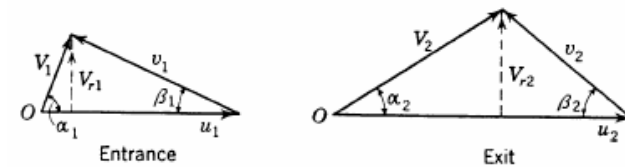
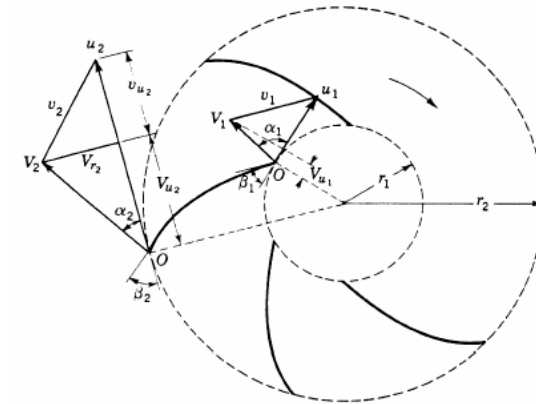
$$\frac{p_1}{\rho g} + \frac{V_1^2}{2g} + (\Delta h_t)_{1 \rightarrow 2} = \frac{p_2}{\rho g} + \frac{V_2^2}{2g}$$

$$\frac{p_1}{\rho g} + \frac{V_1^2}{2g} + \frac{U_2 v_{\theta 2} - U_1 v_{\theta 1}}{g} = \frac{p_2}{\rho g} + \frac{V_2^2}{2g}$$

The law of cosines $V^2 = W^2 + U^2 - 2WU \cos \beta$

$$v_{\theta} = V \cos \alpha = U - W \cos \beta$$

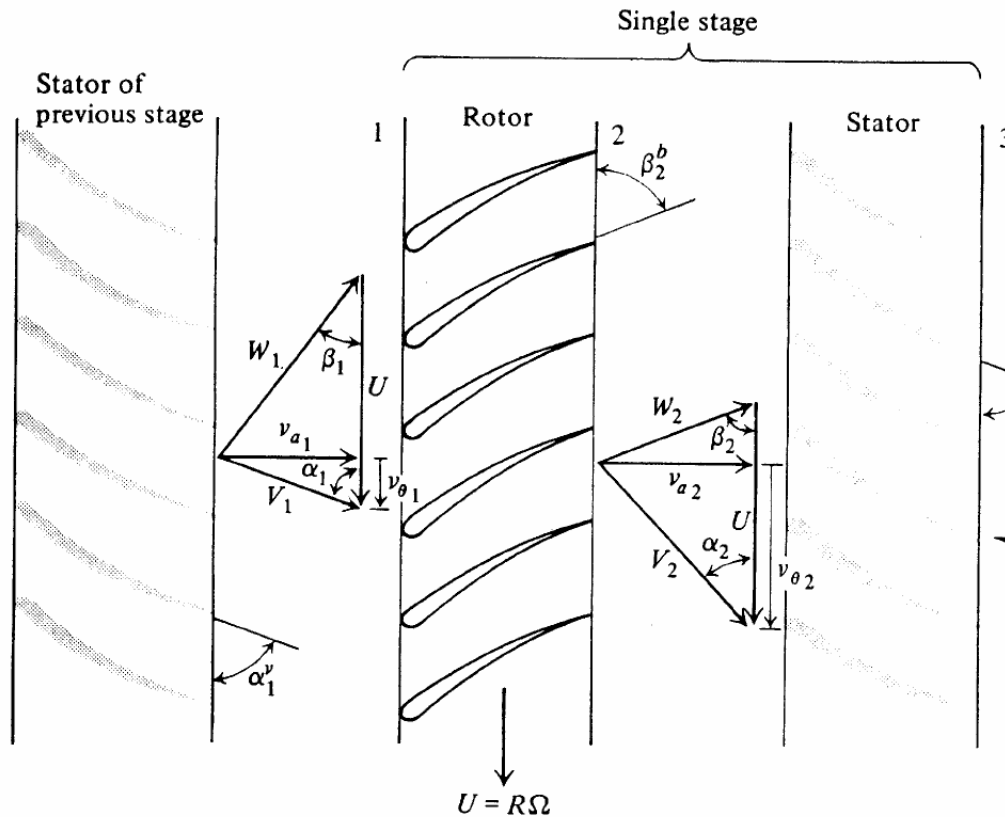
$$V^2 = W^2 + U^2 - 2U(U - v_{\theta})$$



$$\frac{p_2 - p_1}{\rho g} + \frac{W_2^2 - W_1^2}{2g} - \frac{U_2^2 - U_1^2}{2g} = 0$$

the ideal (no friction) static-pressure change for an incom-pressible flow through a turbomachine.

the axial velocity be nearly constant



$$v_{a1} = v_{a2} = v_{a3} \equiv v_a$$

The rotor speed at 1 and 2

$$U_1 = U_2 \equiv U = R\Omega$$

the head change across the rotor

$$(\Delta h_t)_{1 \rightarrow 2} = \frac{U}{g} (v_{\theta 2} - v_{\theta 1})$$

the velocity triangles

$$v_{\theta 1} = v_a \cot \alpha_1$$

$$v_{\theta 2} = U - v_a \cot \beta_2$$

Figure 12.10 Stage velocity triangles.

$$\beta_2 \approx \beta_2^b$$

$$\alpha_1 \approx \alpha_1^v \quad \alpha_3 \approx \alpha_3^v$$

the total head change across the stage

$$(\Delta h_t)_{1 \rightarrow 2} = \frac{U^2}{g} \left[1 - \frac{v_a}{U} (\cot \beta_2 + \cot \alpha_1) \right]$$

head coefficient $\Psi = g(\Delta h_t)_{1 \rightarrow 2} / U^2$, a measure of the total head change.

capacity coefficient $\Phi = v_a / U$, a measure of the flow rate.

$$(\Delta h_t)_{1 \rightarrow 2} = \frac{U^2}{g} \left[1 - \frac{v_a}{U} (\cot \beta_2 + \cot \alpha_1) \right] \quad \Psi = 1 - (\cot \beta_2 + \cot \alpha_1) \Phi$$

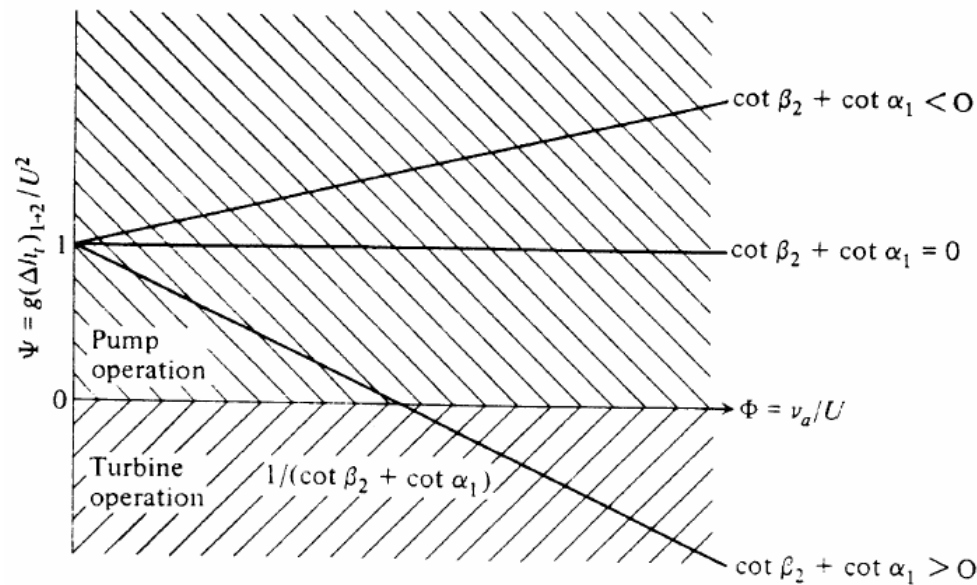


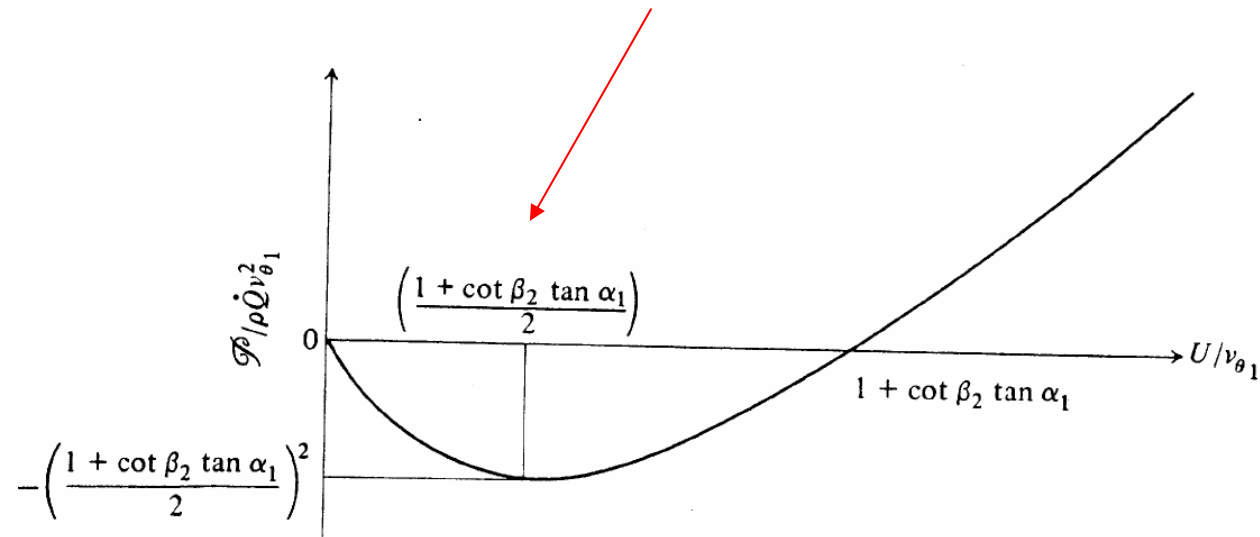
Figure 12.11 Ideal characteristic curve for an axial-flow turbomachine.

Ψ is positive for pumps since they increase the head of the flow, $(\Delta h_t)_{1 \rightarrow 2} > 0$;
 Ψ is negative for turbines since they extract work from the flow and decrease the head, $(\Delta h_t)_{1 \rightarrow 2} < 0$.

$$(\Delta h_t)_{1 \rightarrow 2} = \frac{\mathcal{F}_{\text{shaft}}}{\dot{m}g} = \frac{\Omega}{g} [(rv_\theta)_2 - (rv_\theta)_1]$$

$$(\Delta h_t)_{1 \rightarrow 2} = \frac{U^2}{g} \left[1 - \frac{v_a}{U} (\cot \beta_2 + \cot \alpha_1) \right]$$

→ $\frac{\mathcal{F}}{\rho \dot{Q} v_{\theta 1}^2} = \frac{U}{v_{\theta 1}} \left[\frac{U}{v_{\theta 1}} - (1 + \cot \beta_2 \tan \alpha_1) \right]$ *power coefficient.*



$U/v_{\theta 1} < 1 + \cot \beta_2 \tan \alpha_1$ $\mathcal{F}/\rho \dot{Q} v_{\theta 1}^2 < 0$ turbine operation

$U/v_{\theta 1} > 1 + \cot \beta_2 \tan \alpha_1$ $\mathcal{F}/\rho \dot{Q} v_{\theta 1}^2 > 0$ pump operation

$U/v_{\theta 1} = \frac{1}{2}(1 + \cot \beta_2 \tan \alpha_1)$ $P = P_{\text{max}}$

Bernoulli's equation

$$\rightarrow \frac{p_2 - p_1}{\rho g} + \frac{W_2^2 - W_1^2}{2g} - \frac{U_2^2 - U_1^2}{2g} = 0$$

$$U_1 = U_2$$

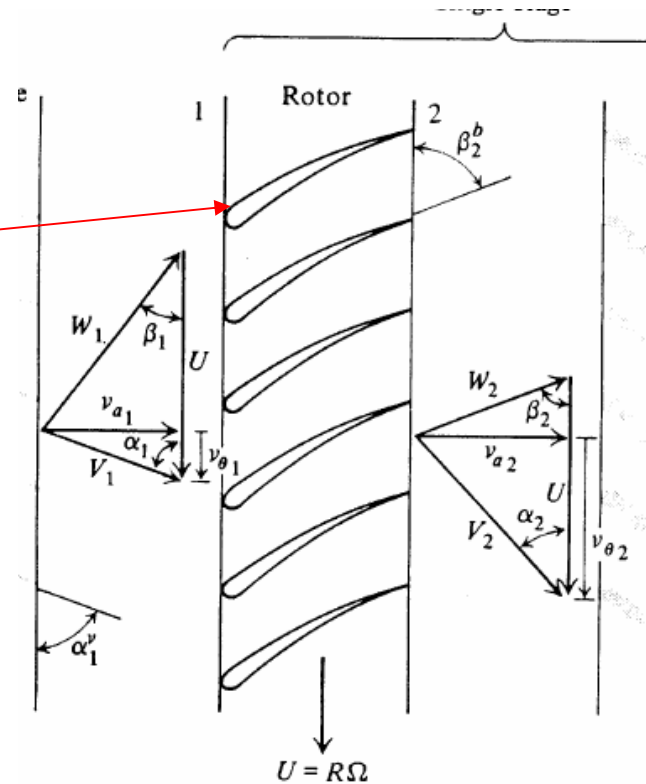
the static pressure change across the rotor

$$\rightarrow p_2 - p_1 = \frac{1}{2}\rho(W_1^2 - W_2^2)$$

because $v_{\theta 2} > v_{\theta 1}$ and $v_{a1} = v_{a2}$

$$W_1 > W_2$$

$$p_2 - p_1 > 0$$



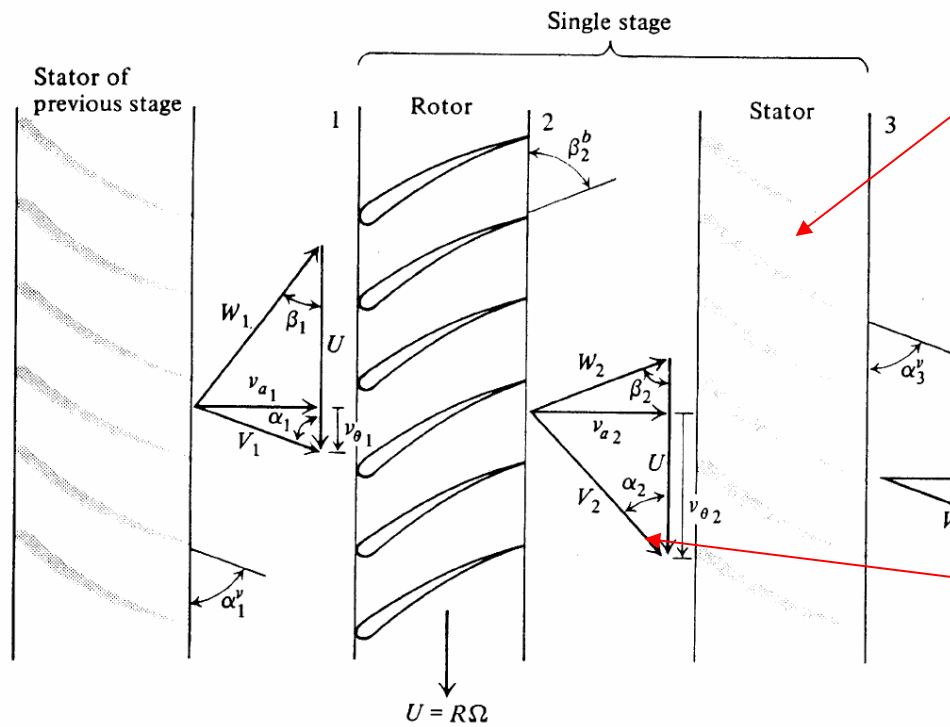


Figure 12.10 Stage velocity triangles.

The stator is stationary, $U = 0$,
no work is done on the flow.

$$\frac{p_1}{\rho g} + \frac{V_1^2}{2g} + \frac{U_2 v_{\theta 2} - U_1 v_{\theta 1}}{g} = \frac{p_2}{\rho g} + \frac{V_2^2}{2g}$$

$$\Rightarrow p_3 - p_2 = \frac{1}{2}\rho(V_2^2 - V_3^2)$$

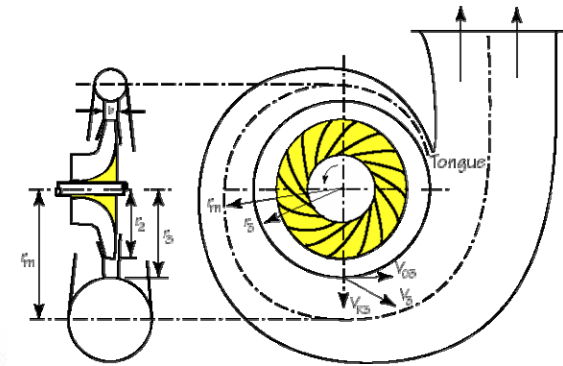
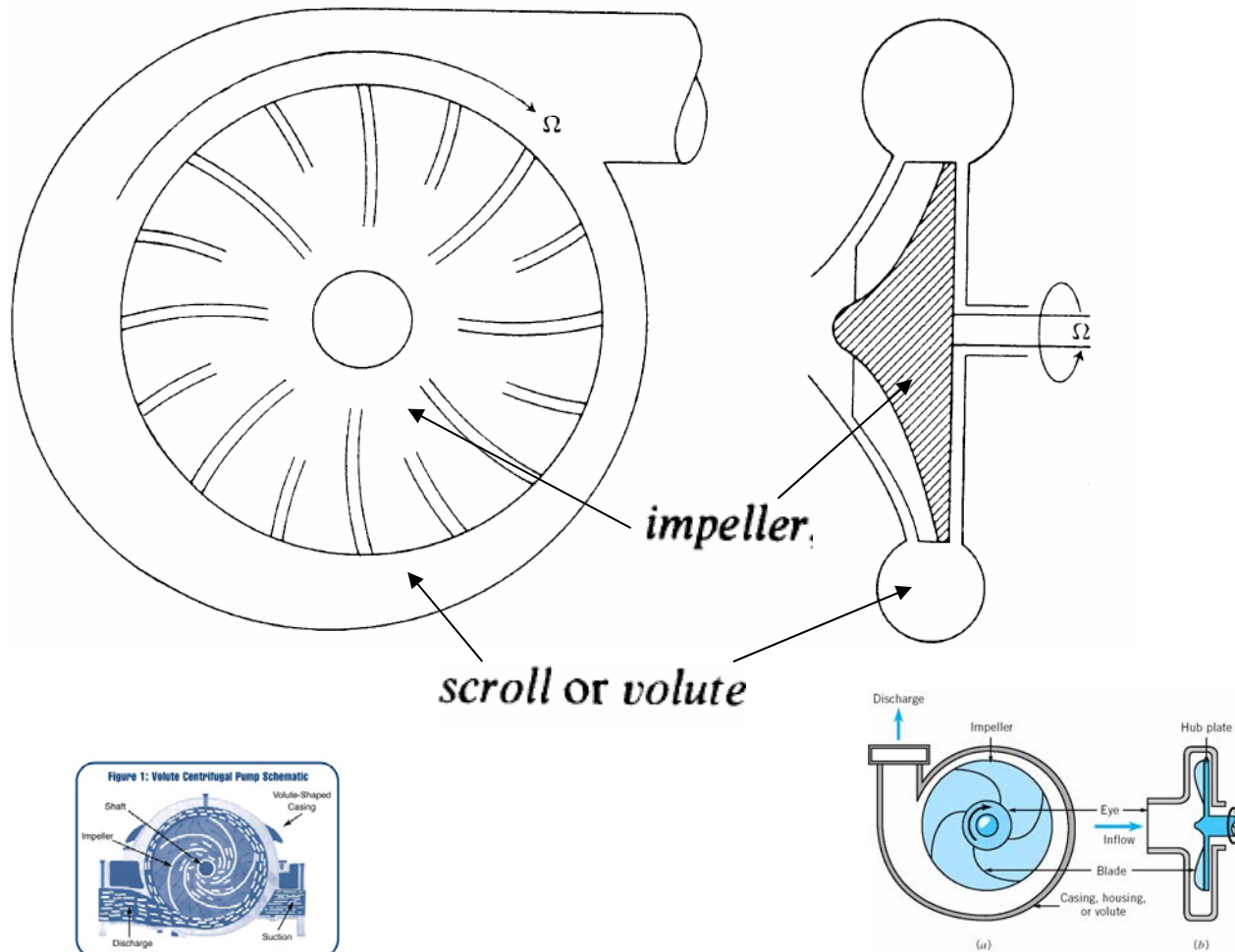
$$V_2 > V_3$$

$$p_3 - p_2 > 0$$

the pressure rises across the stator. The stator acts as a diffuser.

Centrifugal Turbomachines

The flow through a centrifugal turbomachine is primarily in the radial direction, outward for a pump and usually inward for a turbine.



centrifugal pump

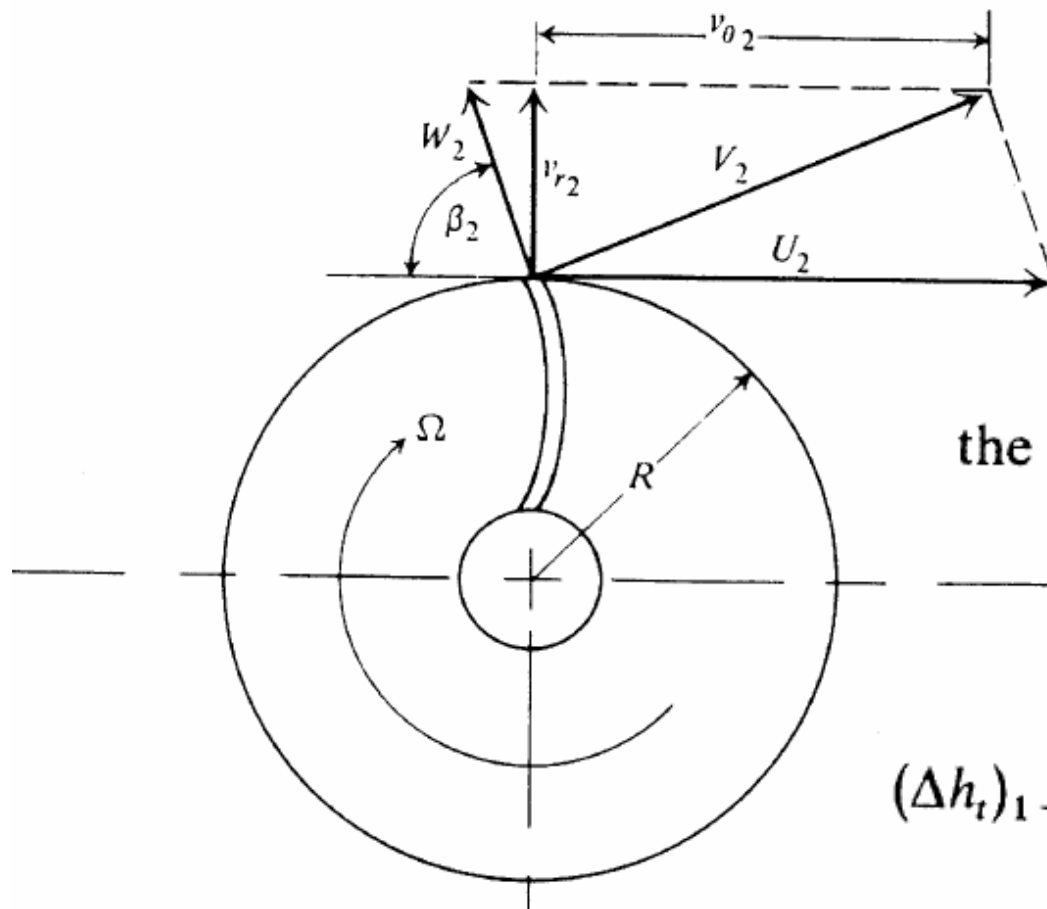


Figure 12.21 Velocity triangle for centrifugal turbomachine.

$$v_{\theta 2} = U_2 - v_{r2} \cot \beta_2$$

$$v_{\theta 1} = 0 \quad V_1 \equiv v_{r1}$$

the head change across the blades is

$$(\Delta h_t)_{1 \rightarrow 2} = \frac{U_2 v_{\theta 2} - U_1 v_{\theta 1}}{g}$$

$$(\Delta h_t)_{1 \rightarrow 2} = \frac{U_2 v_{\theta 2}}{g} = \frac{U_2}{g} (U_2 - v_{r2} \cot \beta_2)$$

the volume flow rate \dot{Q}

$$\dot{Q} = 2\pi R b_2 v_{r2}$$

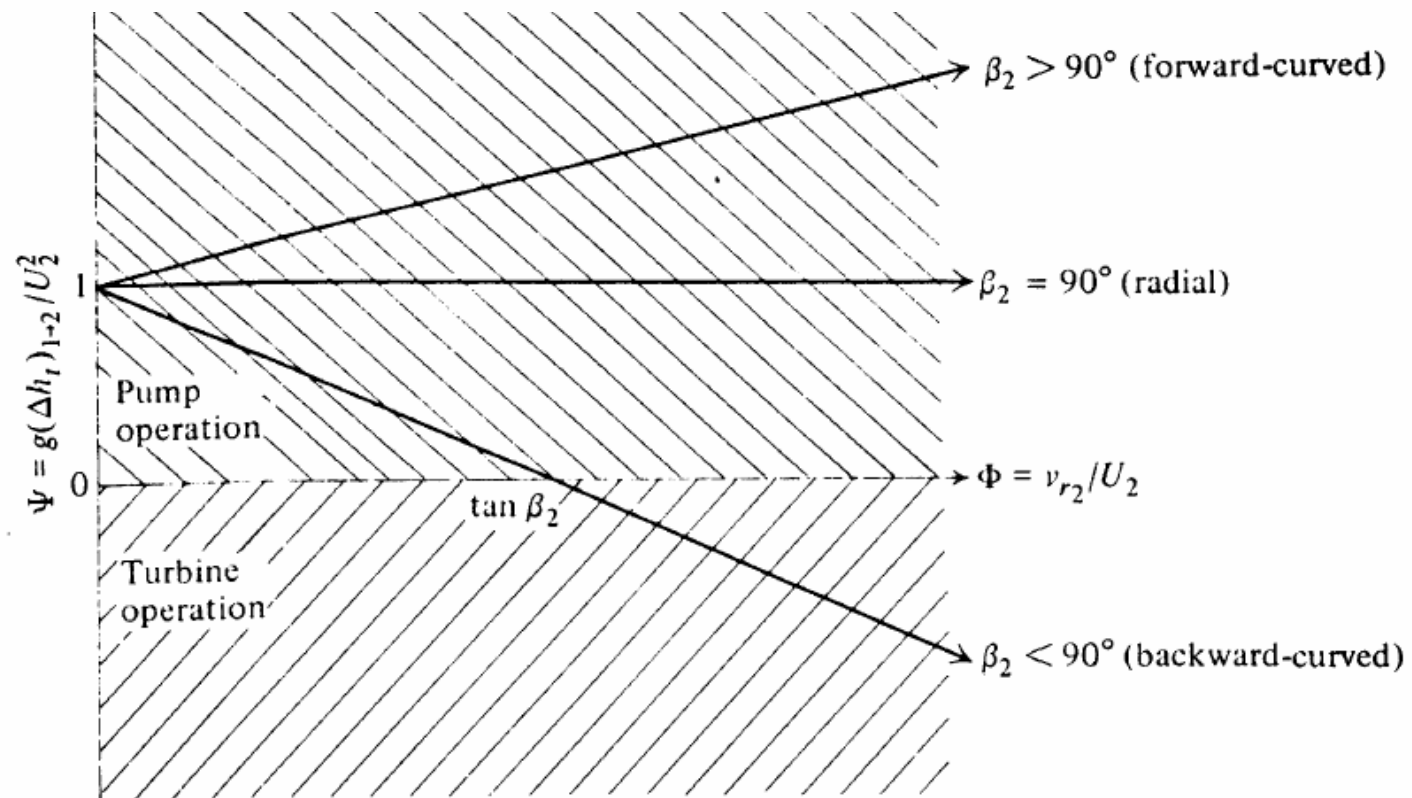
b_2 is the width of the tip of the impeller.

The capacity coefficient for a centrifugal turbomachine is

$$\Phi = \frac{v_{r2}}{U_2} = \frac{\dot{Q}}{2\pi R^2 b_2 \Omega}$$

$$\text{head coefficient } \Psi = g(\Delta h_t)_{1 \rightarrow 2} / U_2^2 = 1 - \Phi \cot \beta_2$$

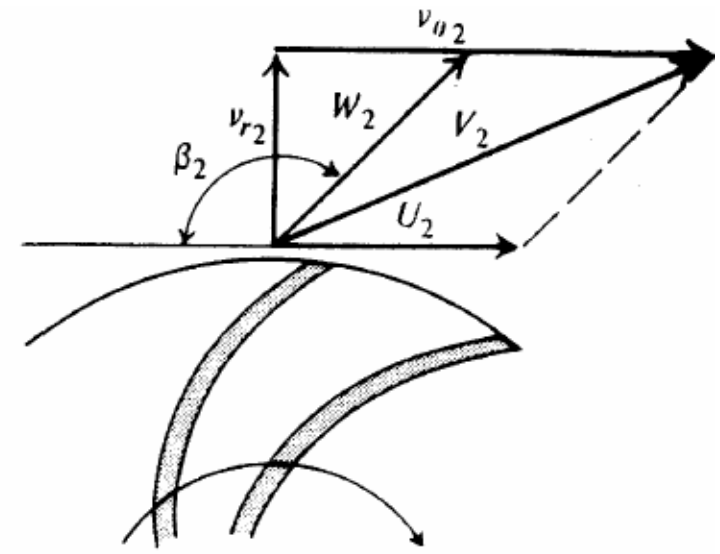
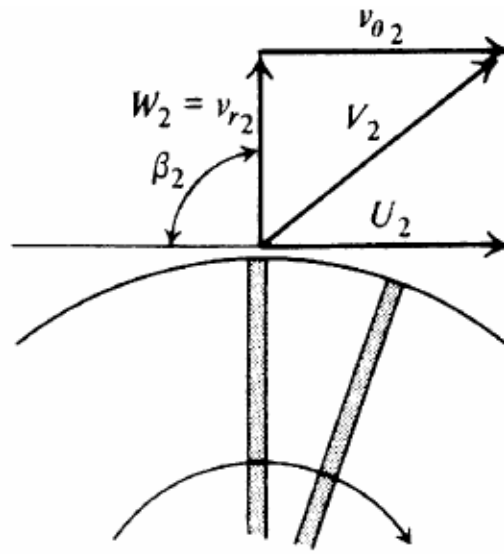
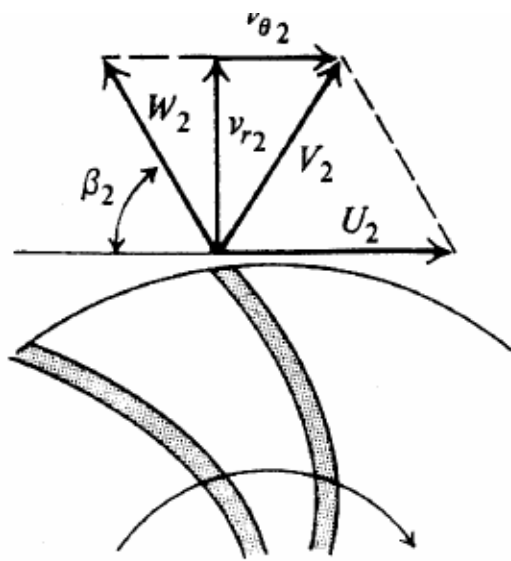
Ideal characteristic curve for centrifugal turbomachine.



$\beta_2 < 90^\circ$

$\beta_2 = 90^\circ$

$\beta_2 > 90^\circ$



(a)

(b)

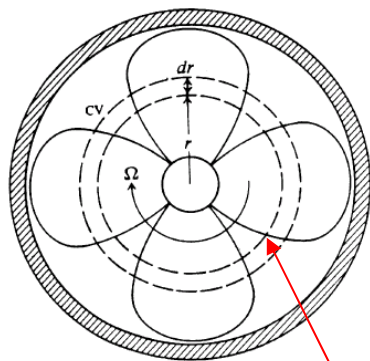
(c)

Figure 12.23 Types of blade-tip curvature: (a) backward-curved blades, $\beta_2 < 90^\circ$; (b) radial blades, $\beta_2 = 90^\circ$; forward-curved blades, $\beta_2 > 90^\circ$.

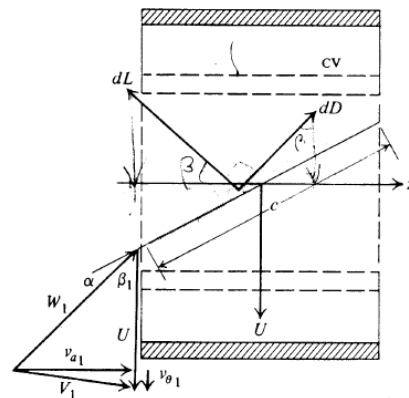
12.3 BLADE-ELEMENT THEORY

Section 12.2 analyzed turbomachinery performance assuming that the flow takes place between infinitesimally spaced and infinitesimally thin blades and vanes.

In this section we consider the opposite limiting case, that of flow over blades so widely spaced that there is negligible interaction between the flows over neighboring blades; each blade acts as an isolated airfoil.



Blade-element control volume.



the lift and drag forces on
Blade-element control volume.

$$dL = C_L \frac{1}{2} \rho W_1^2 c dr$$

$$dD = C_D \frac{1}{2} \rho W_1^2 c dr$$

c is the chord of the airfoil section.

The force of the blade acting on the control volume in the tangential direction is

$$dF_{B/CV_\theta} = dL \sin \beta_1 + dD \cos \beta_1 = (C_L \sin \beta_1 + C_D \cos \beta_1) \frac{1}{2} \rho W_1^2 c dr$$

The force of the blade acting on the control volume in the axial direction

$$dF_{B/CV_z} = dL \cos \beta_1 - dD \sin \beta_1 = (C_L \cos \beta_1 - C_D \sin \beta_1) \frac{1}{2} \rho W_1^2 c dr$$

The total head and static-pressure change across the blades

Pump: the total head increases with the tangential force and the static pressure ($p_2 - p_1$) rises with the axial force.

By momentum equation to the control volume in the axial or Z direction

$$n dF_{B/CV_z} + (p_1 - p_2)2\pi r dr = \cancel{dm}(v_{a_2} - v_{a_1}) \quad v_{a_1} = v_{a_2}$$

● **static-pressure change across the blades**

$$\begin{aligned} \rightarrow p_2 - p_1 &\equiv (\Delta p)_{1 \rightarrow 2} = \frac{n dF_{B/CV_z}}{2\pi r dr} \\ &= \frac{1}{2}\rho W_1^2 \frac{nc}{2\pi r} (C_L \cos \beta_1 - C_D \sin \beta_1) \end{aligned}$$

$$\rightarrow \left(\frac{\Delta p}{\rho g} \right)_{1 \rightarrow 2} = \frac{W_1^2}{2g} \frac{nc}{2\pi r} C_L \cos \beta_1 \left(1 - \frac{\tan \beta_1}{C_L/C_D} \right)$$

The quantity $nc/2\pi r$, called the solidity, is a measure of the pitch or spacing of the blades.

- The total head change across the blades

The torque acting on the control volume is

$$d\mathcal{T}_{\text{shaft}} = rn dF_{\text{B/CV}_\theta} = (C_L \sin \beta_1 + C_D \cos \beta_1) \frac{1}{2} \rho W_1^2 n c r dr$$

The total head change across the blades is then

$$(\Delta h_t)_{1 \rightarrow 2} = \frac{\Omega d\mathcal{T}_{\text{shaft}}}{g \dot{m}} = \frac{W_1^2}{2g} \frac{U}{v_a} \frac{nc}{2\pi r} C_L \sin \beta_1 \left(1 + \frac{\cot \beta_1}{C_L/C_D} \right)$$

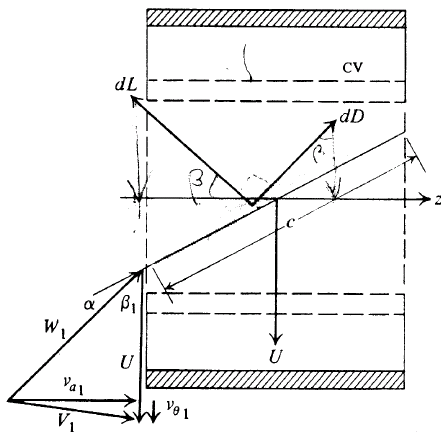
$$\dot{m} = \rho 2\pi r dr v_a$$

$$\tau\Omega = \dot{W} h = \gamma \dot{Q} h = \rho g \dot{Q} h$$

No inlet guide vanes and the flow comes axially onto the blade with $v_\theta = 0$ and

$$U_1 = W_1 \cos \beta_1, \quad V_a = W_1 \sin \beta_1$$

The static-pressure rise across the blades



$$\left(\frac{\Delta p}{\rho g} \right)_{1 \rightarrow 2} = \frac{W_1^2}{2g} \frac{nc}{2\pi r} C_L \cos \beta_1 \left(1 - \frac{\tan \beta_1}{C_L/C_D} \right)$$

$$= \frac{U^2}{2g} \frac{nc}{2\pi r \cos \beta_1} C_L \left(1 - \frac{\tan \beta_1}{C_L/C_D} \right)$$

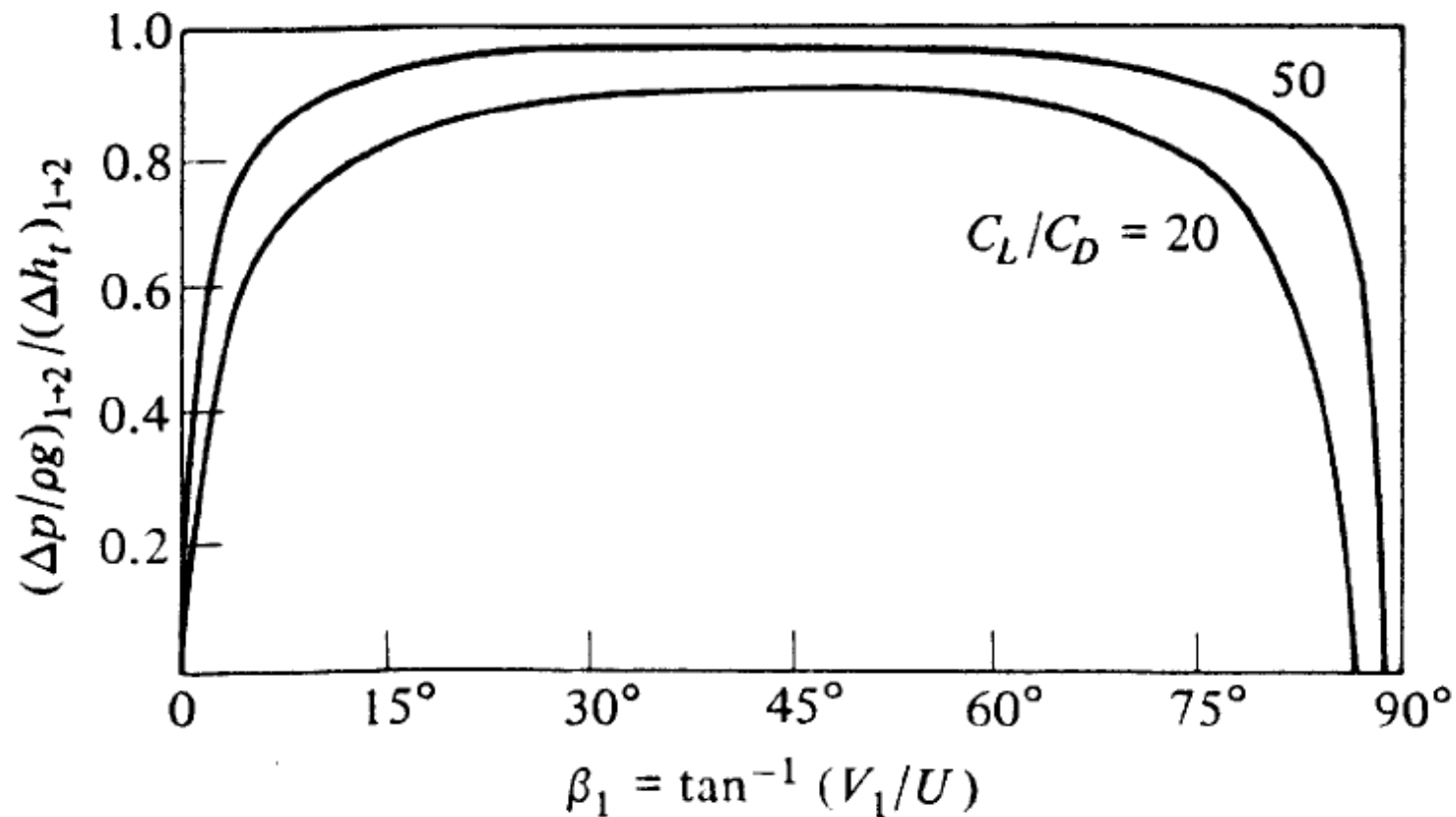
the total head change

$$(\Delta h_t)_{1 \rightarrow 2} = \frac{W_1^2}{2g} \frac{U}{v_a} \frac{nc}{2\pi r} C_L \sin \beta_1 \left(1 + \frac{\cot \beta_1}{C_L/C_D} \right)$$

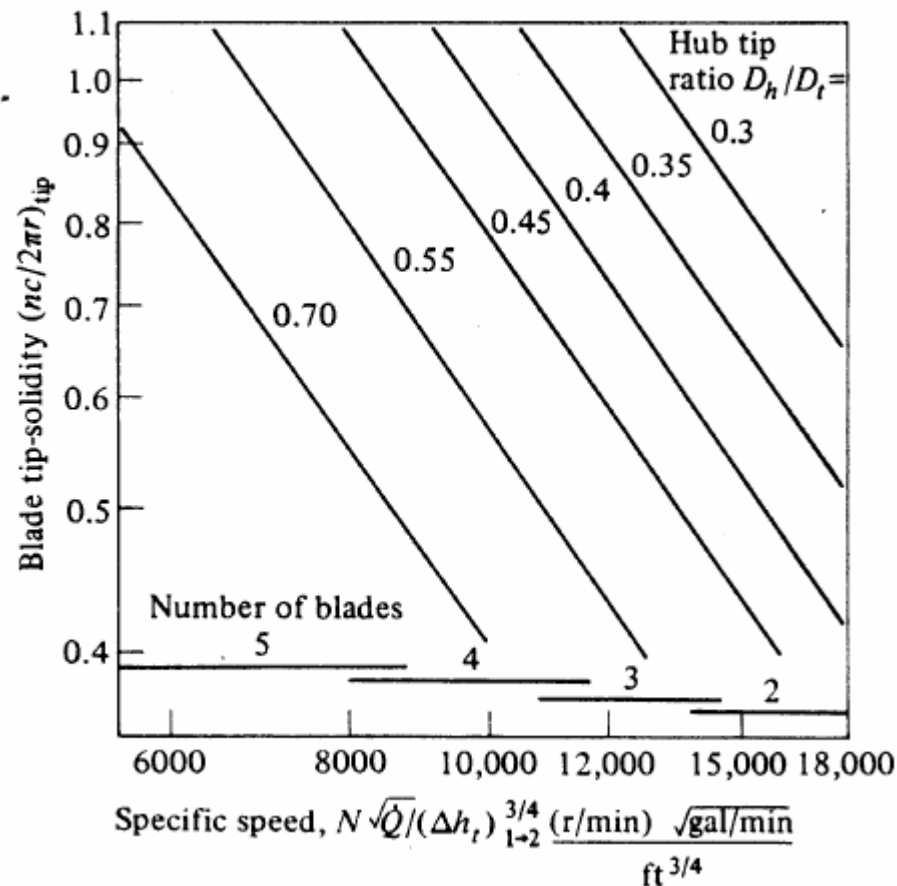
$$= \frac{U^2}{2g} \frac{nc}{2\pi r \cos \beta_1} C_L \left(1 + \frac{\cot \beta_1}{C_L/C_D} \right)$$

The local degree of reaction, which is the ratio of the static-pressure rise to the total head increase at some radial location.

$$R = \frac{(\Delta p / \rho g)_{1 \rightarrow 2}}{(\Delta h_t)_{1 \rightarrow 2}} = \frac{1 - (\tan \beta_1) / (C_L / C_D)}{1 + (\cot \beta_1) / (C_L / C_D)}$$



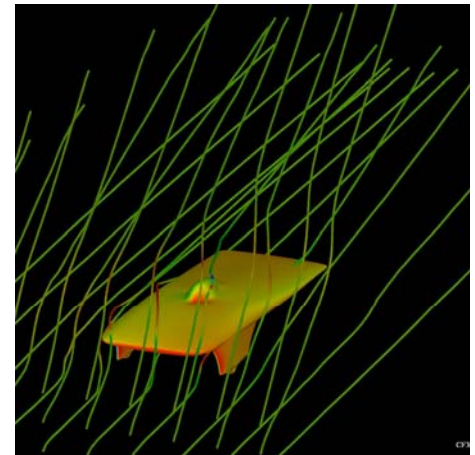
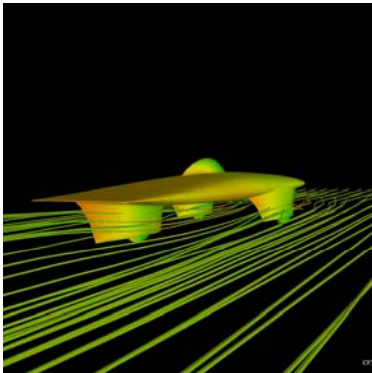
The solidity can be visualized as a measure of the cross-sectional area blockage caused by the blades. Increased solidity increases the interference between adjacent blades and causes the assumption of isolated airfoil flow to break down. Figure 12.27 shows that the same solidity can be obtained for different numbers of blades. Experimental testing has shown that maximum efficiency is usually obtained at a solidity of 0.4 to 0.5. For mechanical-strength considerations, the solidity at the hub is usually 1.25 to 1.30 times the solidity at the blade tip.



Chapter 2

Introduction of CFD

計算流體力學 簡介



高等流體機械設計

=流體機械(Turbomachinery)設計

+CAD(Computer-Aided Design and Drafting)

+CFD(Computational Fluid Dynamics)

+CAM(Computer-Aided Manufacture)

1.1 What is CFD (Computational Fluid Dynamics)

☛ 計算流體力學(Computational Fluid Dynamics)是藉由電腦來模擬流體運動過程的一門學問，其內容主要是流體力學、熱傳學、數學、數值方法及電腦科技等的整合。

☛ 應用範圍也非常廣，航太、汽車、船舶、土木、機械、化工、醫工、電子、材料、大氣與海洋等均涵蓋在內，例如飛機與汽車之外形設計，各類引擎燃燒室及冷凍空調系統設計，流體機械、空氣及水污染物擴散預測，建築結構物如超高大樓、隧道及橋樑等受風及水流的影響，心臟與血管內的血流流動，高速火車進出隧道的噪音題等，都可利用計算流體力學來研究與解決這些問題。

☛ 由於流體運動本身具**三維性**、**時變性**與**非線性**等特質，因此其物理現象非常複雜。早期的流體力學研究主要是借助於**理論分析**與**實驗**，然而傳統的理論分析方法由於**有許多假設與簡化**，所以其能解決的問題通常**有限**。

☛ 近年來，隨著**電腦計算速度與記憶容量**不斷地**增進**，計算流體力學所能解決問題的尺度與複雜度也逐漸加大，時至今日，**計算流體力學**已成為學界研究流體力學的主要利器之一，與**理論流力**和**實驗流力**構成現代研究流體力學之**三大主流**。此一分析工具除了適於**探討參數變化的影響**外，因其而建立的分析資料庫，**更可以減少實驗所需的工時而縮短設計時程**。

☛ 計算流體力學的發展大約**始於1950年代**（或更早些），剛開始是由航太工業、汽車工業領軍，再帶動所有與流體力學有關的其他行業而蓬勃發展。現今歐美各國政府機關，如國家實驗室及一些特殊任務導向機關，每年均投入十分龐大之人力與物力在計算流體力學的研究，許多著名大學及大企業（如飛機、汽車等重工業）本身也都擁有「計算流體力學研究中心」。同時，歐美的民間工程顧問公司對於計算流體力學之研發也有許多貢獻，開發了不少有用的套裝軟體，如CFX、UNIC、CFD2000、FIDAP、FLUENT等，都被工業界廣泛地使用。

1.2 How does a CFD code work?

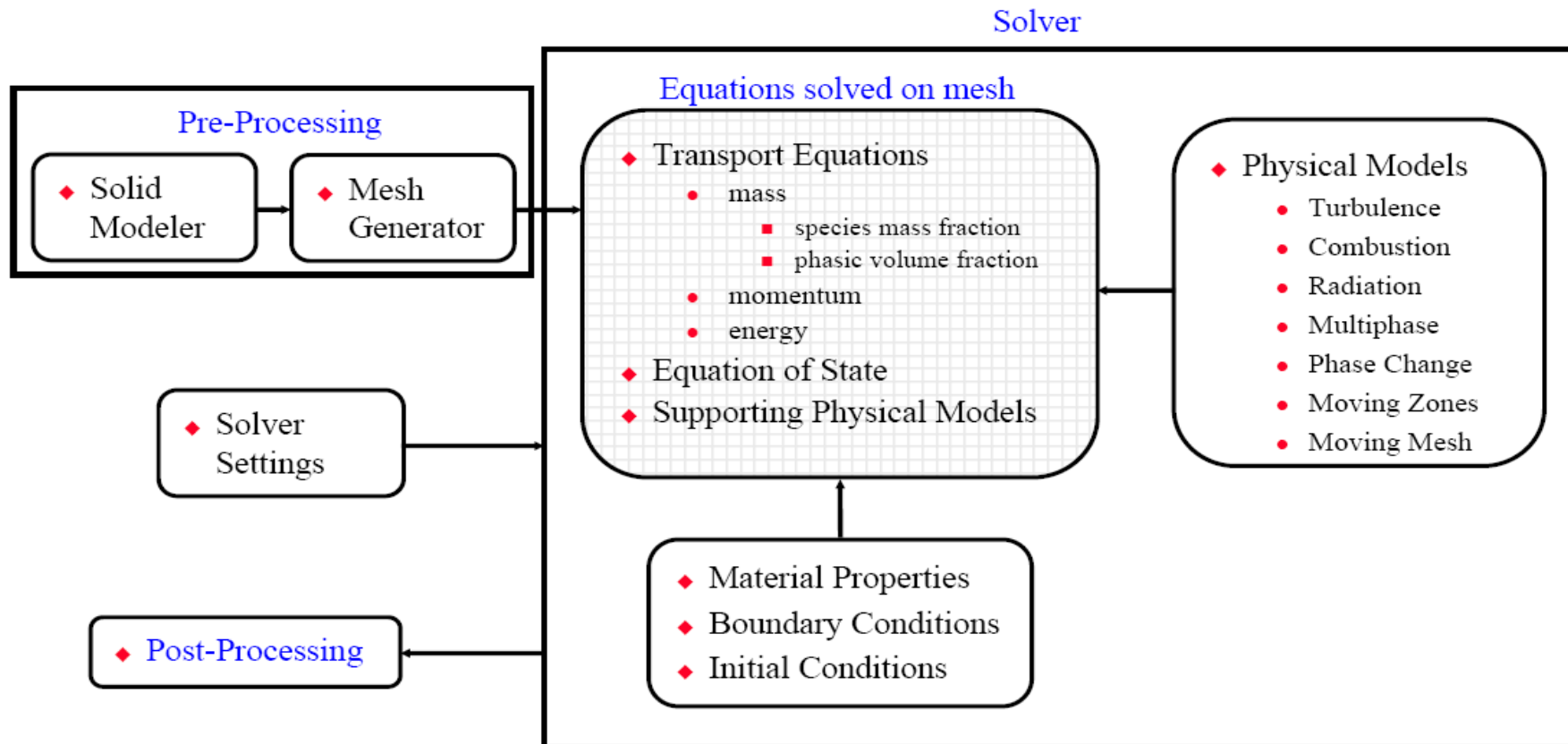
A CFD code contains three main elements:

(1) Pre-processor(前處理)-autocad

(2) Solver(求解器)

(3) Post-processor(後處理)

CFD Modeling Overview



(1) Pre-processor(前處理)

The activities at the pre-processing stage involve:

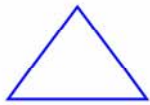
- Definition of the geometry of the region of interest: the computational domain.
- Grid generation—the sub-division of the domain into a number of smaller, non-overlapping sub-domains: a *grid* (or *mesh*) of *cells* (or *control volumes* or *elements*).
- Selection of the physical and chemical phenomena that need to be modelled.
- Definition of fluid properties.
- Specification of appropriate boundary conditions at cells which coincide with or touch the domain boundary.

可壓縮及不可壓縮流場、層流與擾流問題、暫態與穩態、化學變化、多相流問題、Bubble 問題、熱傳、幅射、moving grid。(Chapter 2 and 3)

Design and Create the Grid

◆ Problem Identification and Pre-Processing

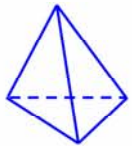
1. Define your modeling goals.
2. Identify the domain you will model.
3. Design and create the grid.



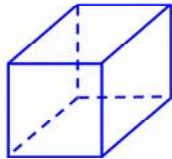
triangle



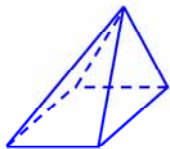
quadrilateral



tetrahedron



hexahedron



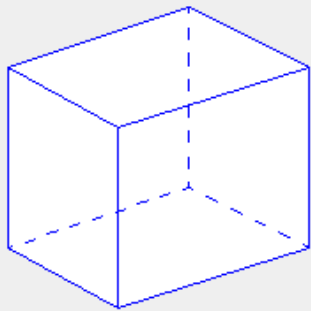
pyramid



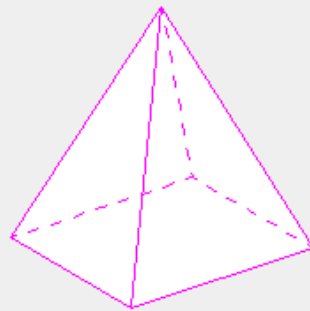
prism/wedge

- ◆ Can you benefit from Mixsim, Icepak, or Airpak?
- ◆ Can you use a quad/hex grid or should you use a tri/tet grid or hybrid grid?
 - How complex is the geometry and flow?
 - Will you need a non-conformal interface?
- ◆ What degree of grid resolution is required in each region of the domain?
 - Is the resolution sufficient for the geometry?
 - Can you predict regions with high gradients?
 - Will you use adaption to add resolution?
- ◆ Do you have sufficient computer memory?
 - How many cells are required?
 - How many models will be used?

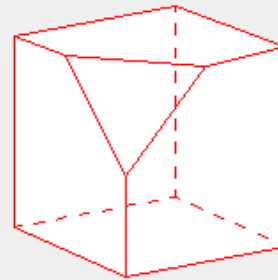
※ Finite Volume method !



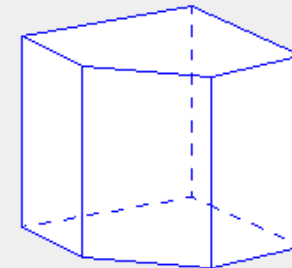
Hexahedral



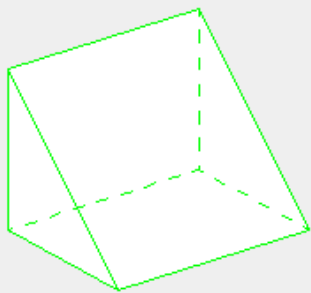
Pyramid



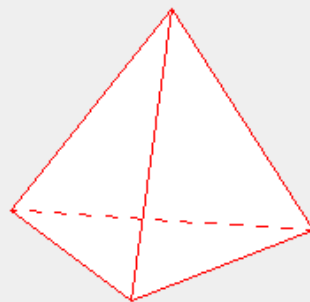
Corner Cut Polyhedral #1



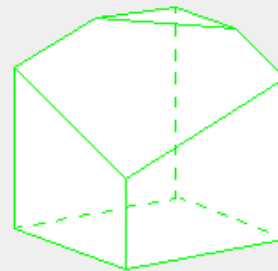
Edge Cut Polyhedral



Prismatic



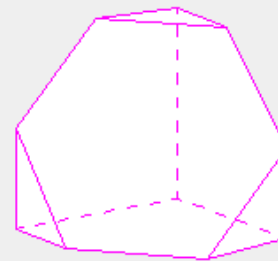
Tetrahedral



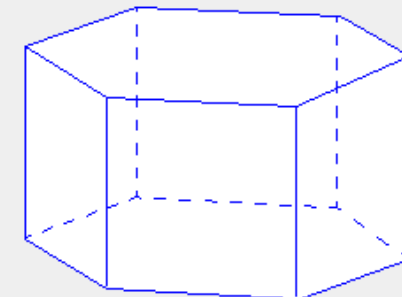
Corner Cut Polyhedral #2



Off Cut to Polyhedral #2



Corner Cut Polyhedral #3



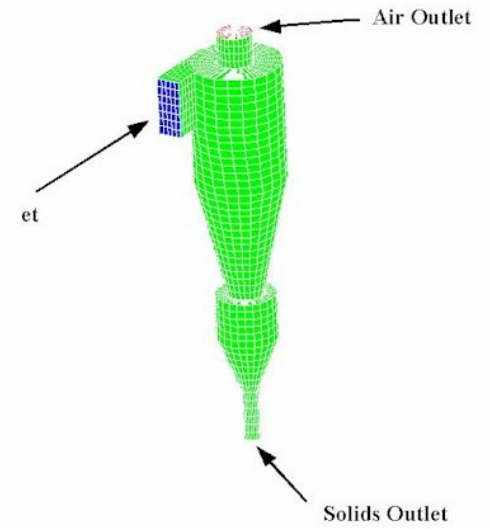
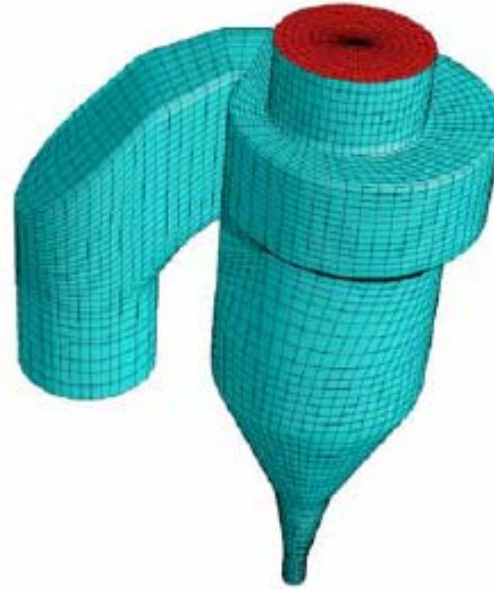
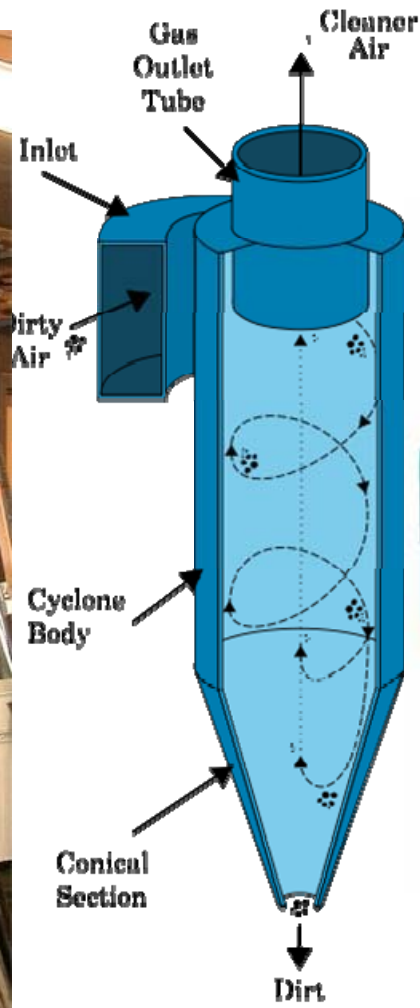
Multi-Edge Cut Polyhedral

Traditional CFD Cell Shapes

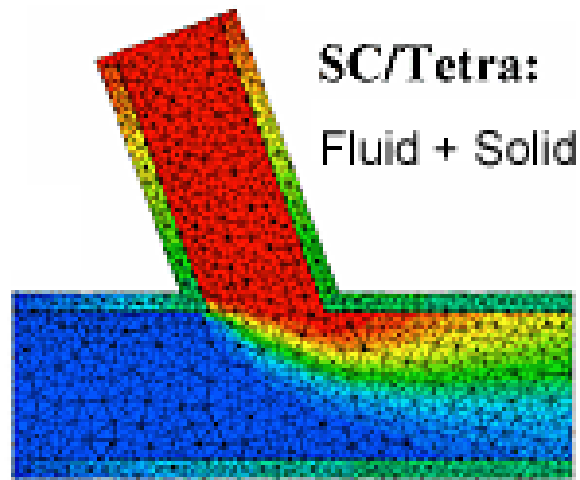
Hexa Based Polyhedral CFD Cells



Example: Cyclone Separator



Example of Volume Mapping



-
-
-
-

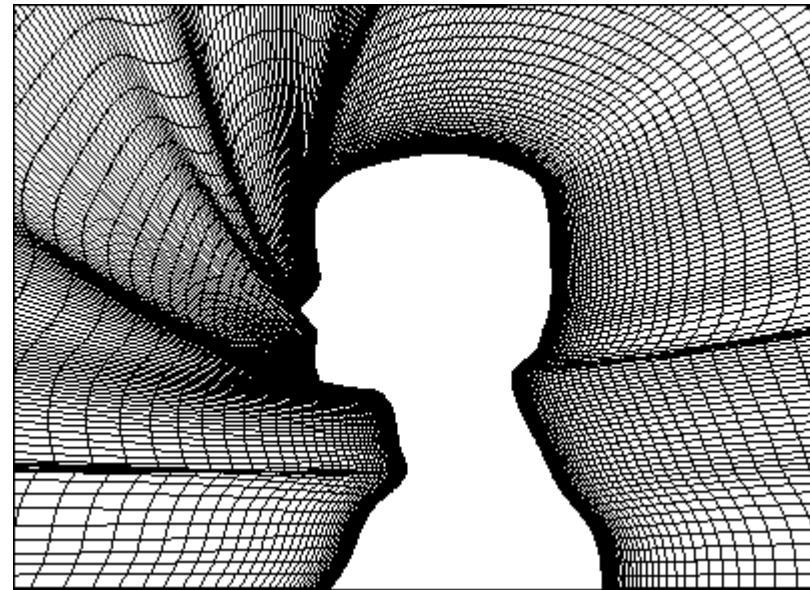
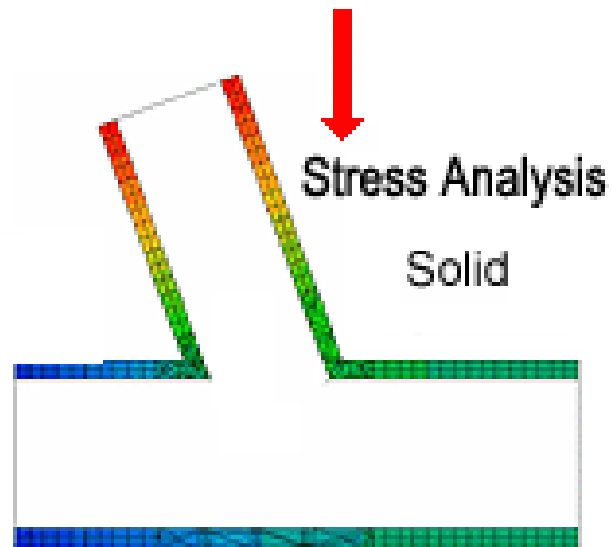


Figure 1: Transfinite grid (2-D) around a human head

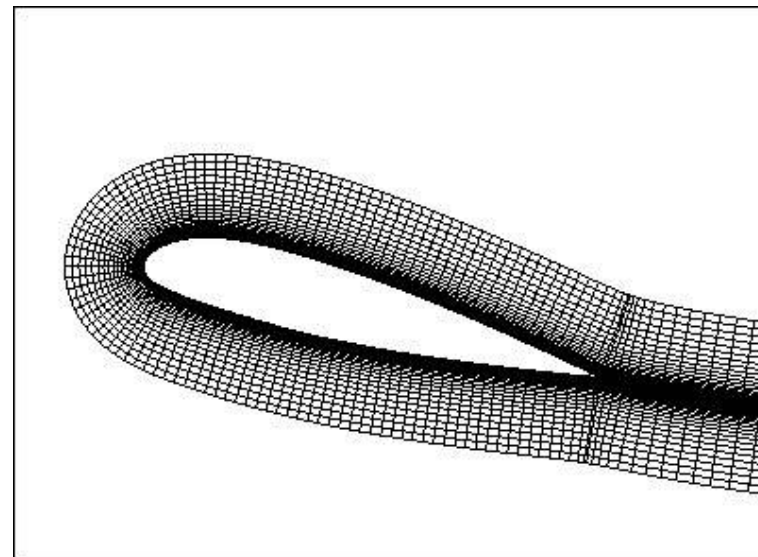


Figure 2 Airfoil grid (hyperbolic)

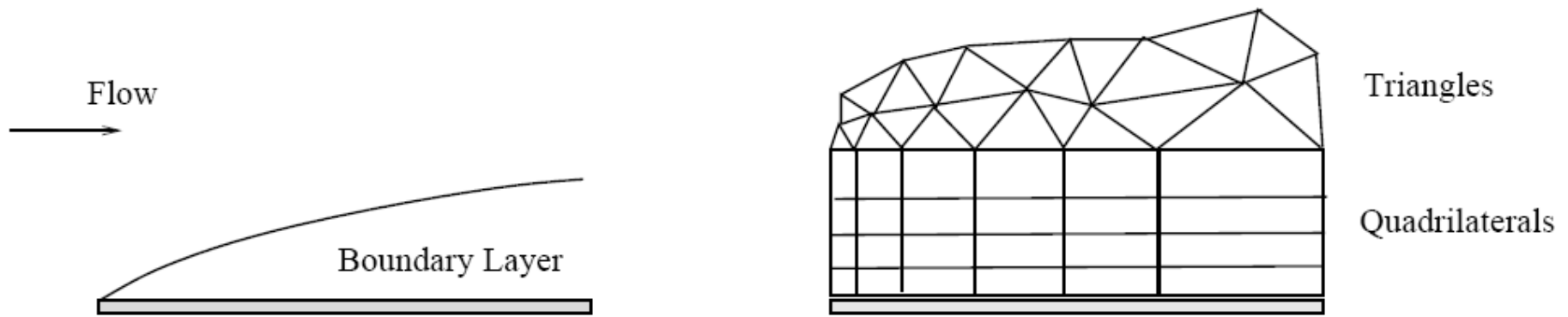
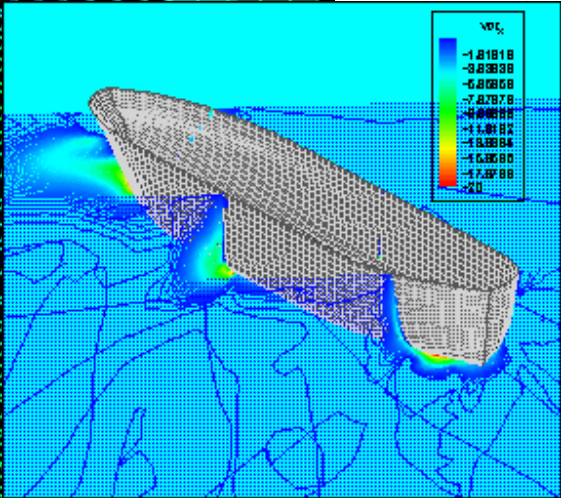
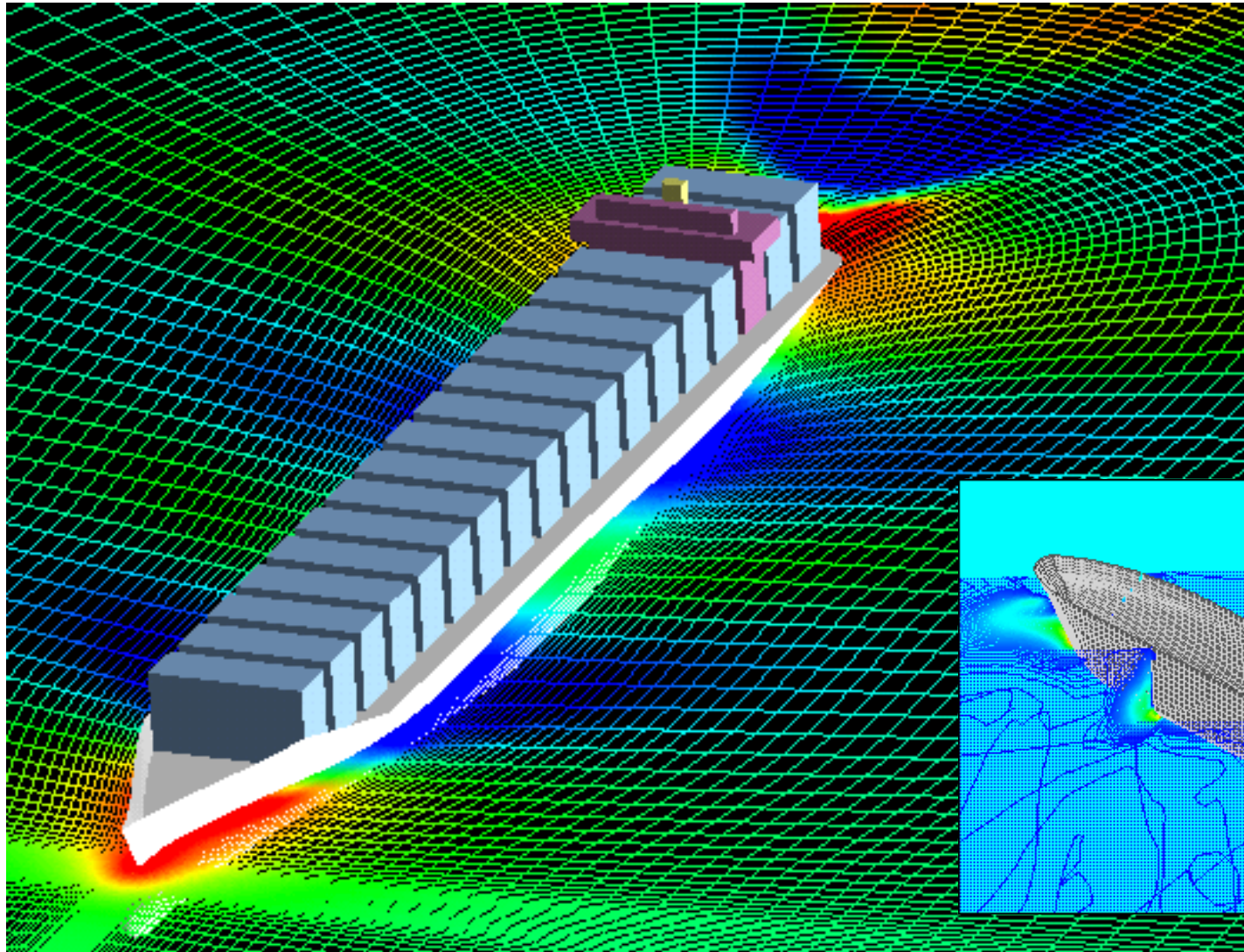
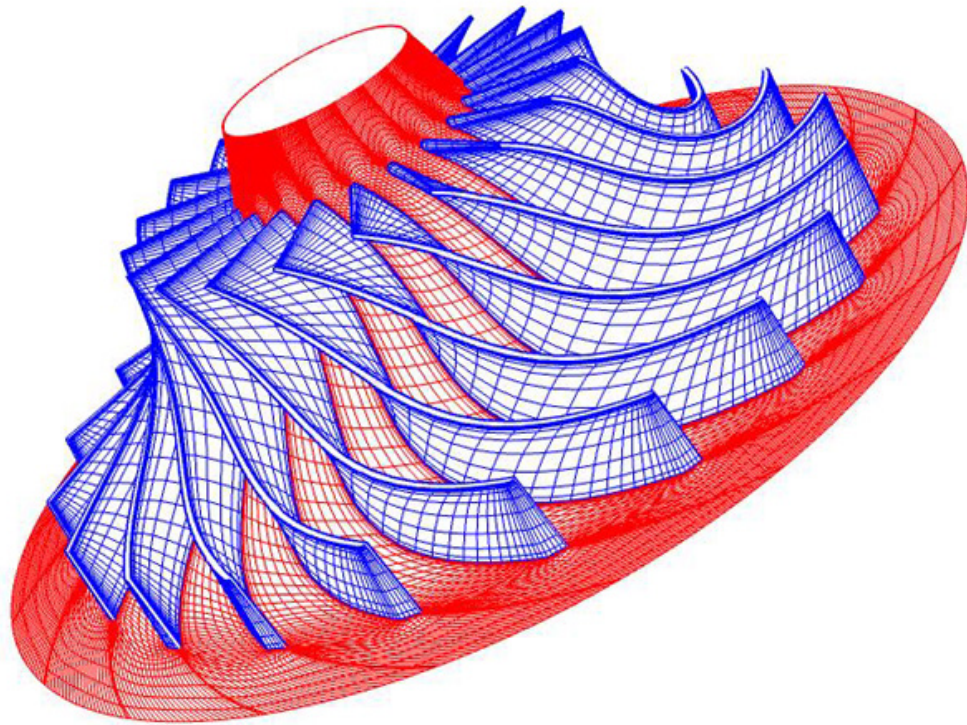
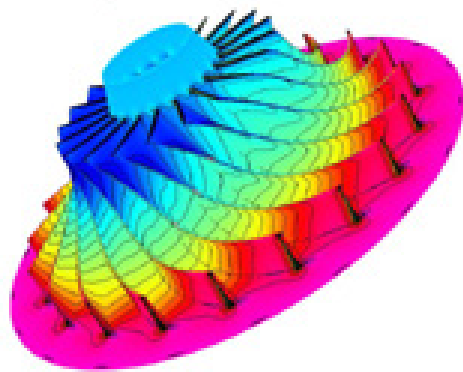


Figure 2.9: Hybrid Mesh in Boundary Layer

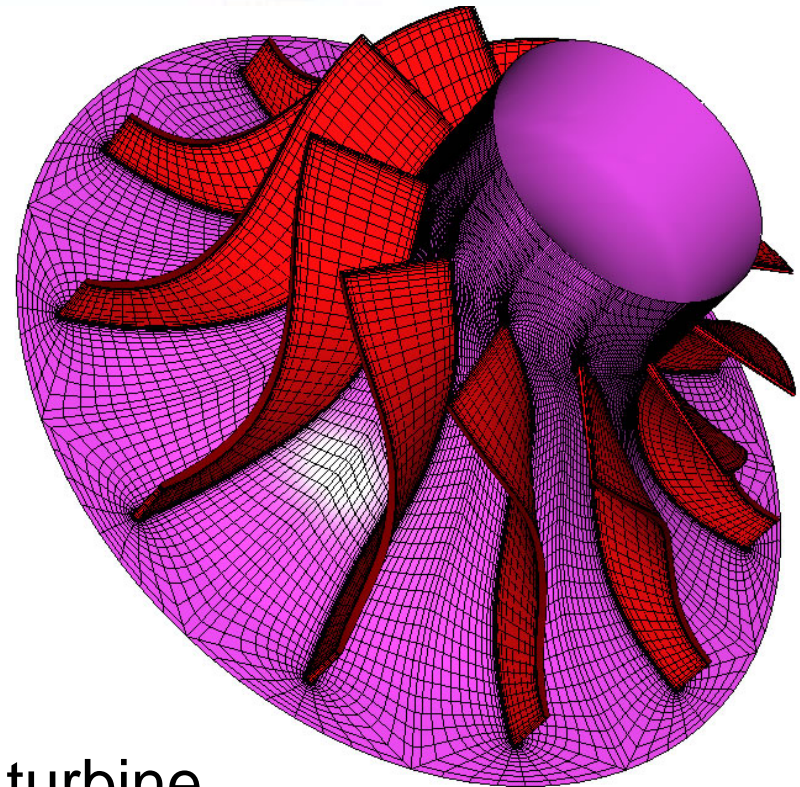




centrifugal impeller

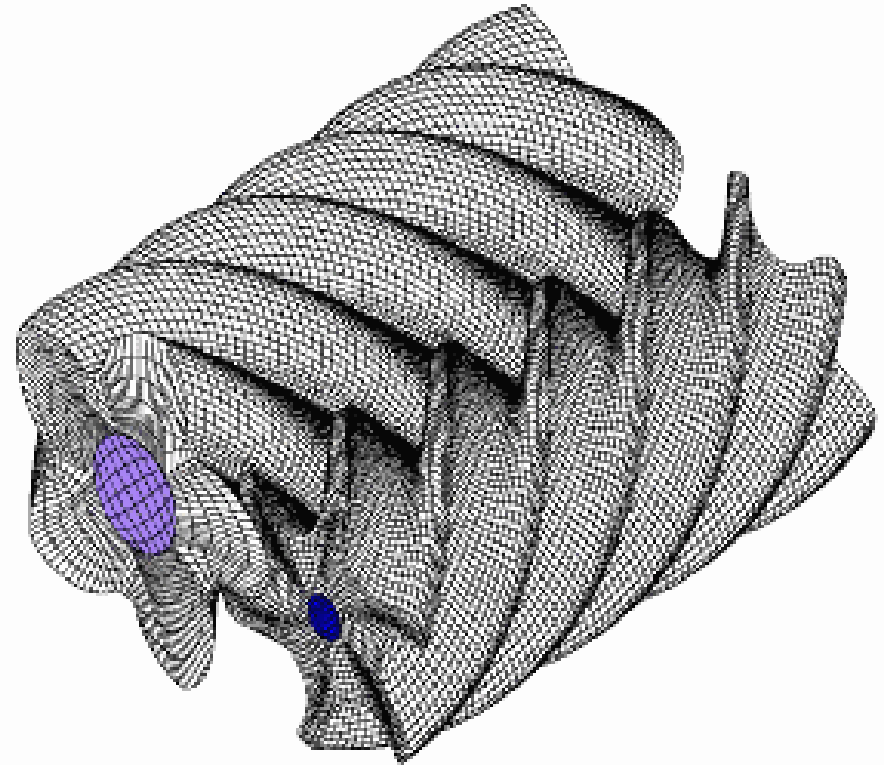
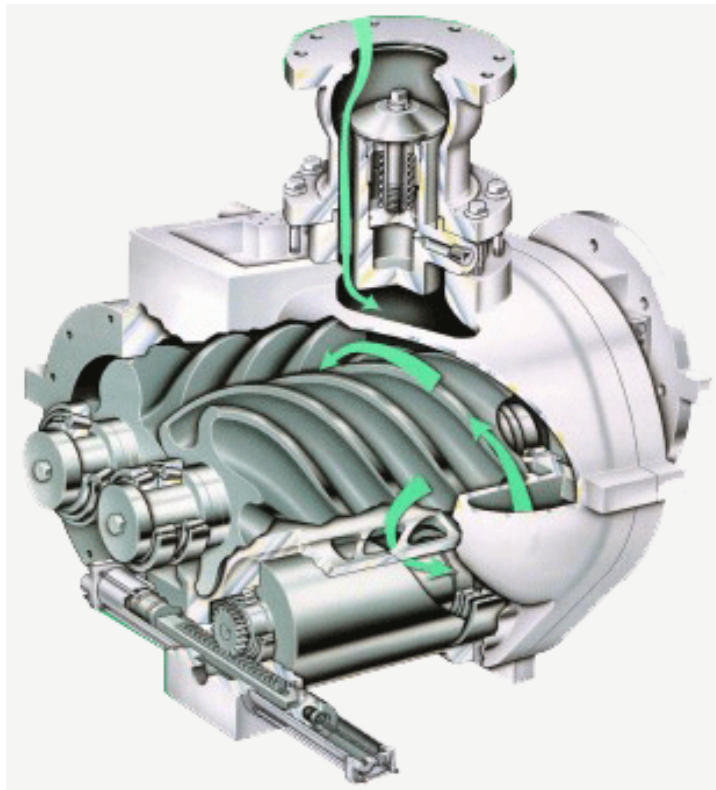


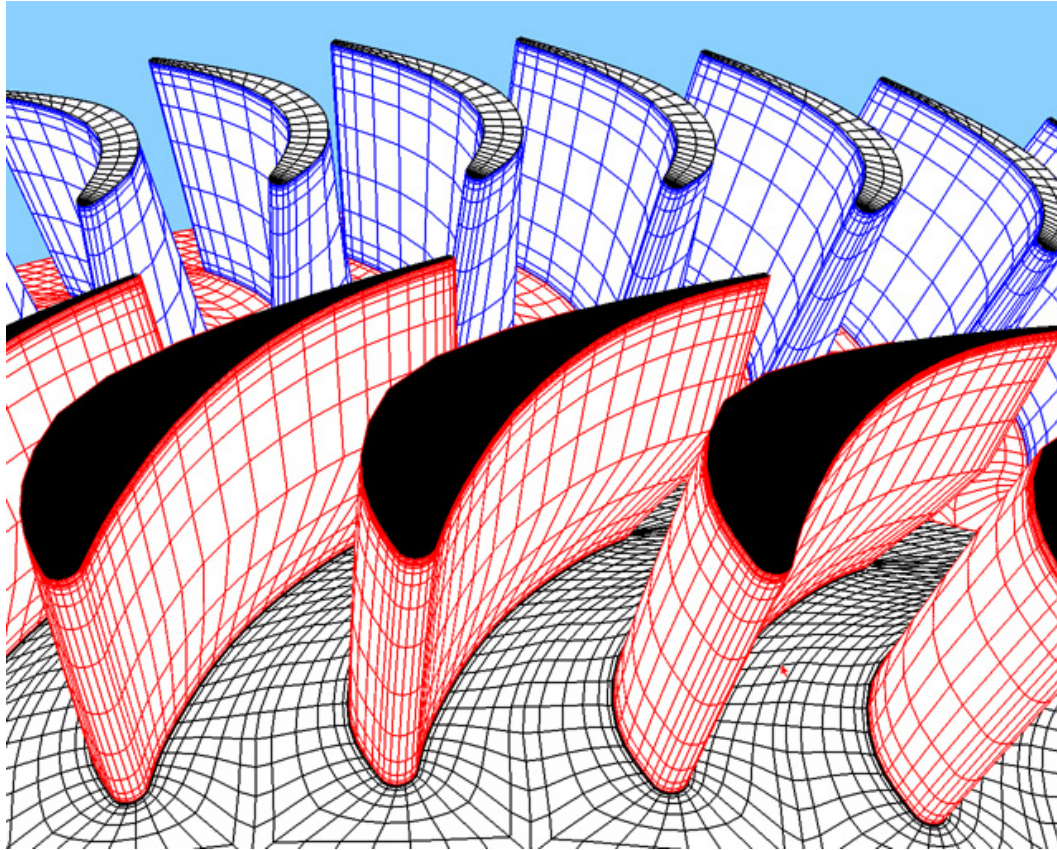
Impellor of centrifugal compressor



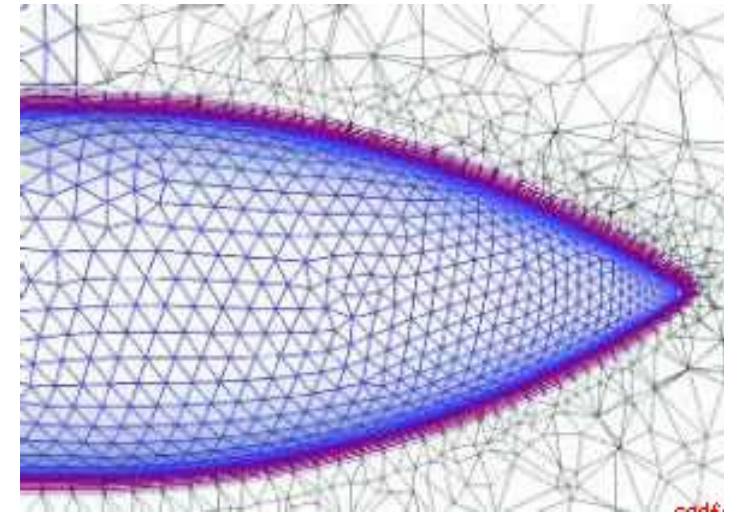
radial turbine

Screw compressor





Multiblock grid, SSME fuel turbine 1st stage



A rigid, viscous mesh attached to the store surface is used to model the boundary layer.

(2) Solver(求解器)

There are three distinct streams of numerical solution techniques:

- Finite difference method
- Finite element method
- Spectral method

The basis of the solver perform the following step:

- Approximation of the unknown flow variables by means of simple functions.
- Discretisation by substitution of the approximations into the governing flow equations and subsequent mathematical manipulations.
- Solution of the algebraic equations.

i. e.

(a) P. D. E. (partial differential equation) ➡ F. D. E (finite difference equation)

(b) To find the all the FDE's of grid points inside the computational domain

(c) To find the solutions of the algebraic equations.

Set Up the Numerical Model

- ◆ Solver Execution
 - 4. Set up the numerical model.
 - 5. Compute and monitor the solution.

Solving initially in 2D will provide valuable experience with the models and solver settings for your problem in a short amount of time.

- ◆ For a given problem, you will need to:
 - Select appropriate physical models.
 - Turbulence, combustion, multiphase, etc.
 - Define material properties.
 - Fluid
 - Solid
 - Mixture
 - Prescribe operating conditions.
 - Prescribe boundary conditions at all boundary zones.
 - Provide an initial solution.
 - Set up solver controls.
 - Set up convergence monitors.

The finite volume method--a special finite difference formulation

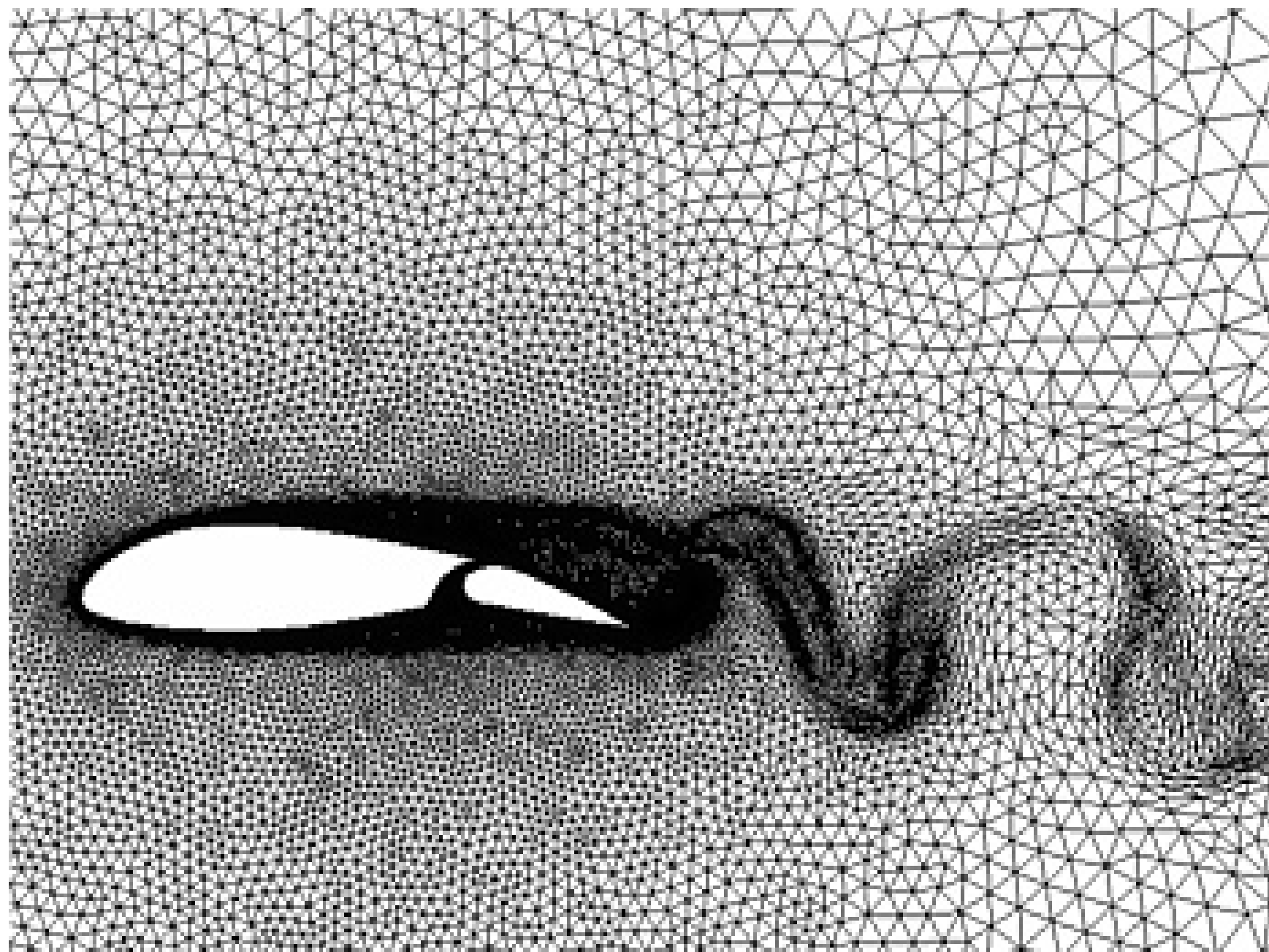
The numerical algorithm consists of the following steps:

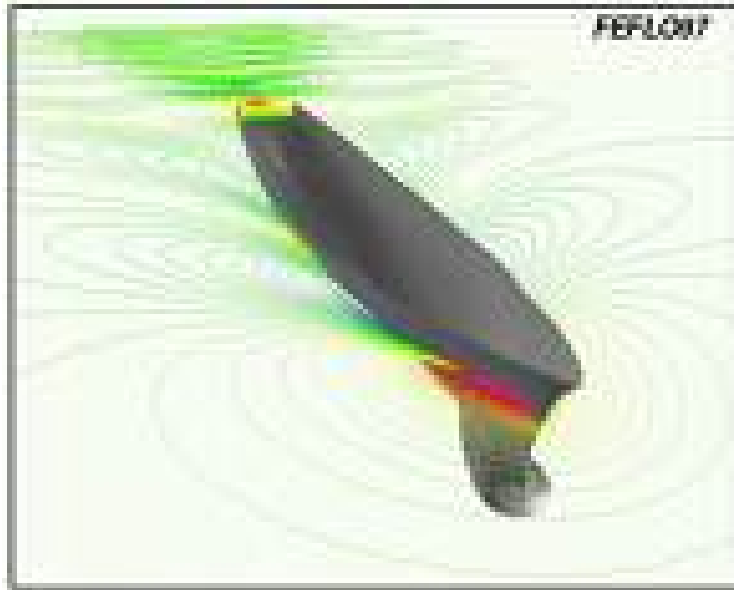
- Formal integration of the governing equations of fluid flow over all the (finite) control volumes of the solution domain.
- Discretisation involves the substitution of a variety of finite-difference-type approximations for the terms in the integrated equation representing flow processes such as convection, diffusion and sources. This converts the integral equations into a system of algebraic equations.
- Solution of the algebraic equations by an iterative method.

(3) Post-processor (後處理)

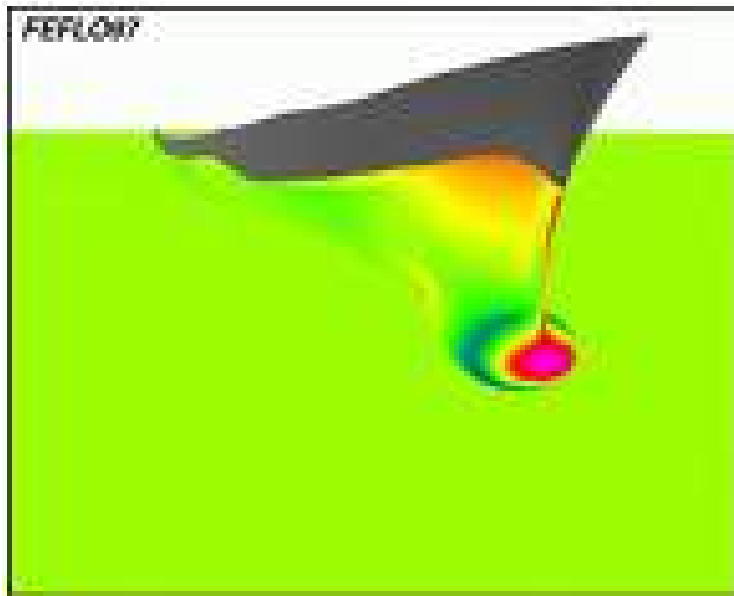
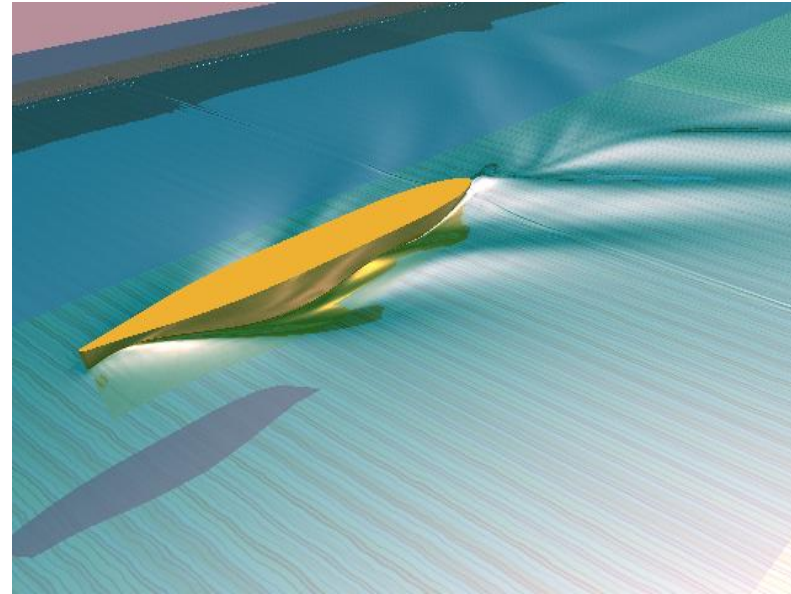
- Domain geometry and grid display
- Vector plots
- Line and shaded contour plots
- 2D and 3D surface plots
- Particle tracking
- View manipulation (translation, rotation, scaling etc.)
- Colour postscript output

More recently these facilities may also include animation for dynamic result display and in addition to graphics all codes produce trustworthy alphanumeric output and have data export facilities for further manipulation external to the code.

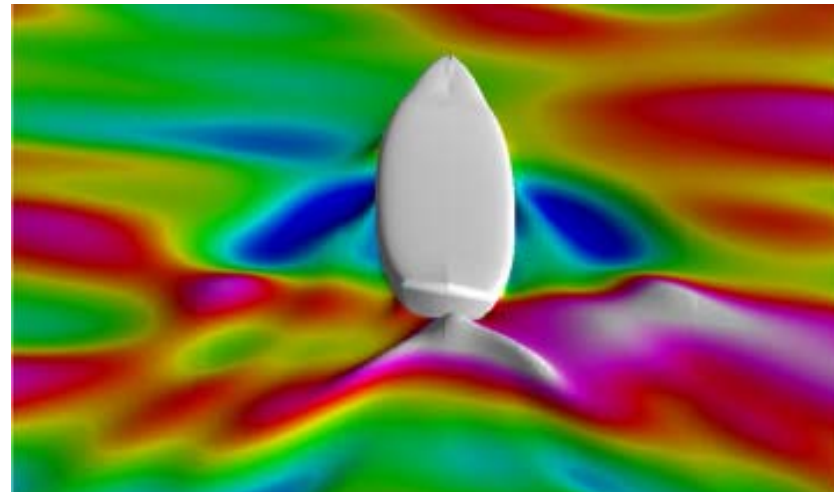


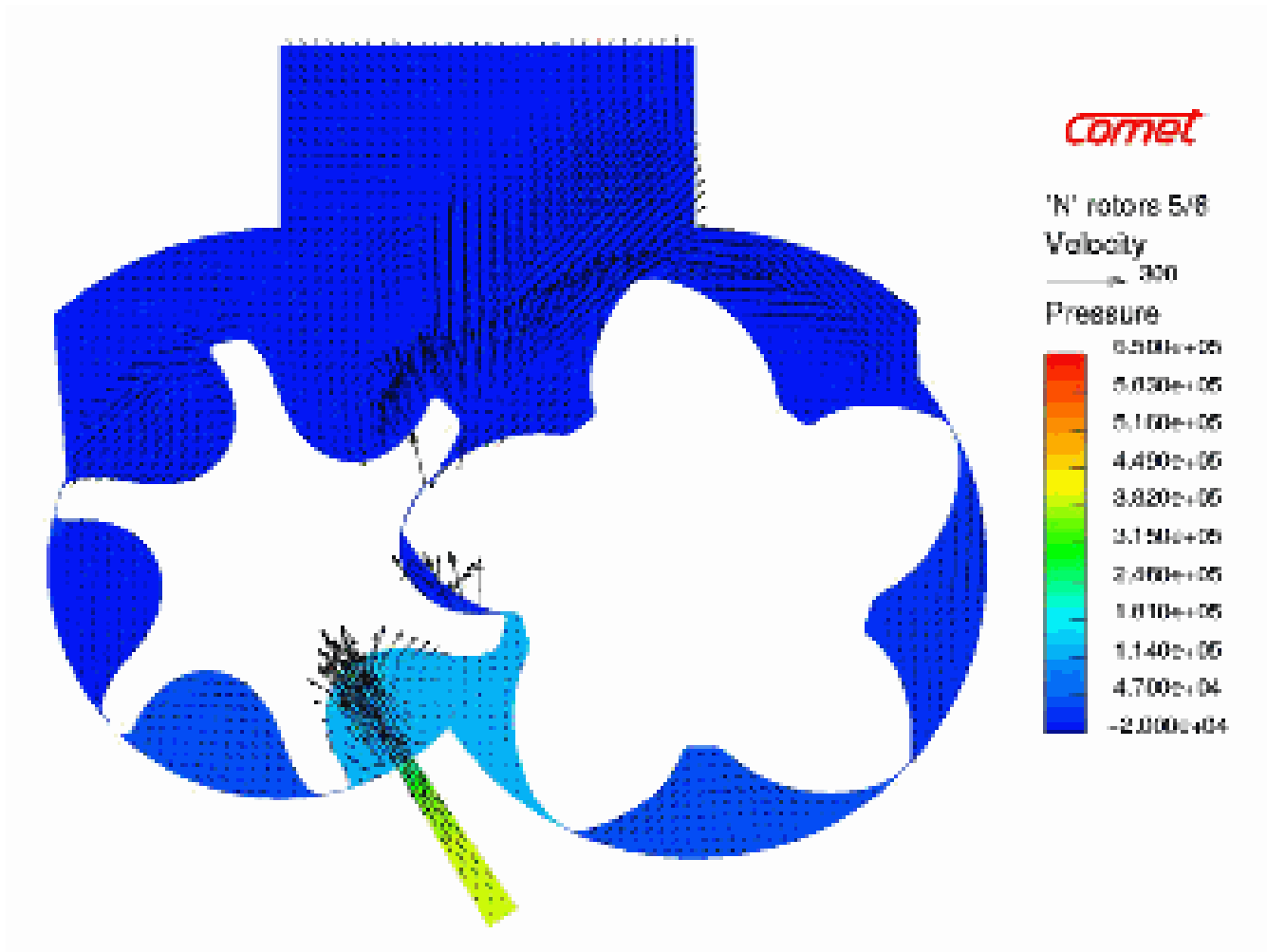


Free Surface Height

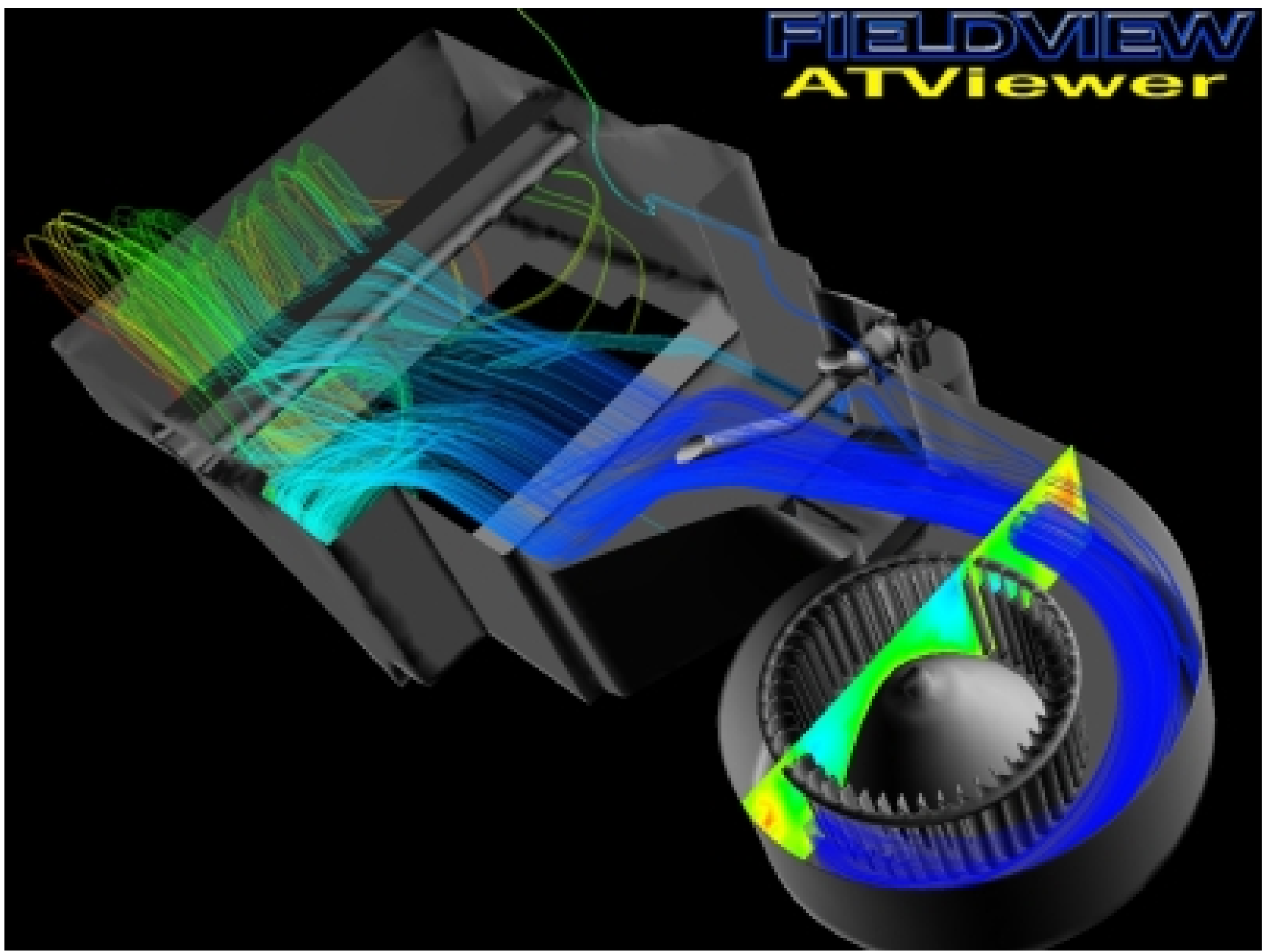


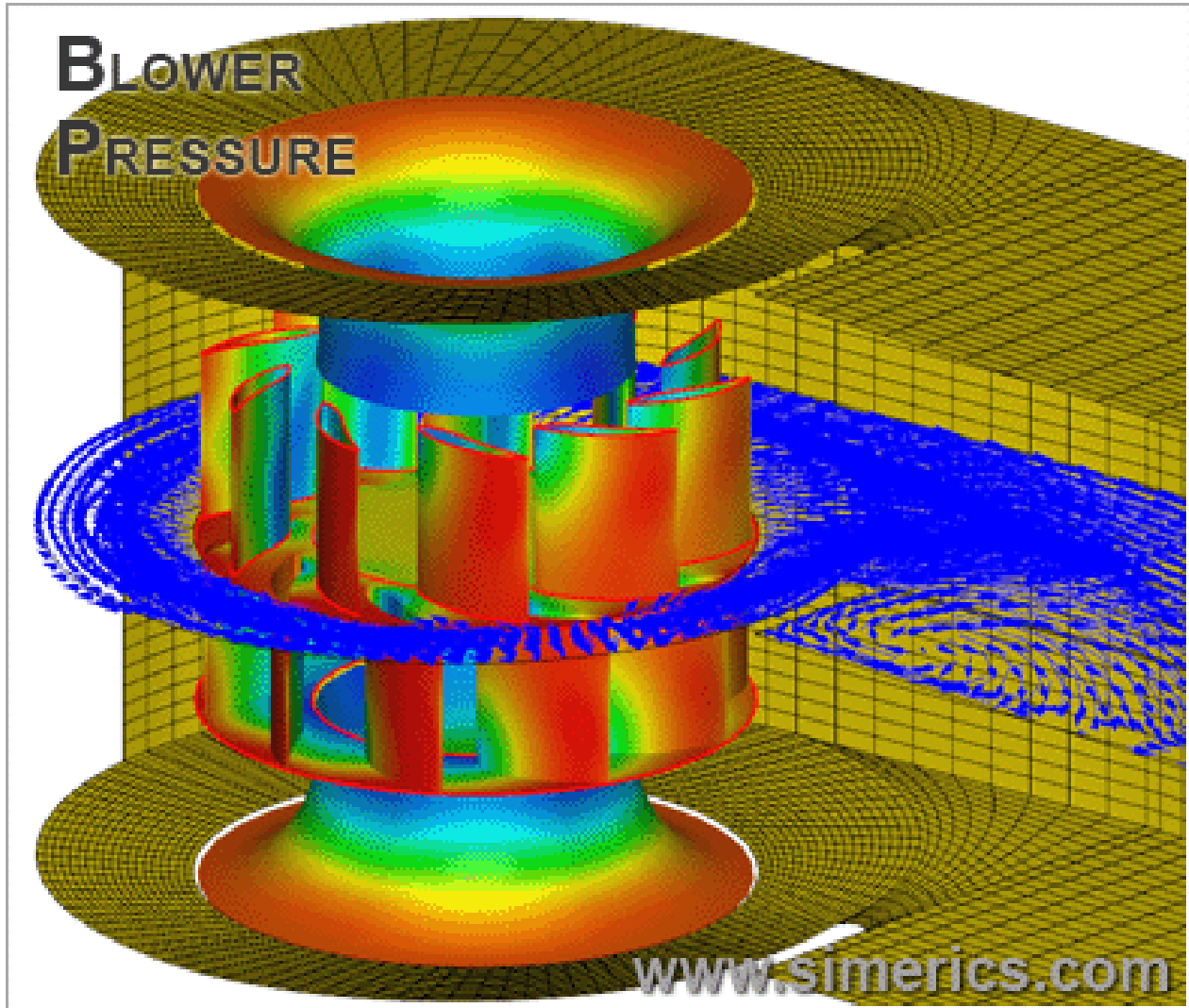
Surface Pressure

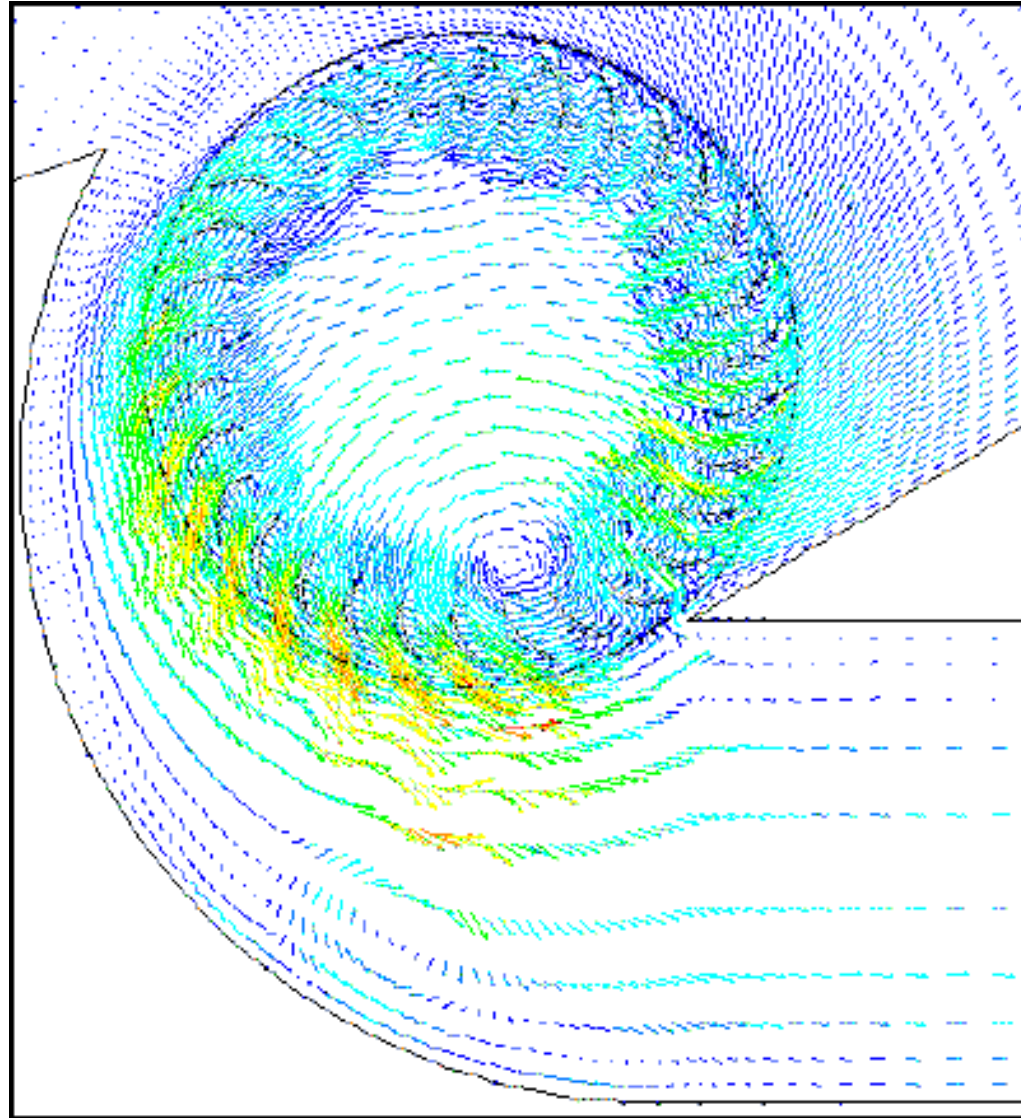




FIELDVIEW ATViewer







Consider Revisions to the Model

- ◆ Post-Processing

- 6. Examine the results.

- 7. Consider revisions to the model.

- ◆ Are physical models appropriate?

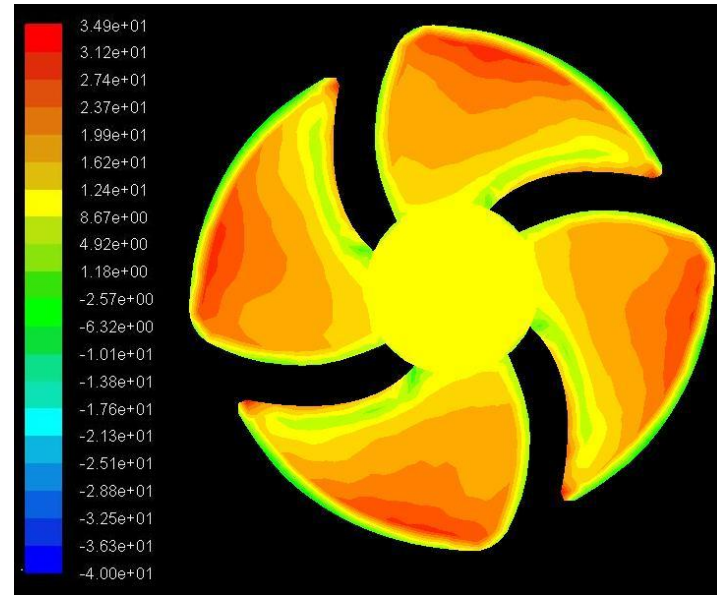
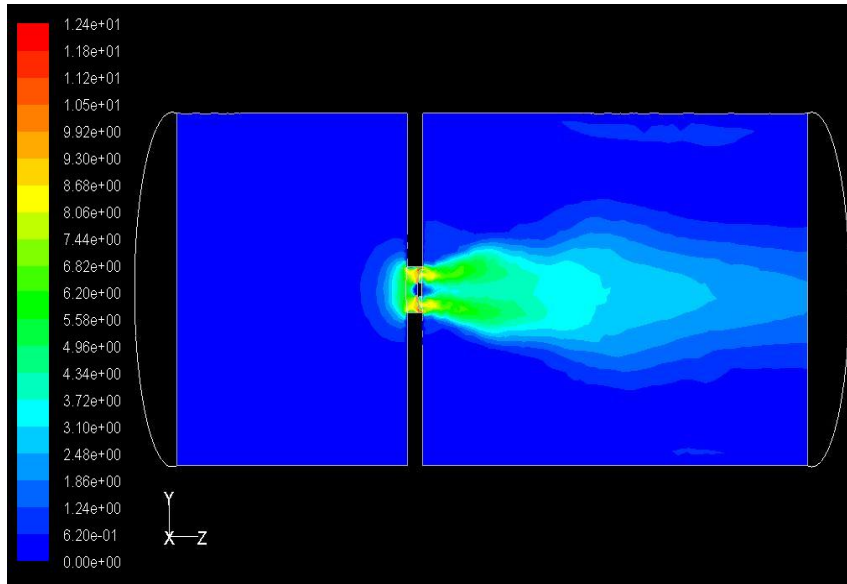
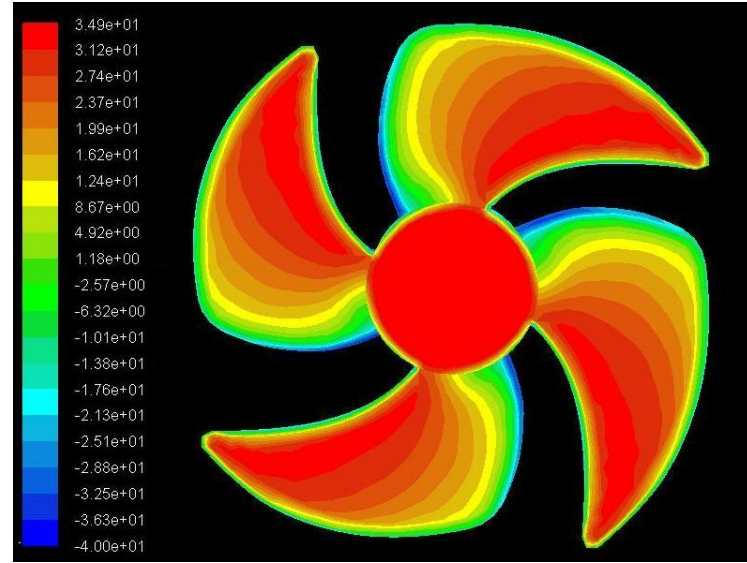
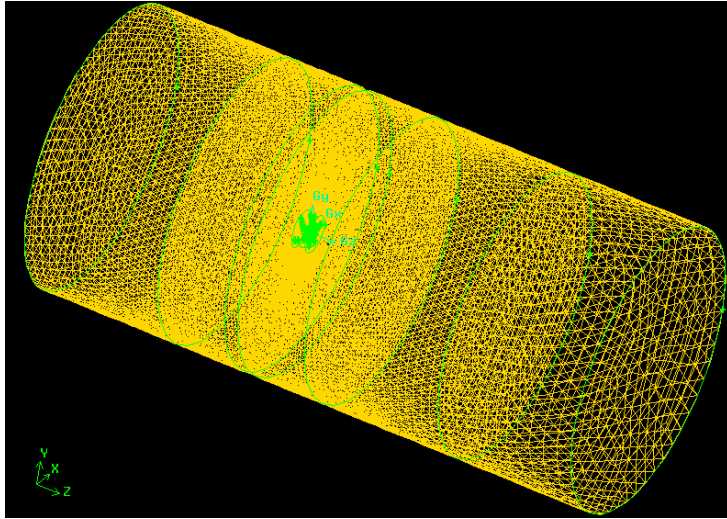
- Is flow turbulent?
 - Is flow unsteady?
 - Are there compressibility effects?
 - Are there 3D effects?

- ◆ Are boundary conditions correct?

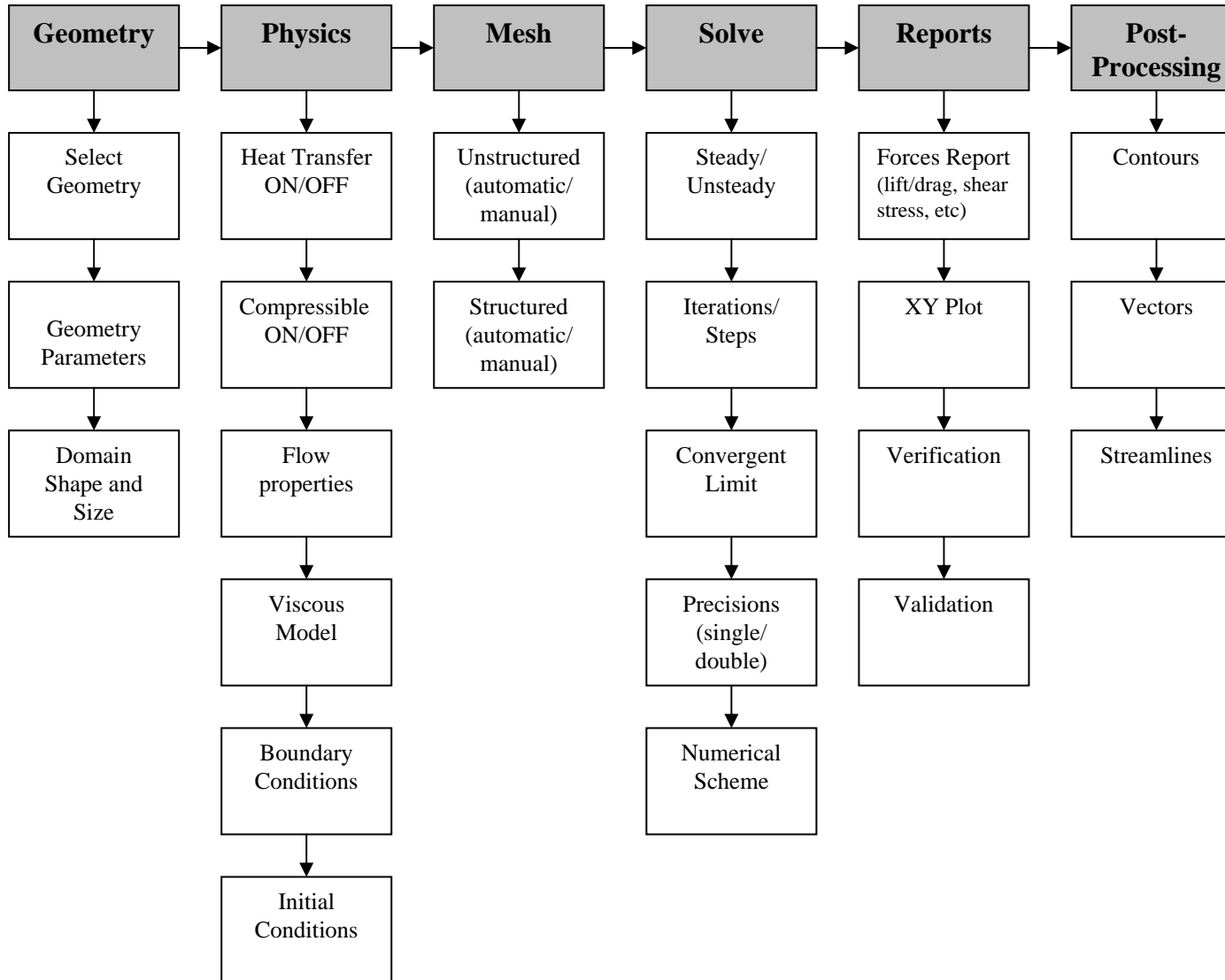
- Is the computational domain large enough?
 - Are boundary conditions appropriate?
 - Are boundary values reasonable?

- ◆ Is grid adequate?

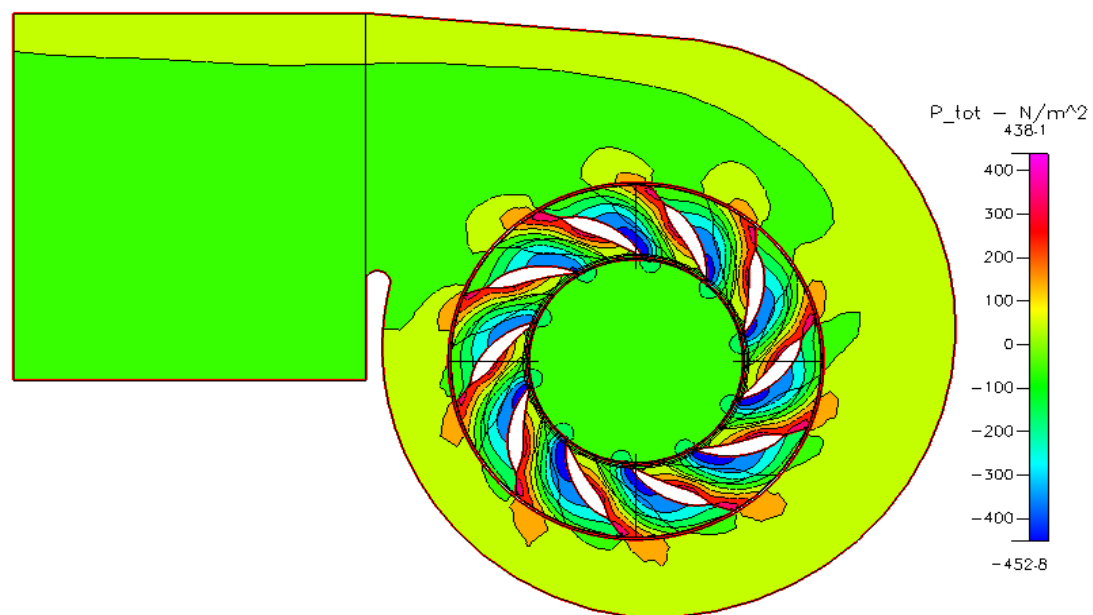
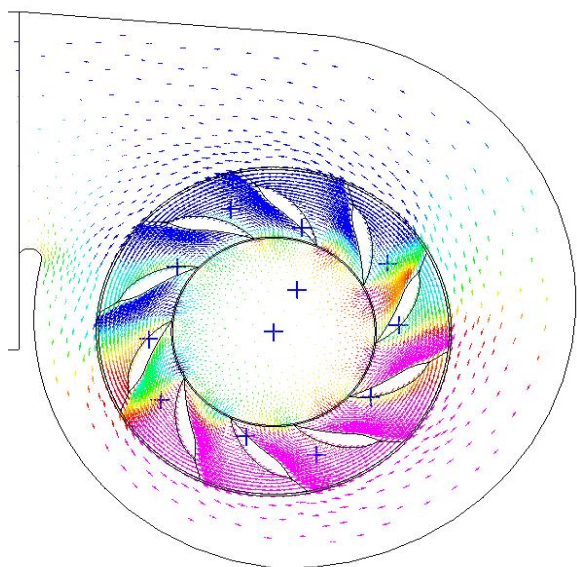
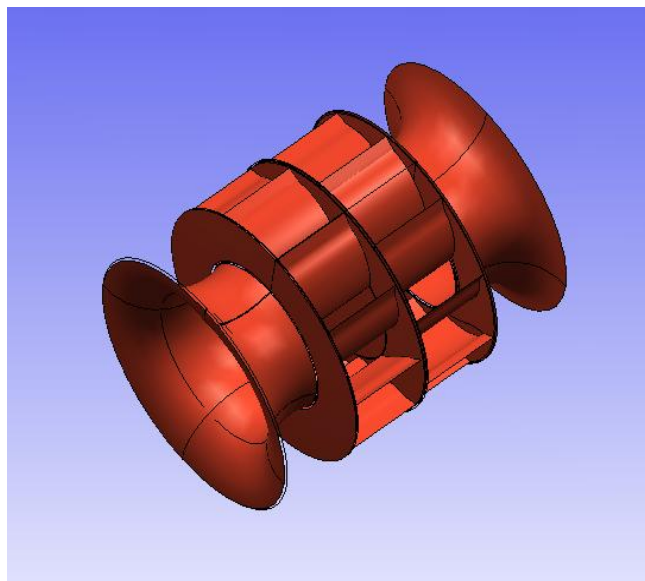
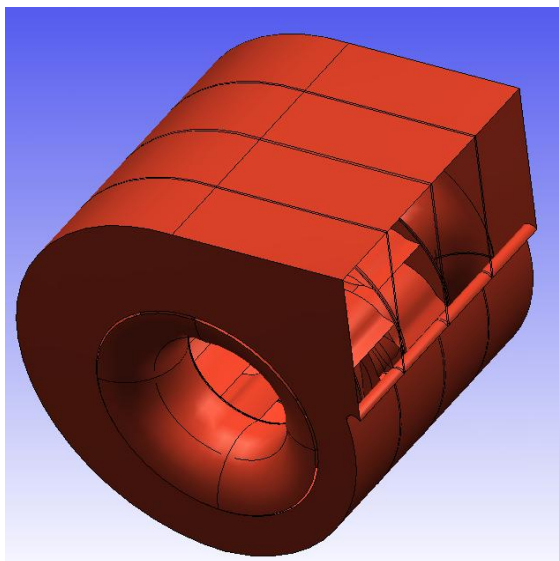
- Can grid be adapted to improve results?
 - Does solution change significantly with adaption, or is the solution grid independent?
 - Does boundary resolution need to be improved?



Road Map for CFD

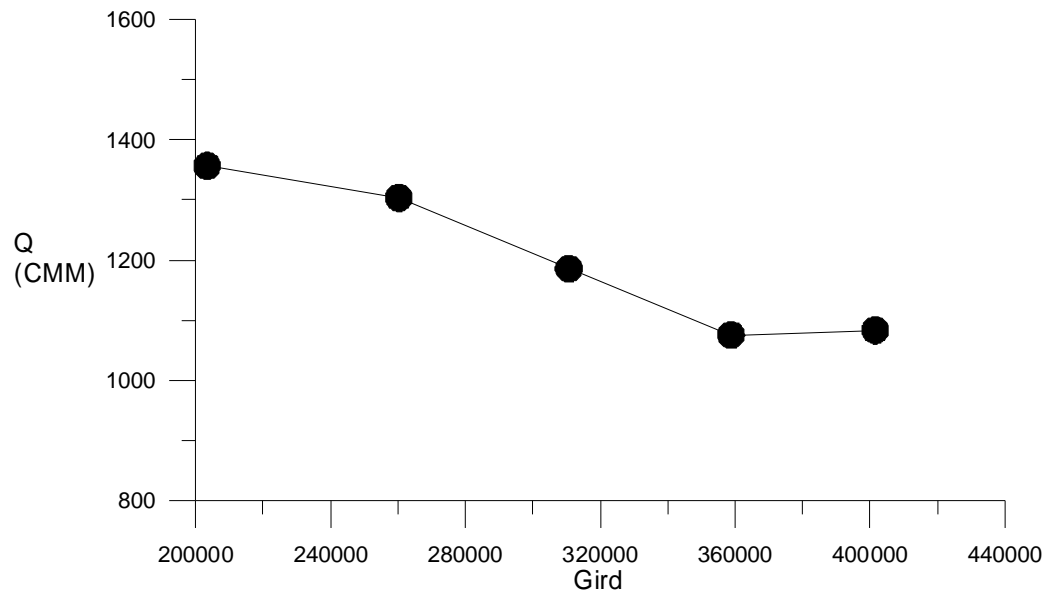


Example 工業級雙吸入式翼型離心風機之開發



格點獨立

為了能使本文研究中模型獲得較精確、較快速收斂的結果，本文以網格數 203, 380、260, 260、310, 650、358, 780、401, 550 五種網格數作檢測。將計算結果個別比對出口風量比較不同網格數的差異，如圖所示。依格點數最多 401, 550 之收斂圈數約為 8 圈比較最候一圈的出口風量，由圖可知格點數 358, 780 與格點數 401, 1550 之出口風量誤差率小於 1%。為了節省運算時間固採用 358, 780 的格點數為基礎。



● A CFDRC code work of CFDRC software

以計算流體力學軟體CFDRC為例，其邊界條件設定、數值計算及結果分析主要步驟如下：

前處理(pre-processing)：使用Autodesk公司研發的AutoCad 2000及ESI公司所開發的CFD-GEOM 進行幾何模型的建立、網格的劃分和邊界條件的設定。

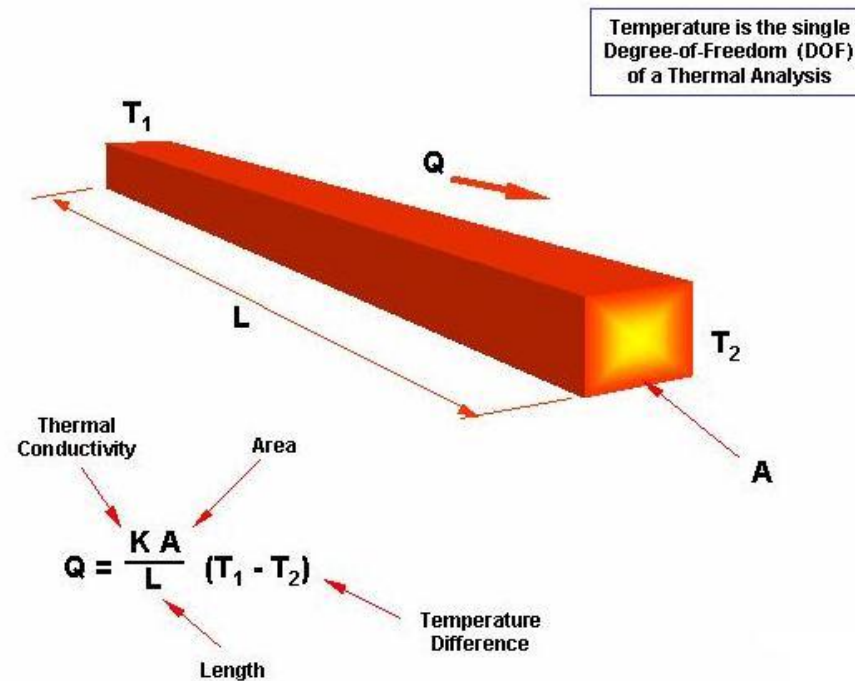
求解器(solver)：利用CFD-ACE讀取前處理的資料，輸入流場型態、初使邊界條件、並選用所需之解法，進行迭帶求解運算。

後處理(post-processing)：將求解過後的資料匯入CFD-VIEW中繪製壓力場、速度場等相關流場解析的資料圖，利用Grapher 4繪製成圖表，以利數據分析。

Chapter 3

The Finite Volume Method for Diffusion (Conduction) Problem

Conduction Heat Transfer



- 4.1 Introduction
- 4.2 Finite volume method for one-dimensional steady state diffusion
- 4.3 Worked examples: one-dimensional steady state diffusion
- 4.4 Finite volume method for two-dimensional diffusion problems
- 4.5 Finite volume method for three-dimensional diffusion problems
- 4.6 Summary of discretised equations for diffusion problems

Finite-Volume Method

Finite-Volume methods are related to finite-difference method, but they are derived based on the integral form of the conservation law—this allows us to represent discontinuities accurately and, as we saw, conservative formulations accurately capture shock speeds.

2.4 Conservative form of the governing equations of a compressible Newtonian fluid

Mass	$\frac{\partial \rho}{\partial t} + \text{div}(\rho \mathbf{u}) = 0$	(2.4)
x-momentum	$\frac{\partial(\rho u)}{\partial t} + \text{div}(\rho u \mathbf{u}) = -\frac{\partial p}{\partial x} + \text{div}(\mu \text{ grad } u) + S_{Mx}$	(2.37a)
y-momentum	$\frac{\partial(\rho v)}{\partial t} + \text{div}(\rho v \mathbf{u}) = -\frac{\partial p}{\partial y} + \text{div}(\mu \text{ grad } v) + S_{My}$	(2.37b)
z-momentum	$\frac{\partial(\rho w)}{\partial t} + \text{div}(\rho w \mathbf{u}) = -\frac{\partial p}{\partial z} + \text{div}(\mu \text{ grad } w) + S_{Mz}$	(2.37c)
Internal energy	$\frac{\partial(\rho i)}{\partial t} + \text{div}(\rho i \mathbf{u}) = -p \text{ div } \mathbf{u} + \text{div}(k \text{ grad } T) + \Phi + S_i$	(2.38)
Equations of state	$p = p(\rho, T)$ and $i = i(\rho, T)$	(2.28)
	e.g. perfect gas $p = \rho RT$ and $i = C_v T$	(2.29)

General form:

$$\frac{\partial(\rho \phi)}{\partial t} + \text{div}(\rho \phi \mathbf{u}) = \text{div}(\Gamma \text{ grad } \phi) + S_\phi$$

ϕ equal to 1, u , v , w and i (or T or h_0)

2.5 Differential and integral forms of the general transport equations

$$\frac{\partial(\rho\phi)}{\partial t} + \text{div}(\rho\phi\mathbf{u}) = \text{div}(\Gamma \text{ grad } \phi) + S_\phi$$

The integration over a 3-D control volume CV yields

$$\int_{CV} \frac{\partial(\rho\phi)}{\partial t} dV + \int_{CV} \text{div}(\rho\phi\mathbf{u})dV = \int_{CV} \text{div}(\Gamma \text{ grad } \phi)dV + \int_{CV} S_\phi dV$$

using Gauss' divergence theorem. $\int_{CV} \text{div } \mathbf{a}dV = \int_A \mathbf{n} \cdot \mathbf{a}dA$

$$\rightarrow \frac{\partial}{\partial t} \left(\int_{CV} \rho\phi dV \right) + \int_A \mathbf{n} \cdot (\rho\phi\mathbf{u})dA = \int_A \mathbf{n} \cdot (\Gamma \text{ grad } \phi)dA + \int_{CV} S_\phi dV$$

Rate of increase of ϕ	+	Net rate of decrease of ϕ due to convection across the boundaries	=	Rate of increase of ϕ due to diffusion across the boundaries	+	Net rate of creation of ϕ
-------------------------------	---	---	---	--	---	-----------------------------------

Comparison:

$$\frac{\partial(\rho\phi)}{\partial t} + \text{div}(\rho\phi\mathbf{u}) = \text{div}(\Gamma \text{grad } \phi) + S_\phi$$

Rate of increase of ϕ of fluid element + Net rate of flow of ϕ out of fluid element = Rate of increase of ϕ due to diffusion + Rate of increase of ϕ due to sources

$$\frac{\partial}{\partial t} \left(\int_{CV} \rho\phi dV \right) + \int_A \mathbf{n} \cdot (\rho\phi\mathbf{u}) dA = \int_A \mathbf{n} \cdot (\Gamma \text{grad } \phi) dA + \int_{CV} S_\phi dV$$

Rate of increase of ϕ + Net rate of decrease of ϕ due to convection across the boundaries = Rate of increase of ϕ due to diffusion across the boundaries + Net rate of creation of ϕ

In steady state problems

$$\frac{\partial}{\partial t} \left(\int_{CV} \rho \phi dV \right) + \int_A \mathbf{n} \cdot (\rho \phi \mathbf{u}) dA = \int_A \mathbf{n} \cdot (\Gamma \text{ grad } \phi) dA + \int_{CV} S_\phi dV$$

→
$$\int_A \mathbf{n} \cdot (\rho \phi \mathbf{u}) dA = \int_A \mathbf{n} \cdot (\Gamma \text{ grad } \phi) dA + \int_{CV} S_\phi dV$$

In time-dependent problems

→
$$\int_{\Delta t} \frac{\partial}{\partial t} \left(\int_{CV} (\rho \phi) dV \right) dt + \int_{\Delta t} \int_A \mathbf{n} \cdot (\rho \phi \mathbf{u}) dA dt$$
$$= \int_{\Delta t} \int_A \mathbf{n} \cdot (\Gamma_\phi \text{ grad } \phi) dA dt + \int_{\Delta t} \int_{CV} S_\phi dV dt$$

The problem of Steady heat conduction
with heat generation (source)

$$\text{i.e. } \mathbf{u}=0, \text{ and } \frac{\partial(\rho\phi)}{\partial t} = 0$$

$$\cancel{\frac{\partial(\rho\phi)}{\partial t}} + \cancel{\text{div}(\rho\phi\mathbf{u})} = \text{div}(\Gamma \text{ grad } \phi) + S_\phi$$

➔ $\text{div}(\Gamma \text{ grad } \phi) + S_\phi = 0$

➔ $\nabla \bullet (\nabla \phi) + S_\phi = 0$

1-D steady-state diffusion (conduction)

➔ $\frac{d}{dx} \left(\Gamma \frac{d\phi}{dx} \right) + S = 0$

The finite difference method

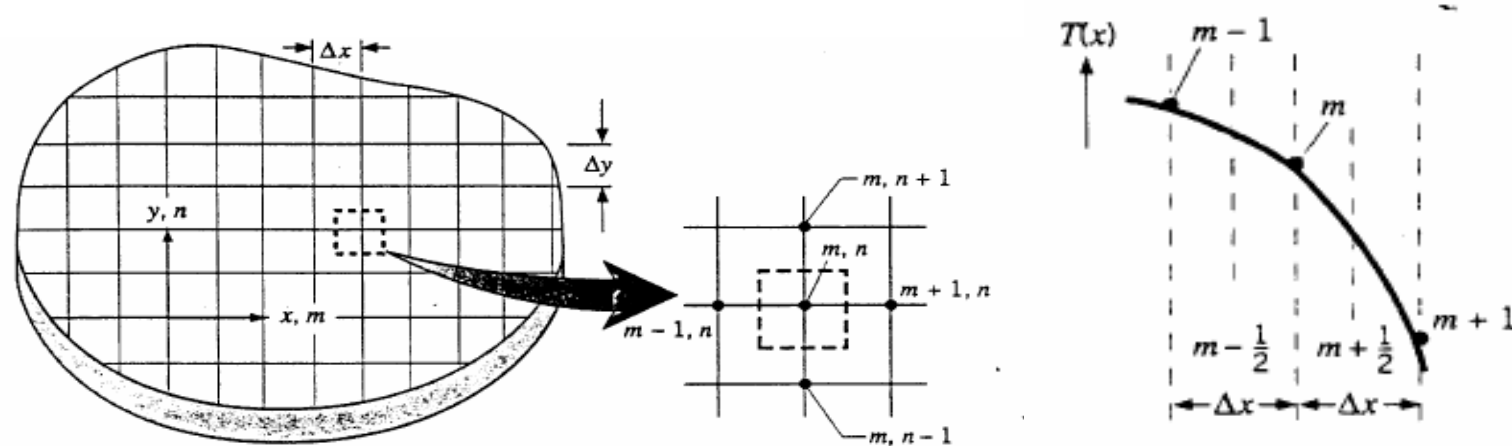


FIGURE 4.5 Two-dimensional conduction. (a) Nodal network. (b) Finite-difference approximation.

$$\left. \frac{\partial T}{\partial x} \right|_{m+1/2, n} \approx \frac{T_{m+1, n} - T_{m, n}}{\Delta x}$$

$$\left. \frac{\partial T}{\partial x} \right|_{m-1/2, n} \approx \frac{T_{m, n} - T_{m-1, n}}{\Delta x}$$

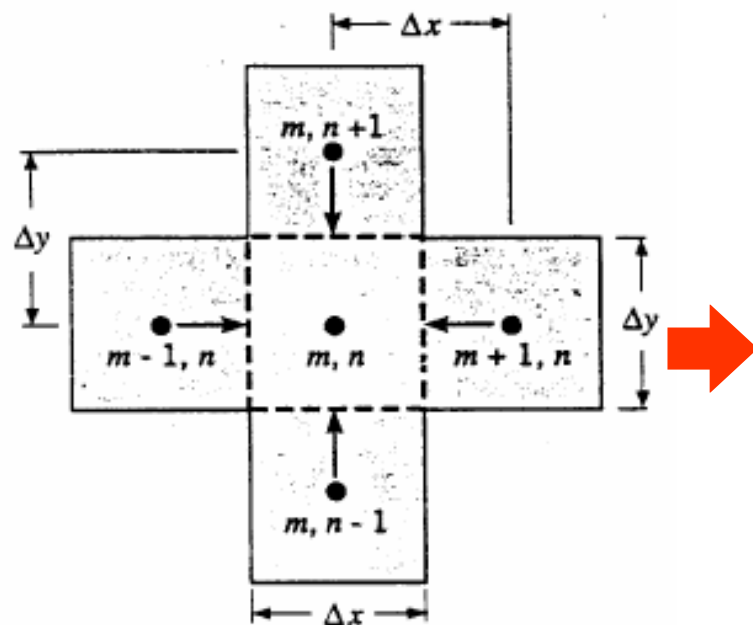
$$\begin{aligned} \left. \frac{\partial^2 T}{\partial x^2} \right|_{m, n} &\approx \frac{\left. \frac{\partial T}{\partial x} \right|_{m+1/2, n} - \left. \frac{\partial T}{\partial x} \right|_{m-1/2, n}}{\Delta x} \\ &\approx \frac{T_{m+1, n} + T_{m-1, n} - 2T_{m, n}}{(\Delta x)^2} \end{aligned}$$

$$\begin{aligned} \left. \frac{\partial^2 T}{\partial y^2} \right|_{m, n} &\approx \frac{\left. \frac{\partial T}{\partial y} \right|_{m, n+1/2} - \left. \frac{\partial T}{\partial y} \right|_{m, n-1/2}}{\Delta y} \\ &\approx \frac{T_{m, n+1} - T_{m, n-1} - 2T_{m, n}}{(\Delta y)^2} \end{aligned}$$

Finite-Difference Form of the Heat Equation

$$\frac{\partial^2 T}{\partial x^2} + \frac{\partial^2 T}{\partial y^2} = 0 \quad \Delta x = \Delta y \quad \rightarrow \quad T_{m,n+1} + T_{m,n-1} + T_{m+1,n} + T_{m-1,n} - 4T_{m,n} = 0$$

The Energy Balance Method



$$\dot{E}_{in} + \dot{E}_g = 0$$

$$\sum_{i \rightarrow (m,n)} q_{(i) \rightarrow (m,n)} + \dot{q}(\Delta x \cdot \Delta y \cdot 1) = 0$$

$$q_{(m-1,n) \rightarrow (m,n)} = k(\Delta y \cdot 1) \frac{T_{m-1,n} - T_{m,n}}{\Delta x}$$

$$q_{(m+1,n) \rightarrow (m,n)} = k(\Delta y \cdot 1) \frac{T_{m+1,n} - T_{m,n}}{\Delta x}$$

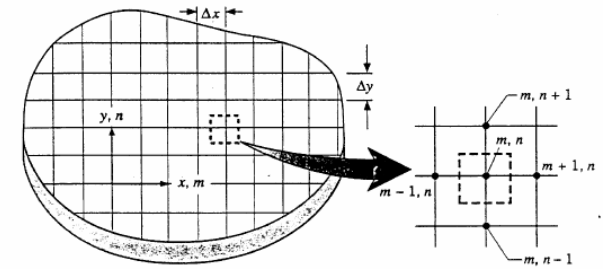
$$q_{(m,n+1) \rightarrow (m,n)} = k(\Delta x \cdot 1) \frac{T_{m,n+1} - T_{m,n}}{\Delta y}$$

$$q_{(m,n-1) \rightarrow (m,n)} = k(\Delta x \cdot 1) \frac{T_{m,n-1} - T_{m,n}}{\Delta y}$$

$$\rightarrow \quad T_{m,n+1} + T_{m,n-1} + T_{m+1,n} + T_{m-1,n} + \frac{\dot{q}(\Delta x)^2}{k} - 4T_{m,n} = 0$$

The Matrix Inversion Method

Discretising equations



$$a_{11}T_1 + a_{12}T_2 + a_{13}T_3 + \dots + a_{1N}T_N = C_1$$

$$a_{21}T_1 + a_{22}T_2 + a_{23}T_3 + \dots + a_{2N}T_N = C_2$$

$$\vdots \quad \quad \quad \vdots \quad \quad \quad \vdots \quad \quad \quad \vdots \quad \quad \quad \vdots \quad \quad \quad \vdots$$

$$a_{N1}T_1 + a_{N2}T_2 + a_{N3}T_3 + \dots + a_{NN}T_N = C_N$$

$$[A][T] = [C]$$

$$A \equiv \begin{bmatrix} a_{11} & a_{12} & \dots & a_{1N} \\ a_{21} & a_{22} & \dots & a_{2N} \\ \vdots & \vdots & & \vdots \\ a_{N1} & a_{N2} & \dots & a_{NN} \end{bmatrix}, \quad T \equiv \begin{bmatrix} T_1 \\ T_2 \\ \vdots \\ T_N \end{bmatrix}, \quad C \equiv \begin{bmatrix} C_1 \\ C_2 \\ \vdots \\ C_N \end{bmatrix}$$

The solution vector may now be expressed as

$$[T] = [A]^{-1}[C]$$

$$[A]^{-1} \equiv \begin{bmatrix} b_{11} & b_{12} & \cdots & b_{1N} \\ b_{21} & b_{22} & \cdots & b_{2N} \\ \vdots & \vdots & & \vdots \\ b_{N1} & b_{N2} & \cdots & b_{NN} \end{bmatrix}$$

$$T_1 = b_{11}C_1 + b_{12}C_2 + \cdots + b_{1N}C_N$$

$$T_2 = b_{21}C_1 + b_{22}C_2 + \cdots + b_{2N}C_N$$

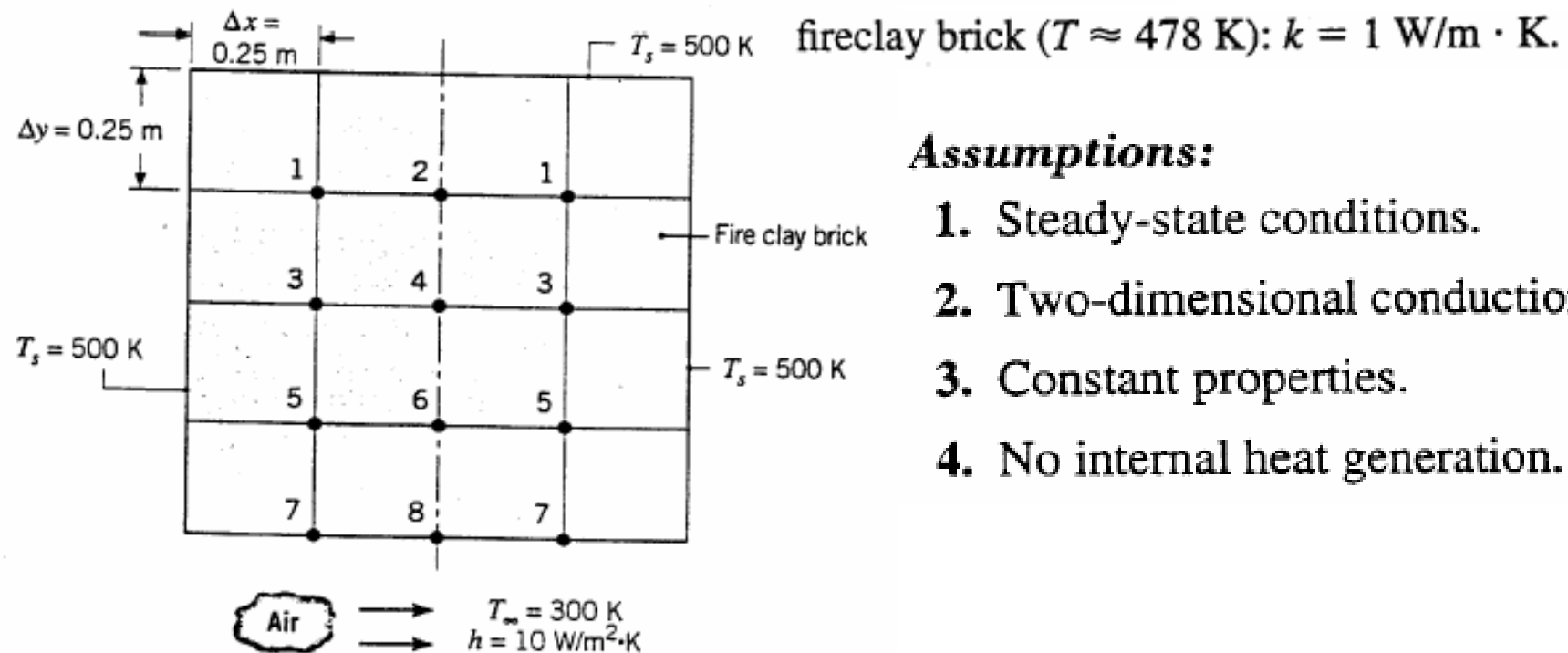
$$\vdots \quad \quad \quad \vdots \quad \quad \quad \vdots \quad \quad \quad \vdots \quad \quad \quad \vdots$$

$$T_N = b_{N1}C_1 + b_{N2}C_2 + \cdots + b_{NN}C_N$$

EXAMPLE

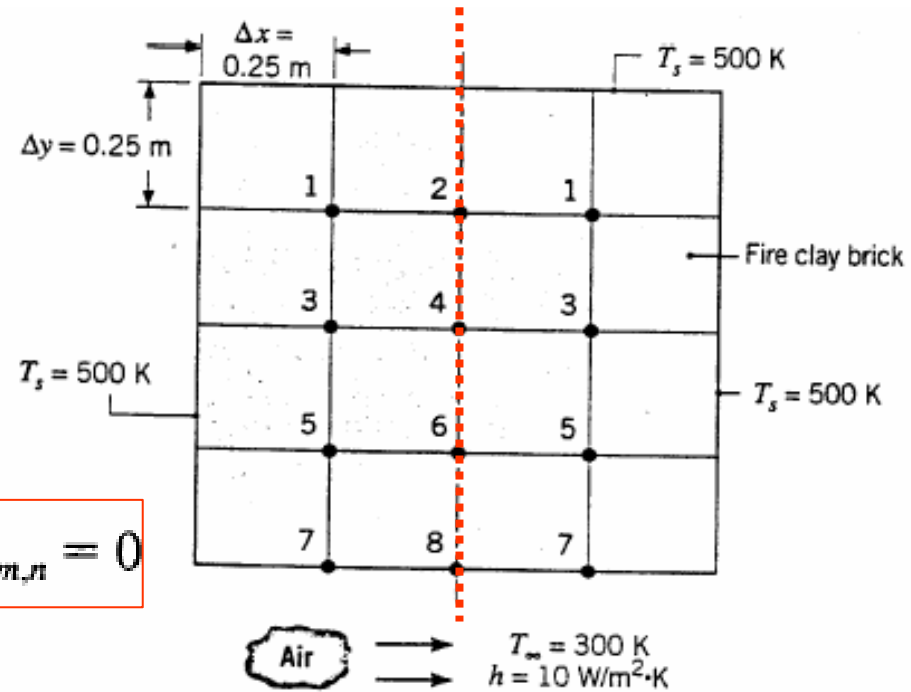
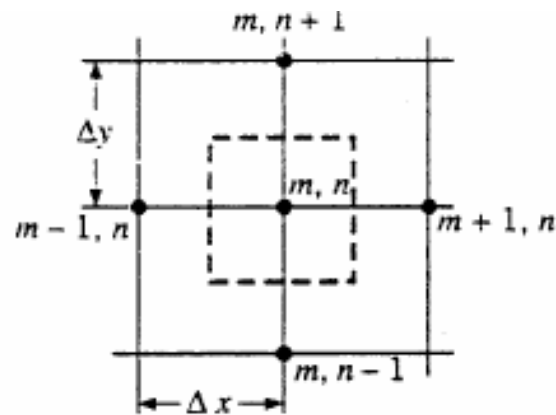
A large industrial furnace is supported on a long column of fireclay brick, which is 1 m by 1 m on a side. During steady-state operation, installation is such that three surfaces of the column are maintained at 500 K while the remaining surface is exposed to an airstream for which $T_\infty = 300$ K and $h = 10$ W/m² · K. Using a grid of $\Delta x = \Delta y = 0.25$ m, determine the two-dimensional temperature distribution in the column and the heat rate to the airstream per unit length of column

Find: Temperature distribution and heat rate per unit length.



Assumptions:

1. Steady-state conditions.
2. Two-dimensional conduction.
3. Constant properties.
4. No internal heat generation.



$$T_{m,n+1} + T_{m,n-1} + T_{m+1,n} + T_{m-1,n} - 4T_{m,n} = 0$$

$$\text{Node 1: } T_2 + T_3 + 1000 - 4T_1 = 0$$

$$\text{Node 3: } T_1 + T_4 + T_5 + 500 - 4T_3 = 0$$

$$\text{Node 5: } T_3 + T_6 + T_7 + 500 - 4T_5 = 0$$

$$\text{Node 2: } 2T_1 + T_4 + 500 - 4T_2 = 0$$

$$\text{Node 4: } T_2 + 2T_3 + T_6 - 4T_4 = 0$$

$$\text{Node 6: } T_4 + 2T_5 + T_8 - 4T_6 = 0$$

$$h \Delta x / k = 2.5,$$

$$\text{Node 7: } 2T_5 + T_8 + 2000 - 9T_7 = 0$$

$$\text{Node 8: } 2T_6 + 2T_7 + 1500 - 9T_8 = 0$$

Discretising finite-difference equations is as follows:

$$\begin{aligned} -4T_1 + T_2 + T_3 + 0 + 0 + 0 + 0 + 0 &= -1000 \\ 2T_1 + -4T_2 + 0 + T_4 + 0 + 0 + 0 + 0 &= -500 \\ T_1 + 0 + -4T_3 + T_4 + T_5 + 0 + 0 + 0 &= -500 \\ 0 + T_2 + 2T_3 + -4T_4 + 0 + T_6 + 0 + 0 &= 0 \\ 0 + 0 + T_3 + 0 + -4T_5 + T_6 + T_7 + 0 &= -500 \\ 0 + 0 + 0 + T_4 + 2T_5 + -4T_6 + 0 + T_8 &= 0 \\ 0 + 0 + 0 + 0 + 2T_5 + 0 + -9T_7 + T_8 &= -2000 \\ 0 + 0 + 0 + 0 + 0 + 2T_6 + 2T_7 + 9T_8 &= -1500 \end{aligned}$$



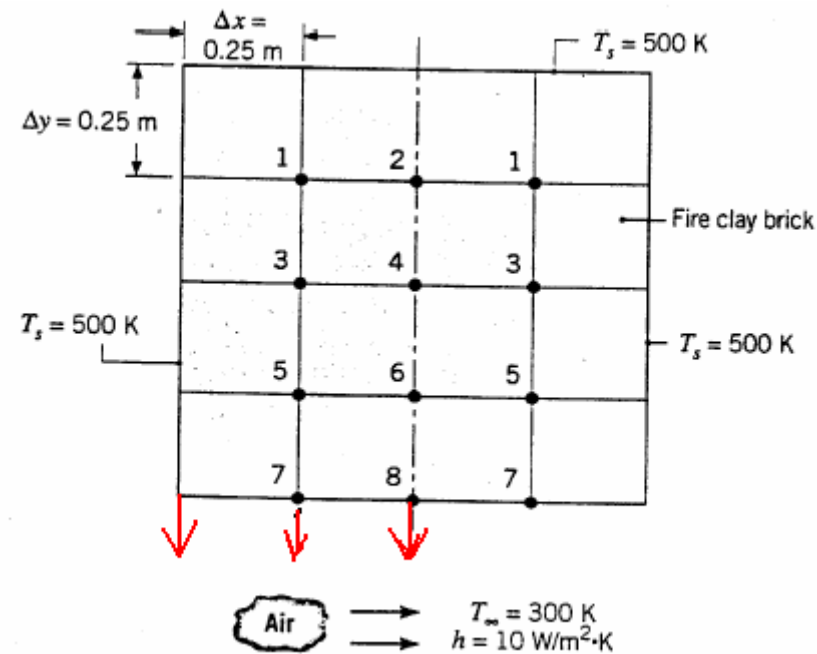
$$[A][T] = [C]$$

$$[A] = \begin{bmatrix} -4 & 1 & 1 & 0 & 0 & 0 & 0 & 0 \\ 2 & -4 & 0 & 1 & 0 & 0 & 0 & 0 \\ 1 & 0 & -4 & 1 & 1 & 0 & 0 & 0 \\ 0 & 1 & 2 & -4 & 0 & 1 & 0 & 0 \\ 0 & 0 & 1 & 0 & -4 & 1 & 1 & 0 \\ 0 & 0 & 0 & 1 & 2 & -4 & 0 & 1 \\ 0 & 0 & 0 & 0 & 2 & 0 & -9 & 1 \\ 0 & 0 & 0 & 0 & 0 & 2 & 2 & -9 \end{bmatrix} \quad [C] = \begin{bmatrix} -1000 \\ -500 \\ -500 \\ 0 \\ -500 \\ 0 \\ -2000 \\ -1500 \end{bmatrix}$$



$$[T] = [A]^{-1}[C]$$

$$[T] = \begin{bmatrix} T_1 \\ T_2 \\ T_3 \\ T_4 \\ T_5 \\ T_6 \\ T_7 \\ T_8 \end{bmatrix} = \begin{bmatrix} 489.30 \\ 485.15 \\ 472.07 \\ 462.01 \\ 436.95 \\ 418.74 \\ 356.99 \\ 339.05 \end{bmatrix} \text{ K}$$



The heat rate from the column to the airstream may be computed from the expression

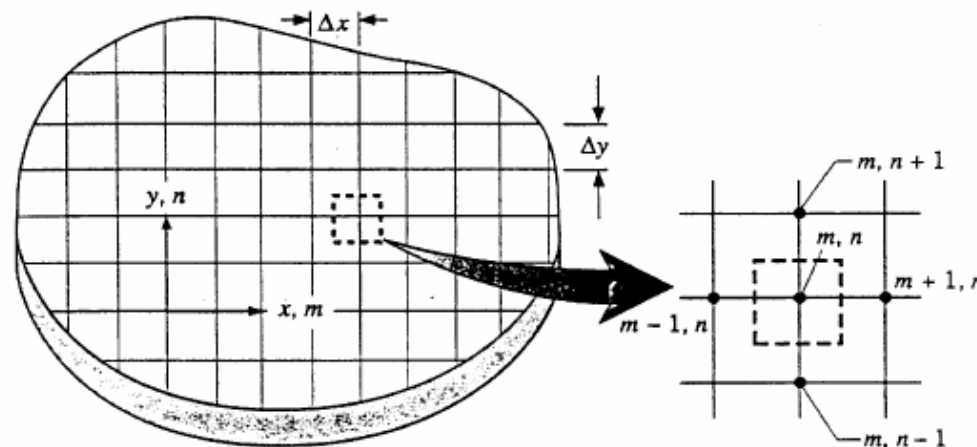
$$\left(\frac{q}{L}\right) = 2h \left[\left(\frac{\Delta x}{2}\right) (T_s - T_\infty) + \Delta x (T_7 - T_\infty) + \left(\frac{\Delta x}{2}\right) (T_8 - T_\infty) \right]$$

$$= 2 \times 10 \text{ W/m}^2 \cdot \text{K} [(0.125 \text{ m} (200 \text{ K})$$

$$+ 0.25 \text{ m} (56.99 \text{ K}) + 0.125 \text{ m} (39.05 \text{ K})] = 883 \text{ W/m}$$

Control Volume Approach

- 1 Let us imagine that we divide the rectangular region of Figure 12.1a into a finite number of nonoverlapping control volumes (areas, since our region is two-dimensional). These control volumes are chosen such that each one completely engulfs only one grid point.
 - 2 The main idea behind this approach is to *integrate* the differential equation over each control volume using chosen (assumed) profiles for the unknown variable ϕ in order to evaluate the required integrals.
 - 3 Once we complete this task, we have in our hands the discretized form of the differential equation, a form that contains the values of ϕ for a group of neighboring grid points. It is worth noting that we are free to assume different profiles for ϕ to approximate different terms in the differential equation.



The finite volume method--a special finite difference formulation

The numerical algorithm consists of the following steps:

- Formal integration of the governing equations of fluid flow over all the (finite) control volumes of the solution domain.
- Discretisation involves the substitution of a variety of finite-difference-type approximations for the terms in the integrated equation representing flow processes such as convection, diffusion and sources. This converts the integral equations into a system of algebraic equations.
- Solution of the algebraic equations by an iterative method.

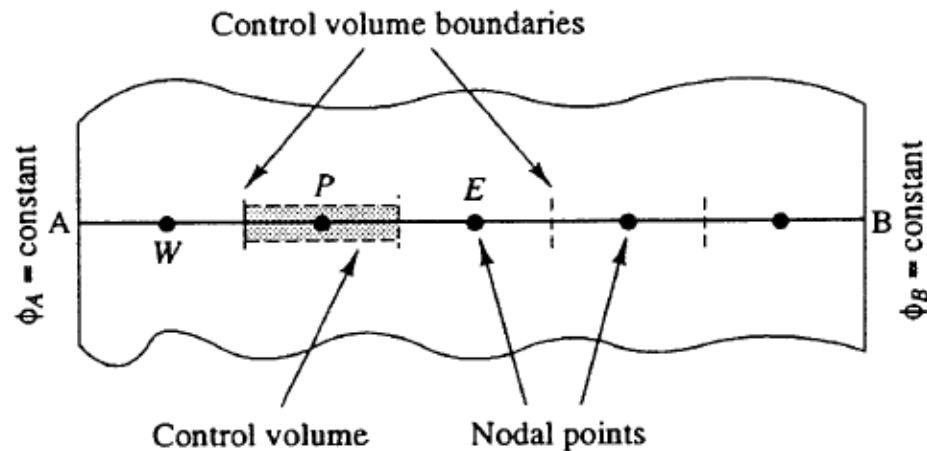
The main advantage of the control volume method:

It is important to realize that if the differential equation expresses the conservation of some quantity like, for example, energy in the First Law of Thermodynamics for an *infinitesimal* control volume, then the discretization equation is the exact representation of the conservation of that quantity in a *finite* control volume. This is the main advantage of the control-volume formulation method: quantities such as mass, momentum, and energy are conserved exactly over any number of control volumes and, therefore, over the entire region, regardless of the coarseness of the mesh that defines the control volumes. To illustrate this method consider the following simple example.

4.2 Finite volume method for one-dimensional steady state diffusion

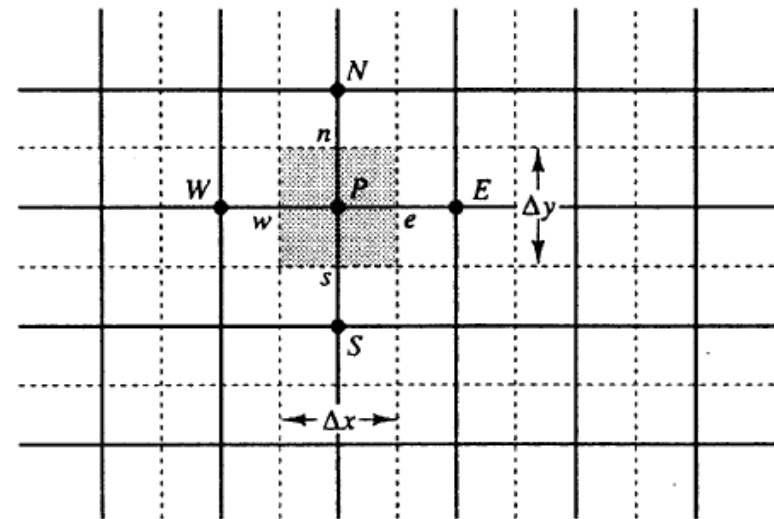
Step 1: Grid generation

The first step is to divide the computational domain into discrete control volumes.



1-D

W:west
E:east
N:north
S:south



2-D

Step 2: discretisation 離散化

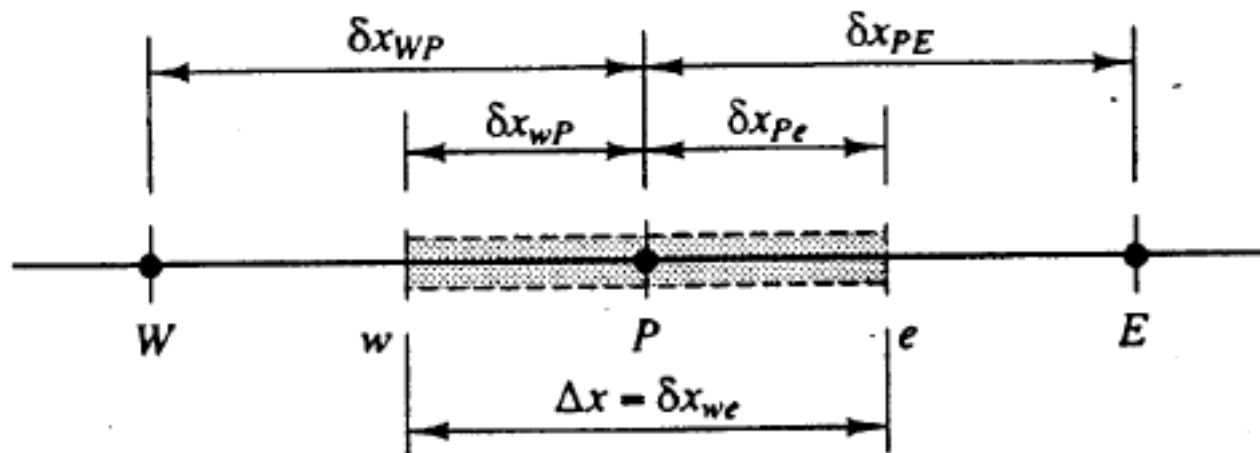
The key step of the finite volume method is the integration of the governing equation (or equations) over a control volume to yield a discretised equation at its nodal point P . For the control volume defined above this gives

$$\frac{d}{dx} \left(\Gamma \frac{d\phi}{dx} \right) + S = 0$$

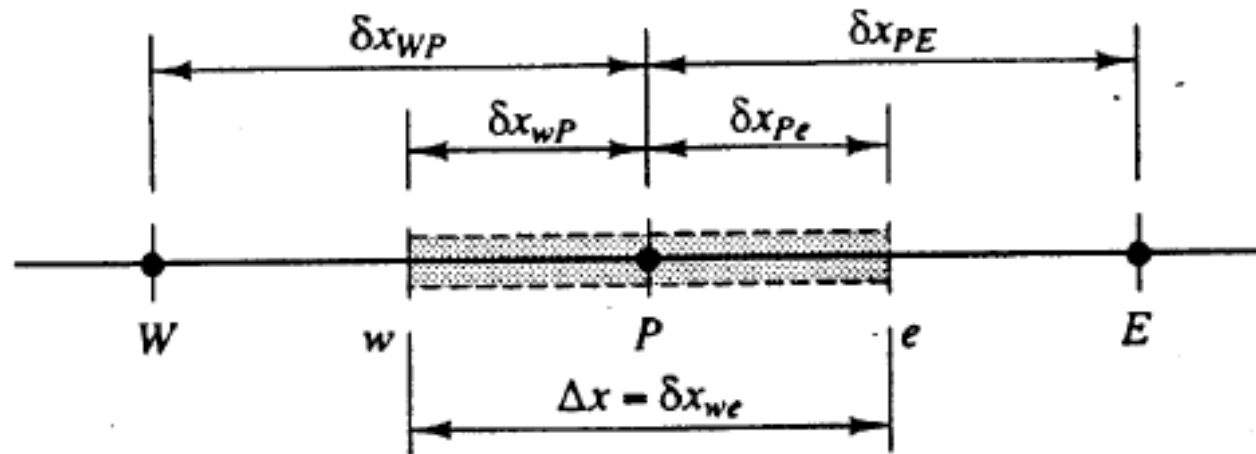
$$\int_{CV} \text{div}(\Gamma \text{grad } \phi) dV + \int_{CV} S_{\phi} dV = \int_{A_{-}} \mathbf{n} \cdot (\Gamma \text{grad } \phi) dA + \int_{CV} S_{\phi} dV = 0$$



$$= \left(\Gamma A \frac{d\phi}{dx} \right)_e - \left(\Gamma A \frac{d\phi}{dx} \right)_w + \bar{S} \Delta V = 0$$



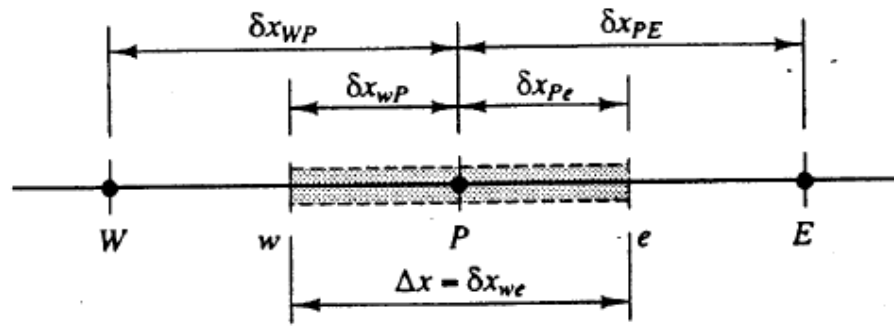
In the finite volume discretisation procedure



$$\left(\frac{\partial \phi}{\partial x}\right)_e = \frac{\phi_E - \phi_P}{\Delta x} = \frac{\phi_E - \phi_P}{2(\Delta x/2)} (+O(\Delta x^2))$$

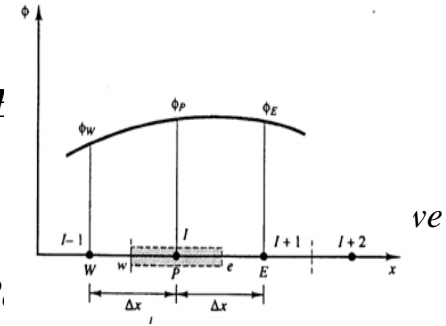
(1) The gradient at a cell face “e” is a central difference with second-order accuracy

(2) After grid refinement the error reduces more quickly in a second-order accurate differencing scheme than in a first-order accurate scheme



$$\delta x_{WP} = \delta x_{PI} \quad ?$$

$$\delta x_{WP} = \delta x_{PI} \quad ?$$



Assumption: Linear approximation and central differencing

$$\Gamma_w = \frac{\Gamma_W + \Gamma_P}{2} \quad \left(\Gamma A \frac{d\phi}{dx} \right)_e = \Gamma_e A_e \left(\frac{\phi_E - \phi_P}{\delta x_{PE}} \right) \quad \bar{S} \Delta V = S_u + S_p \phi_P$$

$$\Gamma_e = \frac{\Gamma_P + \Gamma_E}{2} \quad \left(\Gamma A \frac{d\phi}{dx} \right)_w = \Gamma_w A_w \left(\frac{\phi_P - \phi_W}{\delta x_{WP}} \right)$$

$$\int_{\Delta V} \frac{d}{dx} \left(\Gamma \frac{d\phi}{dx} \right) dV + \int_{\Delta V} S dV = \left(\Gamma A \frac{d\phi}{dx} \right)_e - \left(\Gamma A \frac{d\phi}{dx} \right)_w + \bar{S} \Delta V = 0$$

$$\Rightarrow \Gamma_e A_e \left(\frac{\phi_E - \phi_P}{\delta x_{PE}} \right) - \Gamma_w A_w \left(\frac{\phi_P - \phi_W}{\delta x_{WP}} \right) + (S_u + S_p \phi_P) = 0$$

$$\Rightarrow \left(\frac{\Gamma_e}{\delta x_{PE}} A_e + \frac{\Gamma_w}{\delta x_{WP}} A_w - S_p \right) \phi_P = \left(\frac{\Gamma_w}{\delta x_{WP}} A_w \right) \phi_W + \left(\frac{\Gamma_e}{\delta x_{PE}} A_e \right) \phi_E + S_u$$

$$\left(\frac{\Gamma_e}{\delta x_{PE}} A_e + \frac{\Gamma_w}{\delta x_{WP}} A_w - S_p \right) \phi_P = \left(\frac{\Gamma_w}{\delta x_{WP}} A_w \right) \phi_W + \left(\frac{\Gamma_e}{\delta x_{PE}} A_e \right) \phi_E + S_u$$

$$a_P \phi_P = a_W \phi_W + a_E \phi_E + S_u$$

$$\bar{S} \Delta V = S_u + S_p \phi_P$$

where

a_W	a_E	a_P
$\frac{\Gamma_w}{\delta x_{WP}} A_w$	$\frac{\Gamma_e}{\delta x_{PE}} A_e$	$a_W + a_E - S_p$

In practical situations, as illustrated later, the source term S may be a function of the dependent variable. In such cases the finite volume method approximates the source term by means of a linear form: $\bar{S} \Delta V = S_u + S_p \phi_P$.

Step 3: Solution of Discretization Equations

- ⊖ Discretised equations of the form (4.11) must be set up at each of the nodal points in order to solve a problem. For control volumes that are adjacent to the domain
- ⊖ boundaries the general discretised equation (4.11) is modified to incorporate boundary conditions.
- ⊖ The resulting system of linear algebraic equations is then solved to obtain the distribution of the property ϕ at nodal points. Any suitable matrix solution technique may be enlisted for this task. In Chapter 7 we describe matrix solution methods that are specially designed for CFD procedures.

Step 3: Solution of Discretization Equations

2.4.1 Direct Methods

Using one of the discretization methods described previously, we may write the resulting system of algebraic equations as

$$\mathbf{A}\phi = \mathbf{B} \quad (2.18)$$

where \mathbf{A} is the coefficient matrix, $\phi = [\phi_1, \phi_2, \dots]^T$ is a vector consisting of the discrete values of ϕ , and \mathbf{B} is the vector resulting from the source terms.

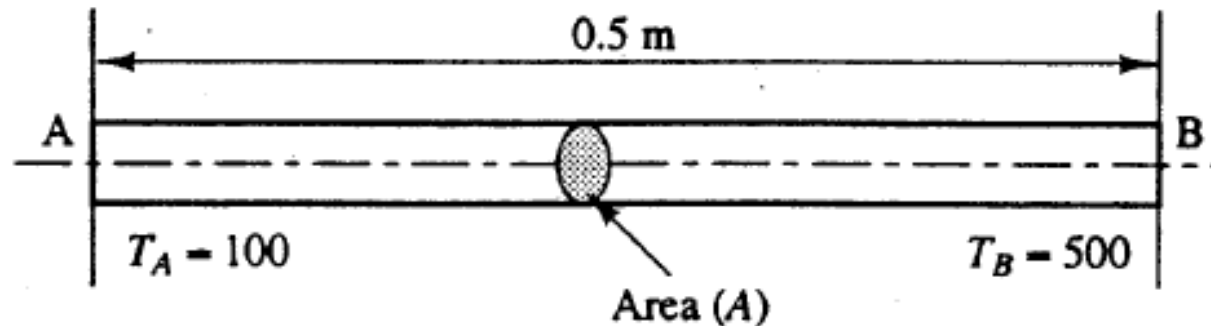
Direct methods solve the equation set 2.18 using the methods of linear algebra. The simplest direct method is inversion, whereby ϕ is computed from

$$\phi = \mathbf{A}^{-1}\mathbf{B} \quad (2.19)$$

$$\mathbf{A} = \begin{bmatrix} x & x & 0 & 0 & 0 \\ x & x & x & 0 & 0 \\ 0 & x & x & x & 0 \\ 0 & 0 & x & x & x \\ 0 & 0 & 0 & x & x \end{bmatrix}$$

4.3 Worked examples:

one-dimensional steady state diffusion



$$A = 10 \times 10^{-3} \text{ m}^2$$

$$k = 1000 \text{ W/m K}$$

1-D steady-state diffusion (conduction) without heat source

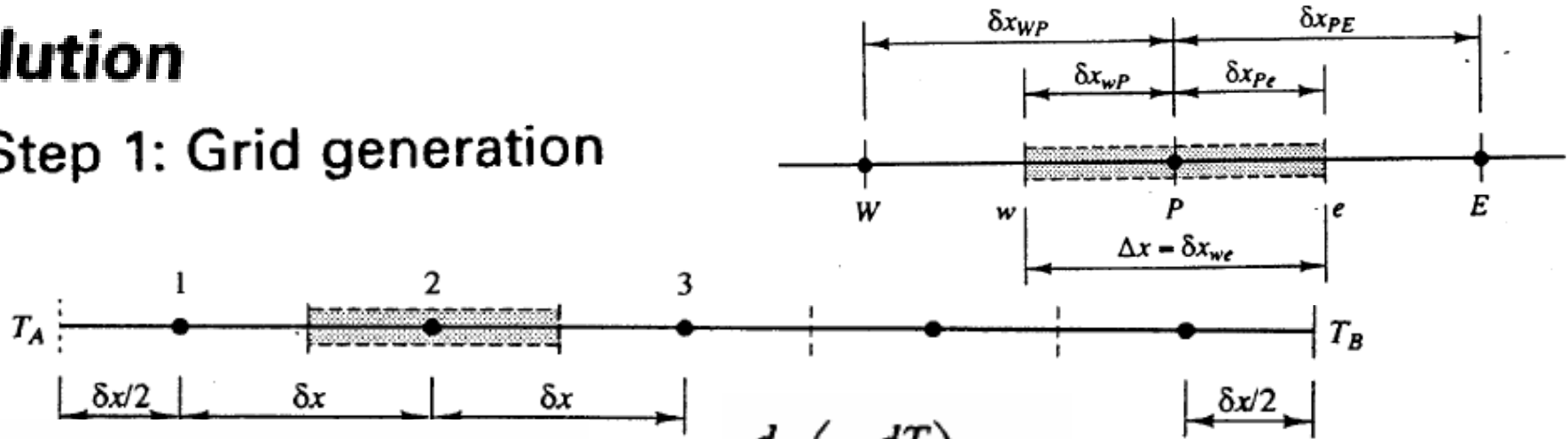
$$\nabla \cdot (\nabla \phi) + S_{\phi} = 0$$

$$\frac{d}{dx} \left(\Gamma \frac{d\phi}{dx} \right) + S = 0$$

$$\frac{d}{dx} \left(k \frac{dT}{dx} \right) = 0$$

Solution

Step 1: Grid generation



Step 2: discretisation

$$\frac{d}{dx} \left(k \frac{dT}{dx} \right) = 0$$

$$\int_{\Delta V} \frac{d}{dx} \left(\Gamma \frac{d\phi}{dx} \right) dV = \left(\Gamma A \frac{d\phi}{dx} \right)_e - \left(\Gamma A \frac{d\phi}{dx} \right)_w = 0$$

$$\rightarrow k_e A_e \left(\frac{T_E - T_P}{\delta x_{PE}} \right) - k_w A_w \left(\frac{T_P - T_W}{\delta x_{WP}} \right) = 0$$

$$\rightarrow \left(\frac{k_e}{\delta x_{PE}} A_e + \frac{k_w}{\delta x_{WP}} A_w \right) T_P = \left(\frac{k_w}{\delta x_{WP}} A_w \right) T_W + \left(\frac{k_e}{\delta x_{PE}} A_e \right) T_E$$

$$a_P T_P = a_W T_W + a_E T_E$$

the discretised equation for nodal points 2, 3 and 4 is

$$a_P T_P = a_W T_W + a_E T_E$$

a_W	a_E	a_P
$\frac{k}{\delta x} A$	$\frac{k}{\delta x} A$	$a_W + a_E$

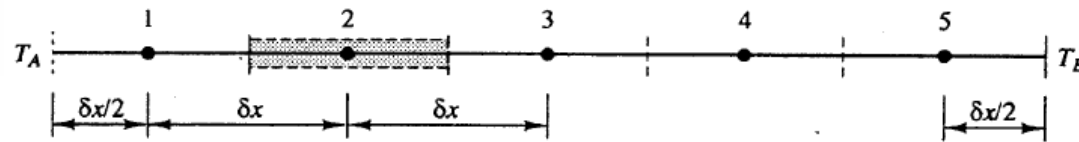


$$a_2 T_2 = a_1 T_1 + a_3 T_3$$

$$a_3 T_3 = a_2 T_2 + a_4 T_4$$

$$a_4 T_4 = a_3 T_3 + a_5 T_5$$

✳ the discretised equation for nodal points boundary Nodes 1 and 5



(P=1 or 5)

$$k_e A_e \left(\frac{T_E - T_P}{\delta x_{PE}} \right) - k_w A_w \left(\frac{T_P - T_W}{\delta x_{WP}} \right) = 0$$

$$kA \left(\frac{T_E - T_P}{\delta x} \right) - kA \left(\frac{T_P - T_A}{\delta x/2} \right) = 0$$

$$\left(\frac{k}{\delta x} A + \frac{2k}{\delta x} A \right) T_P = 0 \cdot T_W + \left(\frac{k}{\delta x} A \right) T_E + \left(\frac{2k}{\delta x} A \right) T_A$$

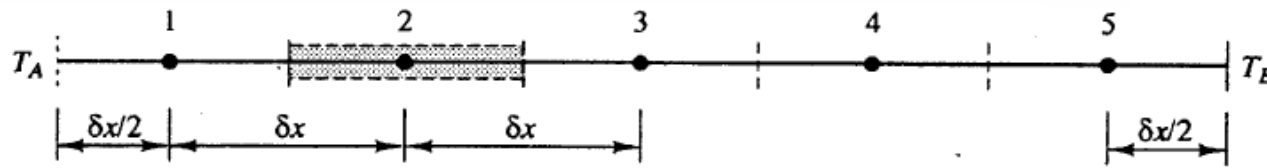
$$a_P T_P = a_W T_W + a_E T_E + S_u$$



$$a_1 T_1 = a_0 T_0 + a_2 T_2 + S_u$$

a_W	a_E	a_P	S_P	S_u
0	$\frac{kA}{\delta x}$	$a_W + a_E - S_P$	$-\frac{2kA}{\delta x}$	$\frac{2kA}{\delta x} T_A$

the discretised equation for nodal point 5 ($P=5$)



$$k_e A_e \left(\frac{T_E - T_P}{\delta x_{PE}} \right) - k_w A_w \left(\frac{T_P - T_W}{\delta x_{WP}} \right) = 0$$

$$kA \left(\frac{T_B - T_P}{\delta x/2} \right) - kA \left(\frac{T_P - T_W}{\delta x} \right) = 0$$

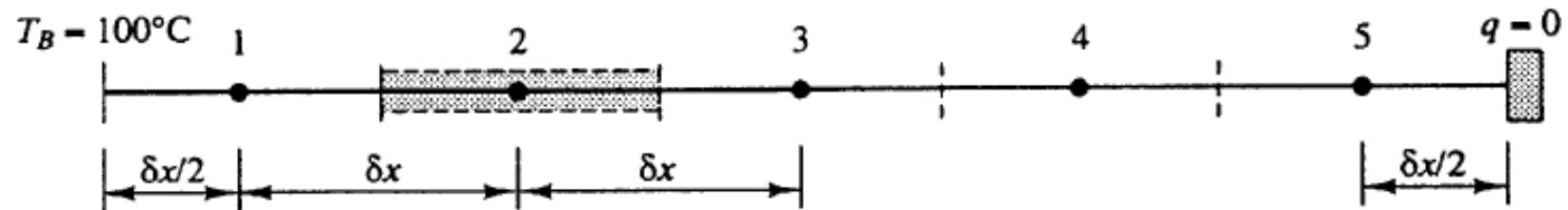
$$\left(\frac{k}{\delta x} A + \frac{2k}{\delta x} A \right) T_P = \left(\frac{k}{\delta x} A \right) T_W + 0 \cdot T_E + \left(\frac{2k}{\delta x} A \right) T_B$$

$$a_P T_P = a_W T_W + a_E T_E + S_u \quad \rightarrow \quad a_5 T_5 = a_4 T_4 + a_E T_E + S_u$$

a_W	a_E	a_P	S_P	S_u
$\frac{kA}{\delta x}$	0	$-a_W + a_E - S_P$	$-\frac{2kA}{\delta x}$	$\frac{2kA}{\delta x} T_B$

Solution

Step 1: Grid generation



Step 2: discretisation

$$\frac{d}{dx} \left(\frac{dT}{dx} \right) - n^2 (T - T_\infty) = 0 \text{ where } n^2 = hp/(kA)$$

Integration of the above equation over a control volume gives

$$\int_{\Delta V} \frac{d}{dx} \left(\frac{dT}{dx} \right) dV - \int_{\Delta V} n^2 (T - T_\infty) dV = 0$$

$$\rightarrow \left[\left(A \frac{dT}{dx} \right)_e - \left(A \frac{dT}{dx} \right)_w \right] - [n^2 (T_P - T_\infty) A \delta x] = 0$$

$$\rightarrow \left[\left(\frac{T_E - T_P}{\delta x} \right) - \left(\frac{T_P - T_W}{\delta x} \right) \right] - [n^2(T_P - T_\infty)\delta x] = 0$$

$$\rightarrow \left(\frac{1}{\delta x} + \frac{1}{\delta x} \right) T_P = \left(\frac{1}{\delta x} \right) T_W + \left(\frac{1}{\delta x} \right) T_E + n^2\delta x T_\infty - n^2\delta x T_P$$

For interior nodal points 2, 3 and 4, the discretisation equation

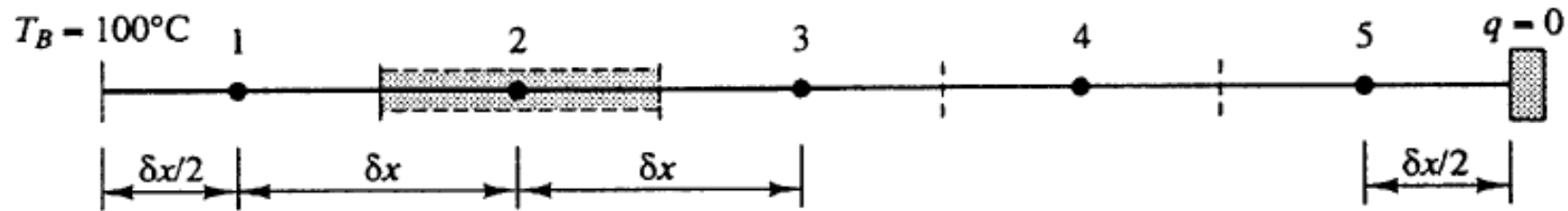
$$a_2 T_2 = a_1 T_1 + a_3 T_3 + S_u$$

$$a_P T_P = a_W T_W + a_E T_E + S_u \rightarrow a_3 T_3 = a_2 T_2 + a_4 T_4 + S_u$$

$$a_4 T_4 = a_3 T_3 + a_5 T_5 + S_u$$

a_W	a_E	a_P	S_P	S_u
$\frac{1}{\delta x}$	$\frac{1}{\delta x}$	$a_W + a_E - S_P$	$-n^2\delta x$	$n^2\delta x T_\infty$

at boundary node 1



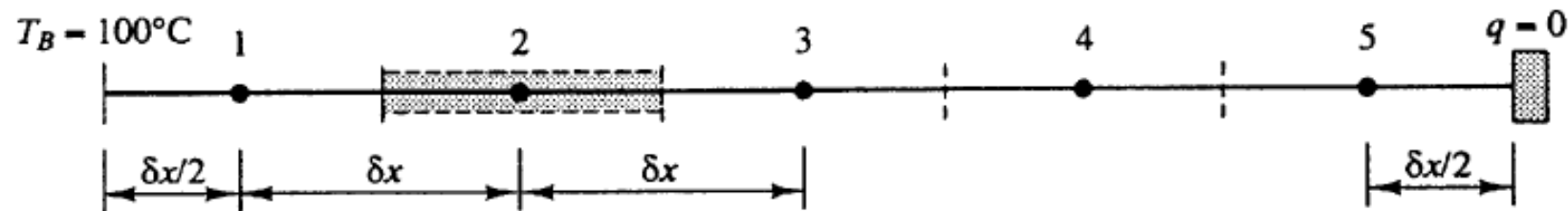
$$\left[\left(\frac{T_E - T_P}{\delta x} \right) - \left(\frac{T_P - T_W}{\delta x} \right) \right] - [n^2(T_P - T_\infty)\delta x] = 0$$

➔
$$\left[\left(\frac{T_E - T_P}{\delta x} \right) - \left(\frac{T_P - T_B}{\delta x/2} \right) \right] - [n^2(T_P - T_\infty)\delta x] = 0$$

➔
$$a_P T_P = a_W T_W + a_E T_E + S_u \quad \rightarrow \quad a_1 T_1 = a_W T_W + a_2 T_2 + S_u$$

a_W	a_E	a_P	S_p	S_u
0	$\frac{1}{\delta x}$	$a_W + a_E - S_p$	$-n^2\delta x - \frac{2}{\delta x}$	$n^2\delta x T_\infty + \frac{2}{\delta x} T_B$

at boundary node 5



$$\left[\left(\frac{T_E - T_P}{\delta x} \right) - \left(\frac{T_P - T_W}{\delta x} \right) \right] - [n^2(T_P - T_\infty)\delta x] = 0$$

→ $\left[0 - \left(\frac{T_P - T_W}{\delta x} \right) \right] - [n^2(T_P - T_\infty)\delta x] = 0$

→ $a_P T_P = a_W T_W + a_E T_E + S_u \rightarrow a_5 T_5 = a_4 T_4 + a_E T_E + S_u$

a_W	a_E	a_P	S_P	S_u
$\frac{1}{\delta x}$	0	$a_W + a_E - S_P$	$-n^2 \delta x$	$n^2 \delta x T_\infty$

The matrix form of the equations set is

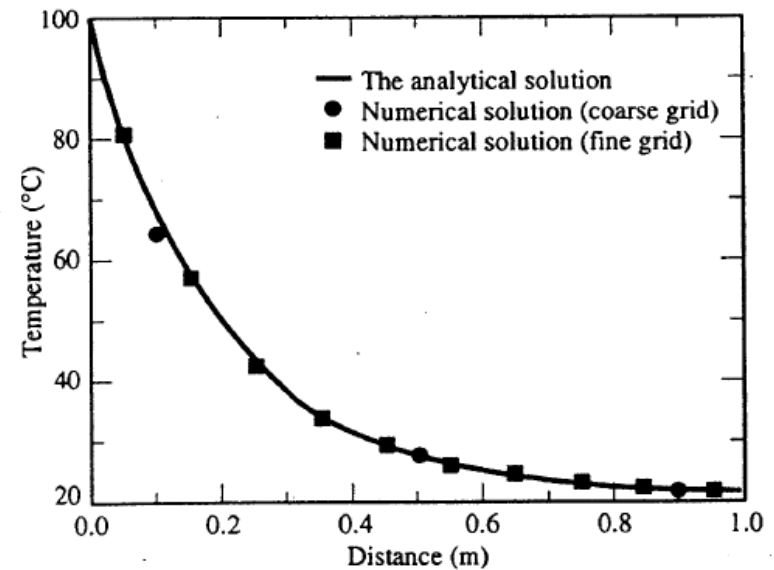
$$\begin{aligned}
 a_1 T_1 &= a_W T_W + a_2 T_2 + S_u \\
 a_2 T_2 &= a_1 T_1 + a_3 T_3 + S_u \\
 a_3 T_3 &= a_2 T_2 + a_4 T_4 + S_u \\
 a_4 T_4 &= a_3 T_3 + a_5 T_5 + S_u \\
 a_5 T_5 &= a_4 T_4 + a_E T_E + S_u
 \end{aligned}$$

$$\begin{bmatrix} 20 & -5 & 0 & 0 & 0 \\ -5 & 15 & -5 & 0 & 0 \\ 0 & -5 & 15 & -5 & 0 \\ 0 & 0 & -5 & 15 & -5 \\ 0 & 0 & 0 & -5 & 10 \end{bmatrix}
 \begin{bmatrix} T_1 \\ T_2 \\ T_3 \\ T_4 \\ T_5 \end{bmatrix}
 =
 \begin{bmatrix} 1100 \\ 100 \\ 100 \\ 100 \\ 100 \end{bmatrix}$$

The solution to the above system is

$$\begin{bmatrix} T_1 \\ T_2 \\ T_3 \\ T_4 \\ T_5 \end{bmatrix}
 =
 \begin{bmatrix} 64.22 \\ 36.91 \\ 26.50 \\ 22.60 \\ 21.30 \end{bmatrix}$$

The maximum deviation is **2%**

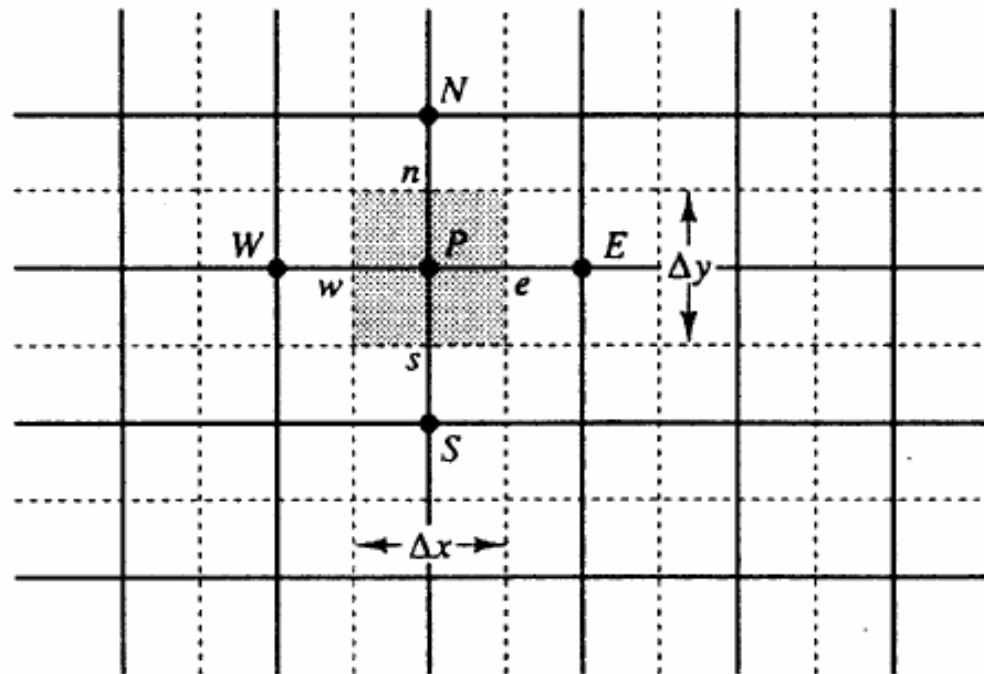


4.4 Finite volume method for two-dimensional diffusion problems

the two-dimensional steady state diffusion equation

$$\nabla \cdot (\nabla \phi) + S_\phi = 0 \quad \rightarrow \quad \frac{\partial}{\partial x} \left(\Gamma \frac{\partial \phi}{\partial x} \right) + \frac{\partial}{\partial y} \left(\Gamma \frac{\partial \phi}{\partial y} \right) + S = 0$$

Step 1: Grid generation



Step 2: discretisation

Integration of the above equation over a control volume gives

$$\int_{\Delta V} \frac{\partial}{\partial x} \left(\Gamma \frac{\partial \phi}{\partial x} \right) dx \cdot dy + \int_{\Delta V} \frac{\partial}{\partial y} \left(\Gamma \frac{\partial \phi}{\partial y} \right) dx \cdot dy + \int_{\Delta V} S_{\phi} dV = 0$$

$$A_e = A_w = \Delta y \text{ and } A_n = A_s = \Delta x,$$

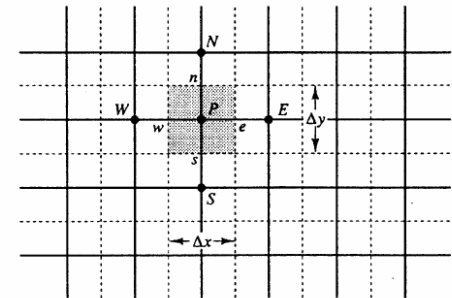
$$\rightarrow \left[\Gamma_e A_e \left(\frac{\partial \phi}{\partial x} \right)_e - \Gamma_w A_w \left(\frac{\partial \phi}{\partial x} \right)_w \right] + \left[\Gamma_n A_n \left(\frac{\partial \phi}{\partial y} \right)_n - \Gamma_s A_s \left(\frac{\partial \phi}{\partial y} \right)_s \right] + \bar{S} \Delta V = 0$$

$$\text{Flux across the west face} = \Gamma_w A_w \frac{\partial \phi}{\partial x} \Big|_w = \Gamma_w A_w \frac{(\phi_P - \phi_W)}{\delta x_{WP}}$$

$$\text{Flux across the east face} = \Gamma_e A_e \frac{\partial \phi}{\partial x} \Big|_e = \Gamma_e A_e \frac{(\phi_E - \phi_P)}{\delta x_{PE}}$$

$$\text{Flux across the south face} = \Gamma_s A_s \frac{\partial \phi}{\partial y} \Big|_s = \Gamma_s A_s \frac{(\phi_P - \phi_S)}{\delta y_{SP}}$$

$$\text{Flux across the north face} = \Gamma_n A_n \frac{\partial \phi}{\partial y} \Big|_n = \Gamma_n A_n \frac{(\phi_N - \phi_P)}{\delta y_{PN}}$$



$$\rightarrow \Gamma_e A_e \frac{(\phi_E - \phi_P)}{\delta x_{PE}} - \Gamma_w A_w \frac{(\phi_P - \phi_W)}{\delta x_{WP}} + \Gamma_n A_n \frac{(\phi_N - \phi_P)}{\delta y_{PN}} - \Gamma_s A_s \frac{(\phi_P - \phi_S)}{\delta y_{SP}} + \bar{S} \Delta V = 0$$

$$\rightarrow \left(\frac{\Gamma_w A_w}{\delta x_{WP}} + \frac{\Gamma_e A_e}{\delta x_{PE}} + \frac{\Gamma_s A_s}{\delta y_{SP}} + \frac{\Gamma_n A_n}{\delta y_{PN}} - S_p \right) \phi_P = \left(\frac{\Gamma_w A_w}{\delta x_{WP}} \right) \phi_W + \left(\frac{\Gamma_e A_e}{\delta x_{PE}} \right) \phi_E + \left(\frac{\Gamma_s A_s}{\delta y_{SP}} \right) \phi_S + \left(\frac{\Gamma_n A_n}{\delta y_{PN}} \right) \phi_N + S_u$$

$$A_w = A_e = \Delta y; A_n = A_s = \Delta x.$$

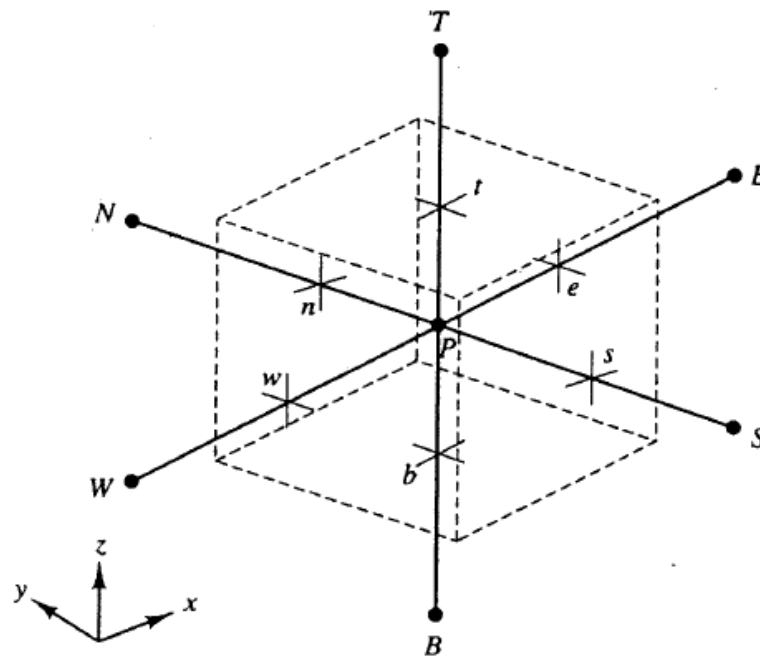
$$\rightarrow a_P \phi_P = a_W \phi_W + a_E \phi_E + a_S \phi_S + a_N \phi_N + S_u$$

a_W	a_E	a_S	a_N	a_P
$\frac{\Gamma_w A_w}{\delta x_{WP}}$	$\frac{\Gamma_e A_e}{\delta x_{PE}}$	$\frac{\Gamma_s A_s}{\delta y_{SP}}$	$\frac{\Gamma_n A_n}{\delta y_{PN}}$	$a_W + a_E + a_S + a_N - S_p$

4.5 Finite volume method for three-dimensional diffusion problems

Steady state diffusion in a three-dimensional situation is governed by

$$\nabla \cdot (\nabla \phi) + S_{\phi} = 0 \quad \rightarrow \quad \frac{\partial}{\partial x} \left(\Gamma \frac{\partial \phi}{\partial x} \right) + \frac{\partial}{\partial y} \left(\Gamma \frac{\partial \phi}{\partial y} \right) + \frac{\partial}{\partial z} \left(\Gamma \frac{\partial \phi}{\partial z} \right) + S = 0$$



A cell in three dimensions and neighbouring nodes

Integration of Equation (4.58) over the control volume shown gives

$$\begin{aligned} & \left[\Gamma_e A_e \left(\frac{\partial \phi}{\partial x} \right)_e - \Gamma_w A_w \left(\frac{\partial \phi}{\partial x} \right)_w \right] + \left[\Gamma_n A_n \left(\frac{\partial \phi}{\partial y} \right)_n - \Gamma_s A_s \left(\frac{\partial \phi}{\partial y} \right)_s \right] \\ & + \left[\Gamma_t A_t \left(\frac{\partial \phi}{\partial z} \right)_t - \Gamma_b A_b \left(\frac{\partial \phi}{\partial z} \right)_b \right] + \bar{S} \Delta V = 0 \end{aligned}$$

$$\begin{aligned} & \left[\Gamma_e \frac{(\phi_E - \phi_P) A_e}{\delta x_{PE}} - \Gamma_w \frac{(\phi_P - \phi_W) A_w}{\delta x_{WP}} \right] \\ & + \left[\Gamma_n \frac{(\phi_N - \phi_P) A_n}{\delta y_{PN}} - \Gamma_s \frac{(\phi_P - \phi_S) A_s}{\delta y_{SP}} \right] \\ & + \left[\Gamma_t \frac{(\phi_T - \phi_P) A_t}{\delta z_{PT}} - \Gamma_b \frac{(\phi_P - \phi_B) A_b}{\delta z_{BP}} \right] + (S_u + S_p \phi_P) = 0 \end{aligned}$$

$$a_P \phi_P = a_W \phi_W + a_E \phi_E + a_S \phi_S + a_N \phi_N + a_B \phi_B + a_T \phi_T + S_u$$

a_W	a_E	a_S	a_N	a_B	a_T	a_P
$\frac{\Gamma_w A_w}{\delta x_{WP}}$	$\frac{\Gamma_e A_e}{\delta x_{PE}}$	$\frac{\Gamma_s A_s}{\delta y_{SP}}$	$\frac{\Gamma_n A_n}{\delta y_{PN}}$	$\frac{\Gamma_b A_b}{\delta z_{BP}}$	$\frac{\Gamma_t A_t}{\delta z_{PT}}$	$a_W + a_E + a_S + a_N$ $+ a_B + a_T - S_p$

4.6 Summary of discretised equations for diffusion problems

- The discretised equations for one-, two- and three dimensional diffusion problems

$$a_P \phi_P = \sum a_{nb} \phi_{nb} + S_u \quad a_P = \sum a_{nb} - S_D$$

	a_w	a_E	a_S	a_N	a_B	A_T
1D	$\frac{\Gamma_w A_w}{\delta x_{WP}}$	$\frac{\Gamma_e A_e}{\delta x_{PE}}$	-	-	-	-
2D	$\frac{\Gamma_w A_w}{\delta x_{WP}}$	$\frac{\Gamma_e A_e}{\delta x_{PE}}$	$\frac{\Gamma_s A_s}{\delta y_{SP}}$	$\frac{\Gamma_n A_n}{\delta y_{PN}}$	-	-
3D	$\frac{\Gamma_w A_w}{\delta x_{WP}}$	$\frac{\Gamma_e A_e}{\delta x_{PE}}$	$\frac{\Gamma_s A_s}{\delta y_{SP}}$	$\frac{\Gamma_n A_n}{\delta y_{PN}}$	$\frac{\Gamma_b A_b}{\delta y_{BP}}$	$\frac{\Gamma_t A_t}{\delta z_{PT}}$

Source terms $\bar{S} \Delta V = S_u + S_p \phi_P$ and specifying values for S_u and S_p .

For a one-dimensional control volume of width $\Delta \zeta$ with a boundary B:

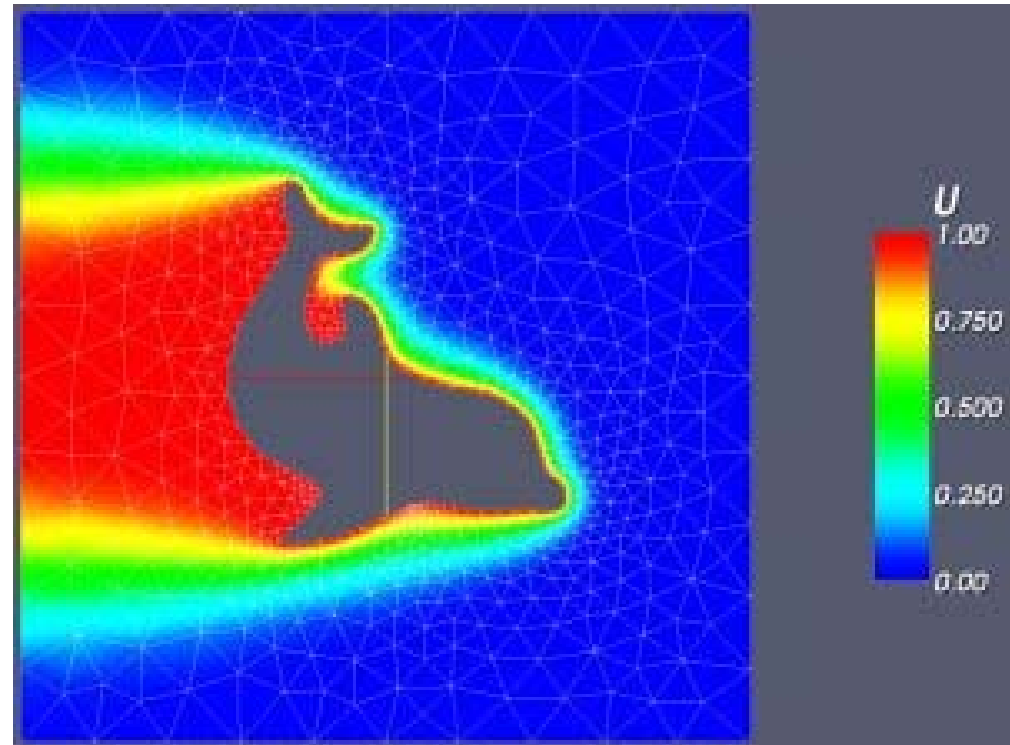
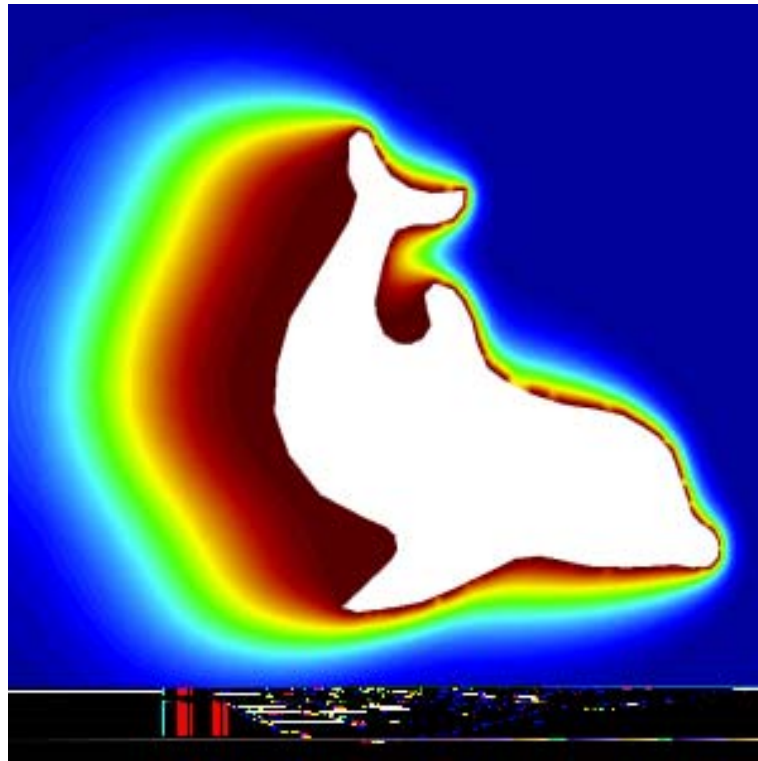
source contributions : fixed value ϕ_B : $S_u = \frac{2k_B A_B}{\Delta \zeta} \phi_B$;

$$S_p = -\frac{2k_B A_B}{\Delta \zeta}$$

fixed flux q_B : $S_u + S_p \phi_P = q_B$

Chapter 4

The Finite Volume Method for Convection-Diffusion Problems



2.4 Conservative form of the governing equations of a compressible Newtonian fluid

Mass	$\frac{\partial \rho}{\partial t} + \text{div}(\rho \mathbf{u}) = 0$	(2.4)
x-momentum	$\frac{\partial(\rho u)}{\partial t} + \text{div}(\rho u \mathbf{u}) = -\frac{\partial p}{\partial x} + \text{div}(\mu \text{grad } u) + S_{Mx}$	(2.37a)
y-momentum	$\frac{\partial(\rho v)}{\partial t} + \text{div}(\rho v \mathbf{u}) = -\frac{\partial p}{\partial y} + \text{div}(\mu \text{grad } v) + S_{My}$	(2.37b)
z-momentum	$\frac{\partial(\rho w)}{\partial t} + \text{div}(\rho w \mathbf{u}) = -\frac{\partial p}{\partial z} + \text{div}(\mu \text{grad } w) + S_{Mz}$	(2.37c)
Internal energy	$\frac{\partial(\rho i)}{\partial t} + \text{div}(\rho i \mathbf{u}) = -p \text{div } \mathbf{u} + \text{div}(k \text{grad } T) + \Phi + S_i$	(2.38)
Equations of state	$p = p(\rho, T) \text{ and } i = i(\rho, T)$	(2.28)
	e.g. perfect gas	
	$p = \rho RT \text{ and } i = C_v T$	(2.29)

General form:

$$\frac{\partial(\rho \phi)}{\partial t} + \text{div}(\rho \phi \mathbf{u}) = \text{div}(\Gamma \text{grad } \phi) + S_\phi$$

$$\frac{\partial(\rho\phi)}{\partial t} + \text{div}(\rho\phi\mathbf{u}) = \text{div}(\Gamma \text{ grad } \phi) + S_\phi$$

using Gauss' divergence theorem. $\int_{CV} \text{div } \mathbf{a} dV = \int_A \mathbf{n} \cdot \mathbf{a} dA$

The steady convection-diffusion equation can be derived from the transport equation for a general property Φ by deleting the transient term

$$\int_A \mathbf{n} \cdot (\rho\phi\mathbf{u}) dA = \int_A \mathbf{n} \cdot (\Gamma \text{ grad } \phi) dA + \int_{CV} S_\phi dV$$

5.2 Steady one-dimensional convection and diffusion

The governing equations for the 1-D steady flow without heat source is

→ $\frac{d(\rho u)}{dx} = 0$
Mass

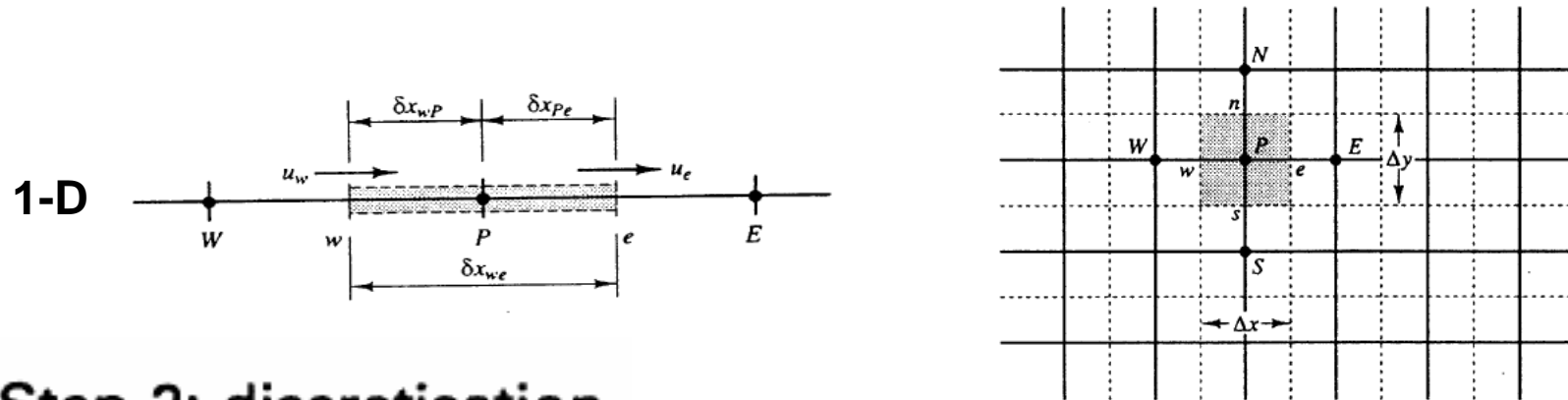
$$\frac{d}{dx}(\rho u \phi) = \frac{d}{dx} \left(\Gamma \frac{d\phi}{dx} \right)$$

x-momentum

Finite volume method for 1-D steady state convection and diffusion

Step 1: Grid generation

The first step is to divide the computational domain into discrete control volumes.

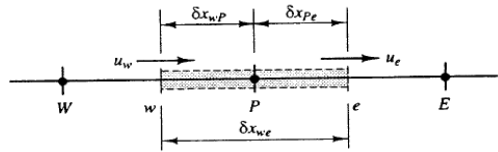


Step 2: discretisation

$$\int_A \mathbf{n} \cdot (\rho \phi \mathbf{u}) dA = \int_A \mathbf{n} \cdot (\Gamma \text{grad } \phi) dA + \int_{CV} S_\phi dV$$

$$\frac{d}{dx} (\rho u \phi) = \frac{d}{dx} \left(\Gamma \frac{d\phi}{dx} \right) \rightarrow (\rho u A \phi)_e - (\rho u A \phi)_w = \left(\Gamma A \frac{\partial \phi}{\partial x} \right)_e - \left(\Gamma A \frac{\partial \phi}{\partial x} \right)_w$$

Integration of transport equation $\frac{d}{dx}(\rho u \phi) = \frac{d}{dx} \left(\Gamma \frac{d\phi}{dx} \right)$ gives



$$(\rho u A \phi)_e - (\rho u A \phi)_w = \left(\Gamma A \frac{\partial \phi}{\partial x} \right)_e - \left(\Gamma A \frac{\partial \phi}{\partial x} \right)_w$$

integration of continuity equation yields $\frac{\partial \rho}{\partial t} + \text{div}(\rho \mathbf{u}) = 0$

$$(\rho u A)_e - (\rho u A)_w = 0 \quad \rightarrow \quad F_e - F_w = 0$$

Definition: the convective mass flux per unit area : $F = \rho u$ [Kg/s m²]

the diffusion conductance at cell faces : $D = \frac{\Gamma}{\delta x}$ [Kg/m · s]

$$F_w = (\rho u)_w, \quad F_e = (\rho u)_e$$

$$D_w = \frac{\Gamma_w}{\delta x_{WP}}, \quad D_e = \frac{\Gamma_e}{\delta x_{PE}}$$

The central differencing scheme

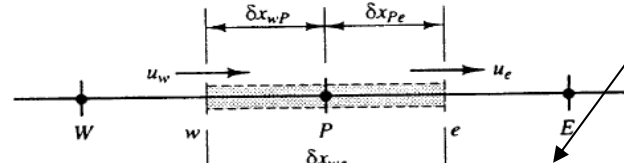
$$\left(\frac{\partial \phi}{\partial x}\right)_P = \frac{\phi_E - \phi_W}{2\Delta x} + O(\Delta x^2)$$

Assumption: **linear interpolation** for transported property Φ and **a uniform grid**

$A = \text{Const.}$

$$\phi_e = (\phi_P + \phi_E)/2$$

$$\phi_w = (\phi_W + \phi_P)/2$$



$$F_w = (\rho u)_w, \quad D_w = \frac{\Gamma_w}{\delta x_{WP}}$$

$$F_e = (\rho u)_e, \quad D_e = \frac{\Gamma_e}{\delta x_{PE}}$$

$$(\rho u A \phi)_e - (\rho u A \phi)_w = \left(\Gamma A \frac{\partial \phi}{\partial x} \right)_e - \left(\Gamma A \frac{\partial \phi}{\partial x} \right)_w$$



$$F_e \phi_e - F_w \phi_w = D_e (\phi_E - \phi_P) - D_w (\phi_P - \phi_W)$$



$$\frac{F_e}{2} (\phi_P + \phi_E) - \frac{F_w}{2} (\phi_W + \phi_P) = D_e (\phi_E - \phi_P) - D_w (\phi_P - \phi_W)$$



$$\left[\left(D_w - \frac{F_w}{2} \right) + \left(D_e + \frac{F_e}{2} \right) \right] \phi_P = \left(D_w + \frac{F_w}{2} \right) \phi_W + \left(D_e - \frac{F_e}{2} \right) \phi_E$$



$$\left[\left(D_w + \frac{F_w}{2} \right) + \left(D_e - \frac{F_e}{2} \right) + (F_e - F_w) \right] \phi_P = \left(D_w + \frac{F_w}{2} \right) \phi_W + \left(D_e - \frac{F_e}{2} \right) \phi_E$$



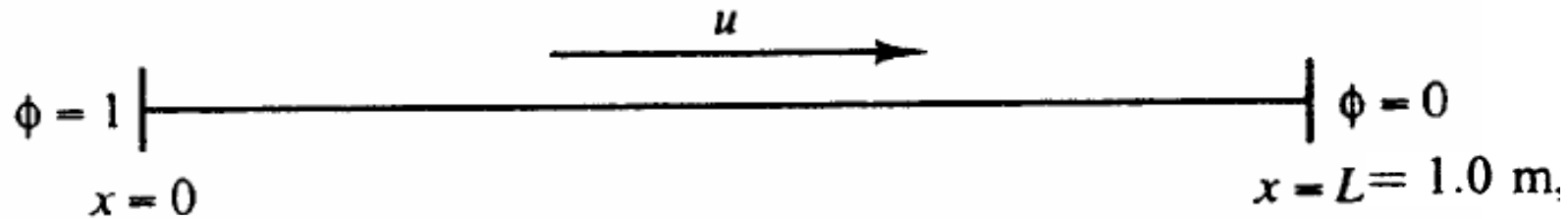
$$a_P \phi_P = a_W \phi_W + a_E \phi_E$$

a_W	a_E	a_P
$D_w + \frac{F_w}{2}$	$D_e - \frac{F_e}{2}$	$a_W + a_E + (F_e - F_w)$

Step 3: Solution of Discretization Equations for all grid nodes

Example 5.1

1-D steady state convection and diffusion, ϕ is the property



x-momentum $\frac{d}{dx}(\rho u \phi) = \frac{d}{dx} \left(\Gamma \frac{d\phi}{dx} \right)$ $\rho = 1.0 \text{ kg/m}^3$, $\Gamma = 0.1 \text{ kg/m/s}$.

Using five equally spaced cells and the central differencing scheme for convection and diffusion

calculate the distribution of ϕ as a function of x for

(i) Case 1: $u = 0.1$ m/s with 5 grid nodes

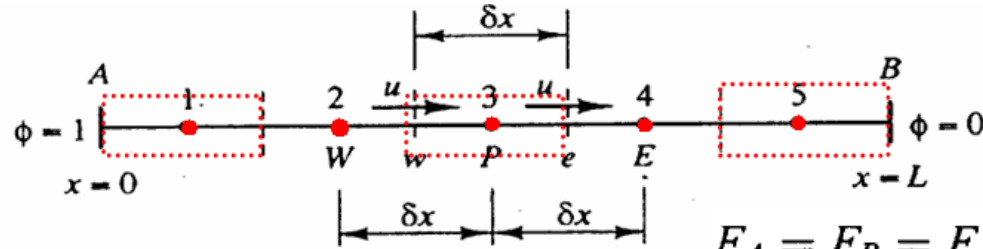
$$\delta x = 1 / 5 = 0.2$$

(ii) Case 2: $u = 2.5$ m/s with 5 grid nodes

(iii) Case 3: $u = 2.5$ m/s with 20 grid nodes

$$\delta x = 1 / 25 = 0.04$$

Solution



$$F_A = F_B = F \text{ and } D_B = 2\Gamma/\delta x = 2D$$

$$\rho = 1.0 \text{ kg/m}^3, \Gamma = 0.1 \text{ kg/m/s}$$

P=1

$$F_e\phi_e - F_w\phi_w = D_e(\phi_E - \phi_P) - D_w(\phi_P - \phi_W)$$

for node 1:

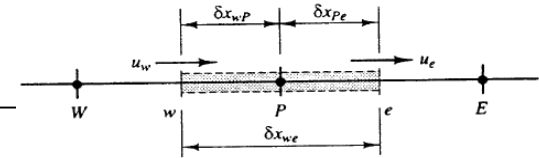
$$\frac{F_e}{2}(\phi_P + \phi_E) - F_A\phi_A = D_e(\phi_E - \phi_P) - D_A(\phi_P - \phi_A)$$

$$\phi_w = \phi_A \quad F_w = F_A$$

$$\Rightarrow a_P\phi_P = a_W\phi_W + a_E\phi_E + S_u \quad a_P = a_W + a_E + (F_e - F_w) - S_D$$

for nodal points 2, 3 and 4:

P=2, 3, 4



$$\left[\left(D_w + \frac{F_w}{2} \right) + \left(D_e - \frac{F_e}{2} \right) + (F_e - F_w) \right] \phi_P = \left(D_w + \frac{F_w}{2} \right) \phi_W + \left(D_e - \frac{F_e}{2} \right) \phi_E$$

$$\Rightarrow a_P\phi_P = a_W\phi_W + a_E\phi_E \quad a_P = a_W + a_E + (F_e - F_w)$$

Boundary node

$$F_e\phi_e - F_w\phi_w = D_e(\phi_E - \phi_P) - D_w(\phi_P - \phi_W) \quad F_A = F_B = F \text{ and } D_B = 2\Gamma/\delta x = 2D$$

for node 5

$$F_B\phi_B - \frac{\Gamma_w}{\gamma}(\phi_P + \phi_W) = D_B(\phi_B - \phi_P) - D_w(\phi_P - \phi_W)$$

P=5

$$\phi_e = \phi_B \quad F_e = F_B$$

$$\Rightarrow a_P\phi_P = a_W\phi_W + a_E\phi_E + S_u \quad a_P = a_W + a_E + (F_e - F_w) - S_P$$

but $F = F_e = F_w = \rho u = 2.5$ $D = D_e = D_w = \Gamma / \delta x = 0.5$
 $F_A = F_B = F$ and $D_B = 2\Gamma / \delta x = 2D$

Node	a_w	a_E	S_p	S_u
1	0	$D - F/2$	$-(2D + F)$	$(2D + F)\phi_A$
2, 3, 4	$D + F/2$	$D - F/2$	0	0
5	$D + F/2$	0	$-(2D - F)$	$(2D - F)\phi_B$

(i) Case 1 $u = 0.1$ m/s: $\rho = 1.0$ kg/m³, $\Gamma = 0.1$ kg/m/s
 $F = \rho u = 0.1$, $D = \Gamma / \delta x = 0.1 / 0.2 = 0.5$ (F/D=0.2)

Node	a_w	a_E	S_u	S_p	$a_p P = a_w + a_E - S_p$
1	0	0.45	$1.1\phi_A$	-1.1	1.55
2	0.55	0.45	0	0	1.0
3	0.55	0.45	0	0	1.0
4	0.55	0.45	0	0	1.0
5	0.55	0	$0.9\phi_B$	-0.9	1.45

$$\begin{bmatrix} 1.55 & -0.45 & 0 & 0 & 0 \\ -0.55 & 1.0 & -0.45 & 0 & 0 \\ 0 & -0.55 & 1.0 & -0.45 & 0 \\ 0 & 0 & -0.55 & 1.0 & -0.45 \\ 0 & 0 & 0 & -0.55 & 1.45 \end{bmatrix} \begin{bmatrix} \phi_1 \\ \phi_2 \\ \phi_3 \\ \phi_4 \\ \phi_5 \end{bmatrix} = \begin{bmatrix} 1.1 \\ 0 \\ 0 \\ 0 \\ 0 \end{bmatrix}$$

using $\phi_A = 1$ and $\phi_B = 0$

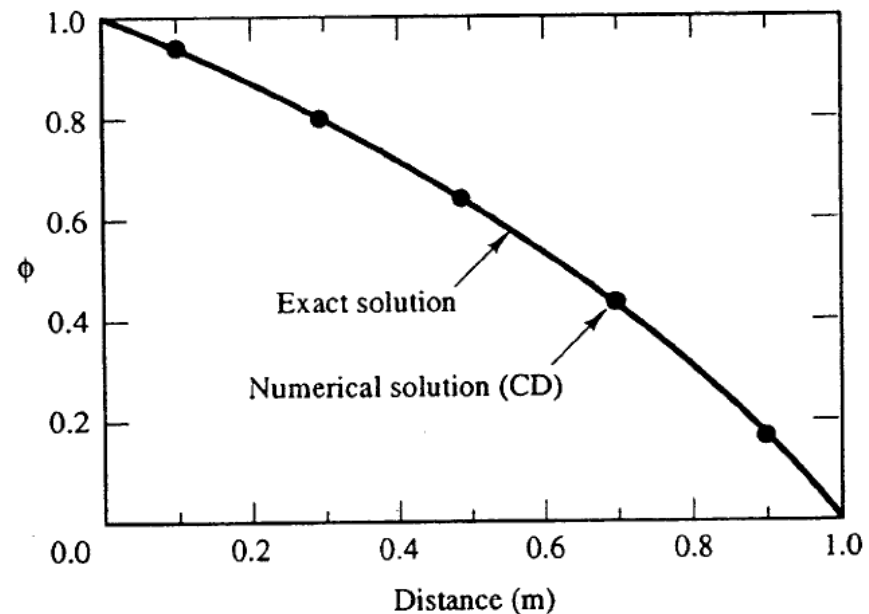
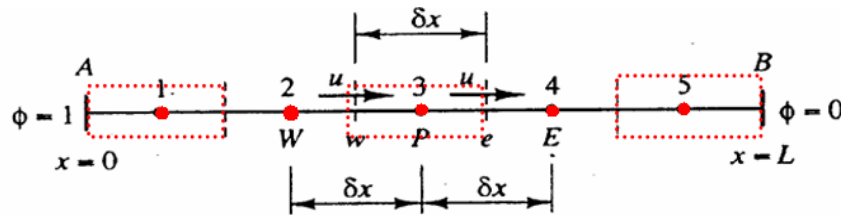
The solution to the above system is

$$\begin{bmatrix} \phi_1 \\ \phi_2 \\ \phi_3 \\ \phi_4 \\ \phi_5 \end{bmatrix} = \begin{bmatrix} 0.9421 \\ 0.8006 \\ 0.6276 \\ 0.4163 \\ 0.1579 \end{bmatrix}$$

Comparison with the analytical solution

$$\frac{\phi - \phi_0}{\phi_L - \phi_0} = \frac{\exp(\rho u x / \Gamma) - 1}{\exp(\rho u L / \Gamma) - 1} \quad \phi(x) = 1 + \frac{1 - \exp(25x)}{7.20 \times 10^{10}}$$

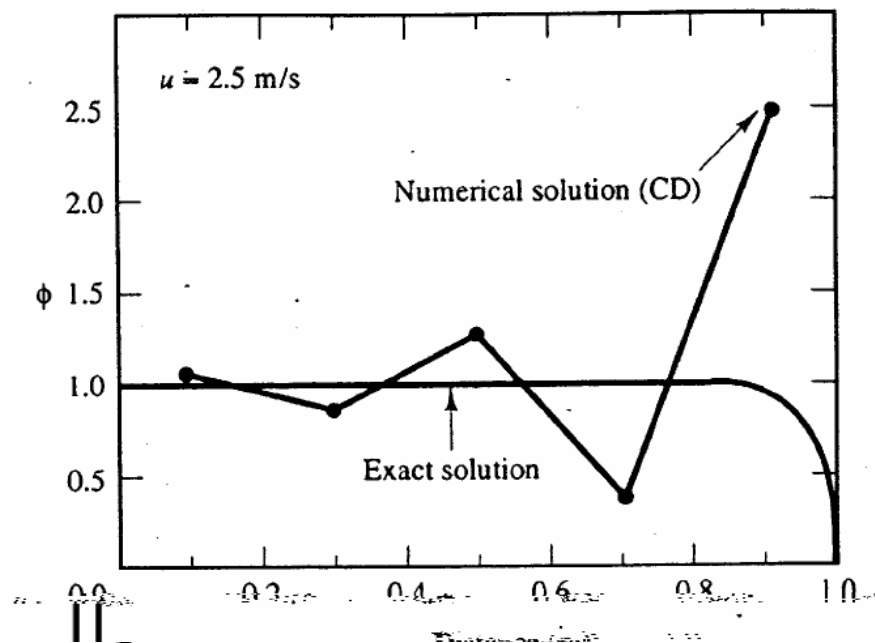
Node	Distance	Finite volume solution	Analytical solution	Difference	Percentage error
1	0.1	0.9421	0.9387	-0.003	-0.36
2	0.3	0.8006	0.7963	-0.004	-0.53
3	0.5	0.6276	0.6224	-0.005	-0.83
4	0.7	0.4163	0.4100	-0.006	-1.53
5	0.9	0.1579	0.1505	-0.007	-4.91



(ii) Case 2: $u = 2.5$ m/s with 5 grid nodes

$$F = \rho u = 2.5, D = \Gamma / \delta x = 0.1 / 0.2 = 0.5 \quad \boxed{(F/D=5)}$$

Node	Distance	Finite volume solution	Analytical solution	Difference	Percentage error
1	0.1	1.0356	1.0000	-0.035	-3.56
2	0.3	0.8694	0.9999	0.131	13.05
3	0.5	1.2573	0.9999	-0.257	-25.74
4	0.7	0.3521	0.9994	0.647	64.70
5	0.9	2.4644	0.9179	-1.546	-168.48

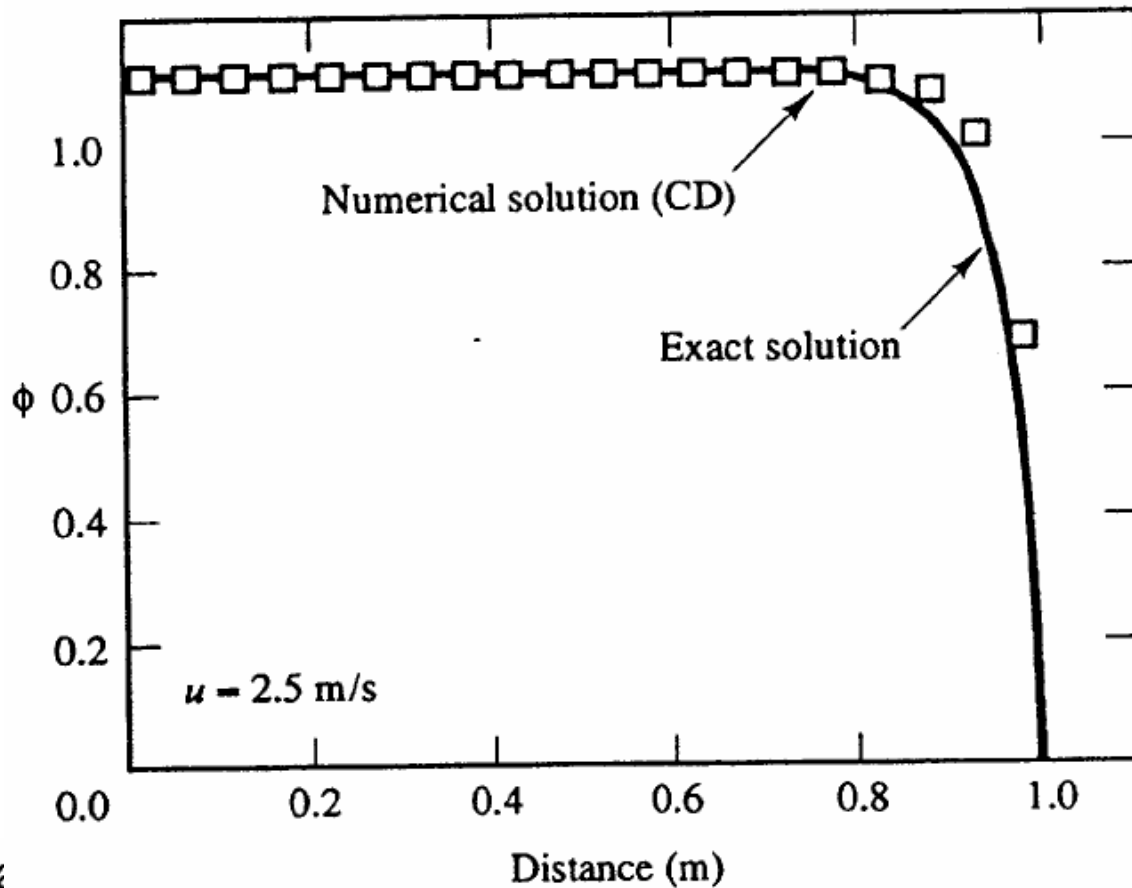


i. e. When the ratio of **F/D** is high the solution based on **central difference scheme** appears the wiggles oscillations (F/D=5)

These oscillations are often called 'wiggles' 扭動

the agreement with the analytical solution is clearly not very good.

(iii) Case 3: $u = 2.5$ m/s with 20 grid nodes ($F/D=1.25$)
 $\delta x = 0.05$, $F = \rho u = 2.5$, $D = \Gamma/\delta x = 0.1/0.05 = 2.0$.
 grid refinement has reduced the F/D ratio from 5 to 1.25.



Grid Independence

The centre

Distance (m)

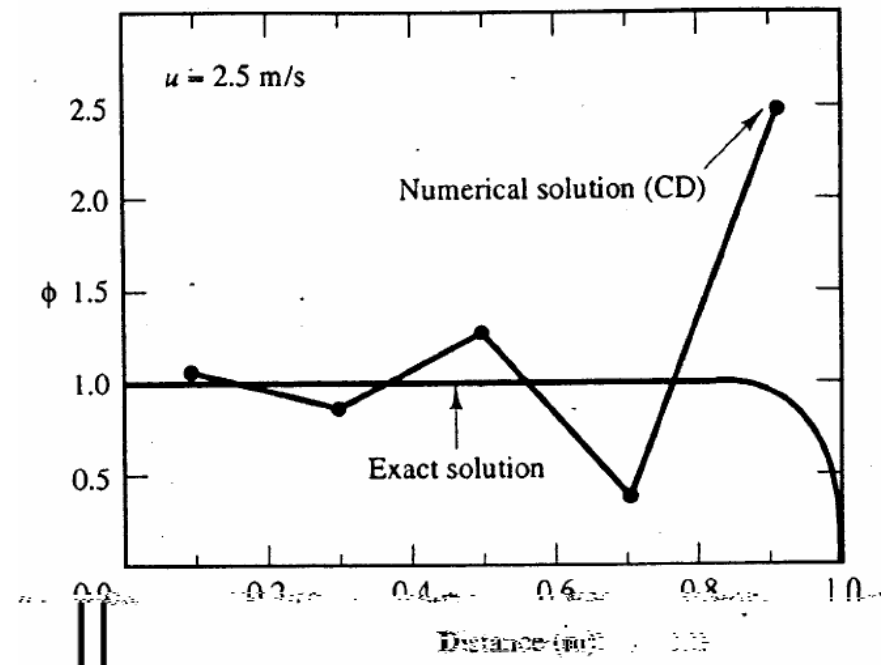
when the F/D ratio is low.

The agreement between the numerical results and the analytical solution is now good

5.4 Properties of discretisation schemes

✘ To avoid the appearance of wiggles in the central difference solution, the discretisation scheme should have the fundamental properties as follows:

- Conservativeness
- Boundedness
- Transportiveness



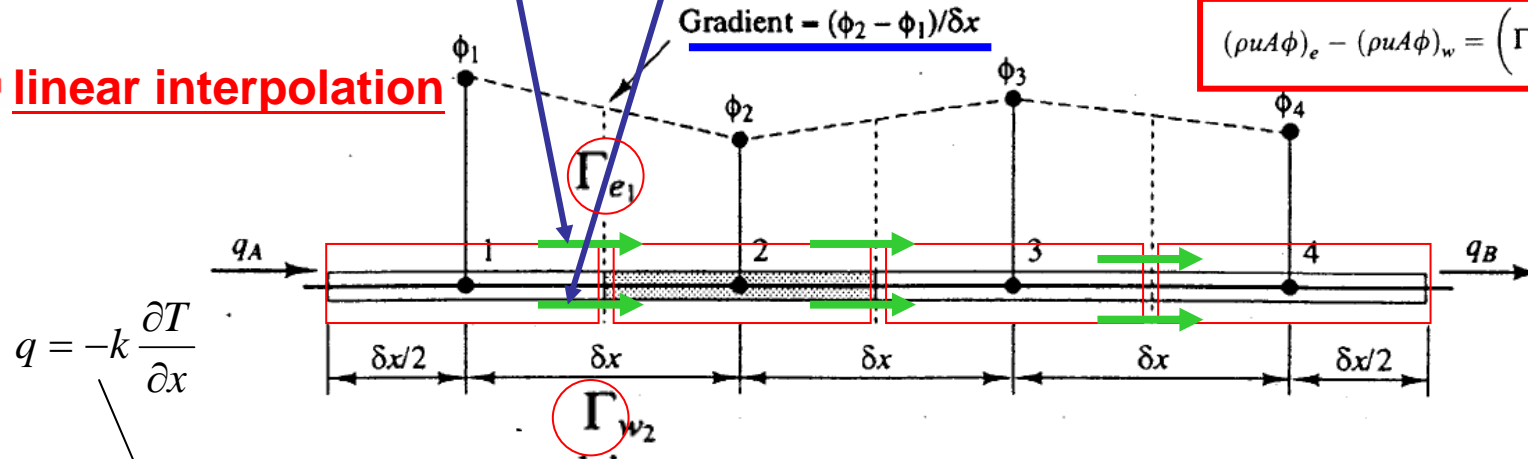
5.4.1 Conservativeness

To ensure conservation of Φ for the whole solution domain in the flux of Φ leaving a control volume across a certain face must be equal to the flux of Φ entering the adjacent control volume through same face i. e.

$$\Gamma_{e_1} = \Gamma_{w_2} \quad \Gamma_{e_2} = \Gamma_{w_3} \quad \Gamma_{e_3} = \Gamma_{w_4} \quad \Gamma_{in} = \Gamma_{out}$$

$$(\rho u A \phi)_e - (\rho u A \phi)_w = \left(\Gamma A \frac{\partial \phi}{\partial x} \right)_e - \left(\Gamma A \frac{\partial \phi}{\partial x} \right)_w$$

● linear interpolation



$$\begin{aligned} & \left[\Gamma_{e_1} \frac{(\phi_2 - \phi_1)}{\delta x} - q_A \right] + \left[\Gamma_{e_2} \frac{(\phi_3 - \phi_2)}{\delta x} - \Gamma_{w_2} \frac{(\phi_2 - \phi_1)}{\delta x} \right] \\ + & \left[\Gamma_{e_3} \frac{(\phi_4 - \phi_3)}{\delta x} - \Gamma_{w_3} \frac{(\phi_3 - \phi_2)}{\delta x} \right] + \left[q_B - \Gamma_{w_4} \frac{(\phi_4 - \phi_3)}{\delta x} \right] \\ & = q_B - q_A \quad \text{Linear function} \\ & \neq q_B - q_A \quad \text{Quadratic function} \end{aligned}$$

5.4.3 Transportiveness

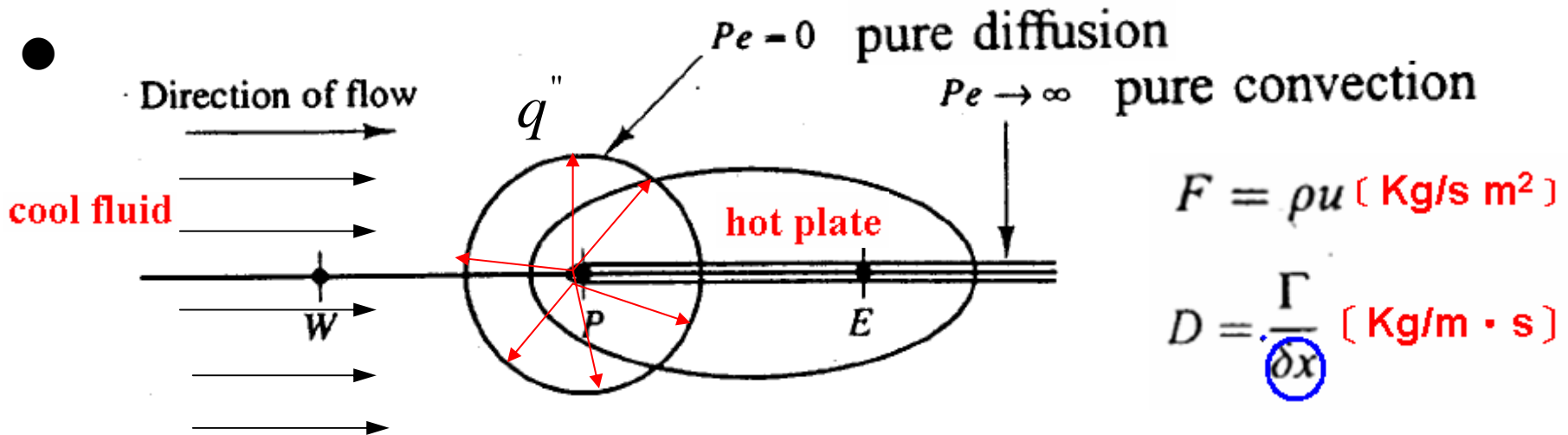
$$Pe = Re Pr = ux / \alpha$$

Convection-Diffusion Problems

- **Definite** a non-dimensional cell Peclet number Pe as a measure of the relative strengths of convection and diffusion

$$Pe = \frac{F}{D} = \frac{\rho u}{\Gamma / \delta x} = \frac{\text{the convective mass flux per unit area}}{\text{diffusion conductance at cell faces}}$$

Low

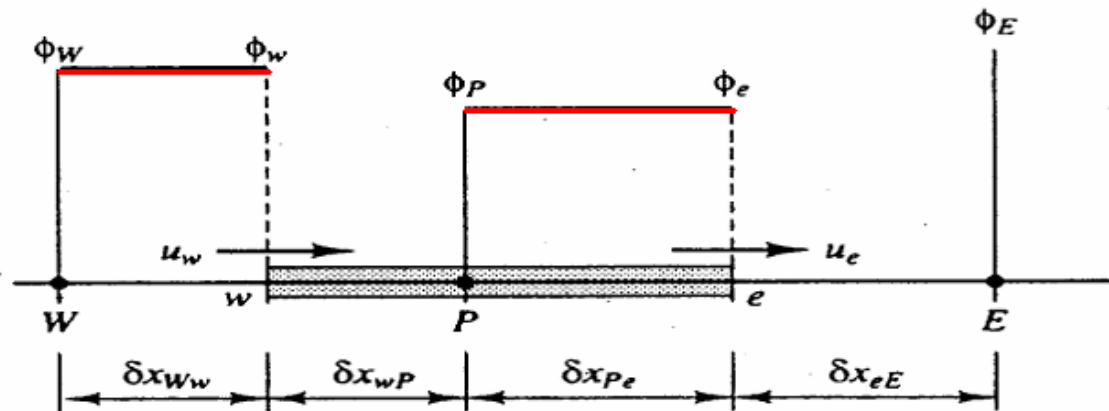


- The relationship between the magnitude of Pe and the directionality of influencing is known as **Transportiveness**

5.6 The upwind differencing scheme

- One of the major inadequacies of the central differencing scheme is its inability to identify flow direction.

Finite volume method for 1-D steady state convection and diffusion



$$F = \rho u \text{ [Kg/s m}^2 \text{]}$$

$$D = \frac{\Gamma}{\delta x} \text{ [Kg/m} \cdot \text{s]}$$

- (1) When the flow is in the positive direction,

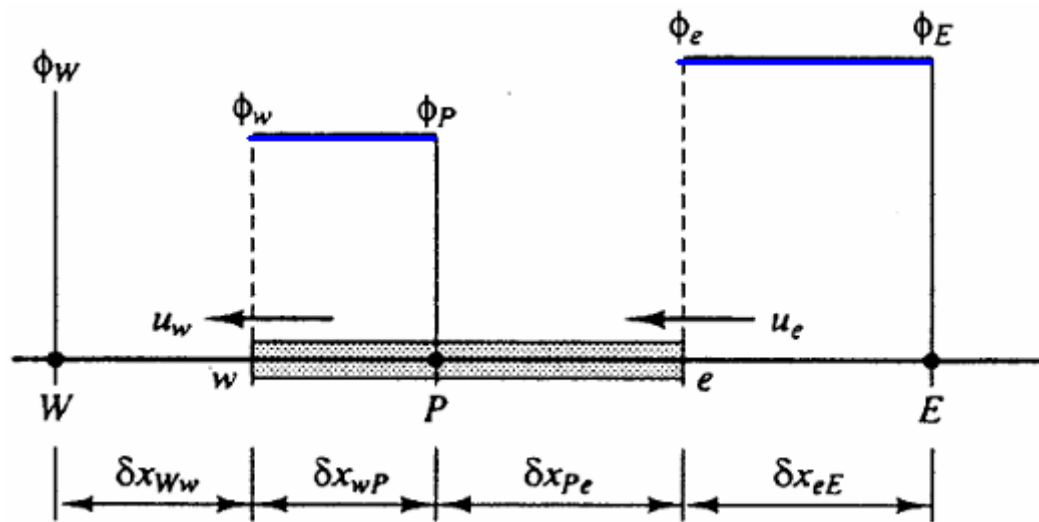
$$\underline{u_w > 0, u_e > 0 (F_w > 0, F_e > 0) \quad \phi_w = \phi_W \text{ and } \phi_e = \phi_P}$$

$$\text{discretised equation } F_e \phi_P - F_w \phi_W = D_e (\phi_E - \phi_P) - D_w (\phi_P - \phi_W)$$

$$(D_w + D_e + F_e) \phi_P = (D_w + F_w) \phi_W + D_e \phi_E$$

$$[(D_w + F_w) + D_e + (F_e - F_w)] \phi_P = (D_w + F_w) \phi_W + D_e \phi_E$$

When the flow is in the negative direction,



$$F = \rho u \text{ [Kg/s m}^2 \text{]}$$

$$D = \frac{\Gamma}{\delta x} \text{ [Kg/m} \cdot \text{s]}$$

$$u_w < 0, u_e < 0 (F_w < 0, F_e < 0) \quad \phi_w = \phi_P \text{ and } \phi_e = \phi_E$$

discretised equation

$$F_e \phi_e - F_w \phi_w = D_e (\phi_E - \phi_P) - D_w (\phi_P - \phi_W)$$

$$\Rightarrow F_e \phi_E - F_w \phi_P = D_e (\phi_E - \phi_P) - D_w (\phi_P - \phi_W)$$

$$\Rightarrow [D_w + (D_e - F_e) + (F_e - F_w)] \phi_P = D_w \phi_W + (D_e - F_e) \phi_E$$

比較 $[(D_w + F_w) + D_e + (F_e - F_w)] \phi_P = (D_w + F_w) \phi_W + D_e \phi_E$

$$a_P \phi_P = a_W \phi_W + a_E \phi_E$$

with central coefficient

$$a_P = a_W + a_E + (F_e - F_w)$$



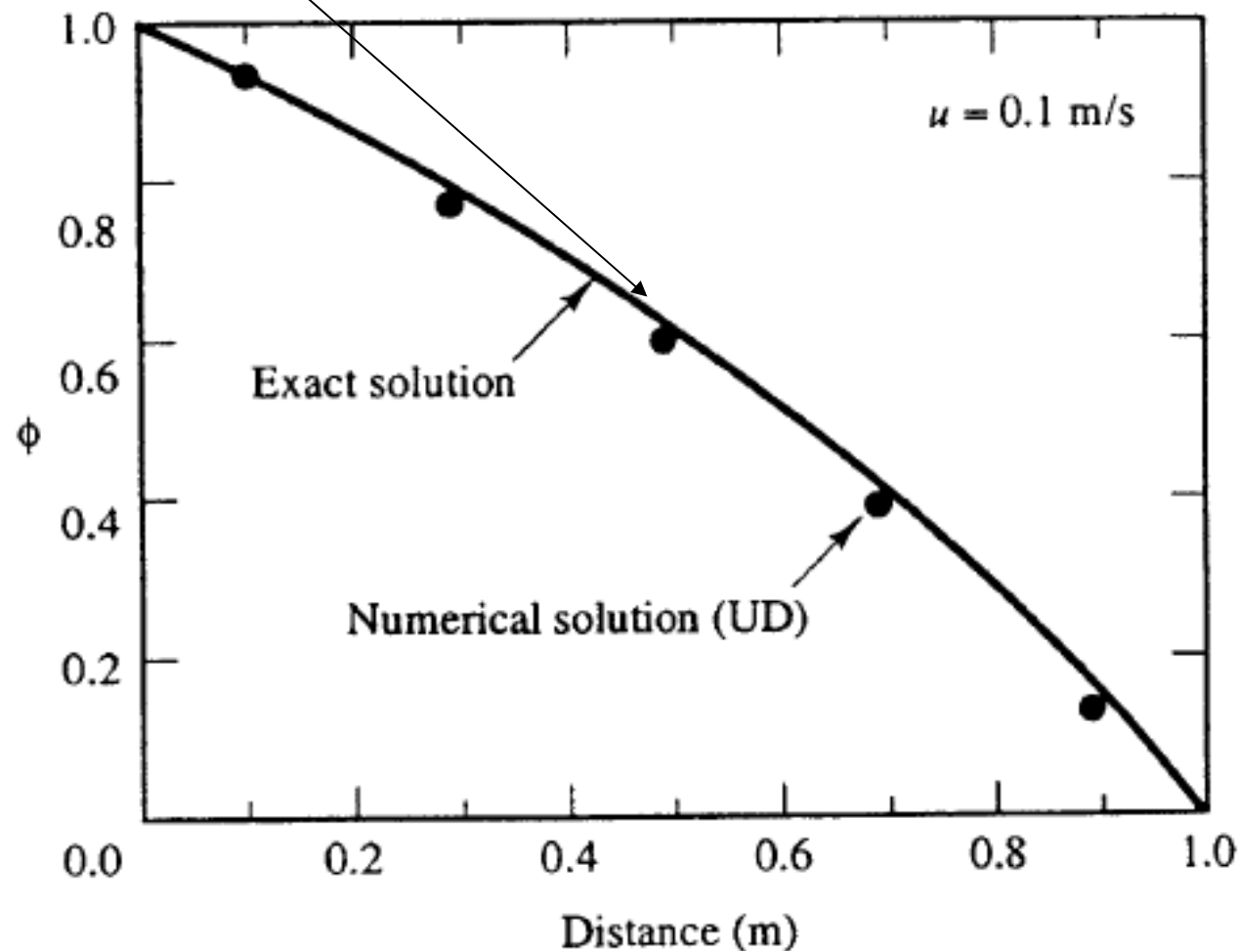
	a_W	a_E
$F_w > 0, F_e > 0$	$D_w + F_w$	D_e
$F_w < 0, F_e < 0$	D_w	$D_e - F_e$

A form of notation for the **neighbour coefficients of the upwind differencing method** that covers both flow directions is given below:

a_W	a_E
$D_w + \max(F_w, 0)$	$D_e + \max(0, -F_e)$

$$\frac{\phi - \phi_0}{\phi_L - \phi_0} = \frac{\exp(\rho u x / \Gamma) - 1}{\exp(\rho u L / \Gamma) - 1}$$

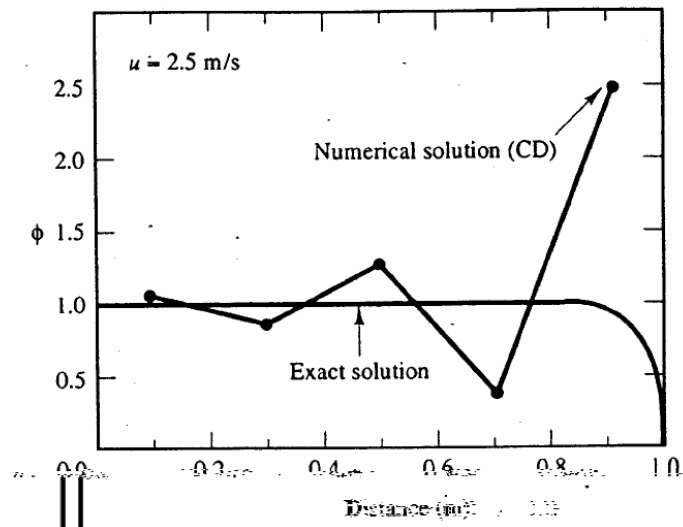
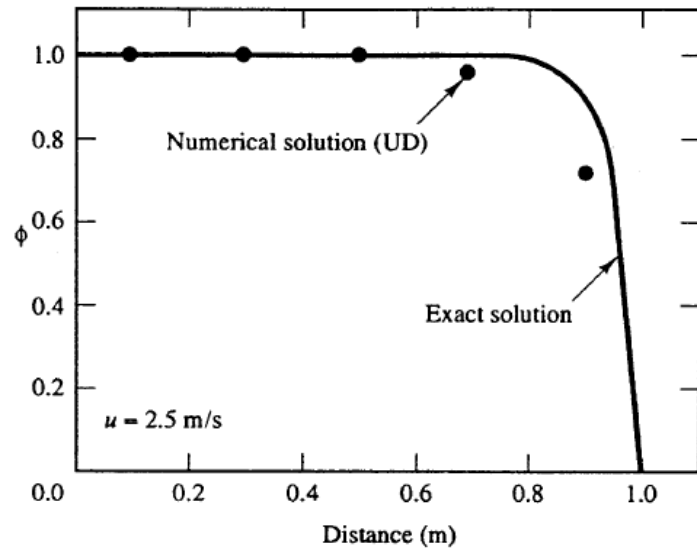
Fig. 5.12 Comparison of the upwind difference numerical results and the analytical solution for Case 1



(ii) Case 2: $u = 2.5$ m/s with 5 grid nodes

$$F = \rho u = 2.5, D = \Gamma / \delta x = 0.1 / 0.2 = 0.5 \quad Pe = 5.$$

Node	Distance	Finite volume solution	Analytical solution	Difference	Percentage error
1	0.1	0.9998	0.9999	0.0001	0.00
2	0.3	0.9987	0.9999	0.001	0.01
3	0.5	0.9921	0.9999	0.007	0.70
4	0.7	0.9524	0.9994	0.047	4.70
5	0.9	0.7143	0.8946	0.180	20.15



The central differencing scheme failed to produce a reasonable result with the same grid resolution. The upwind scheme produces a much more realistic solution that is, however, not very close to the exact solution near boundary B .

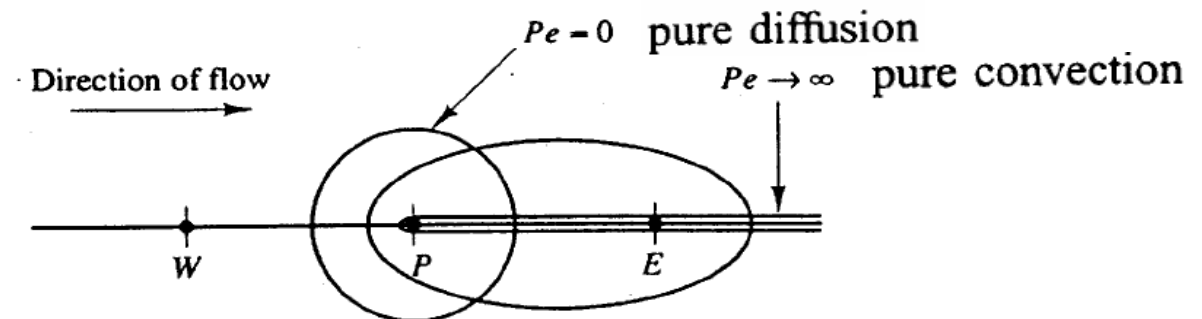
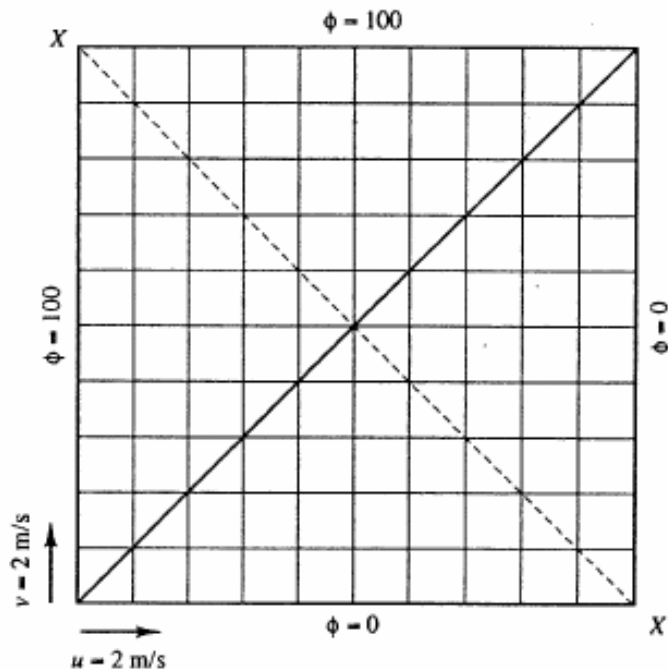
The resulting error caused by upwind method has a diffusion-like appearance (**false diffusion**)

5.6.1 Assessment of the upwind differencing scheme

Conservativeness O. K.

Boundedness O. K.

Transportiveness O. K.



Since there is no physical diffusion the exact solution exhibits a step change of ϕ from 100 to zero when the diagonal X-X crosses the solid diagonal.

5.7 The hybrid differencing scheme Spalding (1972)

The hybrid differencing scheme is based on a combination of central and upwind differencing schemes.

$$Pe = \frac{F}{D} = \frac{\rho u}{\Gamma/\delta x} = \frac{\text{the convective mass flux per unit area}}{\text{diffusion conductance at cell faces}}$$

- for small Peclet numbers ($Pe < 2$) $\rho u < 2\Gamma/\delta x$

The central differencing scheme accurate to second-order

•(3) a central difference formula with second-order accurate. $O(\Delta x^2)$

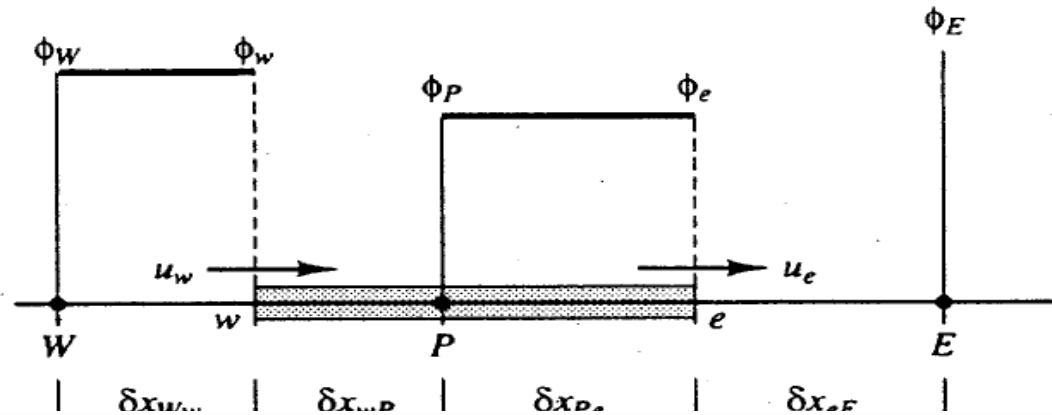
$$\phi(x + \Delta x) - \phi(x - \Delta x) = 2 \left(\frac{\partial \phi}{\partial x} \right)_p \Delta x + \left(\frac{\partial^3 \phi}{\partial x^3} \right)_p \frac{\Delta x^3}{3!} + \dots$$

$$\left(\frac{\partial \phi}{\partial x} \right)_p = \frac{\phi_E - \phi_W}{2\Delta x} + O(\Delta x^2)$$

- for large Peclet numbers ($Pe \geq 2$). $\rho u > 2\Gamma/\delta x$

The upwind scheme is accurate to first order

but accounts for transportiveness



The hybrid differencing formula for the net flux per unit area through the west face is

- (i) for low Peclet numbers $|Pe| < 2$ using central differencing for the convection and diffusion terms.

$$q_w = F_w \left[\frac{1}{2} \left(1 + \frac{2}{Pe_w} \right) \phi_W + \frac{1}{2} \left(1 - \frac{2}{Pe_w} \right) \phi_P \right] \quad \text{for } -2 < Pe_w < 2 \quad \text{(對流與傳導均重要)}$$

- (ii) when $|Pe| > 2$ using upwind differencing schemes for convection and setting the diffusion to zero

$$q_w = F_w A_w \phi_W \quad \text{for } Pe_w \geq 2$$

$$q_w = F_w A_w \phi_P \quad \text{for } Pe_w \leq -2$$

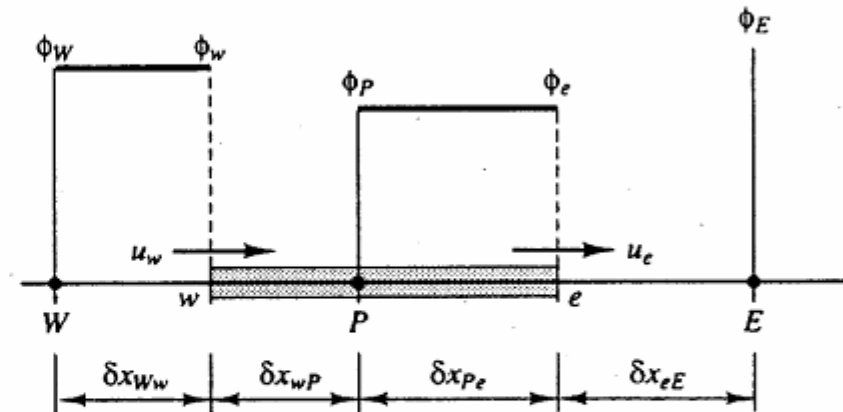
$$\phi_w = \phi_P \quad \text{and} \quad \phi_e = \phi_E$$

for steady one-dimensional convection–diffusion
the hybrid differencing scheme can be written as follows:

the discretised equation

$$a_P \phi_P = a_W \phi_W + a_E \phi_E$$

$$a_P = a_W + a_E + (F_e - F_w)$$



a_W	a_E
$\max \left[F_w, \left(D_w + \frac{F_w}{2} \right), 0 \right]$	$\max \left[-F_e, \left(D_e - \frac{F_e}{2} \right), 0 \right]$

a_W	a_E
$D_w + \max(F_w, 0)$	$D_e + \max(0, -F_e)$

5.7.1 Assessment of the hybrid differencing scheme

The hybrid difference scheme exploits the favourable properties of the upwind and central differencing schemes. It switches to the upwind differencing when the central differencing produces inaccurate results at high Pe numbers. The scheme is fully conservative and since the coefficients are always positive it is unconditionally bounded. • It satisfies the transportiveness requirement by using an upwind formulation for large values of Peclet number. The scheme produces physically realistic solutions and is highly stable when compared with the higher order schemes to be discussed later in the chapter. • Hybrid differencing has been widely used in various computational fluid dynamics (CFD) procedures and has proved to be very useful for predicting practical flows. • The disadvantage is that the accuracy in terms of Taylor series truncation error is only first-order.

5.7.2 Hybrid differencing scheme for multi-dimensional convection–diffusion

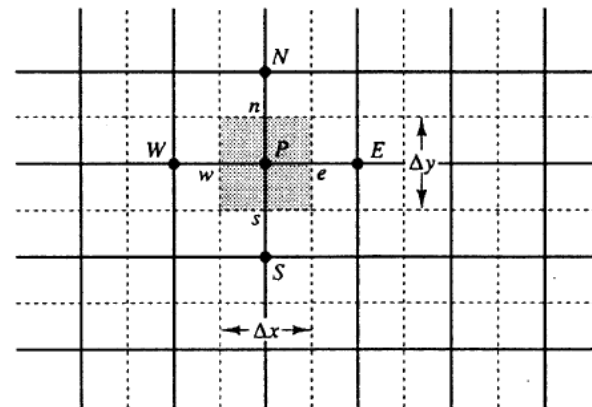
The discretised equation that covers all cases is given by

$$a_P \phi_P = a_W \phi_W + a_E \phi_E + a_S \phi_S + a_N \phi_N + a_B \phi_B + a_T \phi_T$$

with central coefficient

$$a_P = a_W + a_E + a_S + a_N + a_B + a_T + \Delta F$$

and the coefficients of this equation for the **hybrid differencing scheme** are as follows:



	One-dimensional flow	Two-dimensional flow	Three-dimensional flow
a_w	$\max \left[F_w, \left(D_w + \frac{F_w}{2} \right), 0 \right]$	$\max \left[F_w, \left(D_w + \frac{F_w}{2} \right), 0 \right]$	$\max \left[F_w, \left(D_w + \frac{F_w}{2} \right), 0 \right]$
a_e	$\max \left[-F_e, \left(D_e - \frac{F_e}{2} \right), 0 \right]$	$\max \left[-F_e, \left(D_e - \frac{F_e}{2} \right), 0 \right]$	$\max \left[-F_e, \left(D_e - \frac{F_e}{2} \right), 0 \right]$
a_s	-	$\max \left[F_s, \left(D_s + \frac{F_s}{2} \right), 0 \right]$	$\max \left[F_s, \left(D_s + \frac{F_s}{2} \right), 0 \right]$
a_n	-	$\max \left[-F_n, \left(D_n - \frac{F_n}{2} \right), 0 \right]$	$\max \left[-F_n, \left(D_n - \frac{F_n}{2} \right), 0 \right]$
a_b	bottom	-	$\max \left[F_b, \left(D_b + \frac{F_b}{2} \right), 0 \right]$
a_t	top	-	$\max \left[-F_t, \left(D_t - \frac{F_t}{2} \right), 0 \right]$
ΔF	$F_e - F_w$	$F_e - F_w + F_n - F_s$	$F_e - F_w + F_n - F_s + F_t - F_b$

In the above expressions the values of F and D are calculated with the following formulae:

Face	w	e	s	n	b	t
F	$(\rho u)_w A_w$	$(\rho u)_e A_e$	$(\rho v)_s A_s$	$(\rho v)_n A_n$	$(\rho w)_b A_b$	$(\rho w)_t A_t$
D	$\frac{\Gamma_w}{\delta x_{WP}} A_w$	$\frac{\Gamma_e}{\delta x_{PE}} A_e$	$\frac{\Gamma_s}{\delta y_{SP}} A_s$	$\frac{\Gamma_n}{\delta y_{PN}} A_n$	$\frac{\Gamma_b}{\delta z_{PN}} A_b$	$\frac{\Gamma_t}{\delta z_{PT}} A_t$

5.8 The power-law difference scheme Patankar (1980)

- If $0 < Pe < 10$ the flux is evaluated by using a polynomial expression

$$\underline{q_w = F_w[\phi_W - \beta_w(\phi_P - \phi_W)] \quad \text{for } 0 < Pe < 10}$$

$$\text{where } \beta_w = (1 - 0.1Pe_w)^5 / Pe_w$$

diffusion is set to zero when cell Pe exceeds 10.

$$\underline{q_w = F_w\phi_W \quad \text{for } Pe > 10}$$

- The power-law differencing scheme of Patankar (1980) is a more accurate approximation to the one-dimensional exact solution and produces better results than the hybrid scheme.

$$F_e\phi_e - \underline{F_w\phi_w} = D_e(\phi_E - \phi_P) - D_w(\phi_P - \phi_W)$$

for steady one-dimensional convection–diffusion

- The power-law differencing scheme can be written as follows:

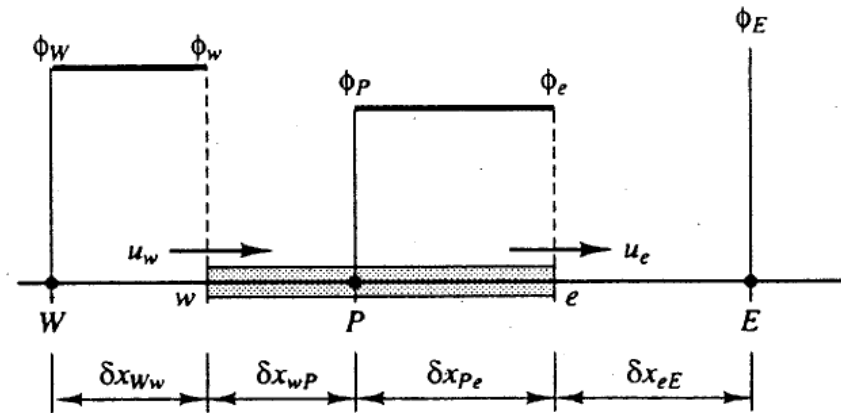
the discretised equation

$$a_P \phi_P = a_W \phi_W + a_E \phi_E$$

$$a_P = a_W + a_E + (F_e - F_w)$$

$$a_W = D_w \max \left[0, (1 - 0.1 |Pe_w|)^5 \right] + \max[F_w, 0]$$

$$a_E = D_e \max \left[0, (1 - 0.1 |Pe_e|)^5 \right] + \max[-F_e, 0]$$



The power-law differencing scheme is more accurate for one-dimensional problems since it attempts to represent the exact solution more closely.

FLUENT version 4.22, use this scheme as the default scheme

a_W	a_E
$D_w + \max(F_w, 0)$	$D_e + \max(0, -F_e)$

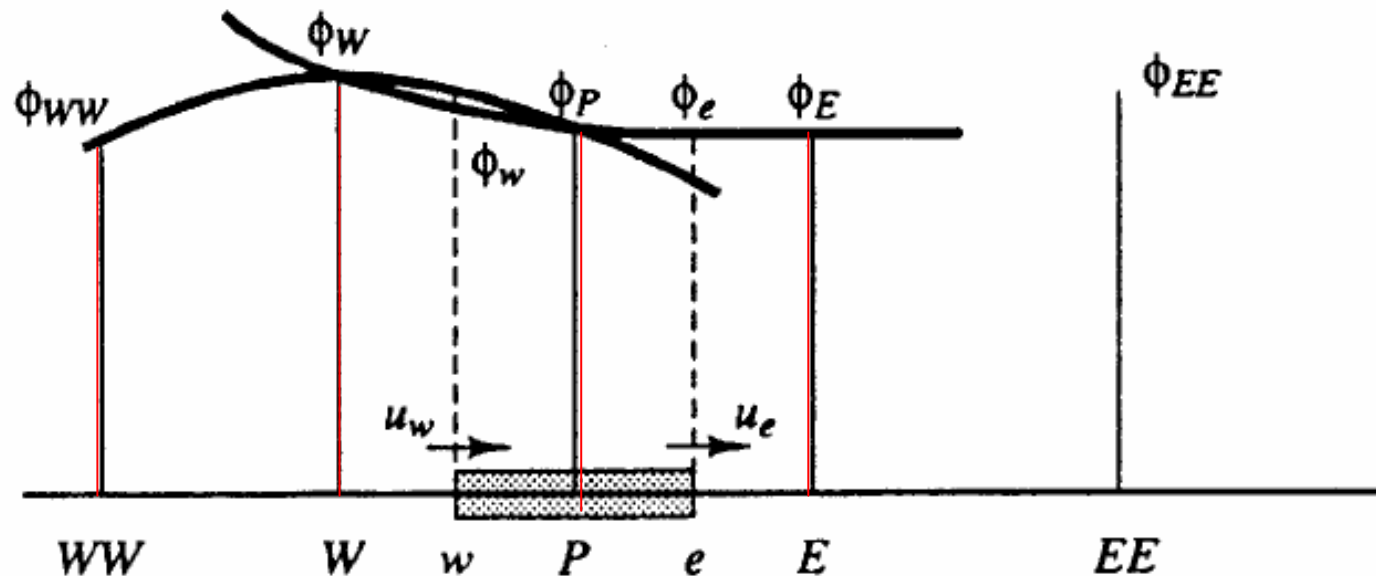
5.9 Higher order differencing schemes for convection – diffusion problems

- The accuracy of hybrid and upwind schemes is only first-order in terms of Taylor series truncation error (TSTE).
- the first-order accuracy makes them prone to numerical diffusion errors.
- Such errors can be minimised by employing higher order discretisation.
- Higher order schemes involve more neighbour points and reduce the discretisation errors by bringing in a wider influence
- The central differencing scheme which has second-order accuracy proved to be unstable and does not possess the transportiveness property. do not take into account the flow direction are unstable and, therefore,
 - more accurate higher order schemes, which preserve upwinding for stability and sensitivity to the flow direction, are needed.

5.9.1 Quadratic upwind differencing scheme: the QUICK scheme

於兩點間之 Φ 值特性以Quadratic interpolation (非以線性關係如 Leonard (1979) central differencing scheme) 來近似

uses a three-point upstream-weighted quadratic interpolation for cell face values.



when $u_w > 0$ and $u_e > 0$ a quadratic fit through WW , W and P is used to evaluate ϕ_w , and a further quadratic fit through W , P and E to calculate ϕ_e .

$$\Phi_w = f(\Phi_P, \Phi_W, \Phi_{WW})$$

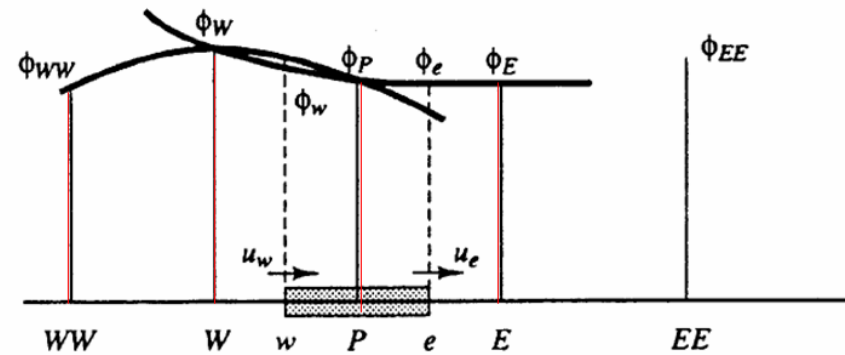
$$\Phi_e = f(\Phi_W, \Phi_P, \Phi_E)$$

$$\underline{\phi_{face} = \frac{6}{8} \phi_{i-1} + \frac{3}{8} \phi_i - \frac{1}{8} \phi_{i-2}}$$

$$\phi_{face} = \frac{6}{8}\phi_{i-1} + \frac{3}{8}\phi_i - \frac{1}{8}\phi_{i-2}$$

$$\text{When } u_w > 0, \quad \phi_w = \frac{6}{8}\phi_W + \frac{3}{8}\phi_P - \frac{1}{8}\phi_{WW}$$

$$\text{When } u_e > 0, \quad \phi_e = \frac{6}{8}\phi_P + \frac{3}{8}\phi_E - \frac{1}{8}\phi_W$$



$$F_e\phi_e - F_w\phi_w = D_e(\phi_E - \phi_P) - D_w(\phi_P - \phi_W)$$

$$\left[F_e \left(\frac{6}{8}\phi_P + \frac{3}{8}\phi_E - \frac{1}{8}\phi_W \right) - F_w \left(\frac{6}{8}\phi_W + \frac{3}{8}\phi_P - \frac{1}{8}\phi_{WW} \right) \right]$$

$$= D_e(\phi_E - \phi_P) - D_w(\phi_P - \phi_W)$$

$$\left[D_w - \frac{3}{8}F_w + D_e + \frac{6}{8}F_e \right] \phi_P = \left[D_w + \frac{6}{8}F_w + \frac{1}{8}F_e \right] \phi_W$$

$$+ \left[D_e - \frac{3}{8}F_e \right] \phi_E - \frac{1}{8}F_w\phi_{WW}$$

$$a_P\phi_P = a_W\phi_W + a_E\phi_E + a_{WW}\phi_{WW}$$

This is now written in the standard form for discretised equations

$$\left[D_w - \frac{3}{8}F_w + D_e + \frac{6}{8}F_e \right] \phi_P = \left[D_w + \frac{6}{8}F_w + \frac{1}{8}F_e \right] \phi_W + \left[D_e - \frac{3}{8}F_e \right] \phi_E - \frac{1}{8}F_w \phi_{WW}$$

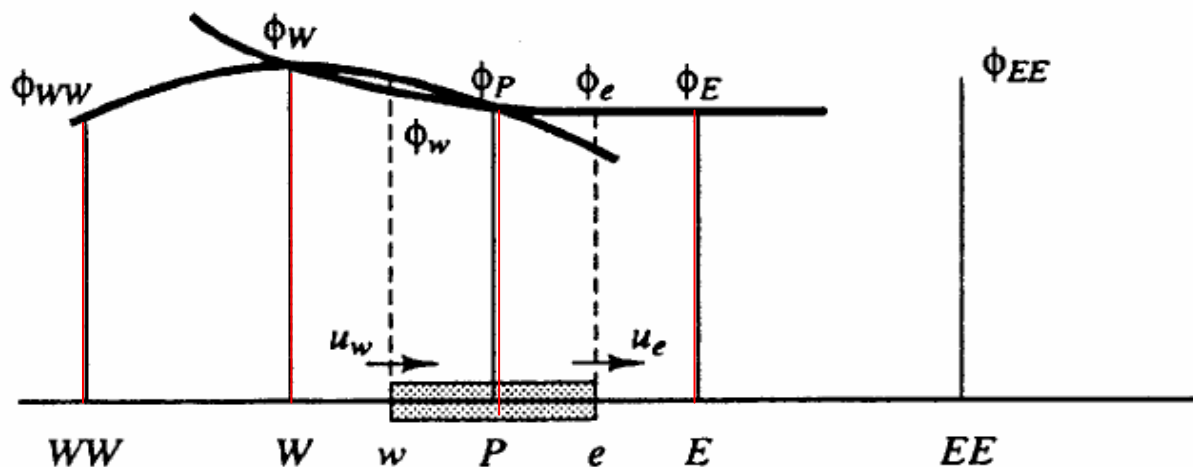
➔ $a_P \phi_P = a_W \phi_W + a_E \phi_E + a_{WW} \phi_{WW}$

when $u_w > 0$ and $u_e > 0$

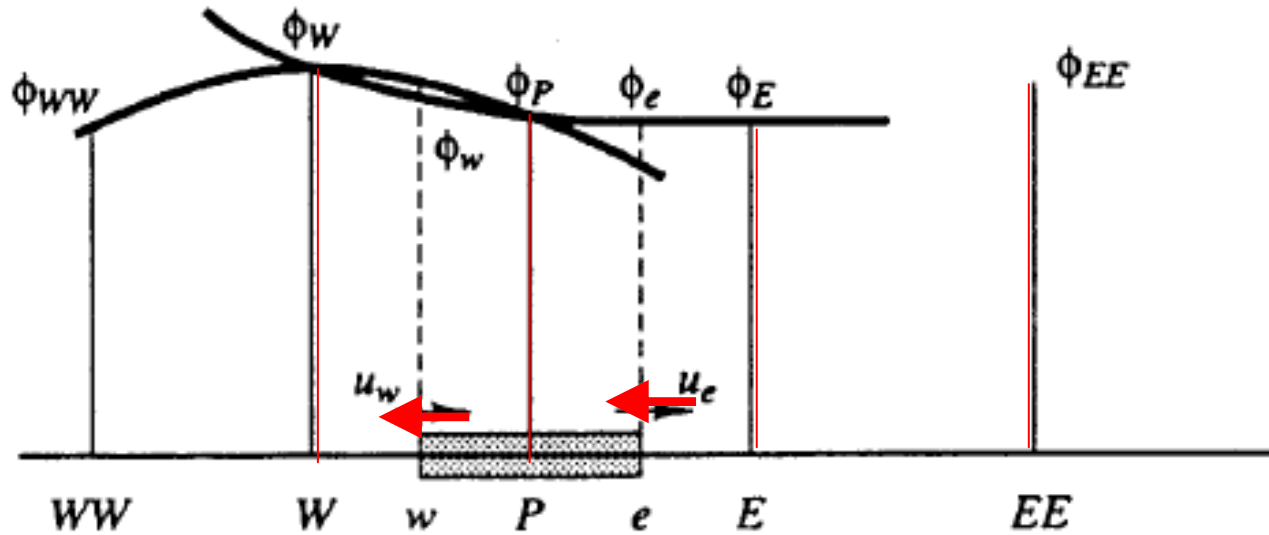
a_W	a_E	a_{WW}	a_P
$D_w + \frac{6}{8}F_w + \frac{1}{8}F_e$	$D_e - \frac{3}{8}F_e$	$-\frac{1}{8}F_w$	<u>$a_W + a_E + a_{WW} + (F_e - F_w)$</u>

$$\Phi_w = f(\Phi_P, \Phi_W, \Phi_{WW})$$

$$\Phi_e = f(\Phi_W, \Phi_P, \Phi_E)$$



For $F_w < 0$ and $F_e < 0$



$$\Phi_w = f(\Phi_W, \Phi_P, \Phi_E)$$

$$\Phi_e = f(\Phi_P, \Phi_E, \Phi_{EE})$$



$$\phi_w = \frac{6}{8}\phi_P + \frac{3}{8}\phi_W - \frac{1}{8}\phi_E$$

$$\phi_e = \frac{6}{8}\phi_E + \frac{3}{8}\phi_P - \frac{1}{8}\phi_{EE}$$

- For $F_w < 0$ and $F_e < 0$

$$F_e \phi_e - F_w \phi_w = D_e(\phi_E - \phi_P) - D_w(\phi_P - \phi_W)$$

$$\left[F_e \left(\frac{6}{8} \phi_E + \frac{3}{8} \phi_P - \frac{1}{8} \phi_{EE} \right) - F_w \left(\frac{6}{8} \phi_P + \frac{3}{8} \phi_W - \frac{1}{8} \phi_{E'} \right) \right]$$

$$= D_e(\phi_E - \phi_P) - D_w(\phi_P - \phi_W)$$

$$a_P \phi_P = a_W \phi_W + a_E \phi_E + a_{EE} \phi_{EE}$$

a_W	a_E	a_{EE}	a_P
$D_w + \frac{3}{8} F_w$	$D_e - \frac{6}{8} F_e - \frac{1}{8} F_w$	$\frac{1}{8} F_e$	$a_W + a_E + a_{EE} + (F_e - F_w)$

Summary

The QUICK scheme for one-dimensional convection–diffusion problems can be summarised as follows:

$$a_P \phi_P = a_W \phi_W + a_E \phi_E + a_{WW} \phi_{WW} + a_{EE} \phi_{EE}$$

with central coefficient $a_P = a_W + a_E + a_{WW} + a_{EE} + (F_e - F_w)$ and neighbour coefficients

a_W	a_{WW}	a_E	a_{EE}		Standard QUICK
$D_w + \frac{6}{8}\alpha_w F_w + \frac{1}{8}\alpha_e F_e + \frac{3}{8}(1 - \alpha_w)F_w$	$-\frac{1}{8}\alpha_w F_w$	$D_e - \frac{3}{8}\alpha_e F_e - \frac{6}{8}(1 - \alpha_e)F_e - \frac{1}{8}(1 - \alpha_w)F_w$	$\frac{1}{8}(1 - \alpha_e)F_e$	a_W	$D_w + \frac{6}{8}\alpha_w F_w + \frac{1}{8}\alpha_e F_e + \frac{3}{8}(1 - \alpha_w)F_w$
				a_{WW}	$-\frac{1}{8}\alpha_w F_w$
				a_E	$D_e - \frac{3}{8}\alpha_e F_e - \frac{6}{8}(1 - \alpha_e)F_e - \frac{1}{8}(1 - \alpha_w)F_w$
				a_{EE}	$\frac{1}{8}(1 - \alpha_e)F_e$

where $\alpha_w = 1$ for $F_w > 0$ and $\alpha_e = 1$ for $F_e > 0$
 $\alpha_w = 0$ for $F_w < 0$ and $\alpha_e = 0$ for $F_e < 0$

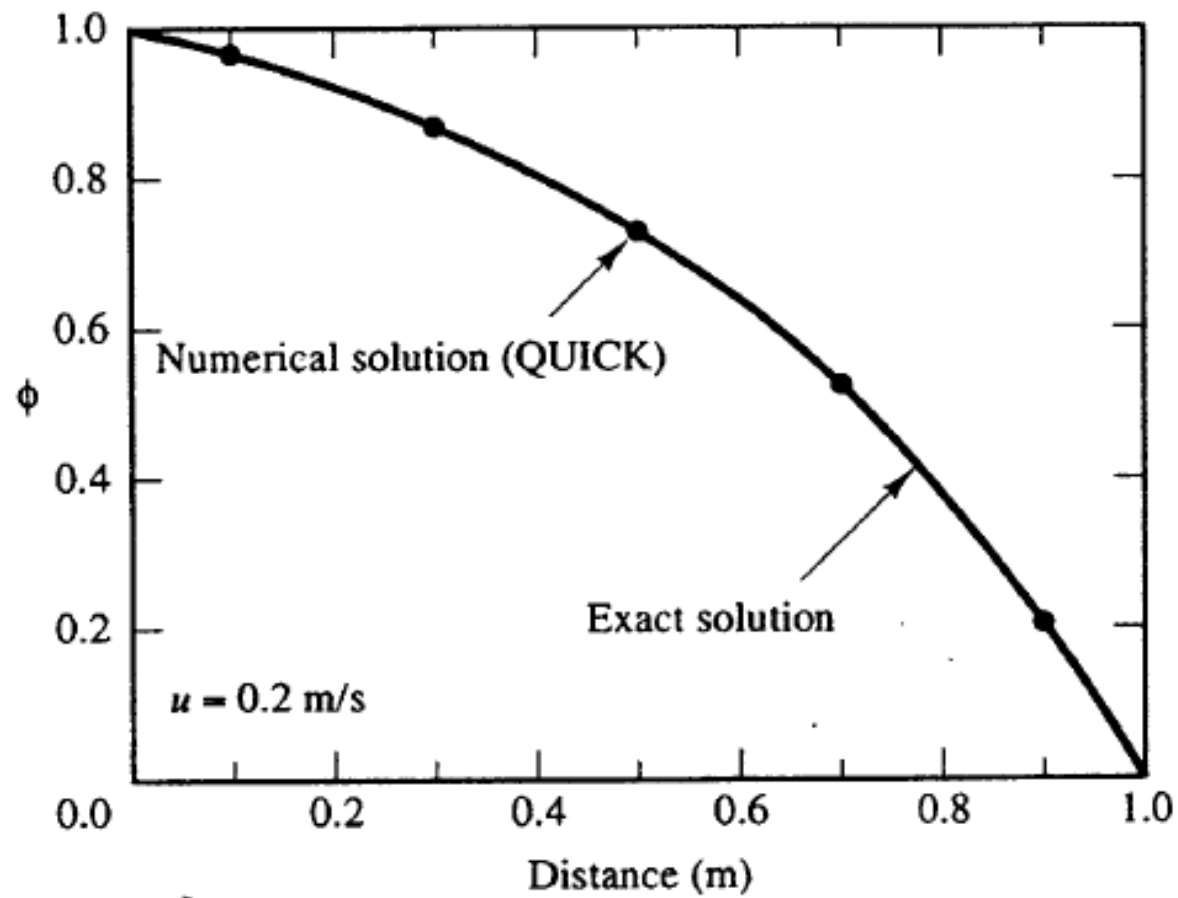
when $u_w > 0$ and $u_e > 0$

a_W	a_E	a_{WW}	a_P
$D_w + \frac{6}{8}F_w + \frac{1}{8}F_e$	$D_e - \frac{3}{8}F_e$	$-\frac{1}{8}F_w$	$a_W + a_E + a_{WW} + (F_e - F_w)$

For $F_w < 0$ and $F_e < 0$

a_W	a_E	a_{EE}	a_P
$D_w + \frac{3}{8}F_w$	$D_e - \frac{6}{8}F_e - \frac{1}{8}F_w$	$\frac{1}{8}F_e$	$a_W + a_E + a_{EE} + (F_e - F_w)$

Comparison with the analytical solution



5.9.2 Assessment of the QUICK scheme

- The scheme uses consistent quadratic profiles – the cell face values of fluxes are always calculated by quadratic interpolation between two bracketing nodes and an upstream node – and is therefore conservative. ● Since the scheme is based on a quadratic function its accuracy in terms of the Taylor series truncation error is third order on a uniform mesh. ● The transportiveness property is built into the scheme as the quadratic function is based on two upstream and one downstream nodal values. ● If the flow field satisfies continuity the coefficient a_p equals the sum of all neighbour coefficients which is desirable for boundedness.

The QUICK scheme is therefore conditionally stable.

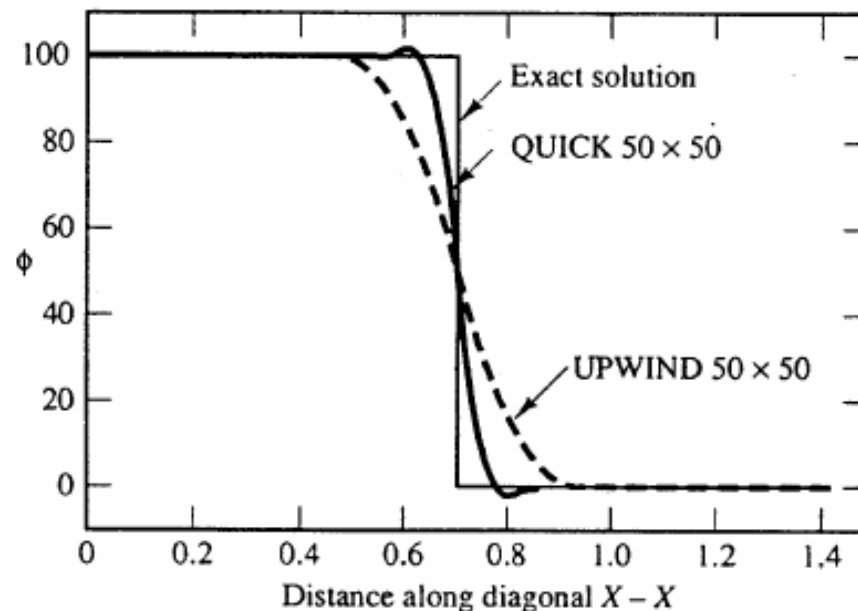
5.9.3 Stability problems of the QUICK scheme and remedies

- Since the QUICK scheme in the form presented above can be unstable due to the appearance of negative main coefficients it has been re-formulated in different ways that alleviate stability problems.

Hayase *et al* (1992)

last authors generalised the approach for re-arranging QUICK schemes and derived a stable and fast converging variant.

5.9.4 General comments on the QUICK differencing scheme



- It can be seen that the QUICK scheme matches the exact solution much more accurately than the upwind scheme on a 50×50 grid.

5.11 Summary

- All the finite volume schemes presented in this chapter describe the effects of simultaneous convection and diffusion by means of discretised equations whose coefficients are weighted combinations of the convective mass flux per unit area F and the diffusion conductance D .
- The discretised equations for a general internal node for the central, upwind and hybrid differencing and the power-law schemes of a one-dimensional convection–diffusion problem take the following form:

$$a_P \phi_P = a_W \phi_W + a_E \phi_E$$

with $a_P = a_W + a_E + (F_e - F_w)$

- The neighbour coefficients for these schemes are

<i>Scheme</i>	a_W	a_E
Central differencing	$D_w + F_w/2$	$D_e - F_e/2$
Upwind differencing	$D_w + \max(F_w, 0)$	$D_e + \max(0, -F_e)$
Hybrid differencing	$\max[F_w, (D_w + F_w/2), 0]$	$\max[-F_e, (D_e - F_e/2), 0]$
Power law	$D_w \max\left[0, (1 - 0.1 Pe_w)^5\right]$ + $\max(F_w, 0)$	$D_e \max\left[0, (1 - 0.1 Pe_e)^5\right]$ + $\max(-F_e, 0)$

- The boundary conditions enter the discretised equations via source terms. Their treatment is specific to each discretisation scheme.
- Discretisation schemes that possess conservativeness, boundedness and transportiveness give physically realistic results and stable iterative solutions:
 - The central differencing method is not suitable for general purpose convection–diffusion problems because it lacks transportiveness and gives unrealistic solutions at large values of the cell Peclet number.
 - Upwind, hybrid and power-law differencing all possess conservativeness, boundedness and transportiveness and are highly stable, but suffer from false diffusion in multi-dimensional flows if the velocity vector is not parallel to one of the co-ordinate directions.
- The discretised equations of the standard QUICK method of Leonard (1979) have the following form for a general internal node point:

$$a_P \phi_P = a_W \phi_W + a_E \phi_E + a_{WW} \phi_{WW} + a_{EE} \phi_{EE}$$

where

$$a_P = a_W + a_E + a_{WW} + a_{EE} + (F_e - F_w)$$

The neighbour coefficients of the standard QUICK scheme are

	Standard QUICK
a_W	$D_w + \frac{6}{8} \alpha_w F_w + \frac{1}{8} \alpha_e F_e + \frac{3}{8} (1 - \alpha_w) F_w$
a_{WW}	$-\frac{1}{8} \alpha_w F_w$
a_E	$D_e - \frac{3}{8} \alpha_e F_e - \frac{6}{8} (1 - \alpha_e) F_e - \frac{1}{8} (1 - \alpha_w) F_w$
a_{EE}	$\frac{1}{8} (1 - \alpha_e) F_e$

with $\alpha_w = 1$ for $F_w > 0$ and $\alpha_e = 1$ for $F_e > 0$

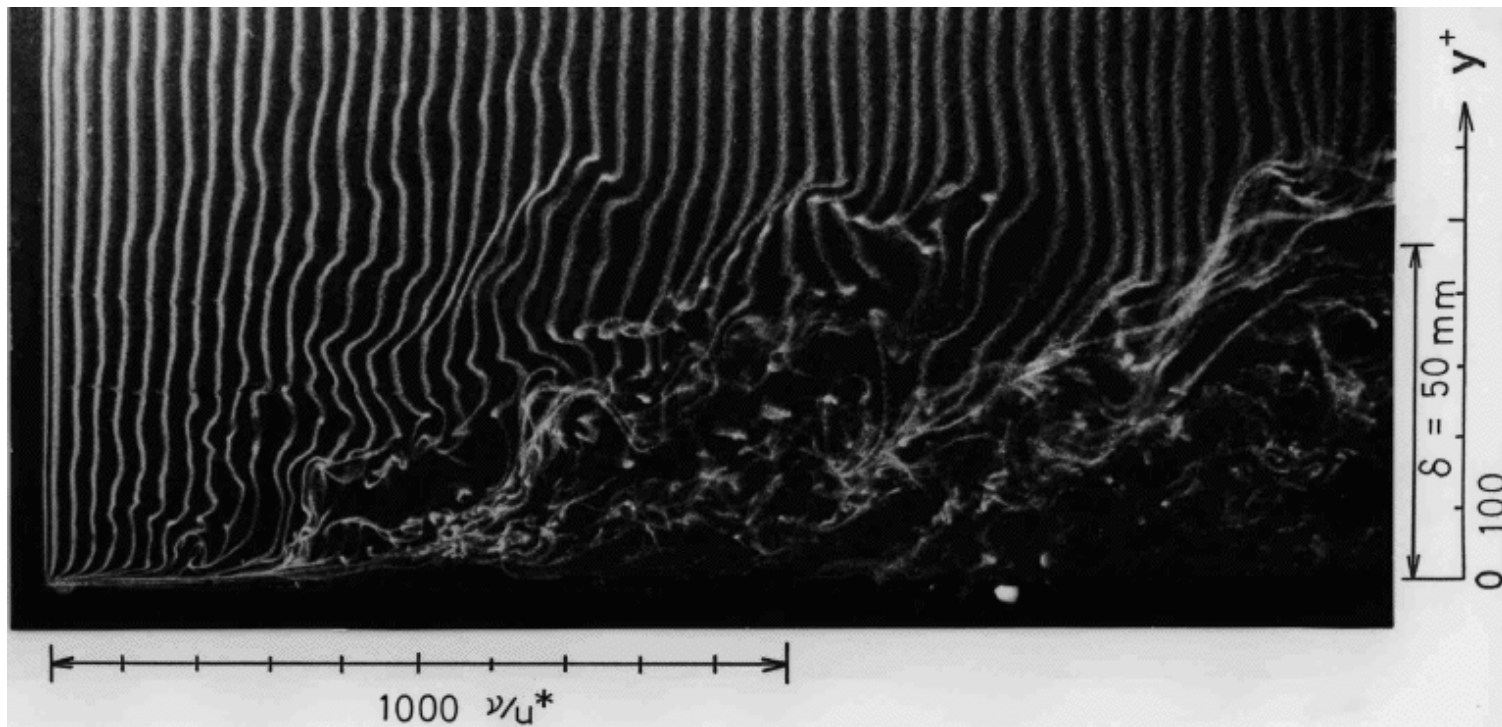
$\alpha_w = 0$ for $F_w < 0$ and $\alpha_e = 0$ for $F_e < 0$

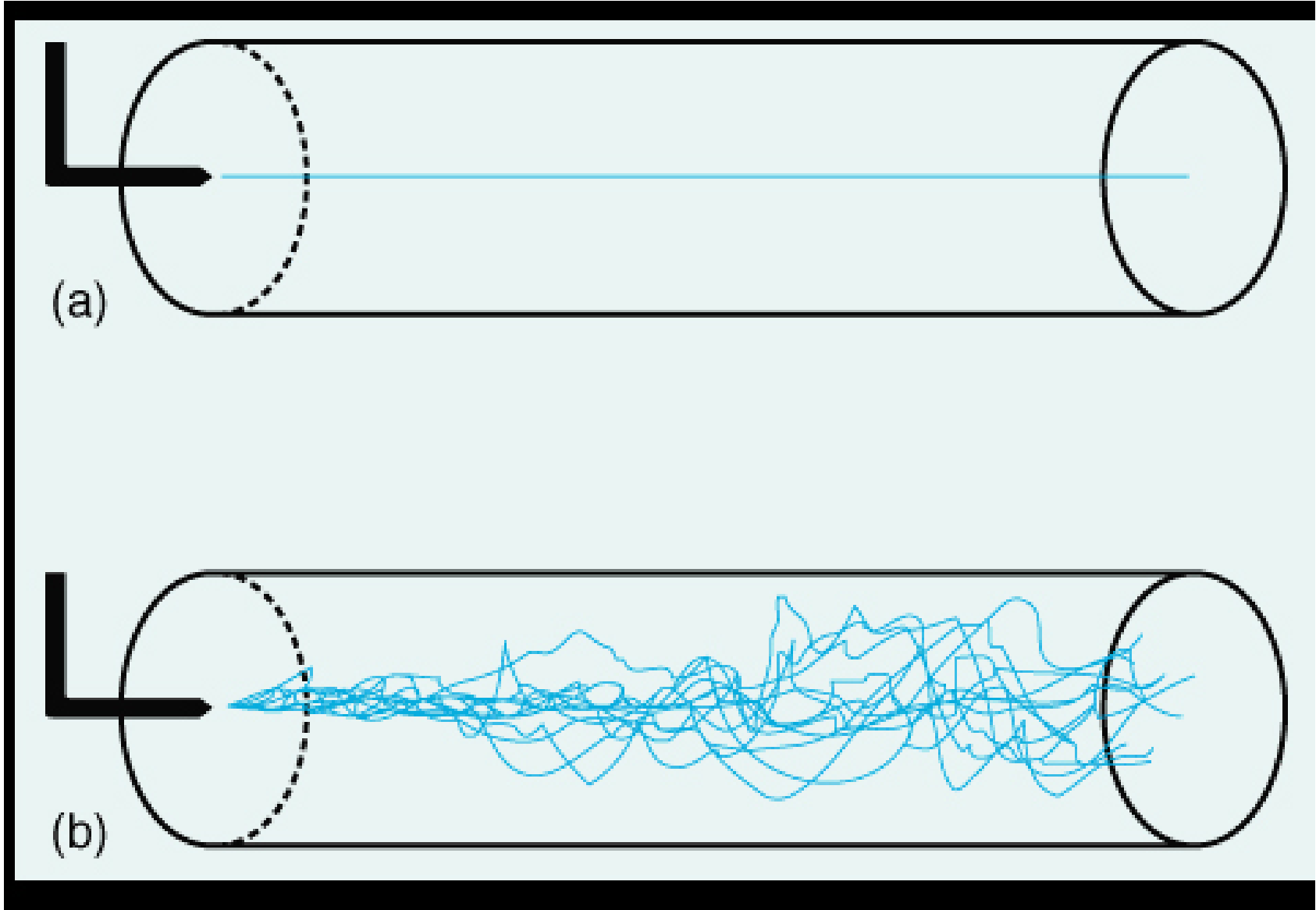
- Higher order schemes, such as QUICK, can minimise false diffusion errors but are less computationally stable.

Nevertheless, if used with care and judgement the QUICK scheme can give very accurate solutions of convection-diffusion problems.

Chapter 5

Turbulence and its Modelling





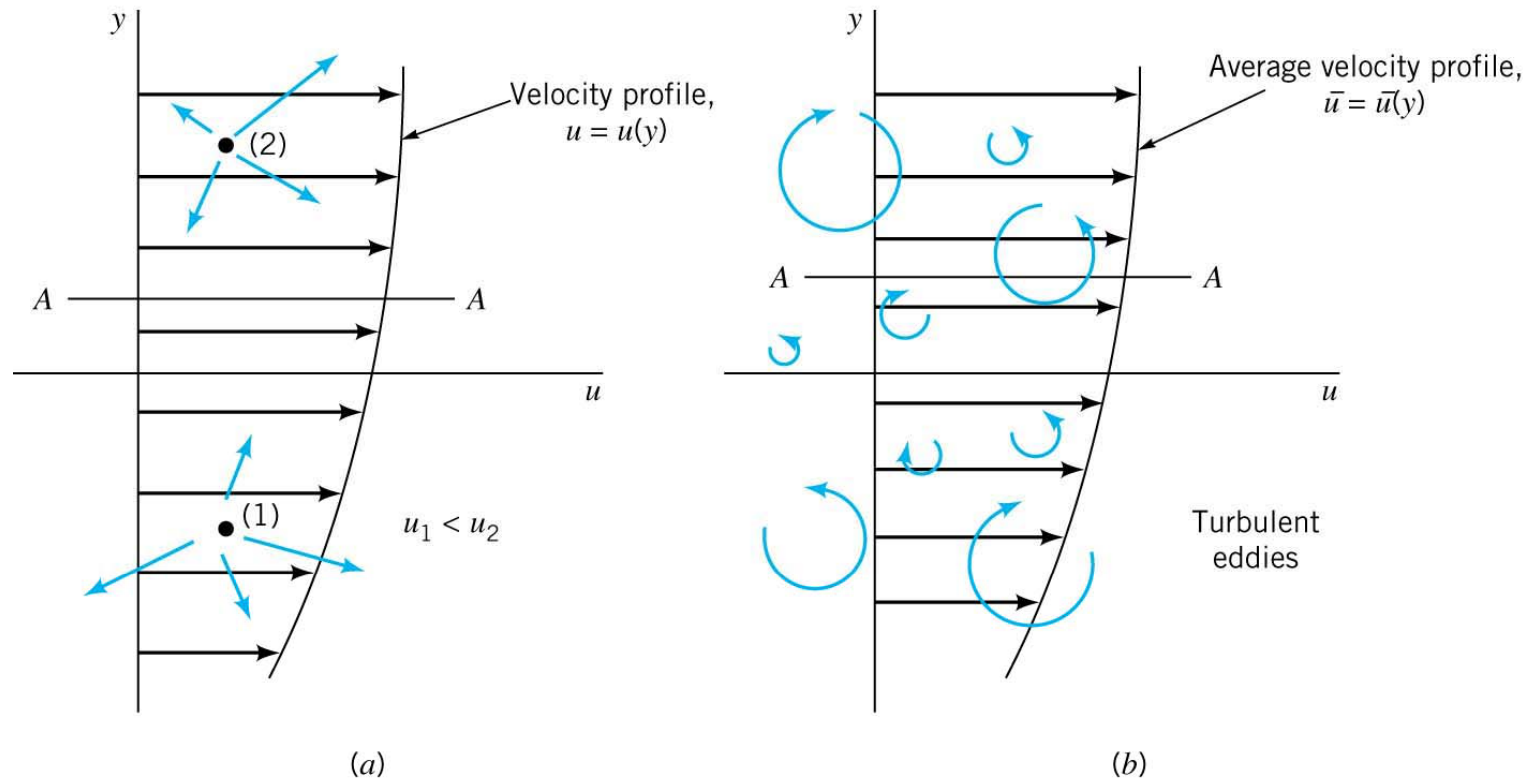
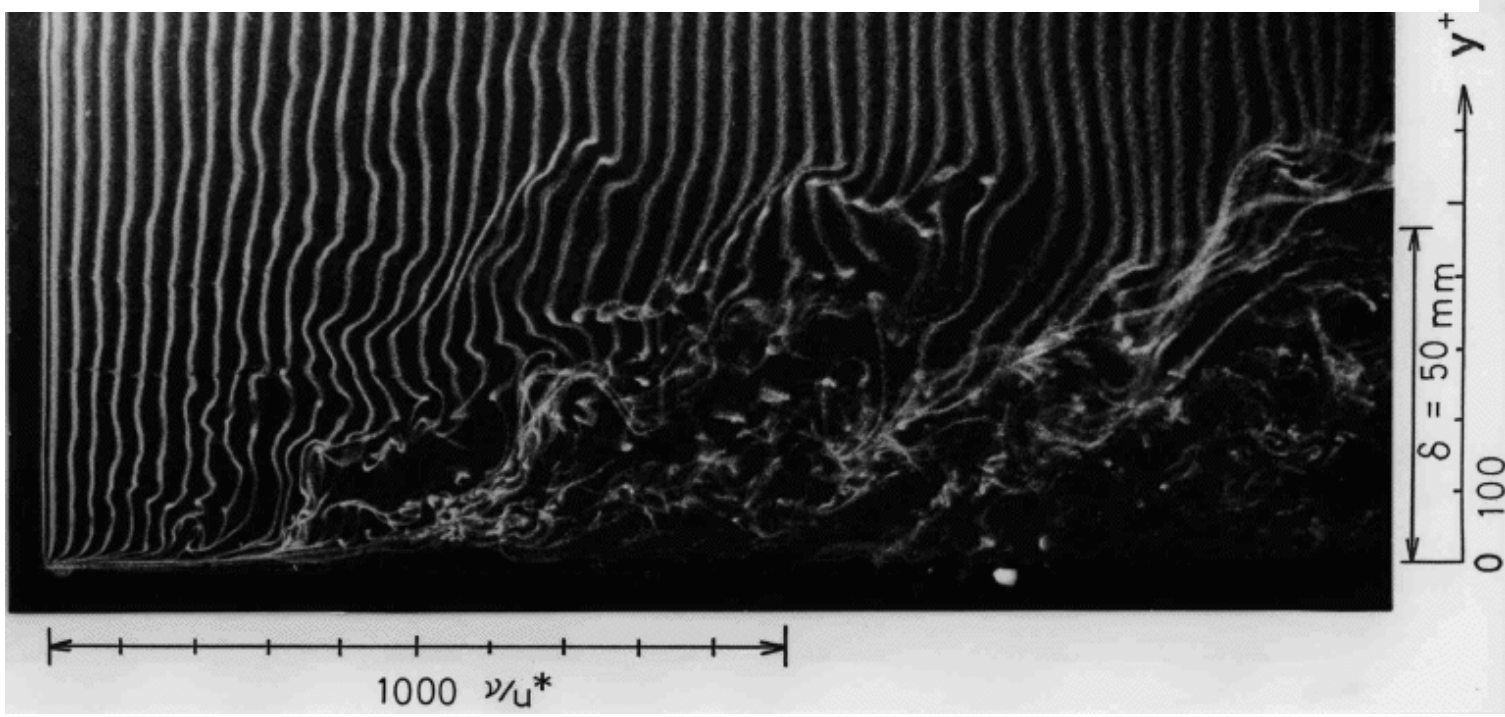
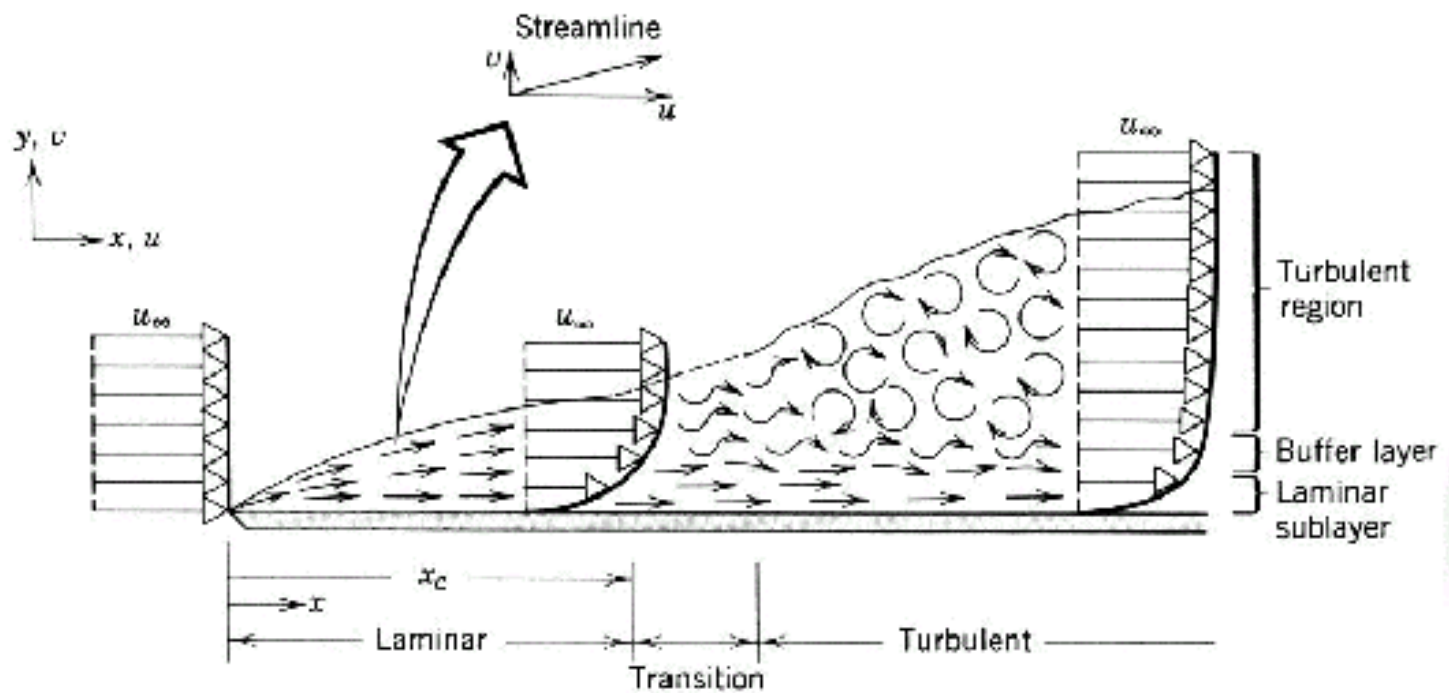
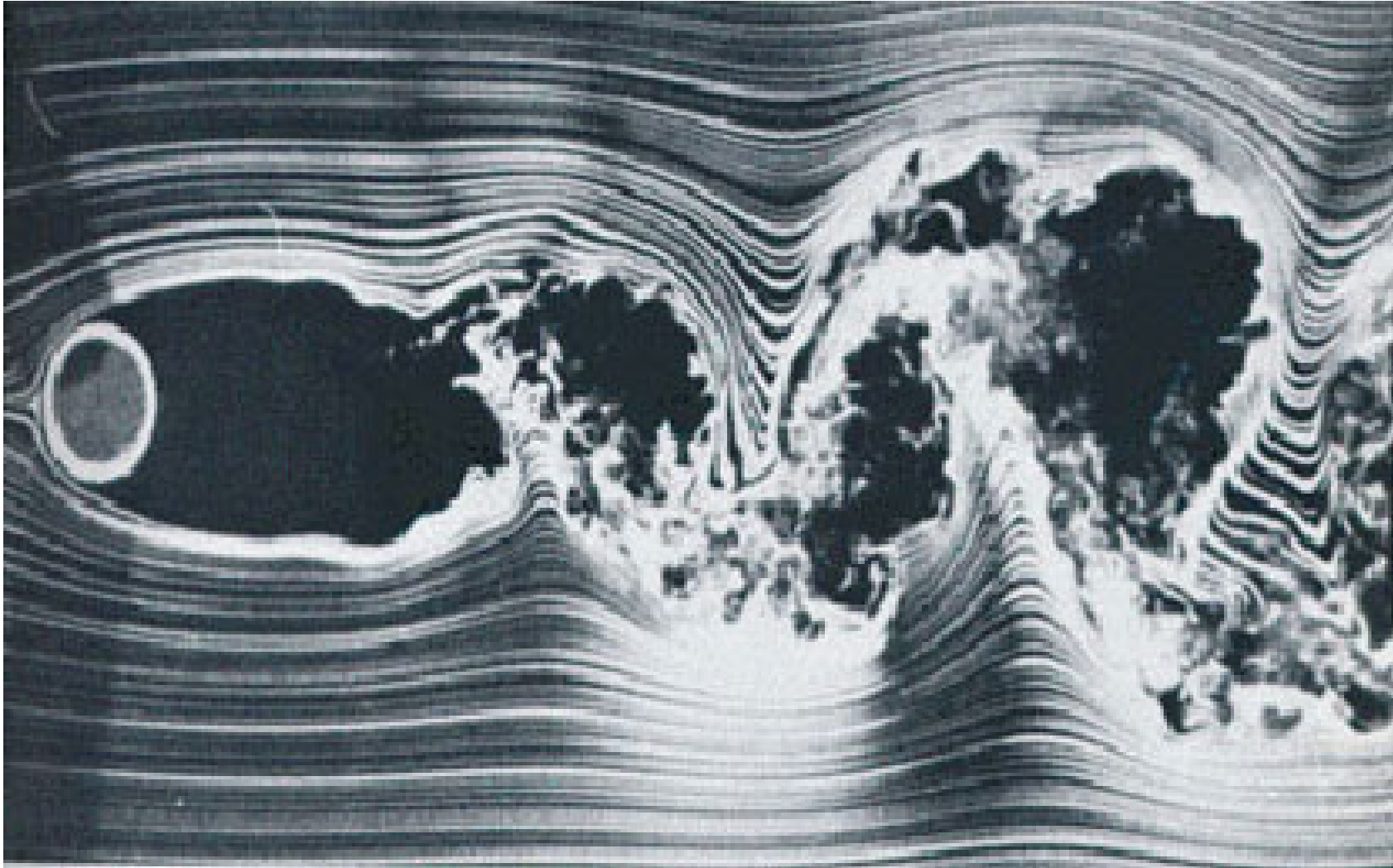


Fig. (a) Laminar flowshear stress caused by random of molecules (b) Turbulent flow as a series of random, 3-D eddies





Turbulence

The nature of turbulence:

irregularity, randomness

diffusivity -- rapid mixing and increased rates
of momentum, energy and mass
large Reynolds numbers

3-D vorticity fluctuations

dissipation -- viscous force perform work which
increases the internal energy at
the expense of kinetic energy of
the turbulence

continuum phenomenon

feature of the fluid flow

Origin of turbulence

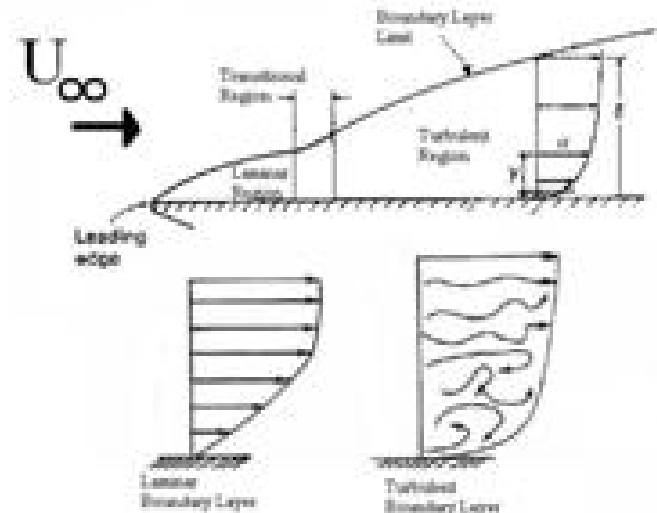
turbulence arise from instabilities at large Re
e.g pipe flow becomes turbulence when

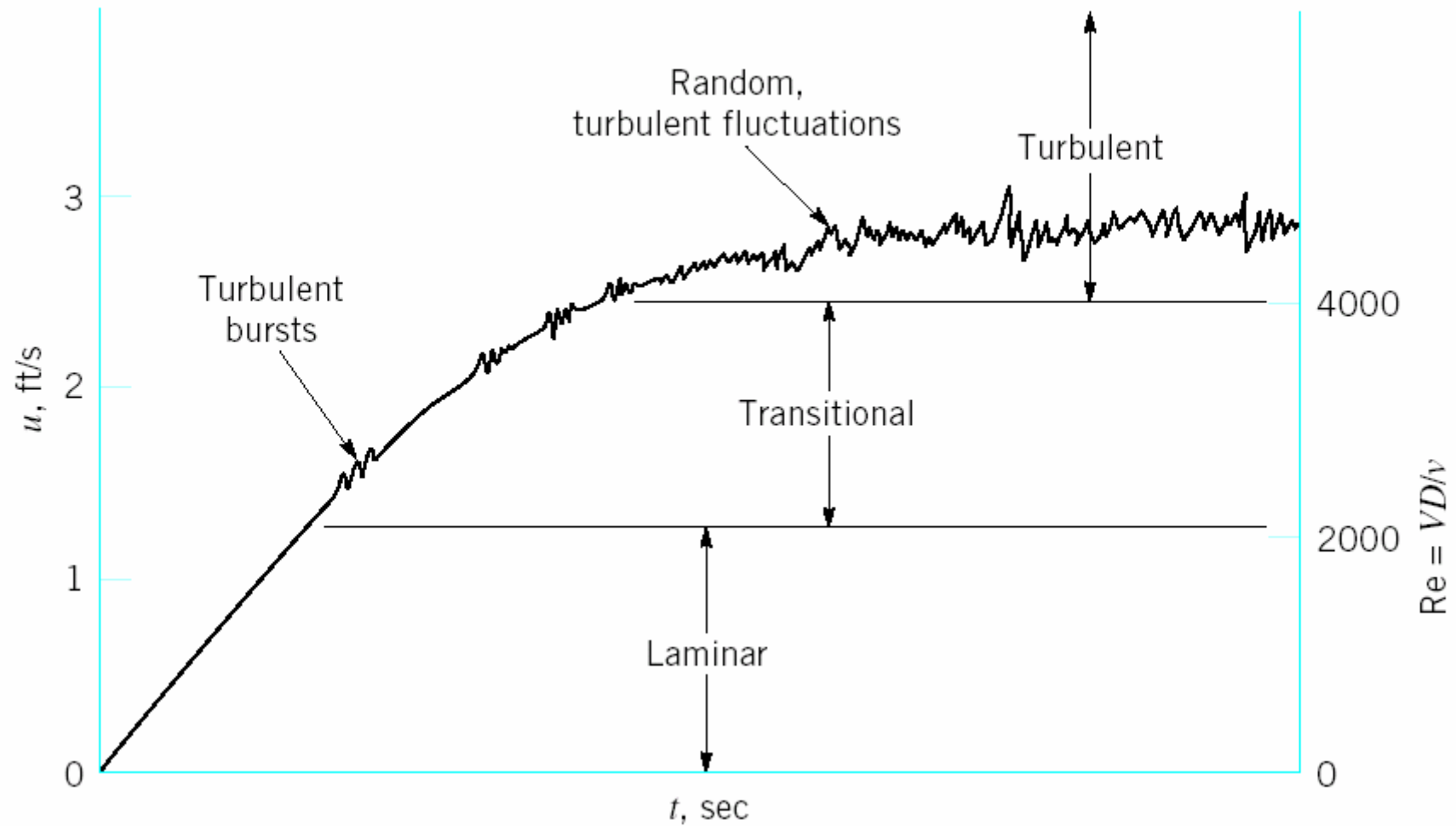
$$Re_D > 2000$$

boundary layer with zero pressure gradient

$$Re_d > 600, d \text{ is the displacement thickness}$$

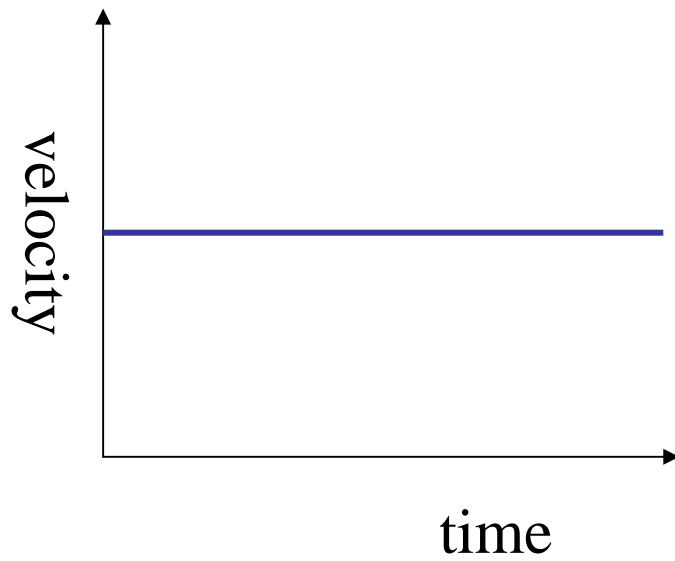
it cannot maintain itself, energy from the surrounding, common source of energy shear in mean flow, thermal ...



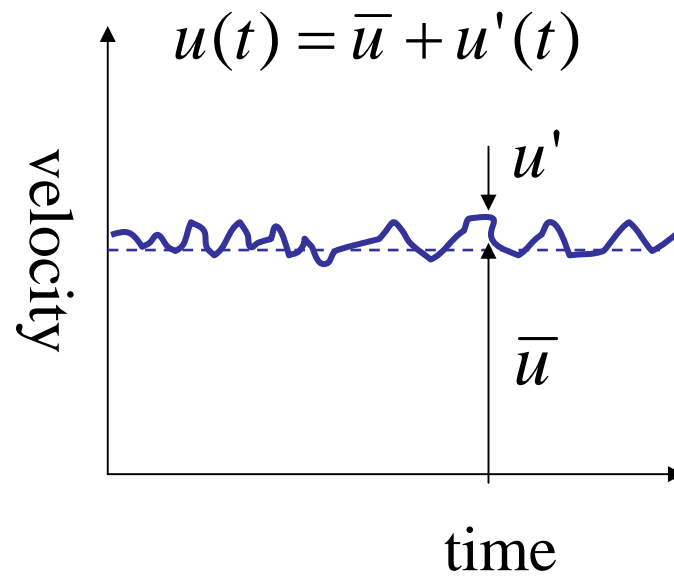


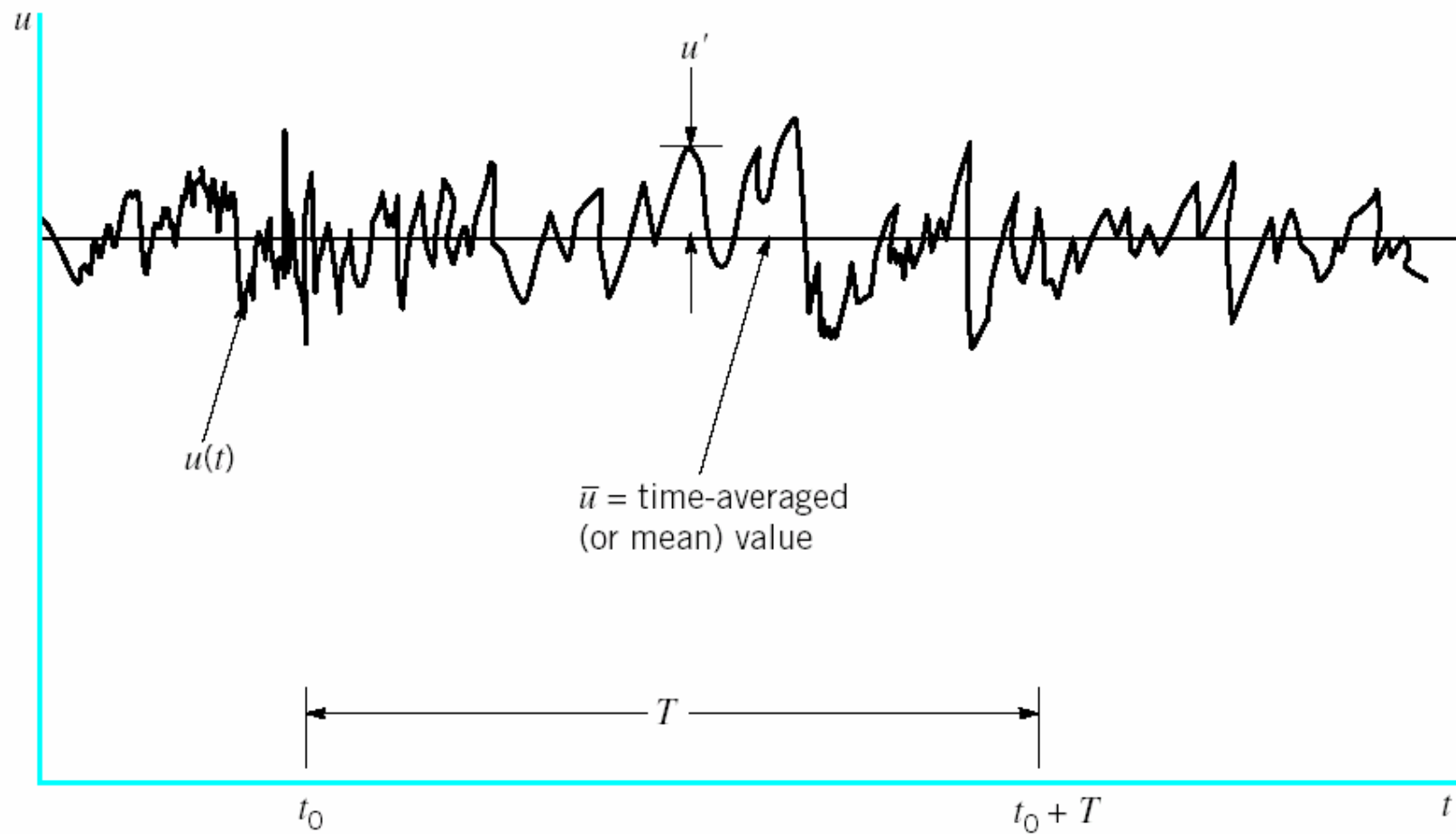
Transition from laminar to turbulent flow in a pipe.

Laminar Flow



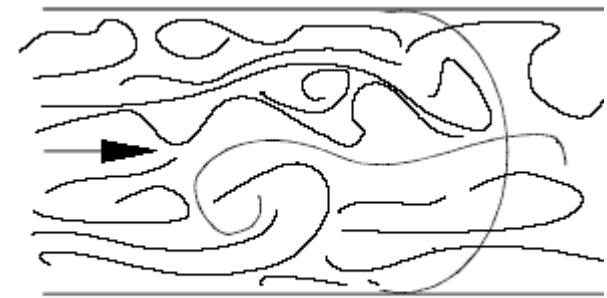
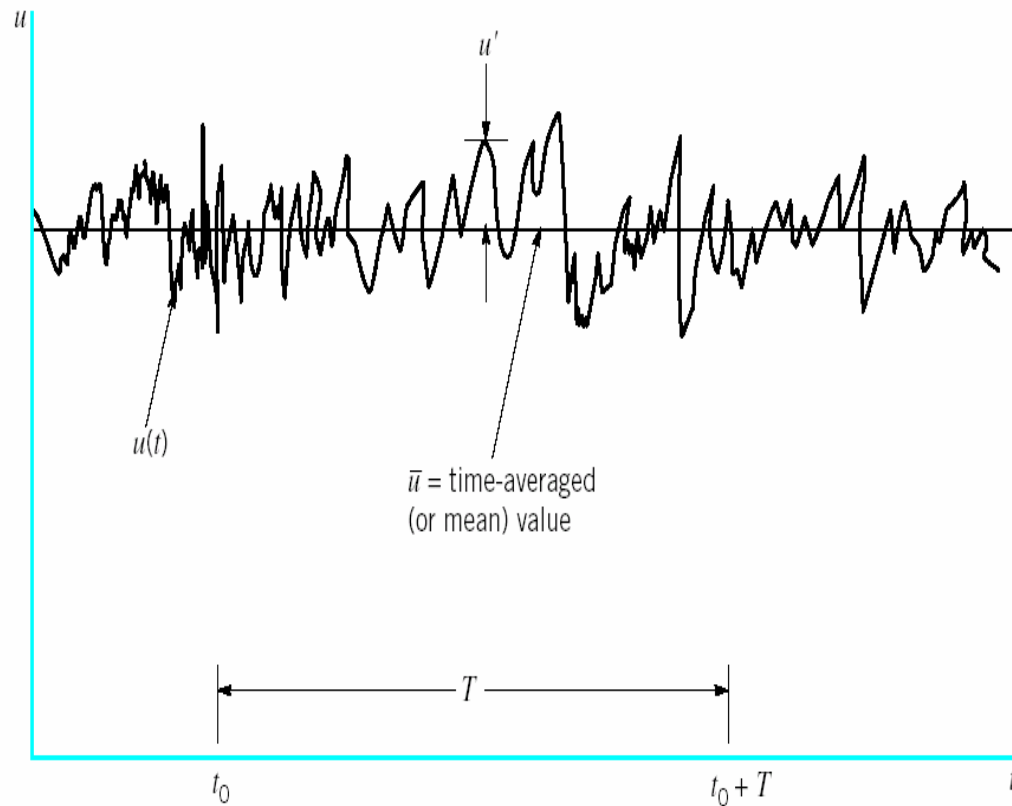
Steady turbulent flow



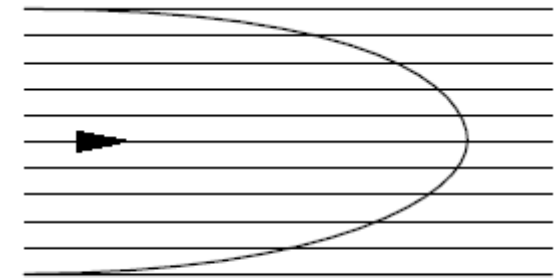


The time-averaged, \bar{u} , and fluctuating, u' , description of a parameter for turbulent flow.

3.1 What is turbulence?



TURBULENT FLOW



LAMINAR FLOW

The time-averaged, \bar{u} , and fluctuating, u' , description of a parameter for turbulent flow.

$$\varphi(t) = \Phi + \varphi'(t)$$

= steady mean component Φ + a time-varying fluctuating component φ'

3.3 Effect of turbulence on time-averaged Navier–Stokes equations

Reynolds equations

Definition : the mean Φ of a flow property φ

$$\Phi = \frac{1}{\Delta t} \int_0^{\Delta t} \varphi(t) dt$$

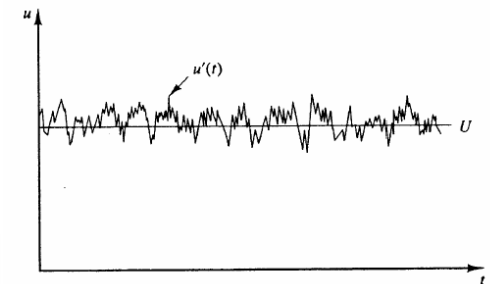
$$\varphi(t) = \Phi + \varphi'(t)$$

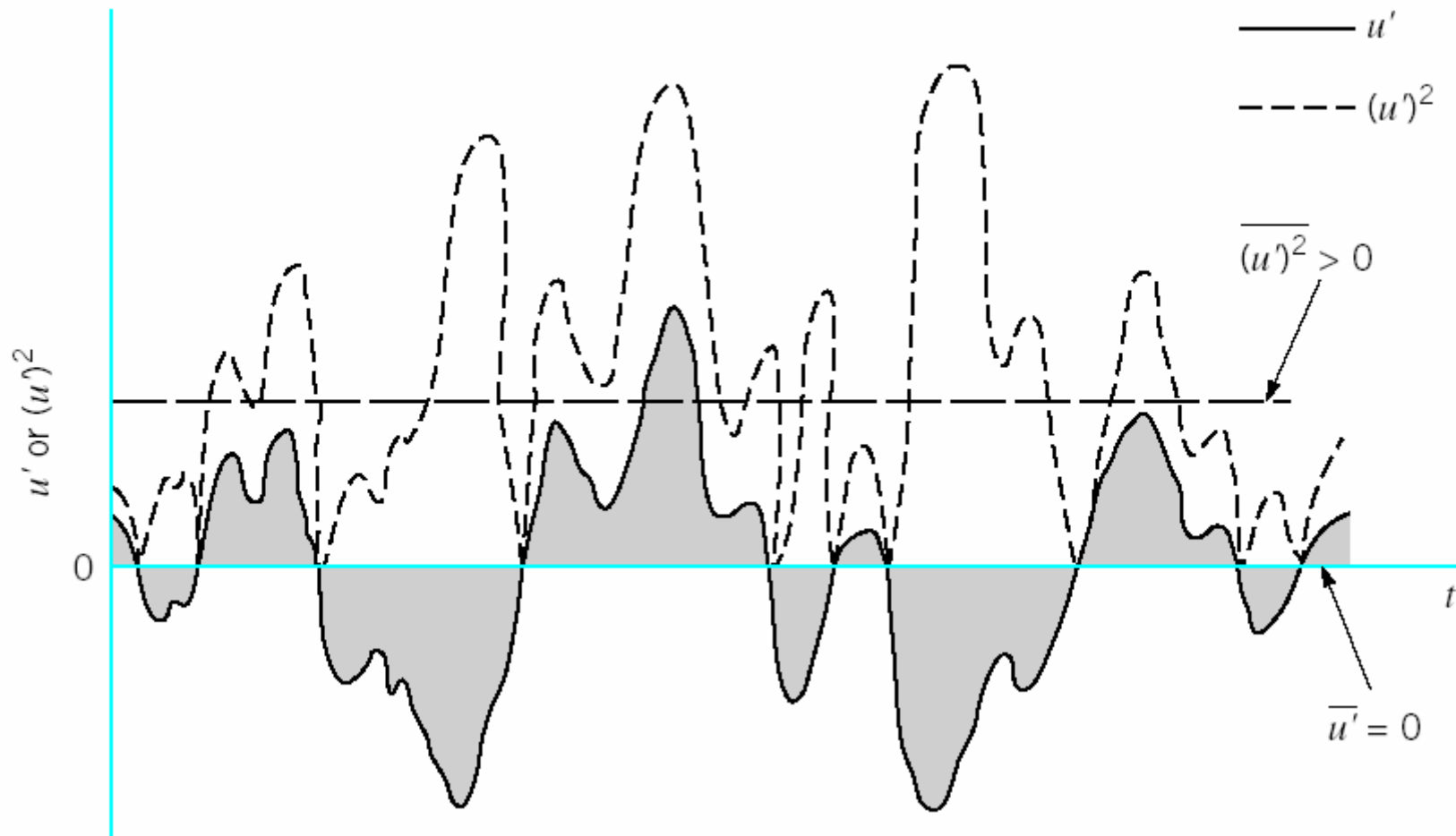
- The time average of the fluctuations φ' is, by definition, zero:

$$\overline{\varphi'} = \frac{1}{\Delta t} \int_0^{\Delta t} \varphi'(t) dt \equiv 0$$

- the root-mean-square (rms) of the fluctuations:

$$\varphi_{rms} = \sqrt{\overline{(\varphi')^2}} = \left[\frac{1}{\Delta t} \int_0^{\Delta t} (\varphi')^2 dt \right]^{1/2}$$





- The kinetic energy k (per unit mass) associated with the turbulence

$$k = \frac{1}{2} \left(\overline{u'^2} + \overline{v'^2} + \overline{w'^2} \right)$$

- The turbulence intensity T_i

$$T_i = \frac{\left(\frac{2}{3}k \right)^{1/2}}{U_{ref}}$$

- The rule of combinations, derivative and integral of two fluctuating properties $\varphi = \Phi + \varphi'$ & $\psi = \Psi + \psi'$

$$\overline{\varphi'} = \overline{\psi'} = 0; \quad \overline{\Phi} = \Phi; \quad \overline{\frac{\partial \varphi}{\partial s}} = \frac{\partial \Phi}{\partial s}; \quad \overline{\int \varphi ds} = \int \Phi ds$$

$$\overline{\varphi + \psi} = \Phi + \Psi; \quad \overline{\varphi\psi} = \Phi\Psi + \overline{\varphi'\psi'}; \quad \overline{\varphi\Psi} = \Phi\Psi; \quad \overline{\varphi'\Psi} = 0$$

- $a = A + a'$ & $\varphi = \Phi + \varphi'$ a : a fluctuating vector quantity

$$\overline{\text{div } \mathbf{a}} = \text{div } \mathbf{A}; \quad \overline{\text{div}(\varphi \mathbf{a})} = \text{div}(\overline{\varphi \mathbf{a}}) = \text{div}(\Phi \mathbf{A}) + \text{div}(\overline{\varphi' \mathbf{a}'});$$

$$\overline{\text{div grad } \varphi} = \text{div grad } \Phi$$

- $\mathbf{u} = \mathbf{U} + \mathbf{u}'; u = U + u'; v = V + v'; w = W + w'; p = P + p'$

$$\overline{\frac{\partial u}{\partial t}} = \frac{\partial U}{\partial t};$$

$$\overline{\text{div}(u\mathbf{u})} = \text{div}(U\mathbf{U}) + \underline{\text{div}(u'\mathbf{u}')}$$

$$\overline{-\frac{1}{\rho} \frac{\partial p}{\partial x}} = -\frac{1}{\rho} \frac{\partial P}{\partial x};$$

$$\overline{v \text{ div grad } u} = v \text{ div grad } U$$

Applying the time average on the instantaneous continuity and Navier-Stokes equation for an incompressible flow with constant

viscosity $\mathbf{u} = \mathbf{U} + \mathbf{u}'; u = U + u'; v = V + v'; w = W + w'; p = P + p'$

$$\overline{div \mathbf{u}} = 0$$

$$\frac{\partial u}{\partial t} + div(u\mathbf{u}) = -\frac{1}{\rho} \frac{\partial p}{\partial x} + \nu div grad u$$

$$\frac{\partial v}{\partial t} + div(v\mathbf{u}) = -\frac{1}{\rho} \frac{\partial p}{\partial y} + \nu div grad v$$

$$\frac{\partial w}{\partial t} + div(w\mathbf{u}) = -\frac{1}{\rho} \frac{\partial p}{\partial z} + \nu div grad w$$

$$\text{div } \mathbf{U} = 0$$



$$\frac{\partial U}{\partial t} + \text{div}(U\mathbf{U}) + \text{div}(\overline{u'u'}) = -\frac{1}{\rho} \frac{\partial P}{\partial x} + \nu \text{div grad } U$$

$$\frac{\partial V}{\partial t} + \text{div}(V\mathbf{U}) + \text{div}(\overline{v'u'}) = -\frac{1}{\rho} \frac{\partial P}{\partial y} + \nu \text{div grad } V$$

$$\frac{\partial W}{\partial t} + \text{div}(W\mathbf{U}) + \text{div}(\overline{w'u'}) = -\frac{1}{\rho} \frac{\partial P}{\partial z} + \nu \text{div grad } W$$

Reynolds stresses



Reynolds equation—Turbulent flow equation for incompressible flows

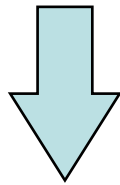
$$\frac{\partial U}{\partial t} + \text{div}(U\mathbf{U}) = -\frac{1}{\rho} \frac{\partial P}{\partial x} + \nu \text{div grad } U + \left[-\frac{\partial \overline{u'^2}}{\partial x} - \frac{\partial \overline{u'v'}}{\partial y} - \frac{\partial \overline{u'w'}}{\partial z} \right]$$

$$\frac{\partial V}{\partial t} + \text{div}(V\mathbf{U}) = -\frac{1}{\rho} \frac{\partial P}{\partial y} + \nu \text{div grad } V + \left[-\frac{\partial \overline{u'v'}}{\partial x} - \frac{\partial \overline{v'^2}}{\partial y} - \frac{\partial \overline{v'w'}}{\partial z} \right]$$

$$\frac{\partial W}{\partial t} + \text{div}(W\mathbf{U}) = -\frac{1}{\rho} \frac{\partial P}{\partial z} + \nu \text{div grad } W + \left[-\frac{\partial \overline{u'w'}}{\partial x} - \frac{\partial \overline{v'w'}}{\partial y} - \frac{\partial \overline{w'^2}}{\partial z} \right]$$

❖ Continuity

$$\frac{\partial u}{\partial x} + \frac{\partial v}{\partial y} + \frac{\partial w}{\partial z} = \frac{\partial(\bar{u} + u')}{\partial x} + \frac{\partial(\bar{v} + v')}{\partial y} + \frac{\partial(\bar{w} + w')}{\partial z}$$



$$\frac{\partial \bar{u}}{\partial x} + \frac{\partial \bar{v}}{\partial y} + \frac{\partial \bar{w}}{\partial z} = 0$$

$$\frac{\partial u'}{\partial x} + \frac{\partial v'}{\partial y} + \frac{\partial w'}{\partial z} = 0$$

$$\rho \frac{Du}{Dt} = \frac{\partial(-p + \tau_{xx})}{\partial x} + \frac{\partial\tau_{yx}}{\partial y} + \frac{\partial\tau_{zx}}{\partial z} + S_{Mx}$$

❖ Momentum Equation for turbulent flow

$$\rho \frac{D\vec{V}}{Dt} + \rho \frac{\partial}{\partial x_j} (\overline{u_i' u_j'}) = \rho \vec{g} + \nabla \bar{p} + \mu \nabla^2 \vec{V}$$



$$\rho \frac{D\vec{V}}{Dt} = \rho \vec{g} - \nabla \bar{p} + \nabla \cdot \tau_{ij}$$

$$\left[\begin{array}{ccc} -\frac{\partial \bar{u}^2}{\partial x} & -\frac{\partial \bar{u}'v'}{\partial y} & -\frac{\partial \bar{u}'w'}{\partial z} \end{array} \right]$$

$$\left[\begin{array}{ccc} -\frac{\partial \bar{u}'v'}{\partial x} & -\frac{\partial \bar{v}^2}{\partial y} & -\frac{\partial \bar{v}'w'}{\partial z} \end{array} \right]$$



$$\tau_{ij} = \mu \left(\frac{\partial u_i}{\partial x_j} + \frac{\partial u_j}{\partial x_i} \right) - \underbrace{\rho \overline{u_i' u_j'}}_{\text{Renolds Stress}}$$

$$\left[\begin{array}{ccc} -\frac{\partial \bar{u}'w'}{\partial x} & -\frac{\partial \bar{v}'w'}{\partial y} & -\frac{\partial \bar{w}^2}{\partial z} \end{array} \right]$$

$$\tau \approx \tau_w = (\mu + \mu_t) \frac{\partial \bar{u}}{\partial y} \approx \rho \kappa^2 y^2 \left| \frac{\partial \bar{u}}{\partial y} \right| \frac{\partial \bar{u}}{\partial y} = \rho v_*^2$$

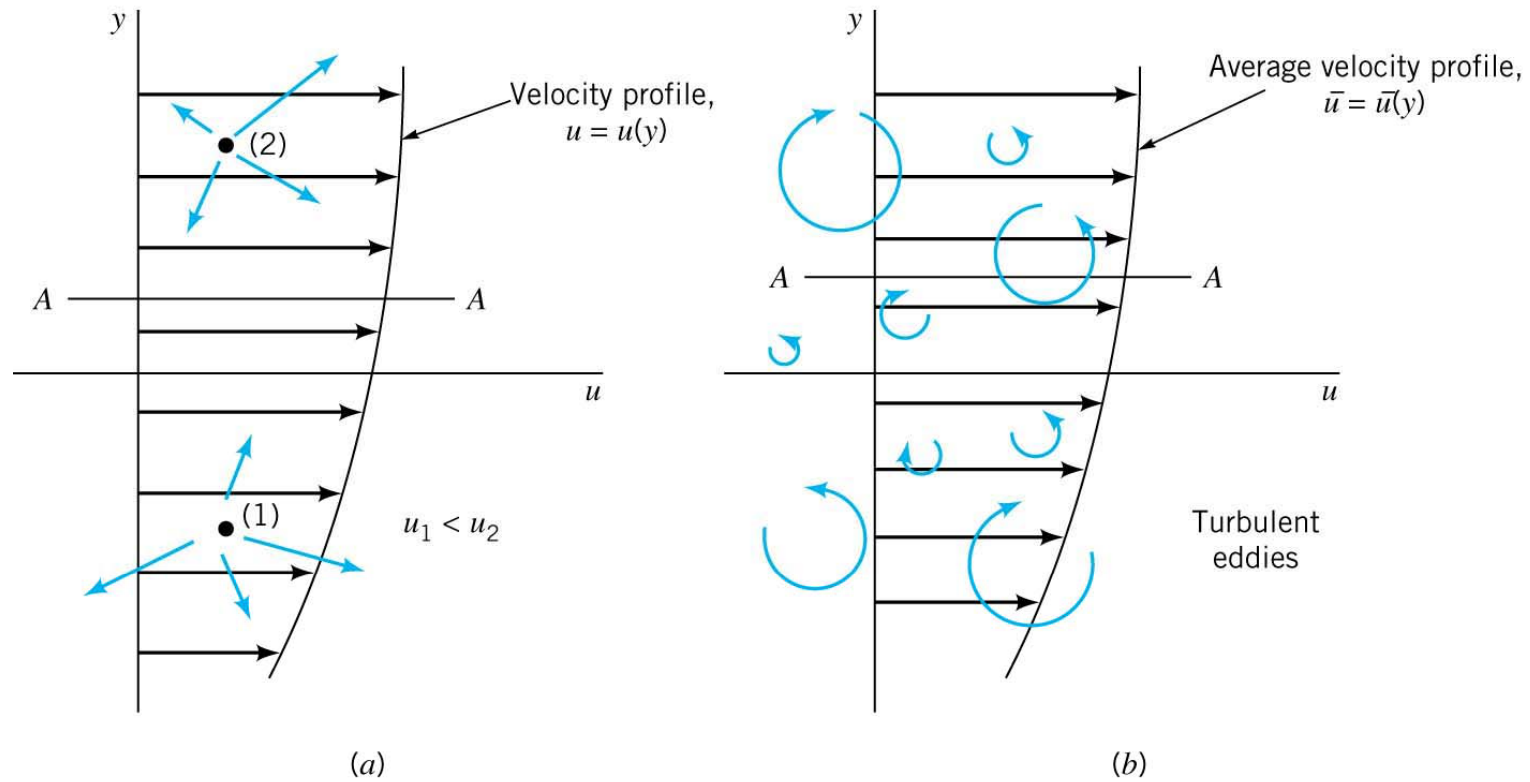


Fig. (a) Laminar flowshear stress caused by random of molecules (b) Turbulent flow as a series of random, 3-D eddies

Reynolds stresses --The six extra stresses

We need either information or a theory to evaluate these terms

$$\tau_{xx} = -\rho \overline{u'^2}$$

$$\tau_{yy} = -\rho \overline{v'^2}$$

$$\tau_{zz} = -\rho \overline{w'^2}$$

$$\tau_{xy} = \tau_{yx} = -\rho \overline{u'v'}$$

$$\tau_{xz} = \tau_{zx} = -\rho \overline{u'w'}$$

$$\tau_{yz} = \tau_{zy} = -\rho \overline{v'w'}$$

Three normal stresses

$$\left[-\frac{\partial \overline{u'^2}}{\partial x} - \frac{\partial \overline{u'v'}}{\partial y} - \frac{\partial \overline{u'w'}}{\partial z} \right]$$

$$\left[-\frac{\partial \overline{u'v'}}{\partial x} - \frac{\partial \overline{v'^2}}{\partial y} - \frac{\partial \overline{v'w'}}{\partial z} \right]$$

$$\left[-\frac{\partial \overline{u'w'}}{\partial x} - \frac{\partial \overline{v'w'}}{\partial y} - \frac{\partial \overline{w'^2}}{\partial z} \right]$$

Three shear stresses

Similar

The time average transport equation for scalar φ

$$\frac{\partial \Phi}{\partial t} + \text{div}(\Phi \mathbf{U}) = \text{div}(\Gamma_{\Phi}^* \text{grad } \Phi) + \left[-\frac{\partial \overline{u' \varphi'}}{\partial x} - \frac{\partial \overline{v' \varphi'}}{\partial y} - \frac{\partial \overline{w' \varphi'}}{\partial z} \right] + S_{\Phi}$$

$$\frac{\partial U}{\partial t} + \text{div}(U \mathbf{U}) = -\frac{1}{\rho} \frac{\partial P}{\partial x} + \nu \text{div grad } U + \left[-\frac{\partial \overline{u'^2}}{\partial x} - \frac{\partial \overline{u'v'}}{\partial y} - \frac{\partial \overline{u'w'}}{\partial z} \right]$$

$$\frac{\partial V}{\partial t} + \text{div}(V \mathbf{U}) = -\frac{1}{\rho} \frac{\partial P}{\partial y} + \nu \text{div grad } V + \left[-\frac{\partial \overline{u'v'}}{\partial x} - \frac{\partial \overline{v'^2}}{\partial y} - \frac{\partial \overline{v'w'}}{\partial z} \right]$$

$$\frac{\partial W}{\partial t} + \text{div}(W \mathbf{U}) = -\frac{1}{\rho} \frac{\partial P}{\partial z} + \nu \text{div grad } W + \left[-\frac{\partial \overline{u'w'}}{\partial x} - \frac{\partial \overline{v'w'}}{\partial y} - \frac{\partial \overline{w'^2}}{\partial z} \right]$$

$$\rho \frac{D \vec{V}}{D t} = \rho \vec{g} + \nabla \bar{p} + \nabla \cdot \tau_{ij}$$

$$\tau_{ij} = \mu \left(\frac{\partial u_i}{\partial x_j} + \frac{\partial u_j}{\partial x_i} \right) - \underbrace{\rho \overline{u_i' u_j'}}_{\text{Reynolds Stress}}$$

Table 3.1 Turbulent flow equations for compressible flows

Reynolds (Turbulent) Stresses

(unknown)待解

Continuity

$$\frac{\partial \rho}{\partial t} + \text{div}(\rho \mathbf{U}) = 0$$

Reynolds equations

$$\frac{\partial(\rho U)}{\partial t} + \text{div}(\rho U \mathbf{U}) = -\frac{\partial P}{\partial x} + \text{div}(\mu \text{grad } U) + \left[\begin{array}{ccc} \frac{\partial(\rho \overline{u'^2})}{\partial x} & \frac{\partial(\rho \overline{u'v'})}{\partial y} & \frac{\partial(\rho \overline{u'w'})}{\partial z} \end{array} \right] + S_{Mx}$$

$$\frac{\partial(\rho V)}{\partial t} + \text{div}(\rho V \mathbf{U}) = -\frac{\partial P}{\partial y} + \text{div}(\mu \text{grad } V) + \left[\begin{array}{ccc} \frac{\partial(\rho \overline{u'v'})}{\partial x} & \frac{\partial(\rho \overline{v'^2})}{\partial y} & \frac{\partial(\rho \overline{v'w'})}{\partial z} \end{array} \right] + S_{My}$$

$$\frac{\partial(\rho W)}{\partial t} + \text{div}(\rho W \mathbf{U}) = -\frac{\partial P}{\partial z} + \text{div}(\mu \text{grad } W) + \left[\begin{array}{ccc} \frac{\partial(\rho \overline{u'w'})}{\partial x} & \frac{\partial(\rho \overline{v'w'})}{\partial y} & \frac{\partial(\rho \overline{w'^2})}{\partial z} \end{array} \right] + S_{Mz}$$

10 unknown $u, v, w, p, -\rho \overline{u'^2}, -\rho \overline{v'^2}, -\rho \overline{w'^2}, -\rho \overline{u'v'}, -\rho \overline{u'w'}, -\rho \overline{v'w'}$

Scalar transport equation

$$\frac{\partial(\rho \Phi)}{\partial t} + \text{div}(\rho \Phi \mathbf{U}) = \text{div}(\Gamma_{\Phi} \text{grad } \Phi) + \left[\begin{array}{ccc} \frac{\partial(\rho \overline{u'\phi'})}{\partial x} & \frac{\partial(\rho \overline{v'\phi'})}{\partial y} & \frac{\partial(\rho \overline{w'\phi'})}{\partial z} \end{array} \right] + S_{\Phi}$$

Reynolds stresses

$$\rho \frac{D\vec{V}}{Dt} = \rho \vec{g} + \nabla \bar{p} + \nabla \cdot \tau_{ij}$$

$$\tau_{ij} = \mu \left(\frac{\partial u_i}{\partial x_j} + \frac{\partial u_j}{\partial x_i} \right) - \underbrace{\rho \overline{u'_i u'_j}}_{\text{Reynolds Stress}}$$

$$\tau_{ij} = \begin{pmatrix} \tau_{xx} & \tau_{xy} & \tau_{xz} \\ \tau_{yx} & \tau_{yy} & \tau_{yz} \\ \tau_{zx} & \tau_{zy} & \tau_{zz} \end{pmatrix}$$

$$\begin{aligned} & \left[\frac{\partial(\rho \overline{u'^2})}{\partial x} - \frac{\partial(\rho \overline{u'v'})}{\partial y} - \frac{\partial(\rho \overline{u'w'})}{\partial z} \right] + \\ & \left[\frac{\partial(\rho \overline{u'v'})}{\partial x} - \frac{\partial(\rho \overline{v'^2})}{\partial y} - \frac{\partial(\rho \overline{v'w'})}{\partial z} \right] + \\ & \left[\frac{\partial(\rho \overline{u'w'})}{\partial x} - \frac{\partial(\rho \overline{v'w'})}{\partial y} - \frac{\partial(\rho \overline{w'^2})}{\partial z} \right] \end{aligned}$$

suffix notation

$$\rightarrow \tau_{ij} = -\rho \overline{u'_i u'_j} = \mu_t \left(\frac{\partial U_i}{\partial x_j} + \frac{\partial U_j}{\partial x_i} \right)$$

(Boussinesq (1877))

turbulent stresses increase as the mean rate of deformation increases

e.g. similar to lamilar flow viscous stress

$$\tau_{ij} = \mu e_{ij} = \mu \left(\frac{\partial u_i}{\partial x_j} + \frac{\partial u_j}{\partial x_i} \right) \quad \tau_{12} = \tau_{xy} = \mu \left(\frac{\partial u_1}{\partial x_2} + \frac{\partial u_2}{\partial x_1} \right) = \mu \left(\frac{\partial u}{\partial y} + \frac{\partial v}{\partial x} \right)$$

μ_t eddy viscosity (Pa s) $\nu_t = \mu_t / \rho$ kinematic eddy viscosity m²/s

3.5 Turbulence models – Reynolds stress equation models

∴ We need either information or a theory to evaluate Reynolds stresses

<u>Classical models</u>	Based on (time-averaged) Reynolds equations <ol style="list-style-type: none">1. zero equation model – mixing length model2. two-equation model – k-ϵ model3. Reynolds stress equation model4. algebraic stress model
<u>Large eddy simulation</u>	Based on space-filtered equations

The **classical models** use the Reynolds equations developed in section 3.3 and form the basis of turbulence calculations in currently available commercial CFD codes. **Large eddy simulations** are turbulence models where the time-dependent flow equations are solved for the mean flow and the largest eddies and where the effects of the smaller eddies are modelled. It was argued earlier that the largest eddies interact strongly with the mean flow and contain most of the energy so this approach results in a good model of the main effects of turbulence. Large eddy

3.5.1 Mixing length model

Similar to laminar flow

$$\tau_{yx} = \mu \frac{du}{dy} \quad \mu = \text{dynamic viscosity} \quad \nu \equiv \frac{\mu}{\rho} \quad \text{kinematic viscosity}$$

The Eddy Viscosity

$$\tau_i = -\rho \overline{u'v'} = \mu_t \frac{\partial \bar{u}}{\partial y}, \quad \mu_t = \text{eddy viscosity}, \quad \overline{u'v'} = \text{eddy diffusivity}$$

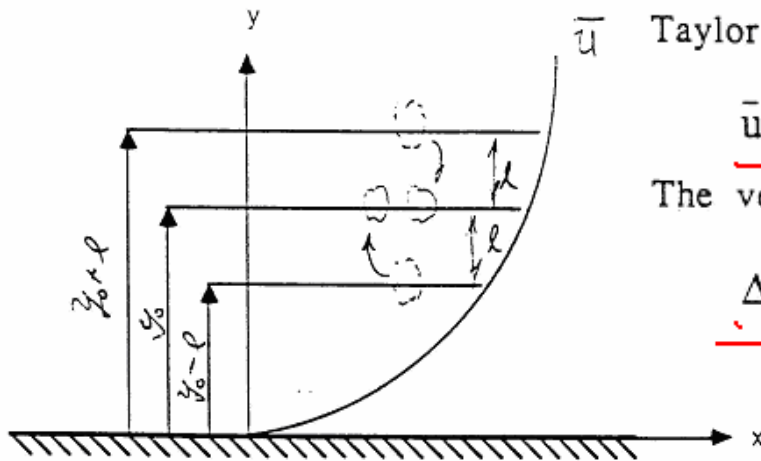
Mixing Length $-\overline{u'v'} \approx (\text{const}) u'_{rms} v'_{rms} \approx (\text{const}) \left(l_1 \frac{\partial \bar{u}}{\partial y} \right) \left(l_2 \frac{\partial \bar{u}}{\partial y} \right)$

Reynolds stresses

$$\tau_{xy} = \tau_{yx} = -\rho \overline{u'v'} = \rho \ell_m^2 \left| \frac{\partial U}{\partial y} \right| \frac{\partial U}{\partial y} = \mu_t \frac{\partial U}{\partial y} \Rightarrow \mu_t \approx \rho \ell_m^2 \left| \frac{\partial U}{\partial y} \right|$$

Prandtl's mixing length model.

Consider a plane, incompressible, and steady mean flow over a wall



Taylor series:

$$\bar{u}(y_0 \pm \ell) = \bar{u}(y_0) \pm \ell \left. \frac{\partial \bar{u}}{\partial y} \right|_{y=y_0} + \dots$$

The velocity difference, hence the fluctuation, are

$$\Delta_{\pm} \bar{u}(y_0) = u'(y_0) \approx \pm \ell \left. \frac{\partial \bar{u}}{\partial y} \right|_{y=y_0}$$

$$\bar{u}' \approx \left(l_1 \frac{\partial \bar{u}}{\partial y} \right)$$

$$|\bar{v}'| \propto |\bar{u}'|$$

$$\mu_t \approx \rho l^2 \left| \frac{\partial \bar{u}}{\partial y} \right|$$

$$-\overline{u'v'} \approx (\text{const}) u'_{rms} v'_{rms} \approx (\text{const}) \left(l_1 \frac{\partial \bar{u}}{\partial y} \right) \left(l_2 \frac{\partial \bar{u}}{\partial y} \right)$$

$$\tau_{xy} = \tau_{yx} = -\rho \overline{u'v'} = \rho \ell^2 \left| \frac{\partial \bar{u}}{\partial y} \right| \frac{\partial \bar{u}}{\partial y} = \mu_t \frac{\partial \bar{u}}{\partial y} \rightarrow \mu_t \approx \rho \ell^2 \left| \frac{\partial \bar{u}}{\partial y} \right| \approx \rho (ky)^2 \left| \frac{\partial \bar{u}}{\partial y} \right|$$

Prandtl's mixing length model. $l = ky$

Mixing length is not a constant. Prandtl suggested that

$$l_m = ky$$

experimental, $k \approx 0.4$

k is called the von Karman mixing length constant

Reynolds stresses

$$\tau_{xy} = \tau_{yx} = -\rho \overline{u'v'} = \rho l^2 \left| \frac{\partial \bar{u}}{\partial y} \right| \frac{\partial \bar{u}}{\partial y} = \mu_t \frac{\partial \bar{u}}{\partial y} \rightarrow \mu_t \approx \rho l^2 \left| \frac{\partial \bar{u}}{\partial y} \right|$$

$$l = ky \rightarrow \mu_t \approx \rho l^2 \left| \frac{\partial \bar{u}}{\partial y} \right| \approx \rho (ky)^2 \left| \frac{\partial \bar{u}}{\partial y} \right|$$

$$-\rho \overline{v'\phi'} = \mu_t / \sigma_t \frac{\partial \Phi}{\partial y} \quad \mu_t \approx \rho l^2 \left| \frac{\partial \bar{u}}{\partial y} \right|$$

σ_t of 0.9 in near wall flows, 0.5 for jets and mixing layers and 0.7 in axisymmetric jets.

Prandtl's mixing length model.

- The boundary layer equation for turbulent flow over a flat plate

$$\rho \left[\bar{u} \frac{\partial \bar{u}}{\partial x} + \bar{v} \frac{\partial \bar{u}}{\partial y} \right] = -\frac{d\bar{p}}{dx} + \frac{\partial \Sigma}{\partial y} \quad \Sigma = \rho(v + v_T) \frac{\partial \bar{u}}{\partial y}$$

Consider parallel flow, the governing equation is

$$\frac{d}{dy} \left[(\mu + \rho v_T) \frac{d\bar{u}}{dy} \right] = -\frac{d\bar{p}}{dx} = 0$$

Let us introduce the dimensionless variables as follow

$$u^+ = \frac{\bar{u}}{u_\tau} = \frac{\bar{u}}{\sqrt{\tau_o/\rho}} = \frac{\bar{u} / U_\infty}{\sqrt{c_f/2}}$$

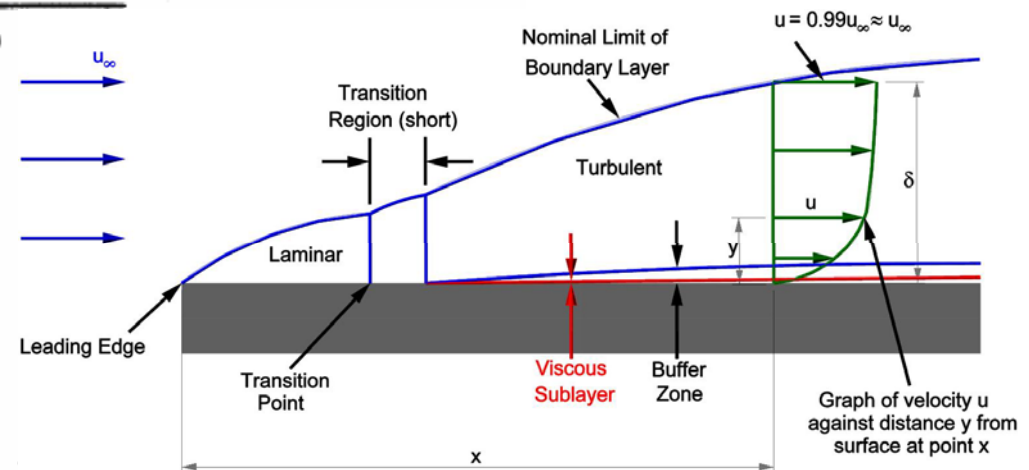
$$y^+ = \frac{yu_\tau}{\nu} = \frac{y\sqrt{\tau_o/\rho}}{\nu} = \frac{yU_\infty\sqrt{c_f/2}}{\nu}$$

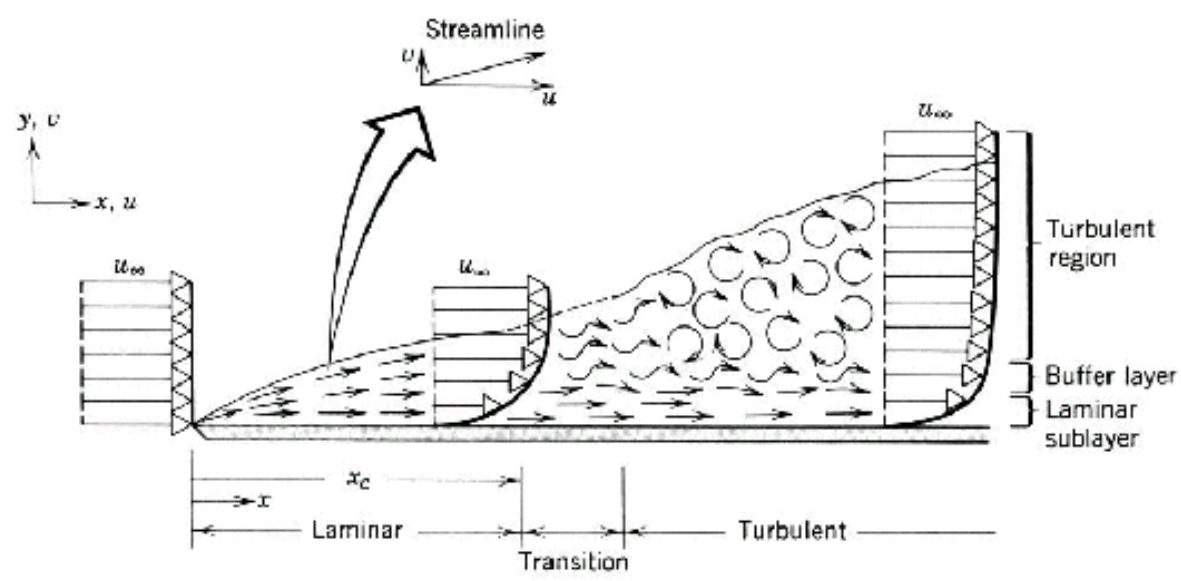
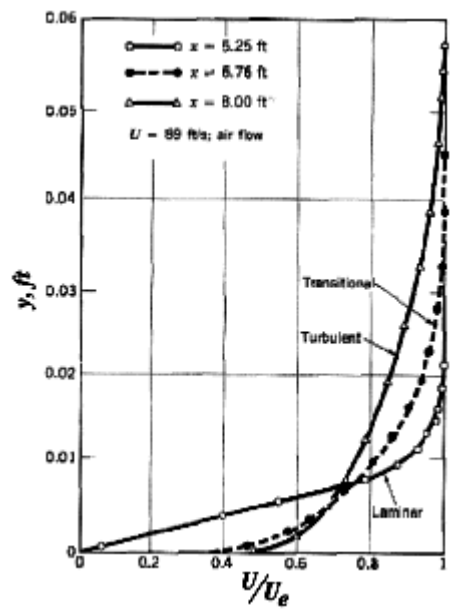
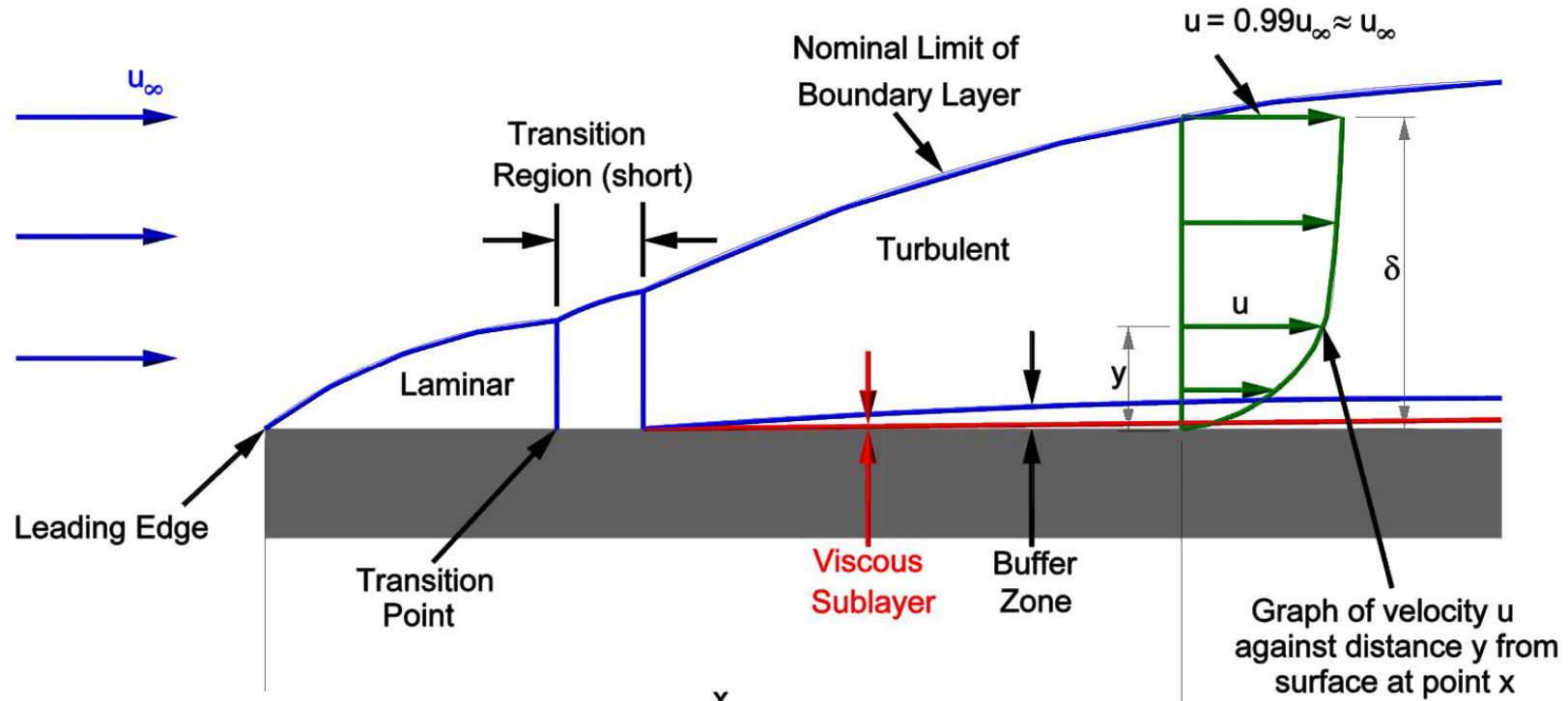
The dimensionless equation is

$$\frac{d}{dy^+} \left[\left(1 + \frac{\nu_T}{\nu} \right) \frac{du^+}{dy^+} \right] = 0$$

Integrating once, we obtain

$$\left(1 + \frac{\nu_T}{\nu} \right) \frac{du^+}{dy^+} = 1$$





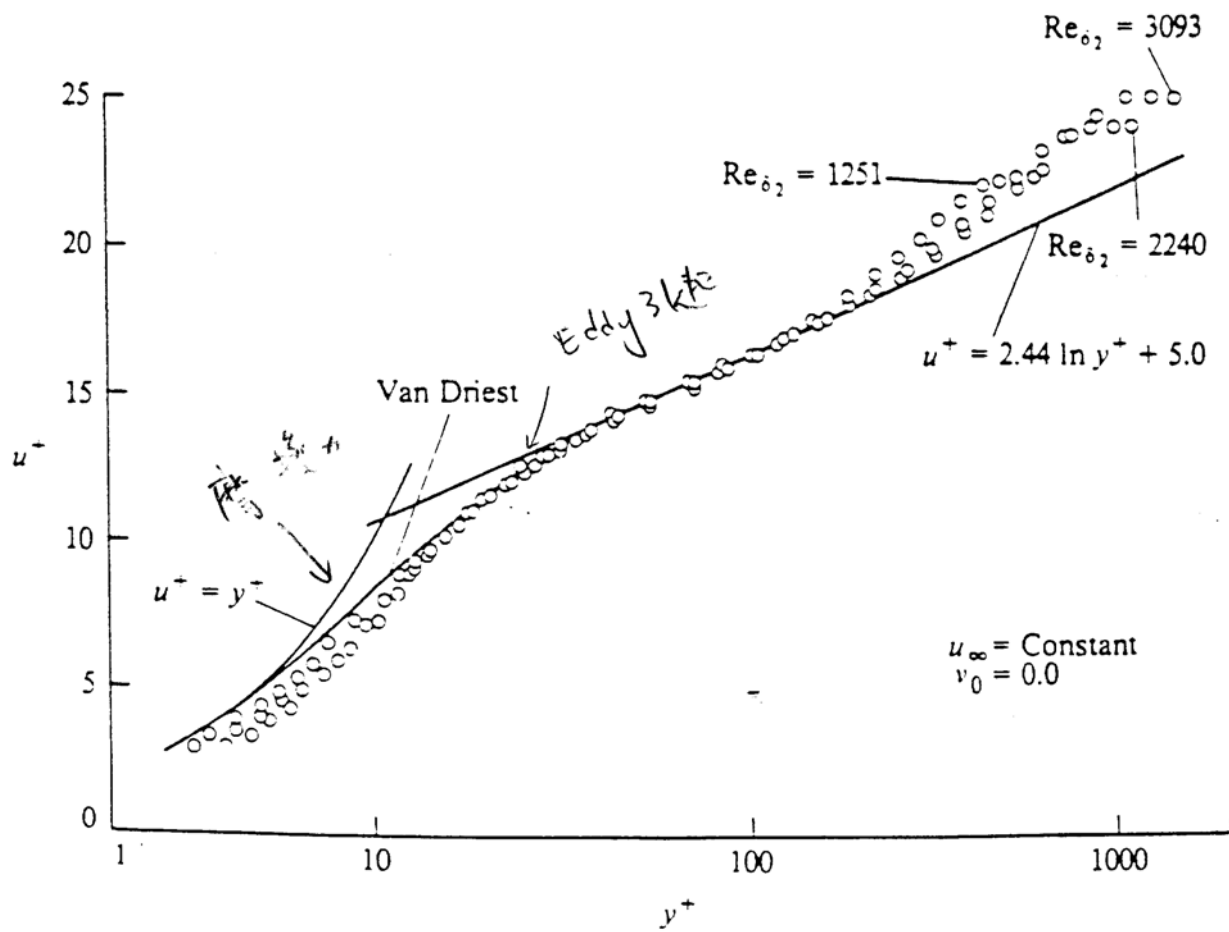


Figure 10-3 Turbulent boundary-layer profiles in wall coordinates (data of Anderson et al.¹³).

$$\left(1 + \frac{\nu_T}{\nu}\right) \frac{du^+}{dy^+} = 1$$

(1) the viscous sublayer $\nu \gg \nu_T$

$$\frac{\nu_T}{\nu} \rightarrow 0$$

ν molecular viscosity
 ν_T eddy viscosity

$$\frac{du^+}{dy^+} = 1 \Rightarrow u^+ = y^+$$

(2) In the fully turbulent region, $\nu \ll \nu_T$

the eddy diffusivity is much larger than the molecular viscosity,

$$\frac{\nu_T}{\nu} \rightarrow \infty \quad \frac{\nu_T}{\nu} \frac{du^+}{dy^+} = 1$$

Substituting the Prandtl's mixing length

$$\therefore \nu_T \approx \ell_m^2 \left| \frac{\partial \bar{u}}{\partial y} \right| = \ell_m^2 \frac{\partial u^+ u_\tau}{\partial y^+ \nu / u_\tau}$$

$$\frac{\nu_T}{\nu} \approx \ell_m^2 \left| \frac{\partial \bar{u}}{\partial y} \right| = \ell_m^2 \frac{u_\tau^2}{\nu^2} \frac{\partial u^+}{\partial y^+}$$

$$u^+ = \frac{\bar{u}}{u_\tau} = \frac{\bar{u}}{\sqrt{\tau_o/\rho}} = \frac{\bar{u}}{\sqrt{c_f/2} U_\infty}$$

$$y^+ = \frac{y u_\tau}{\nu} = \frac{y \sqrt{\tau_o/\rho}}{\nu} = \frac{y U_\infty \sqrt{c_f/2}}{\nu}$$

$$\frac{\nu_T}{\nu} \frac{du^+}{dy^+} = 1 \Rightarrow \ell_m^2 \left| \frac{du^+}{dy^+} \right| \frac{du^+}{dy^+} = 1 \quad \ell_m^+ = \frac{\ell_m u_\tau}{\nu}$$

$$\Rightarrow \frac{du^+}{dy^+} = \frac{1}{k y^+}$$

Integrating,
$$u^+ = \frac{1}{k} \ln y^+ + C$$

This is called the law-of-the-wall.

$$\tau_{xy} = \tau_{yx} = -\rho \overline{u'v'} = \rho \ell_m^2 \left| \frac{\partial U}{\partial y} \right| \frac{\partial U}{\partial y} = \mu_t \frac{\partial U}{\partial y} \rightarrow \mu_t \approx \rho \ell_m^2 \left| \frac{\partial U}{\partial y} \right| \approx \rho (\kappa y)^2 \left| \frac{\partial U}{\partial y} \right|$$

Table 3.3 Mixing lengths for two-dimensional turbulent flows

Flow	Mixing length l_m	L
Mixing layer	0.07L	Layer width
Jet	0.09L	Jet half width
Wake	0.16L	Wake half width
Axisymmetric jet	0.075L	Jet half width
Boundary layer ($\partial p / \partial x = 0$)		
viscous sub-layer and		
log-law layer ($y/L \leq 0.22$)	$\kappa y [1 - \exp(-y^+ / 26)]$	Boundary layer thickness
outer layer ($y/L \geq 0.22$)	0.09L	
Pipes and channels (fully developed flow)	$L[0.14 - 0.08(1 - y/L)^2 - 0.06(1 - y/L)^4]$	Pipe radius or channel half width

Mixing length model assessment

Advantages

- easy to implement and cheap in terms of computing resources
- good predictions for thin shear layers: jets, mixing layers, wakes and boundary layers
- well established

Disadvantages

- completely incapable of describing flows with separation and recirculation
- only calculates mean flow properties and turbulent shear stress

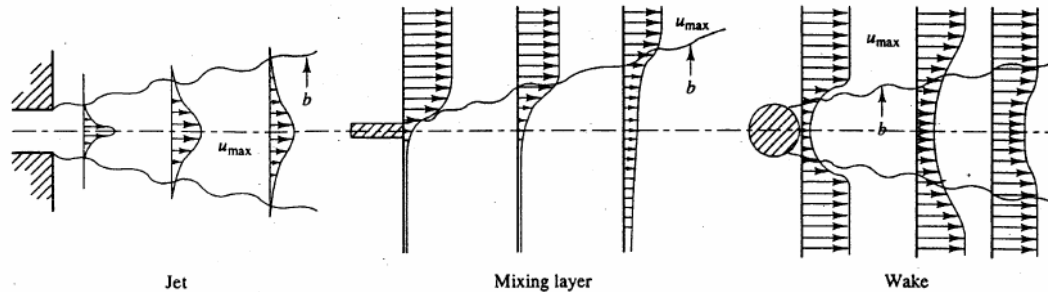
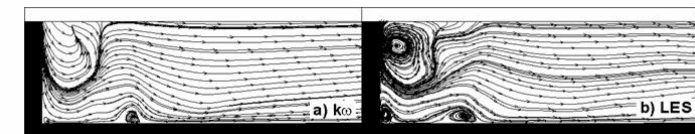
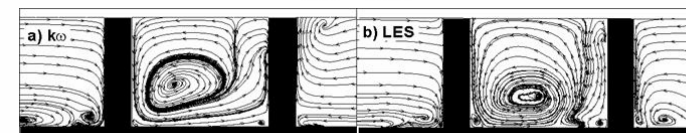


Fig. 3.8 Free turbulent flows



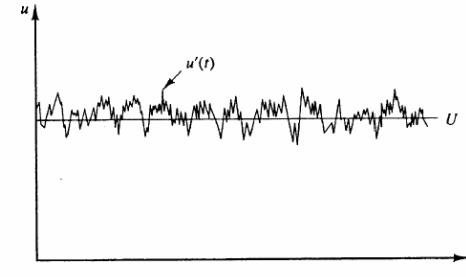
$x/D = 2.75$



$y/D = 3.4375$

3.5.2 The $k-\epsilon$ model

Definition:



instantaneous kinetic energy

$$\underline{k(t) = K + k}$$

the mean kinetic energy

$$\underline{K} = \frac{1}{2} (U^2 + V^2 + W^2)$$

the turbulent kinetic energy

$$\underline{k} = \frac{1}{2} (\overline{u'^2} + \overline{v'^2} + \overline{w'^2}):$$

前述

the turbulent stresses,

$$\tau_{ij} = \begin{pmatrix} \tau_{xx} & \tau_{xy} & \tau_{xz} \\ \tau_{yx} & \tau_{yy} & \tau_{yz} \\ \tau_{zx} & \tau_{zy} & \tau_{zz} \end{pmatrix}$$

$$\tau_{ij} = \rho \overline{u'v'} = 2\mu_t E_{ij}$$

the rate of deformation $e_{ij} =$

$$\begin{pmatrix} e_{xx} & e_{xy} & e_{xz} \\ e_{yx} & e_{yy} & e_{yz} \\ e_{zx} & e_{zy} & e_{zz} \end{pmatrix}$$

fluctuating component

$$e_{ij}(t) = E_{ij} + e'_{ij},$$

mean component,

the rate of deformation

$$e_{ij}(t) = E_{ij} + e'_{ij}, \quad \text{👉}$$

$$e_{xx}(t) = E_{xx} + e'_{xx} = \frac{\partial U}{\partial x} + \frac{\partial u'}{\partial x};$$

$$e_{yy}(t) = E_{yy} + e'_{yy} = \frac{\partial V}{\partial y} + \frac{\partial v'}{\partial y}$$

$$e_{zz}(t) = E_{zz} + e'_{zz} = \frac{\partial W}{\partial z} + \frac{\partial w'}{\partial z}$$

$$e_{xy}(t) = E_{xy} + e'_{xy} = e_{yx}(t) = E_{yx} + e'_{yx} = \frac{1}{2} \left[\frac{\partial U}{\partial y} + \frac{\partial V}{\partial x} \right] + \frac{1}{2} \left[\frac{\partial u'}{\partial y} + \frac{\partial v'}{\partial x} \right]$$

$$e_{xz}(t) = E_{xz} + e'_{xz} = e_{zx}(t) = E_{zx} + e'_{zx} = \frac{1}{2} \left[\frac{\partial U}{\partial z} + \frac{\partial W}{\partial x} \right] + \frac{1}{2} \left[\frac{\partial u'}{\partial z} + \frac{\partial w'}{\partial x} \right]$$

$$e_{yz}(t) = E_{yz} + e'_{yz} = e_{zy}(t) = E_{zy} + e'_{zy} = \frac{1}{2} \left[\frac{\partial V}{\partial z} + \frac{\partial W}{\partial y} \right] + \frac{1}{2} \left[\frac{\partial v'}{\partial z} + \frac{\partial w'}{\partial y} \right]$$

$$\text{👉 } \tau_{ij} = \overline{\rho u' v'} = 2\mu_t E_{ij}$$

$$= \rho C_\mu \frac{k^2}{\varepsilon} \left(\frac{\partial U_i}{\partial x_j} + \frac{\partial U_j}{\partial x_i} \right)$$

$$\tau_i = -\overline{\rho u' v'} = \mu_t \frac{\partial \bar{u}}{\partial y}$$

μ_t = eddy viscosity

Governing equation for mean flow kinetic energy K

$$K = \frac{1}{2} (U^2 + V^2 + W^2)$$

Reynolds equations

$$U \times \frac{\partial(\rho U)}{\partial t} + \text{div}(\rho U U) = -\frac{\partial P}{\partial x} + \text{div}(\mu \text{grad } U) + \left[-\frac{\partial(\rho \overline{u'^2})}{\partial x} - \frac{\partial(\rho \overline{u'v'})}{\partial y} - \frac{\partial(\rho \overline{u'w'})}{\partial z} \right] + S_{Mx}$$

$$V \times \frac{\partial(\rho V)}{\partial t} + \text{div}(\rho V U) = -\frac{\partial P}{\partial y} + \text{div}(\mu \text{grad } V) + \left[-\frac{\partial(\rho \overline{u'v'})}{\partial x} - \frac{\partial(\rho \overline{v'^2})}{\partial y} - \frac{\partial(\rho \overline{v'w'})}{\partial z} \right] + S_{My}$$

$$+ W \times \frac{\partial(\rho W)}{\partial t} + \text{div}(\rho W U) = -\frac{\partial P}{\partial z} + \text{div}(\mu \text{grad } W) + \left[-\frac{\partial(\rho \overline{u'w'})}{\partial x} - \frac{\partial(\rho \overline{v'w'})}{\partial y} - \frac{\partial(\rho \overline{w'^2})}{\partial z} \right] + S_{Mz}$$

$$\begin{aligned} \rightarrow \frac{\partial(\rho K)}{\partial t} &+ \text{div}(\rho K U) = \text{div} \left(-P U + 2\mu U E_{ij} - \rho U \overline{u'_i u'_j} \right) - 2\mu E_{ij} \cdot E_{ij} + \rho \overline{u'_i u'_j} \cdot E_{ij} \\ \text{(I)} & \quad \text{(II)} \quad \quad \text{(III)} \quad \quad \text{(IV)} \quad \quad \text{(V)} \quad \quad \text{(VI)} \quad \quad \text{(VII)} \end{aligned}$$

Rate of change of K of K by convection = of K by pressure + of K by viscous stresses + Transport of K by Reynolds stress - Rate of dissipation of K + Turbulence production

In high Reynolds number flows the turbulent terms (V) and (VII) are always much larger than their viscous counterparts (IV) and (VI)

Governing equation for turbulent kinetic energy k

$$k = \frac{1}{2}(\overline{u'^2} + \overline{v'^2} + \overline{w'^2})$$

$\nabla \cdot$ the instantaneous Navier–Stokes equations

$$u' \times \frac{\partial u}{\partial t} + \text{div}(u\mathbf{u}) = -\frac{1}{\rho} \frac{\partial p}{\partial x} + \nu \text{div grad } u$$

$$v' \times \frac{\partial v}{\partial t} + \text{div}(v\mathbf{u}) = -\frac{1}{\rho} \frac{\partial p}{\partial y} + \nu \text{div grad } v$$

$$+ w' \times \frac{\partial w}{\partial t} + \text{div}(w\mathbf{u}) = -\frac{1}{\rho} \frac{\partial p}{\partial z} + \nu \text{div grad } w$$

$$\rightarrow \frac{\partial(\rho k)}{\partial t} + \text{div}(\rho k \mathbf{U}) = \text{div} \left(-\overline{p' \mathbf{u}'} + 2\overline{\mu \mathbf{u}' e'_{ij}} - \rho \frac{1}{2} \overline{u'_i \cdot u'_i u'_j} \right) - 2\overline{\mu e'_{ij} \cdot e'_{ij}} - \rho \overline{u'_i u'_j} \cdot E_{ij}$$

(I)	(II)	(III)	(IV)	(V)	(VI)	(VII)
Rate of change of k	+ Transport of k by convection	= Transport of k by pressure	+ Transport of k by viscous stresses	+ Transport of k by Reynolds stress	- Rate of dissipation of k	+ Turbulence production

i.e. High Re

$$2\overline{\mu e'_{ij} \cdot e'_{ij}} > 2\overline{\mu \mathbf{u}' e'_{ij}}$$

$$\varepsilon = \frac{-2\overline{\mu e'_{ij} \cdot e'_{ij}}}{\rho} = 2\nu \overline{e'_{ij} \cdot e'_{ij}}$$

☞ Rate of Turbulence dissipation of k (V)

$$-2\mu \overline{e'_{ij} \cdot e'_{ij}} = -2\mu \left(\overline{e'^2_{11}} + \overline{e'^2_{22}} + \overline{e'^2_{33}} + 2\overline{e'^2_{12}} + 2\overline{e'^2_{13}} + 2\overline{e'^2_{23}} \right)$$

The dissipation of turbulent kinetic energy is caused by work done by the smallest eddies against viscous stresses

☞ The rate of dissipation per unit mass,

$$\tau_{ij} = \rho \overline{u'v'} = 2\mu_t E_{ij}$$

$$\varepsilon = \frac{-2\mu \overline{e'_{ij} \cdot e'_{ij}}}{\rho} = 2\nu \overline{e'_{ij} \cdot e'_{ij}} \quad m^2/s^3$$

when the Reynolds number is high, the viscous transport term (IV) is always very small compared to the turbulent transport term (VI).

$$\text{i.e. High Re} \quad 2\mu \overline{e'_{ij} \cdot e'_{ij}} > 2\mu \overline{u' \cdot e'_{ij}}$$

☞ It is possible to develop similar transport equations for all other turbulence quantities including the rate of viscous dissipation ε (see Bradshaw *et al*, 1981). The exact ε -

The k - ε model equations

Two model equations of k and ε for solving k and ε

The **standard k - ε model** (Launder and Spalding, 1974) has two model equations, one for turbulent kinetic energy k and the rate of viscous dissipation ε

☞ $k = \frac{1}{2} (\overline{u'^2} + \overline{v'^2} + \overline{w'^2})$

$$\varepsilon = \frac{-2\mu \overline{e'_{ij} e'_{ij}}}{\rho} = 2\nu \overline{e'_{ij} e'_{ij}}$$

☞ **Definte:** velocity scale $\vartheta = k^{1/2}$ length scale $\ell = \frac{k^{3/2}}{\varepsilon}$

☞ eddy viscosity $\mu_t = C\rho\vartheta\ell = \rho C_\mu \frac{k^2}{\varepsilon}$ C_μ is a dimensionless constant.

☞
$$\tau_{ij} = -\rho \overline{u'_i u'_j} = 2\mu_t E_{ij} = \mu_t \left(\frac{\partial U_i}{\partial x_j} + \frac{\partial U_j}{\partial x_i} \right) = \rho C_\mu \frac{k^2}{\varepsilon} \left(\frac{\partial U_i}{\partial x_j} + \frac{\partial U_j}{\partial x_i} \right)$$

☞ 10 unknown $u, v, w, p, -\rho \overline{u'^2}, -\rho \overline{v'^2}, -\rho \overline{w'^2}, -\rho \overline{u'v'}, -\rho \overline{u'w'}, -\rho \overline{v'w'}$

假如 $k, \varepsilon, \kappa, \mu$ 已知，可求得六個 **Reynolds stress**

eddy viscosity $\mu_t = C\rho\vartheta l = \rho C_\mu \frac{k^2}{\varepsilon}$



The standard model uses the following transport equations used for k and ε :

$$\textcircled{k} \quad \frac{\partial(\rho k)}{\partial t} + \text{div}(\rho k \mathbf{U}) = \text{div} \left[\frac{\mu_t}{\sigma_k} \text{grad } k \right] + 2\mu_t E_{ij} \cdot E_{ij} - \rho \varepsilon$$

$$\textcircled{\varepsilon} \quad \frac{\partial(\rho \varepsilon)}{\partial t} + \text{div}(\rho \varepsilon \mathbf{U}) = \text{div} \left[\frac{\mu_t}{\sigma_\varepsilon} \text{grad } \varepsilon \right] + C_{1\varepsilon} \frac{\varepsilon}{k} 2\mu_t E_{ij} \cdot E_{ij} - C_{2\varepsilon} \rho \frac{\varepsilon^2}{k}$$

Rate of change of k or ε + Transport of k or ε by convection = Transport of k or ε by diffusion + Rate of production of k or ε - Rate of destruction of k or ε

$$C_\mu = 0.09; \quad \sigma_k = 1.00; \quad \sigma_\varepsilon = 1.30; \quad C_{1\varepsilon} = 1.44; \quad C_{2\varepsilon} = 1.92$$

$$\tau_{ij} = \rho \overline{u'_i u'_j} = 2\mu_t E_{ij}$$

👉 Boussinesq relationship :

To compute the Reynolds stresses with the k - ϵ model

$$-\rho \overline{u'_i u'_j} = \mu_t \left(\frac{\partial U_i}{\partial x_j} + \frac{\partial U_j}{\partial x_i} \right) - \frac{2}{3} \rho k \delta_{ij} = 2\mu_t E_{ij} - \frac{2}{3} \rho k \delta_{ij}$$

δ_{ij} , the Kronecker delta ($\delta_{ij} = 1$ if $i = j$ and $\delta_{ij} = 0$ if $i \neq j$)

Example $i = j$ For incompressible flow

the normal stresses $\tau_{xx} = -\rho \overline{u'^2}$, $\tau_{yy} = -\rho \overline{v'^2}$ and $\tau_{zz} = -\rho \overline{w'^2}$.

$$2\mu_t E_{ii} = 2\mu_t \left[\frac{\partial U}{\partial x} + \frac{\partial V}{\partial y} + \frac{\partial W}{\partial z} \right] = 2\mu_t \operatorname{div} \mathbf{U} = 0$$

$$-\rho \overline{u'_i u'_j} = 2\mu_t E_{ij} - \frac{2}{3} \rho k \delta_{ij} \quad \Rightarrow \quad -\rho \overline{u'_i u'_j} = -2\rho k \quad k = \frac{1}{2} (\overline{u'^2} + \overline{v'^2} + \overline{w'^2})$$

Boundary conditions

- inlet: distributions of k and ε must be given
- outlet or symmetry axis: $\partial k / \partial n = 0$ and $\partial \varepsilon / \partial n = 0$
- free stream: $k = 0$ and $\varepsilon = 0$
- solid walls: approach depends on Reynolds number (see below)

(1) for k and ε in internal flows can be obtained from

$$k = \frac{3}{2}(U_{ref} T_i)^2; \quad \varepsilon = C_\mu^{3/4} \frac{k^{3/2}}{\ell}; \quad \ell = 0.07L$$

T_i the turbulence intensity

$$T_i = \frac{\left(\frac{2}{3}k\right)^{1/2}}{U_{ref}}$$

L characteristic length of the equipment (equivalent pipe radius)

(2) **At high Reynolds number the standard k - ϵ model**

the universal distributions near a solid wall $30 < y_p^+ < 500$

log-law $u^+ = \frac{1}{\kappa} \ln y^+ + B = \frac{1}{\kappa} \ln(Ey^+)$ $y^+ = \frac{yu_\tau}{\nu} = \frac{y\sqrt{\tau_o/\rho}}{\nu} = \frac{yU_\infty\sqrt{c_f/2}}{\nu}$

the eddy viscosity formula $\mu_t = C\rho\vartheta\ell = \rho C_\mu \frac{k^2}{\epsilon}$ $u^+ = \frac{\bar{u}}{u_\tau} = \frac{\bar{u}}{\sqrt{\tau_o/\rho}} = \frac{\bar{u}/U_\infty}{\sqrt{c_f/2}}$

Then

$$u^+ = \frac{U}{u_\tau} = \frac{1}{\kappa} \ln(Ey_p^+); \quad k = \frac{u_\tau^2}{\sqrt{C_\mu}}; \quad \epsilon = \frac{u_\tau^3}{\kappa y}$$

Von Karman's constant $\kappa = 0.41$

the wall roughness parameter $E = 9.8$ for smooth walls

For heat transfer (Launder and Spalding, 1974)

$$T^+ \equiv -\frac{(T - T_w)C_p\rho u_\tau}{q_w} = \sigma_{T,t} \left[u^+ + P \left(\frac{\sigma_{T,l}}{\sigma_{T,t}} \right) \right]$$

For heat transfer (Launder and Spalding, 1974)

$$T^+ \equiv - \frac{(T - T_w) C_p \rho u_\tau}{q_w} = \sigma_{T,t} \left[u^+ + P \left(\frac{\sigma_{T,l}}{\sigma_{T,t}} \right) \right]$$

with T_P = temperature at near wall point y_P

T_w = wall temperature

q_w = wall heat flux

C_p = fluid specific heat at constant pressure

$\sigma_{T,t}$ = turbulent Prandtl number

$\sigma_{T,l} = \mu C_p / \Gamma_T =$ Prandtl number

Γ_T = thermal conductivity

(3) At low Reynolds numbers

the log-law is not valid so the above-mentioned boundary conditions cannot be used.

The equations of the low Reynolds number k - ϵ model.

Patel *et al* (1985)

$$\frac{\partial(\rho k)}{\partial t} + \text{div}(\rho k \mathbf{U}) = \text{div} \left[\left(\mu + \frac{\mu_t}{\sigma_k} \right) \text{grad } k \right] + 2\mu_t E_{ij} \cdot E_{ij} - \rho \epsilon$$

$$\begin{aligned} \frac{\partial(\rho \epsilon)}{\partial t} + \text{div}(\rho \epsilon \mathbf{U}) = & \text{div} \left[\left(\mu + \frac{\mu_t}{\sigma_\epsilon} \right) \text{grad } \epsilon \right] \\ & + C_{1\epsilon} f_1 \frac{\epsilon}{k} 2\mu_t E_{ij} \cdot E_{ij} - C_{2\epsilon} f_2 \rho \frac{\epsilon^2}{k} \end{aligned}$$

$$\mu_t = \rho C_\mu f_\mu \frac{k^2}{\epsilon}$$

where wall-damping functions Lam and Bremhorst (1981)

$$f_1 = \left(1 + \frac{0.05}{f_\mu} \right)^3 \quad f_2 = 1 - \exp(-Re_t^2) \quad f_\mu = [1 - \exp(-0.0165 Re_y)]^2 \left(1 + \frac{20.5}{Re_t} \right)$$

$$Re_t = \vartheta \ell / \nu = k^2 / (\epsilon \nu) \quad Re_y = k^{1/2} y / \nu.$$

$$\tau_{ij} = -\rho \overline{u'_i u'_j} = \mu_t \left(\frac{\partial U_i}{\partial x_j} + \frac{\partial U_j}{\partial x_i} \right)$$

$k-\epsilon$ model assessment

Advantages

- simplest turbulence model for which only initial and/or boundary conditions need to be supplied
- excellent performance for many industrially relevant flows
- well established; the most widely validated turbulence model

Disadvantages

- more expensive to implement than mixing length model (two extra PDEs)
 - poor performance in a variety of important cases such as
 - (i) some unconfined flows
 - (ii) flows with large extra strains (e.g. curved boundary layers, swirling flows)
 - (iii) rotating flows
 - (iv) fully developed flows in non-circular ducts
-

3.5.3 Reynolds stress equation models (RSM)

(the second-order or second-moment closure model)

Several major drawbacks of the $k-\epsilon$ model emerge when it is attempted to predict flows with complex strain fields or significant body forces. (e.g. centrifugal force)

Reynolds stress $R_{ij} = -\tau_{ij}/\rho = \overline{u'_i u'_j}$

$$\frac{DR_{ij}}{Dt} = P_{ij} + D_{ij} - \epsilon_{ij} + \Pi_{ij} + \Omega_{ij}$$

Rate of change of $R_{ij} = \overline{u'_i u'_j}$	+	Transport of R_{ij} by convection	=	Rate of production of R_{ij}	+	Transport of R_{ij} by diffusion	-	Rate of dissipation of R_{ij}
				+				
				Transport of R_{ij} due to turbulent pressure- strain interactions	+	Transport of R_{ij} due to rotation		

Equation (3.45) describes six partial differential equations: one for the transport of each of the six independent Reynolds stresses ($\overline{u_1^2}, \overline{u_2^2}, \overline{u_3^2}, \overline{u_1 u_2}, \overline{u_1 u_3}$ and $\overline{u_2 u_3}$)

the pressure-strain correlation term Π_{ij} , and the rotation term Ω_{ij} .

Rate of production of R_{ij} :

$$P_{ij} = - \left(R_{im} \frac{\partial U_j}{\partial x_m} + R_{jm} \frac{\partial U_i}{\partial x_m} \right)$$

Transport of R_{ij} by diffusion:

$$D_{ij} = \frac{\partial}{\partial x_m} \left(\frac{v_t}{\sigma_k} \frac{\partial R_{ij}}{\partial x_m} \right) = \text{div} \left(\frac{v_t}{\sigma_k} \text{grad} (R_{ij}) \right)$$

with $v_t = C_\mu \frac{k^2}{\varepsilon}$; $C_\mu = 0.09$ and $\sigma_k = 1.0$

The diffusion term D_{ij} can be modelled by the assumption that the rate of transport of Reynolds stresses by diffusion is proportional to the gradients of Reynolds stresses

Rate of dissipation of R_{ij} : assuming isotropy of the small dissipative eddies

$$\varepsilon_{ij} = \frac{2}{3} \varepsilon \delta_{ij}$$

$$\varepsilon = \frac{-2\mu \overline{e'_{ij} e'_{ij}}}{\rho} = 2\nu \overline{e'_{ij} e'_{ij}}$$

Transport of R_{ij} due to turbulent pressure-strain interactions:

$$\Pi_{ij} = -C_1 \frac{\varepsilon}{k} \left(R_{ij} - \frac{2}{3}k\delta_{ij} \right) - C_2 \left(P_{ij} - \frac{2}{3}P\delta_{ij} \right)$$

with $C_1 = 1.8$ and $C_2 = 0.6$

Transport of R_{ij} due to the rotation:

$$\Omega_{ij} = -2\omega_k (R_{jm}e_{ikm} + R_{im}e_{jkm})$$

ω_k is the rotation vector

e_{ijk} the alternating symbol:

$= +1$ if i, j and k are different and in cyclic order

$e_{ijk} = -1$ if i, j and k are different and in anti-cyclic order

$= 0$ if any two indices are the same.

The six equations for Reynolds stress transport are solved along with a model equation for the scalar dissipation rate ε .

$$\frac{D\varepsilon}{Dt} = \text{div} \left(\frac{\nu_t}{\sigma_\varepsilon} \text{grad } \varepsilon \right) + C_{1\varepsilon} \frac{\varepsilon}{k} 2\nu_t E_{ij} \cdot E_{ij} - C_{2\varepsilon} \frac{\varepsilon^2}{k}$$

Rate of change of ε	+	Transport of ε by convection	=	Transport of ε by diffusion	+	Rate of production of ε	-	Rate of destruction of ε
------------------------------------	---	--	---	---	---	---	---	--

where $C_{1\varepsilon} = 1.44$ and $C_{2\varepsilon} = 1.92$

The usual boundary conditions for elliptic flows are required for the solution of the Reynolds stress transport equations:

- inlet: specified distributions of R_{ij} and ε
- outlet and symmetry: $\partial R_{ij} / \partial n = 0$ and $\partial \varepsilon / \partial n = 0$
- free stream: $R_{ij} = 0$ and $\varepsilon = 0$
- solid wall: wall functions

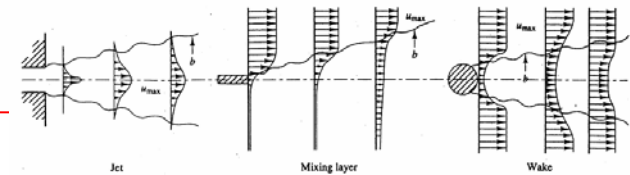


Fig. 3.8 Free turbulent flows

(1) The inlet distributions for R_{ij} :

$$k = \frac{3}{2}(U_{ref} T_i)^2; \quad \varepsilon = C_\mu^{3/4} \frac{k^{3/2}}{\ell}; \quad \ell = 0.07L; \quad \overline{u_1'^2} = k;$$

$$\overline{u_2'^2} = \overline{u_3'^2} = \frac{1}{2}k; \quad \overline{u_i' u_j'} = 0 (i \neq j)$$

the turbulence intensity T_i and a characteristic length L of the equipment (e.g. equivalent pipe radius)

- (2) at high Reynolds numbers wall-function-type boundary conditions $R_{ij} = \overline{u'_i u'_j} = c_{ij} k$ where c_{ij} are obtained from measurements.
- (3) Low Reynolds number modifications to the models can be incorporated to add the effects of molecular viscosity to the diffusion terms and to account for anisotropy in the dissipation rate term in the R_{ij} -equations.

Wall-damping functions $\bar{\varepsilon} (\equiv \varepsilon - 2\nu(\partial k^{1/2}/\partial y)^2)$

Reynolds stress equation models assessment

Advantages

- potentially the most general of all classical turbulence models
- only initial and/or boundary conditions need to be supplied
- very accurate calculation of mean flow properties and all Reynolds stresses for many simple and more complex flows including wall jets, asymmetric channel and non-circular duct flows and curved flows

Disadvantages

- very large computing costs (seven extra PDEs)
 - not as widely validated as the mixing length and $k-\epsilon$ models
 - performs just as poorly as the $k-\epsilon$ model in some flows owing to identical problems with the ϵ -equation modelling (e.g. axisymmetric jets and unconfined recirculating flows)
-

$$\overline{\frac{D}{Dt}} = P_{ij} + D_{ij} - \varepsilon_{ij} + \Pi_{ij} + \Omega_{ij}$$

3.5.4 Algebraic stress equation models (ASM)


assume that the sum of the convection and diffusion terms of the Reynolds stresses is proportional to the sum of the convection and diffusion terms of turbulent kinetic energy.

$$\frac{D\overline{u'_i u'_j}}{Dt} - D_{ij} \approx \frac{\overline{u'_i u'_j}}{k} \cdot \left(\frac{Dk}{Dt} - [k\text{-transport (i.e. div) terms}] \right) = \frac{\overline{u'_i u'_j}}{k} \cdot \left(-\overline{u'_i u'_j} \cdot E_{ij} - \varepsilon \right)$$

Submit into the Reynolds stress transport equation

$$\frac{DR_{ij}}{Dt} = P_{ij} + D_{ij} - \varepsilon_{ij} + \Pi_{ij} + \Omega_{ij} \quad \Omega_{ij} = -2\omega_k (R_{jm} e_{ikm} + R_{im} e_{jkm})$$

$$P_{ij} = - \left(R_{im} \frac{\partial U_j}{\partial x_m} + R_{jm} \frac{\partial U_i}{\partial x_m} \right) \quad \Pi_{ij} = -C_1 \frac{\varepsilon}{k} (R_{ij} - \frac{2}{3}k\delta_{ij}) - C_2 (P_{ij} - \frac{2}{3}P\delta_{ij})$$

 $R_{ij} = \overline{u'_i u'_j} = \frac{2}{3}k\delta_{ij} + \left(\frac{C_D}{C_1 - 1 + \frac{P}{\varepsilon}} \right) (P_{ij} - \frac{2}{3}P\delta_{ij}) \frac{k}{\varepsilon}$

algebraic stress model: a set of six simultaneous algebraic equations for the six unknown Reynolds stresses R_{ij} that can be solved by matrix inversion or iterative techniques if k and ε are known

Algebraic stress equation models

$$R_{ij} = \overline{u'_i u'_j} = \frac{2}{3}k\delta_{ij} + \left(\frac{C_D}{C_1 - 1 + \frac{P}{\varepsilon}} \right) (P_{ij} - \frac{2}{3}P\delta_{ij}) \frac{k}{\varepsilon}$$

$$C_D = 0.55 \quad \text{and} \quad C_1 = 2.2$$

This is a set of six simultaneous algebraic equations for the six unknown Reynolds stresses R_{ij} that can be solved by matrix inversion or iterative techniques if k and ε are known. Therefore, the formulae are solved in conjunction with the standard k - ε model equations (3.34–3.37).

Ⓚ

$$\frac{\partial(\rho k)}{\partial t} + \text{div}(\rho k \mathbf{U}) = \text{div} \left[\frac{\mu_t}{\sigma_k} \text{grad } k \right] + 2\mu_t E_{ij} \cdot E_{ij} - \rho \varepsilon$$

ⓔ

$$\frac{\partial(\rho \varepsilon)}{\partial t} + \text{div}(\rho \varepsilon \mathbf{U}) = \text{div} \left[\frac{\mu_t}{\sigma_\varepsilon} \text{grad } \varepsilon \right] + C_{1\varepsilon} \frac{\varepsilon}{k} 2\mu_t E_{ij} \cdot E_{ij} - C_{2\varepsilon} \rho \frac{\varepsilon^2}{k}$$

$$C_\mu = 0.09; \quad \sigma_k = 1.00; \quad \sigma_\varepsilon = 1.30; \quad C_{1\varepsilon} = 1.44; \quad C_{2\varepsilon} = 1.92$$

Algebraic stress equation models assessment

Advantages

- cheap method to account for Reynolds stress anisotropy
- potentially combines the generality of approach of the RSM (good modelling of buoyancy and rotation effects possible) with the economy of the $k-\epsilon$ model
- successfully applied to isothermal and buoyant thin shear layers
- if convection and diffusion terms are negligible the ASM performs as well as the RSM

Disadvantages

- only slightly more expensive than the $k-\epsilon$ model (two PDEs and a system of algebraic equations)
 - not as widely validated as the mixing length and $k-\epsilon$ models
 - same disadvantages as RSM apply
 - model is severely restricted in flows where the transport assumptions for convective and diffusive effects do not apply – validation is necessary to define the performance limits
-

Turbulent Modelling

Reynolds-Averaged Navier Stokes (RANS)

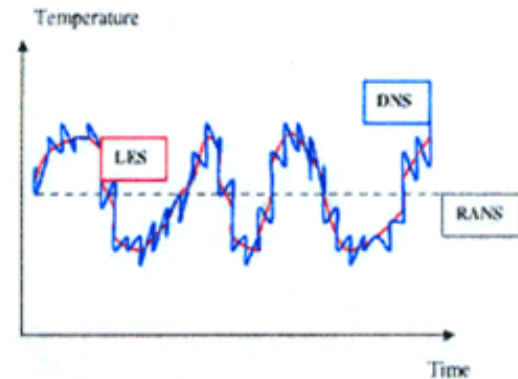
Solve for the mean values of all quantities, the predominant approach in engineering CFD packages.

Large Eddy Simulations (LES)

The turbulent large scales are explicitly calculated whereas the effects of smaller ones are modelled using subgrid closure rules. LES is particularly appealing for IC engine applications, which is attracting more research efforts.

Direct Numerical Simulations (DNS)

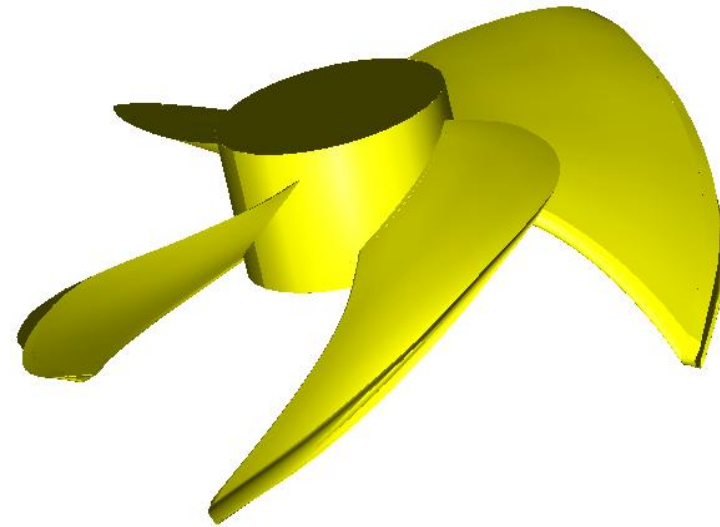
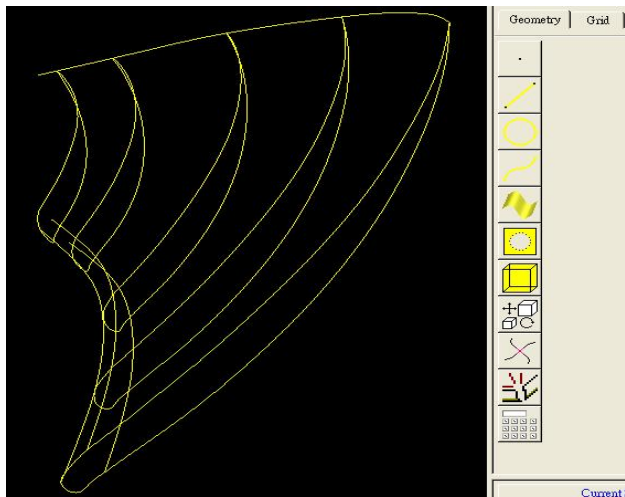
Solve the full instantaneous Navier-Stokes equations without any model for turbulent motions. DNS of IC engine flows is possible, but has not been performed.



Chap 6

軸流式風扇電腦輔助設計分析

Computer-Aided Design and Analysis Axial Flow Fan





簡報內容

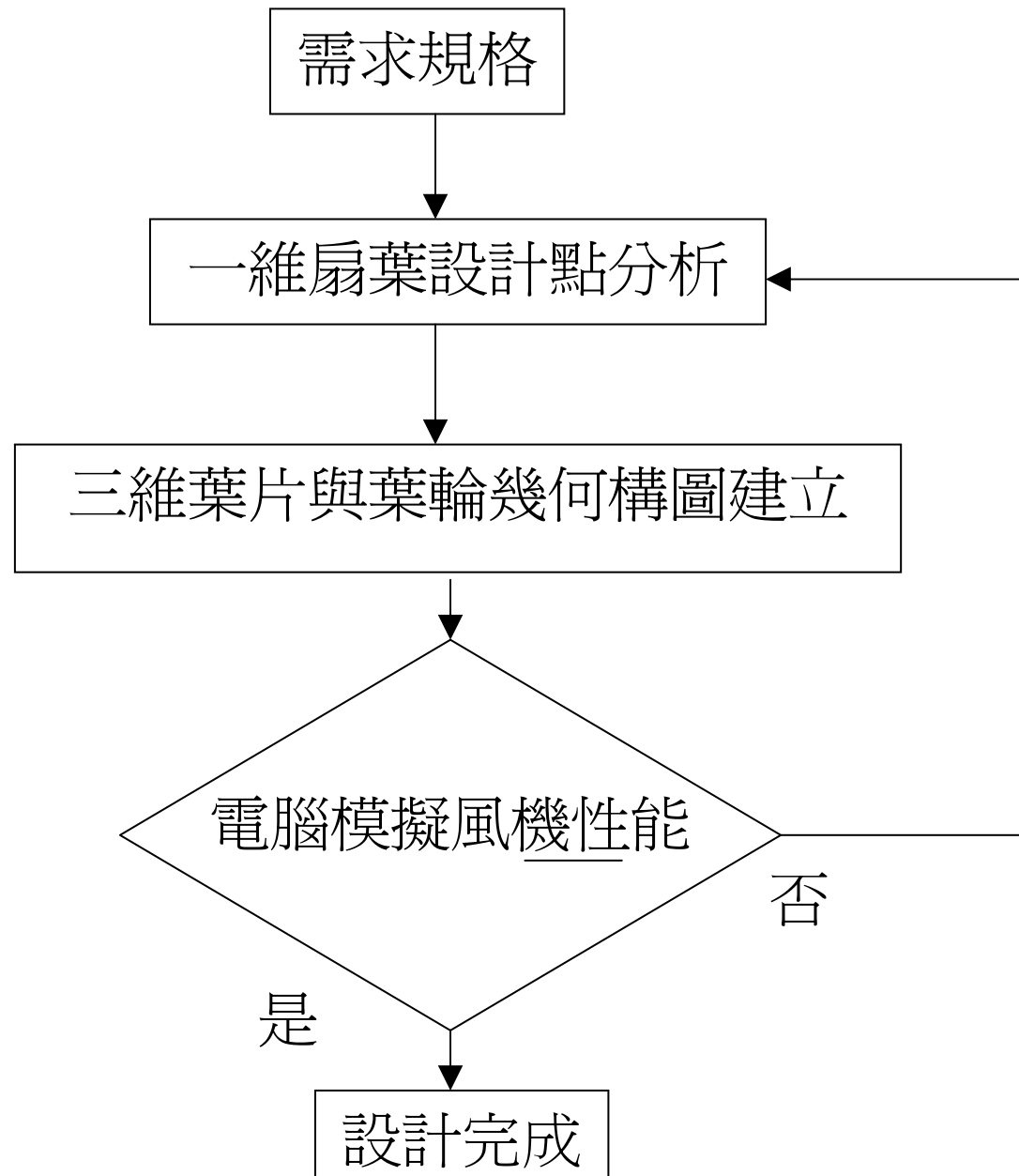
- 一、引言
- 二、一維扇葉設計點分析與設計過程
- 三、流場分析理論
- 四、數值方法
- 五、結果與討論
- 六、結論

一、引言

1.1 緒言

- ❖ 「軸流風機」在日常生活中的應用相當廣範和現代生活息息相關。小至個人電腦及其它電子產品內的散熱裝置，進而家庭用電扇、吹風機、排油煙機、各類空調機內之散熱風扇，乃至於工業用的各式大型送風機、冷卻水塔風扇及大樓通風系統等。
- ❖ 新一代的風機需具備高效率、低噪音、低製造成本和較高的結構安全與環境適應等特性。
- ❖ 電腦輔助設計分析提供快速的設計能力及低成本的性能分析功能，達到精密尺寸的設計製造的要求。

電腦輔助設計風扇流程圖





1.2 研究目的

利用傳統的設計理論與經驗，結合流體計算的方法來建立一套軸流風扇電腦輔助設計與分析的模式，以達到快速、精準的設計要求。

1.3 研究方法

利用一維扇葉設計點理論分析結合電腦模擬分析設計出符合設計需求的風扇。

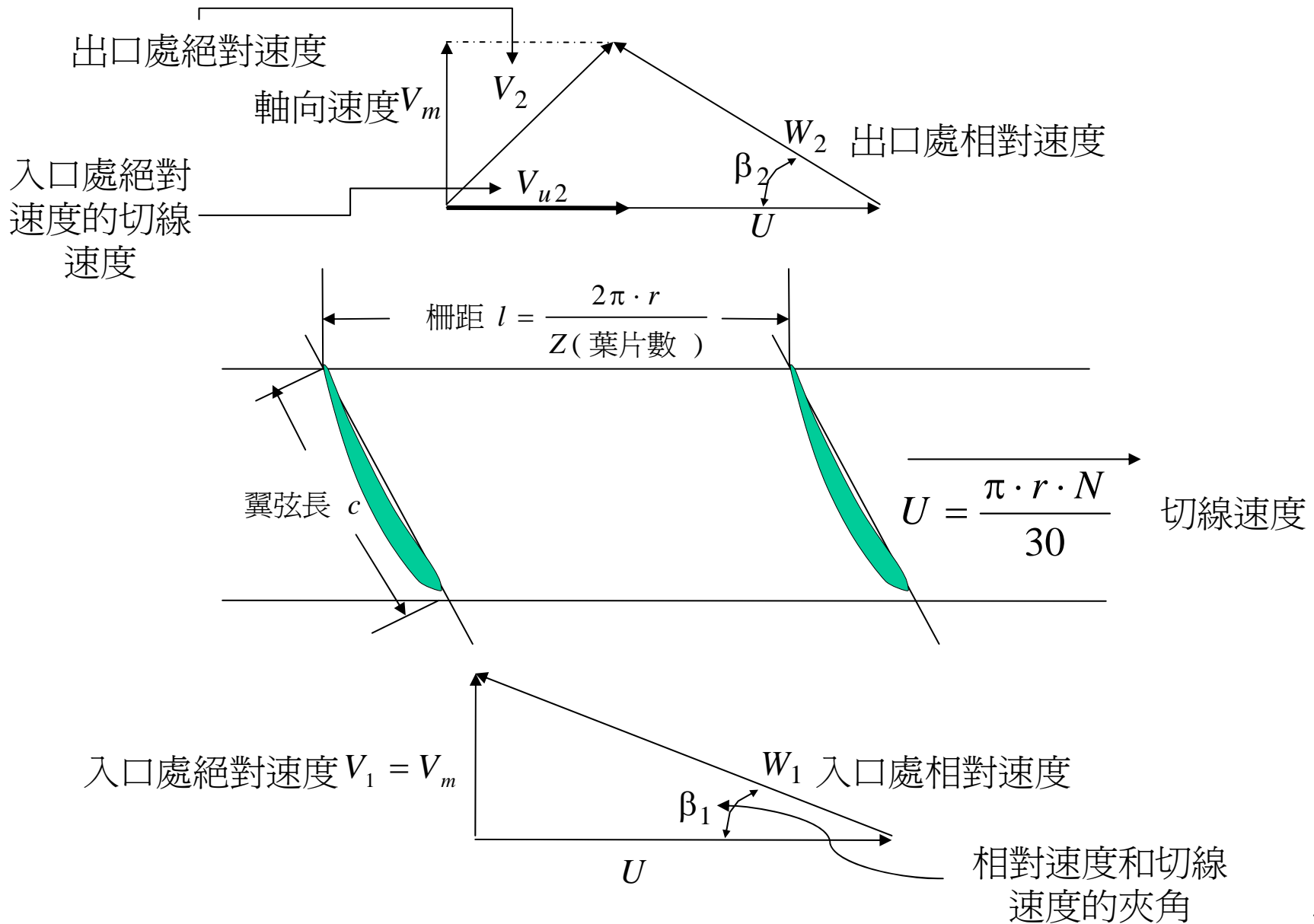


二、一維扇葉設計點理論分析

由於實際的運轉中是有機械摩擦、空氣非理想氣體…等等因素的影響，使得其實際性能不如理論分析的結果好。所以我們必須以理論的分析再加上實驗的結果加以整合分析，進而找出使軸流風扇效率最好之最佳工作設計點

- 一維扇葉設計點
使得水利效率為最佳的設計點
- 一維扇葉設計點理論
使用強制渦動風扇理論及實際的風機設計因子以找出最佳設計點

葉柵和速度三角形

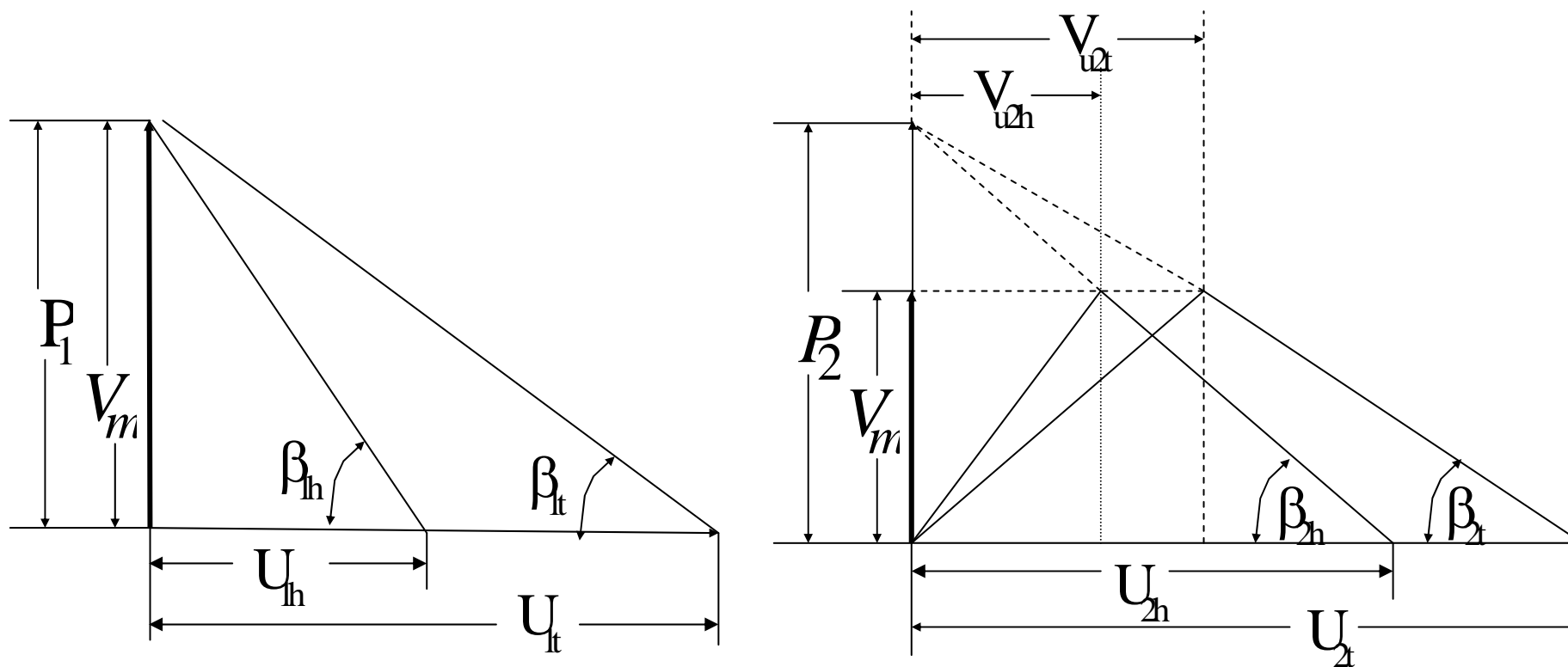




2.1 強制渦動風扇理論之假設

1. 忽略轉子及風道的摩擦阻力。
2. 流體以均勻相同的軸向速度流入風機。
3. 入口滑距 $P1$ 及出口滑距 $P2$ 在任意半徑下皆保持一定。
4. 流體為理想不可壓縮流體。

入口滑距P1及出口滑距P2



2.2 理論揚程

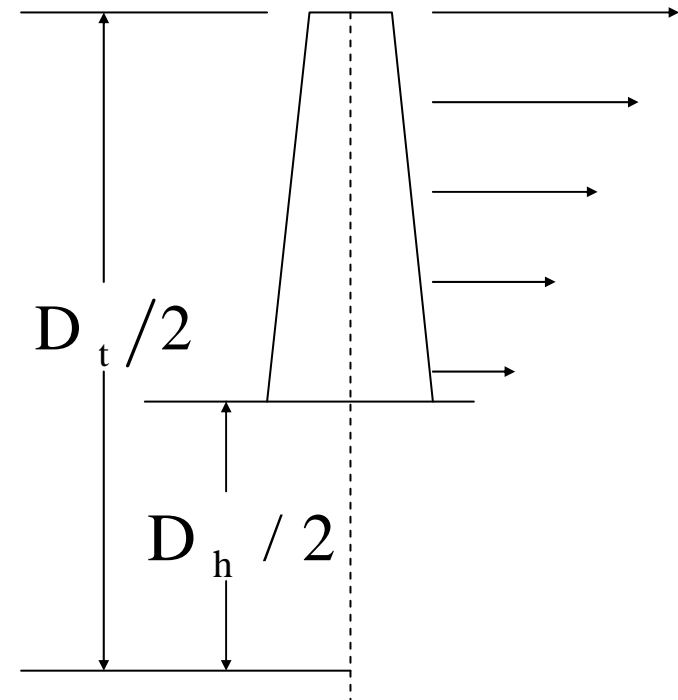
對於一般軸流風機其 Euler's equation

可表示成
$$H_{th} = \frac{U \cdot V_{u2}}{g}$$

由於在強制渦動模式
$$H_{th} = \alpha \cdot r^2$$

故其平均有效揚程
$$H_m \equiv \alpha \cdot r_m^2 = \alpha' \cdot D_m^2$$

$$\Rightarrow \text{平均有效直徑 } D_m = \sqrt{\frac{D_t^2 + D_h^2}{2}}$$



理論揚程跟半徑的平方成正比

2.3 水力效率

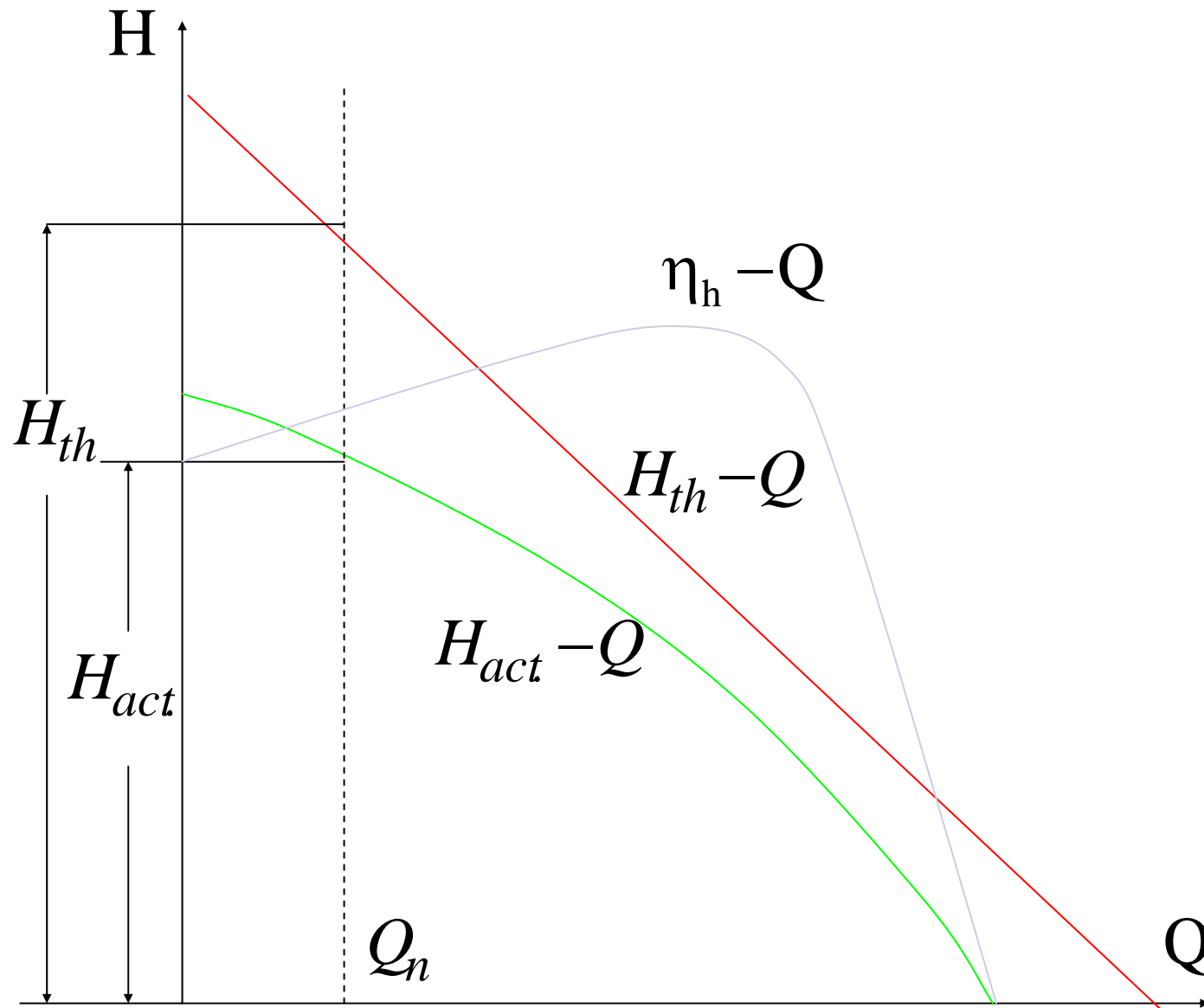
在同一轉速下，採用強制渦動模式的理想風機的

平均揚程與流量的關係為
$$H_m = \frac{U_m^2}{g} - \frac{U_m^2}{g} \left(\frac{1}{P_2 \cdot A} \right) \cdot Q$$

由於在任一流量下其理論揚程和實際揚程會有所差異，

所示其水力效率 $\eta_h = \frac{H_{act.}}{H_{th}}$ 會小於1。

流量 - 揚程曲線



2.4 無因次特性

爲了擴大前述之適用範圍，無因次化是必須的，
以下即爲與風機相關的無因次項定義：

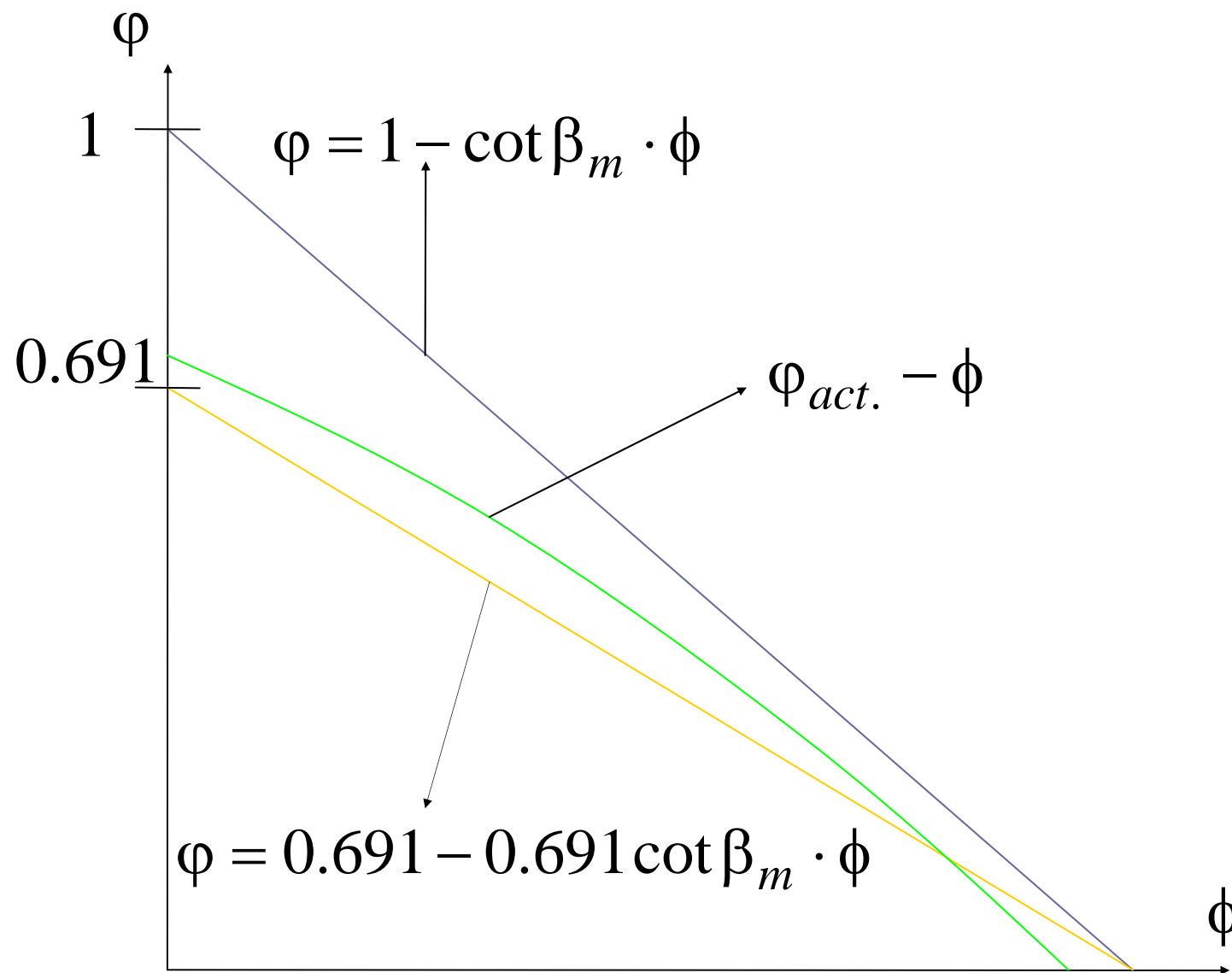
(1) 無因次揚程 $\phi \equiv \frac{H}{U^2/g} = \frac{V_{u2}}{U}$

(2) 無因次流量 $\phi \equiv \frac{V_m}{U}$

(3) 無因次比速率 $\omega_s \equiv \phi_m^{1/2} \cdot \phi_m^{-3/4}$

$$\# \quad n_s = \left[\frac{60 \cdot g^{3/4}}{\sqrt{2\pi}^{1/2}} \right] \cdot \frac{(1 - v^2)^{1/2}}{(1 + v^2)^{1/2}} \cdot \omega_s$$

無因次流量－揚程曲線



0.691

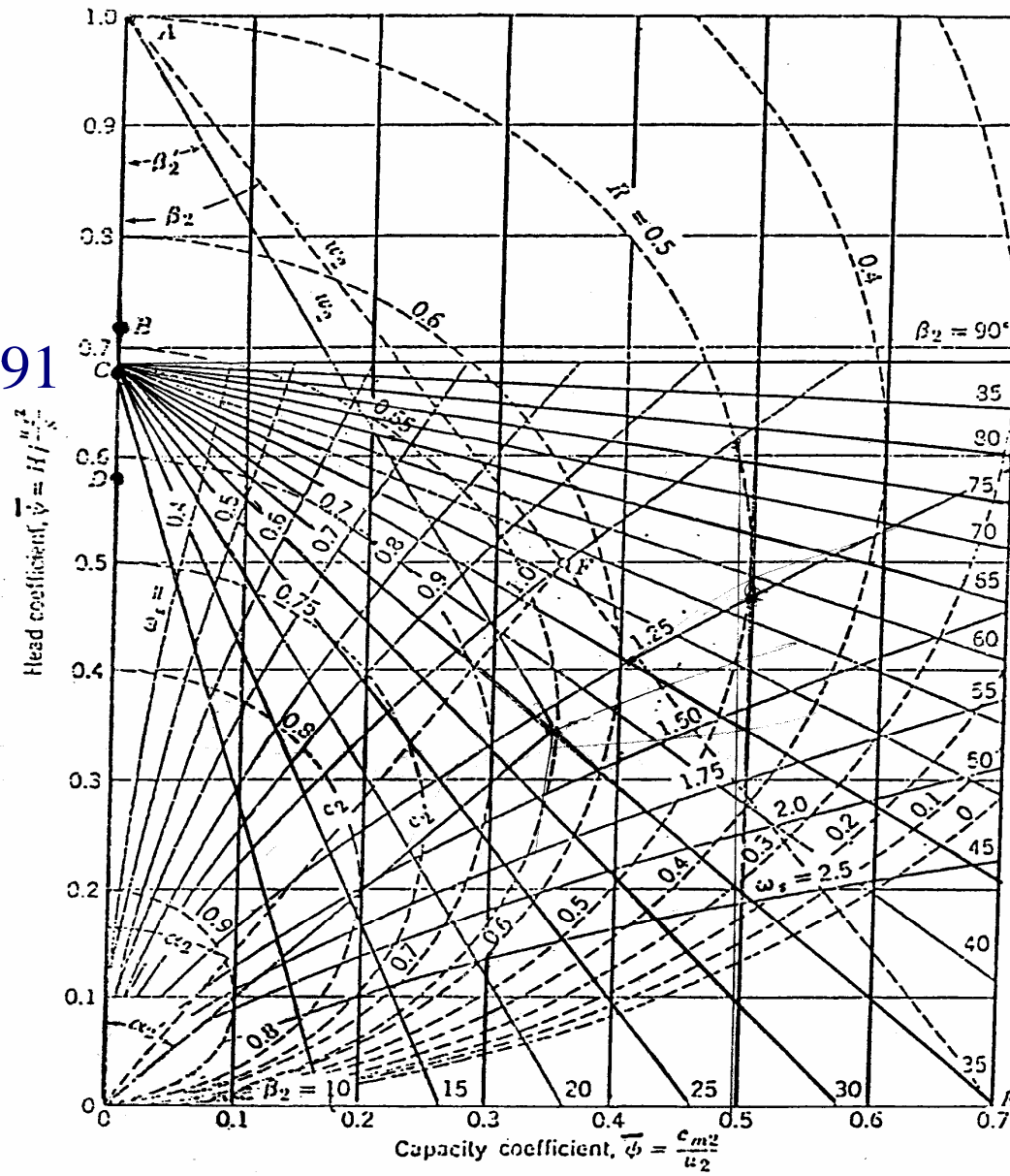


FIG. 9 Stepnoff's chart of centrifugal and axial turboblower characteristics

2.5 風機設計經驗因子

(1) 輪殼比(Hub Ratio)

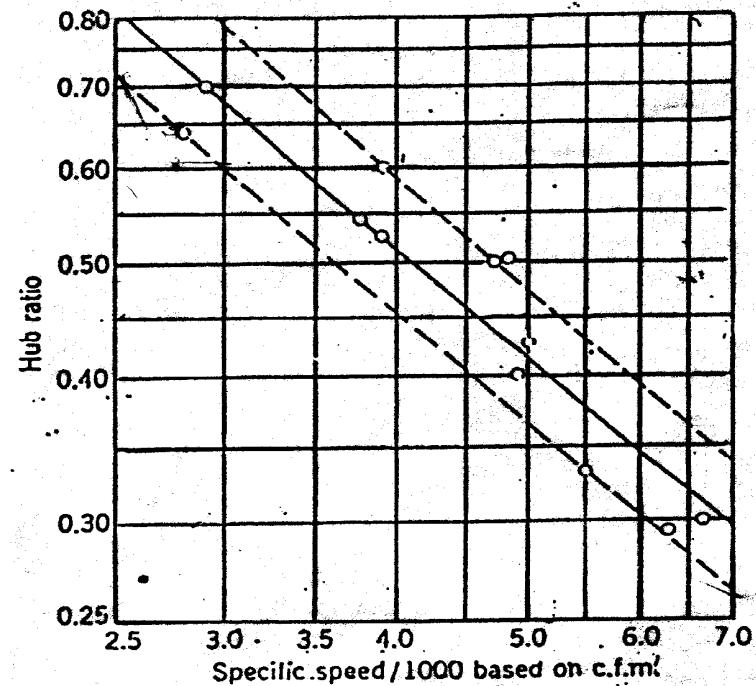
輪殼比 $v \equiv D_h / D_t$ 可參考經實驗得出來的 $v - n_s$ 圖以求得最佳輪殼比。

(2) 葉片數目(Number of Vanes N_b)

$$N_b = \frac{6 \cdot v}{(1 - v)}$$

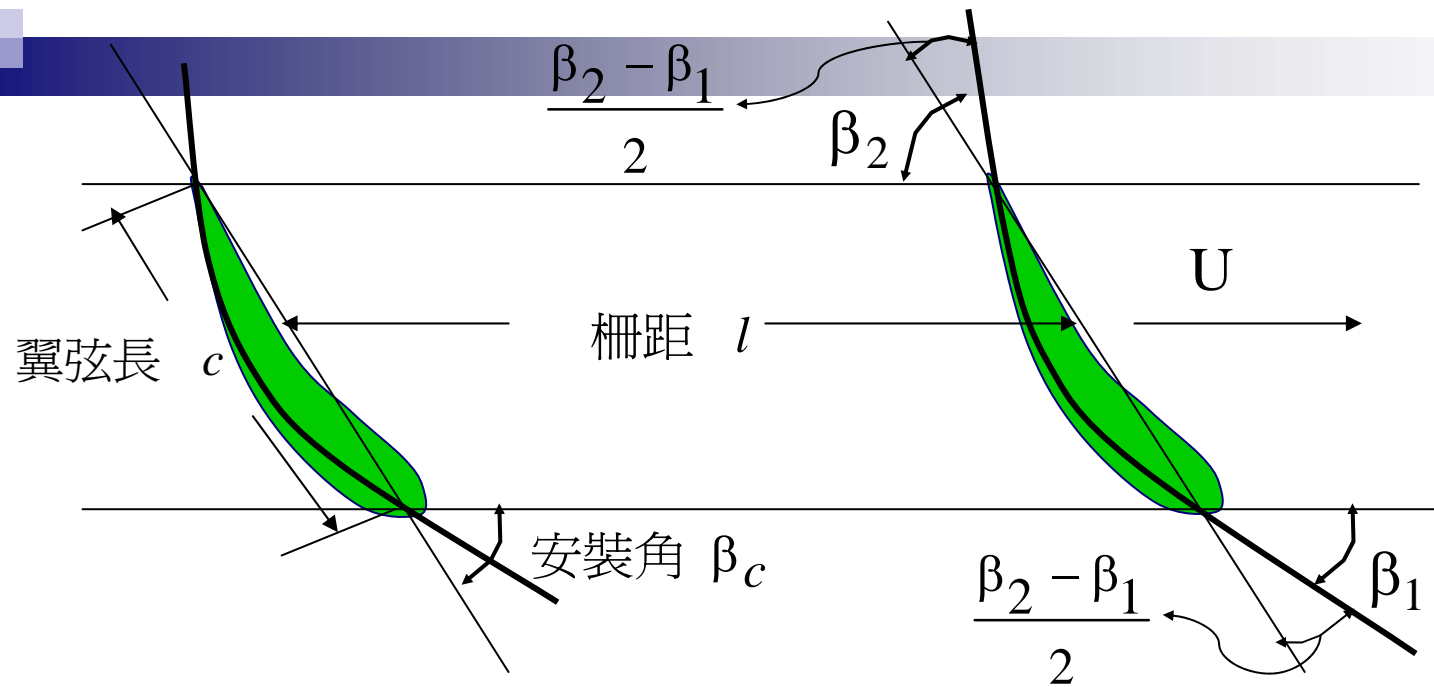
(3) 弦節比(Chord - spacing c/l)

一般而言 $0.5 < c/l < 1.5$

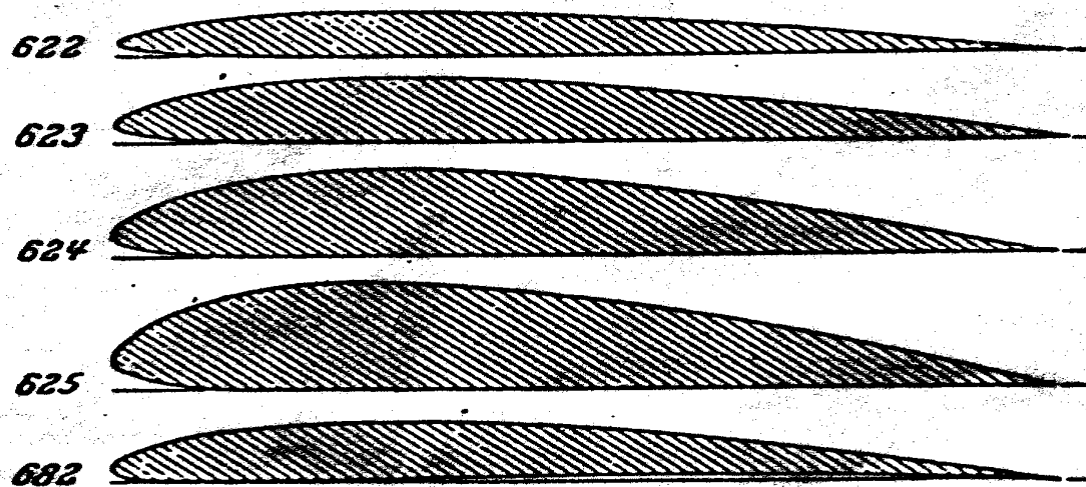


2.6 設計步驟

- (1) 一般而言，在設計基本的風機外型時，必先知道其規格 Q 、 H 、 N 及外徑 D_t 。
- (2) 求出輪轂比 v 、葉片數 N_b 及葉輪直徑 D_h ，及在不同半徑處葉片所須之翼弦長及柵距。此時風機的幾何外型已大致決定。
- (3) 接下來決定不同半徑處的葉片的 β_1 、 β_2 。
- (4) 最後可求出在幾個半徑處葉片之翼型幾何外型、大小及安裝角，再用繪圖軟體畫出三維葉片之幾何外型。



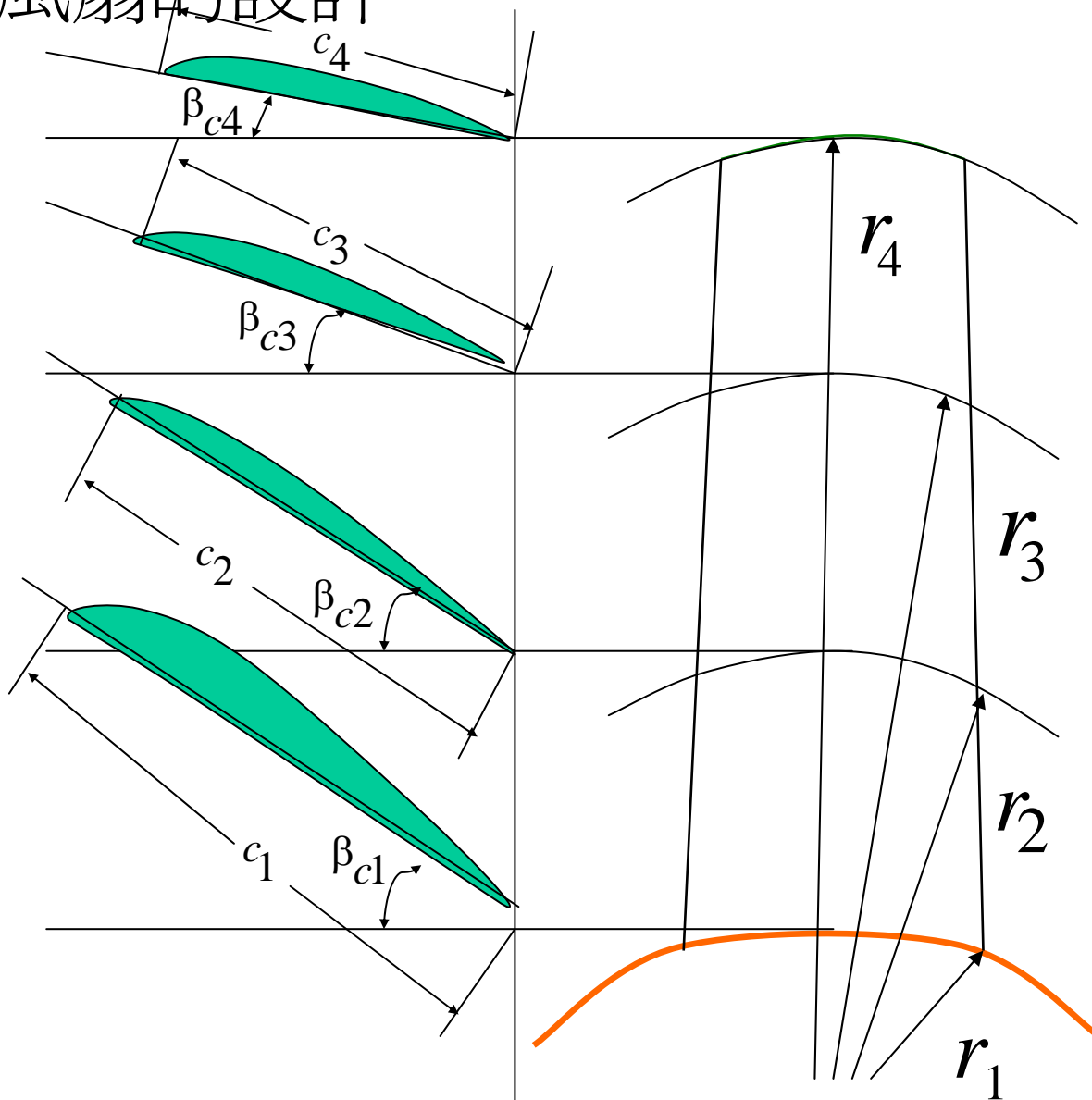
葉片的安裝角



德國標準翼型

(Göttingen profile)

軸流風扇的設計

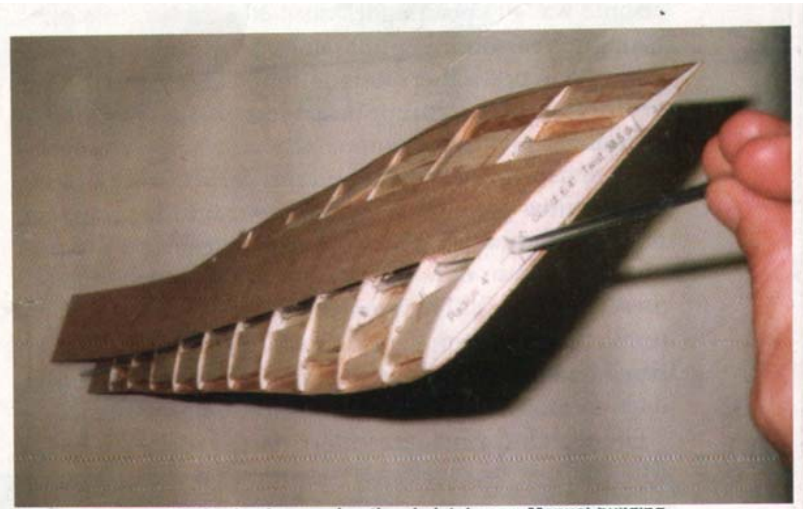
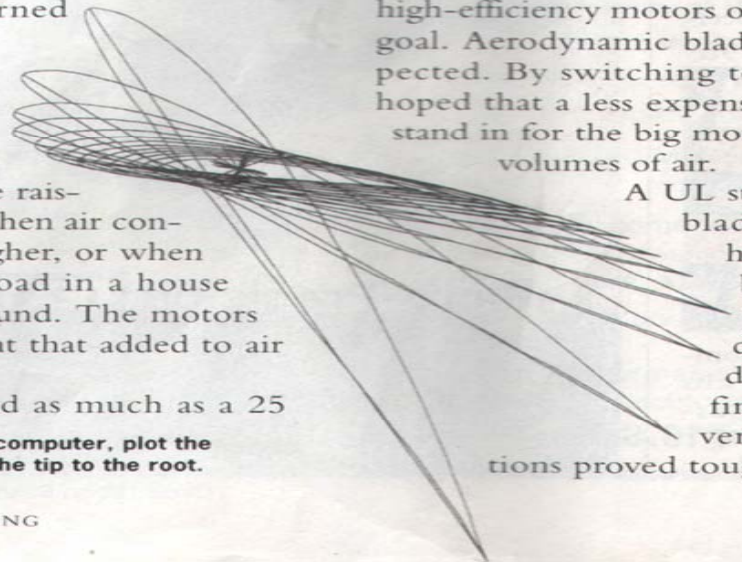


turned

a
ne rais-
When air con-
igher, or when
load in a house
ound. The motors
eat that added to air
ed as much as a 25
/ computer, plot the
the tip to the root.

RING

high-efficiency motors o
goal. Aerodynamic blad
pected. By switching to
hoped that a less expens
stand in for the big mot
volumes of air.
A UL st
blad
h
l
J
d
d
fin
ver
tions proved toug



The first sheets of balsa begin covering the skeletal spar. Manual building methods produced airfoils that came quite close to the original design.



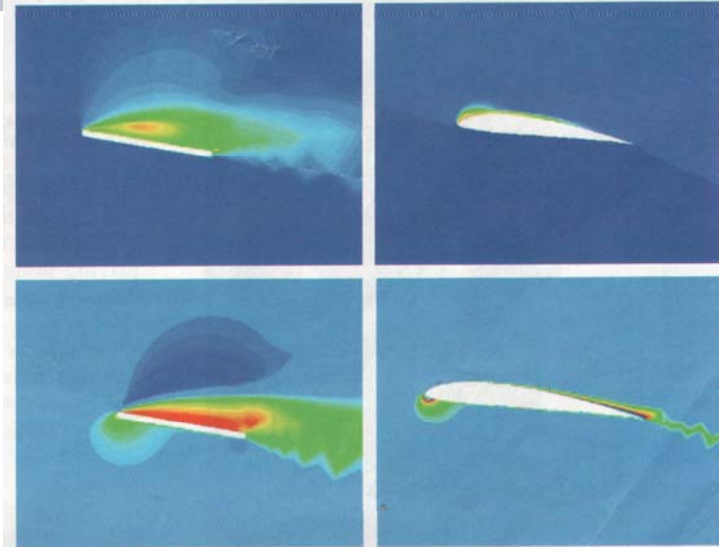
Partway through construction, prototype blade maker Jeff Sonne holds the first of four airfoils he would build by hand. He cut balsa sections of the airfoil from the computer-generated plot.



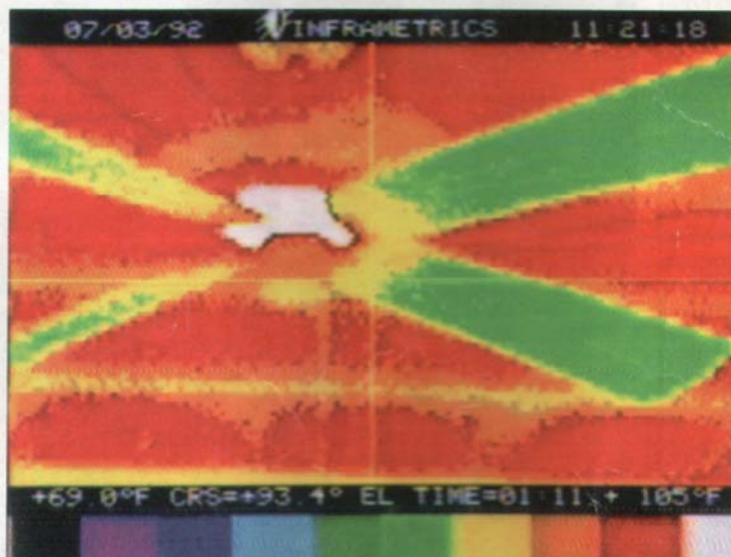
The handbuilt blades proved concepts; then rapid prototyping took over. Guan Su finally worked on the preproduction prototype last summer, following many refinements to the original design.



The Windward II ceiling fan uses a fluorescent bulb to further increase energy savings. A second model uses incandescent light fixtures.



Simulation of energy lost (top) to turbulence (bottom) for flat and aerodynamic profiles. Images depict tip conditions 26 inches from the center. Flat blades pitch to 12 degrees; aero-blades pitch to 6.



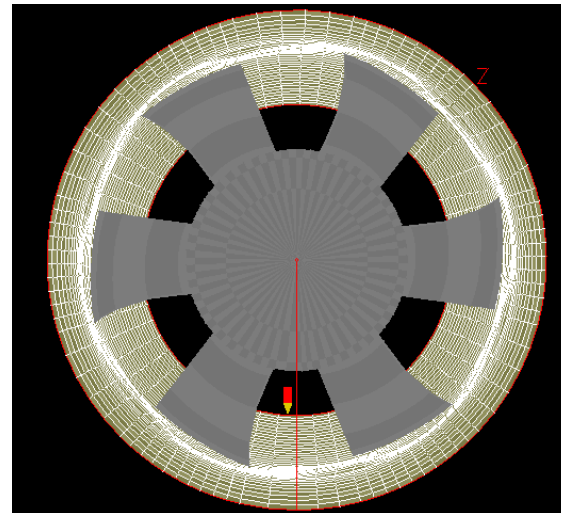
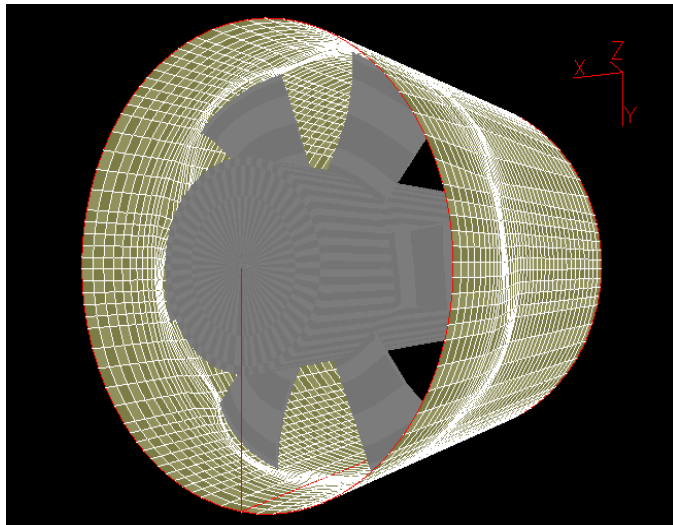
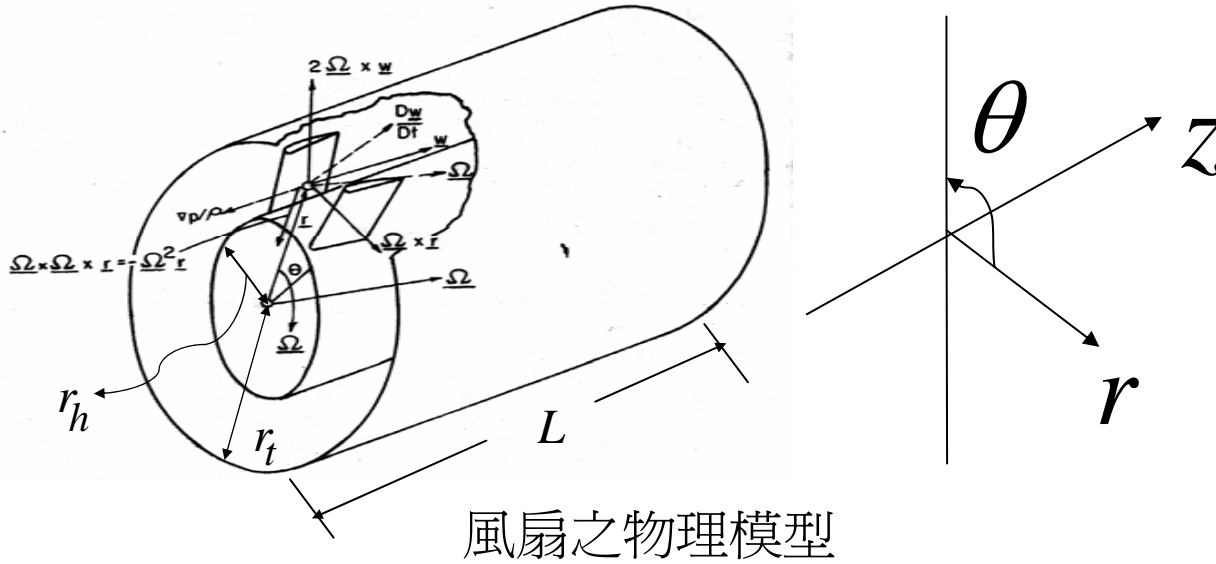
Infrared thermogram of a typical ceiling fan shows heat generated by the motor. Temperature scale at bottom reads from coolest (at left) to hottest.




Using an infrared tachometer, Parker checks prototype's speed during efficiency testing. Fans were evaluated for airflow and power consumption, too.

三、流場分析理論

3.1 系統描述





3.2 基本假設

- (1) 空間內之流體為牛頓流體、不可壓縮的理想氣體。
- (2) 流場為三維穩態紊流流場。
- (3) 流體性質在數值計算之有限體積(finite volume)內，其流體壓力、溫度、密度為均値性(homogeneous)。

3.3 統御方程式

(1) 連續方程式 $\frac{\partial}{\partial x_j}(u_j) = 0$

(2) 動量方程式(採用雷諾平均納威爾-史托克方程式)

$$\frac{\partial}{\partial x_j}(\rho u_j u_i) = -\frac{\partial P}{\partial x_j} + \frac{\partial}{\partial x_j} \left[\mu_{eff} \left(\frac{\partial u_i}{\partial x_j} + \frac{\partial u_j}{\partial x_i} \right) \right] + S_{ui} = 0$$

其中 $\overline{S_u} = -2\overline{\Omega} \times \overline{U} - \overline{\Omega} \times (\overline{\Omega} \times \overline{r})$

為因座標旋轉所產生的源項(Source Term)，包括科氏力(Coriolis Force)和離心力(Centrifugal Force)等。

(3) 紊流動能方程式 $\frac{\partial}{\partial x_j}(\rho u_j k) = \frac{\partial}{\partial x_j} \left(\Gamma_k \frac{\partial k}{\partial x_j} \right) + P_k - \rho \varepsilon$

(4) 紊流動量散逸方程式 $\frac{\partial}{\partial x_j}(\rho u_j \varepsilon) = \frac{\partial}{\partial x_j} \left(\Gamma_\varepsilon \frac{\partial \varepsilon}{\partial x_j} \right) + \frac{\varepsilon}{k} (c_{\varepsilon 1} P_\varepsilon - \rho c_{\varepsilon 2} \varepsilon)$

其中 $P_k = \mu_t \left(\frac{\partial u_i}{\partial x_j} + \frac{\partial u_j}{\partial x_i} \right) \frac{\partial u_i}{\partial x_j}$ $\Gamma_\varepsilon = \mu + \frac{\mu_t}{\sigma_\varepsilon}$ $\Gamma_k = \mu + \frac{\mu_t}{\sigma_k}$ $\mu_t = \rho c_\mu \frac{k^2}{\varepsilon}$

相關設定採用Launder 和 Spalding 的參考值

$$C_\mu = 0.09 \quad C_{\varepsilon 1} = 1.44 \quad C_{\varepsilon 2} = 1.92 \quad \sigma_k = 1 \quad \sigma_\varepsilon = 1.3$$



3.4 邊界條件

- ❖ 入口處： $(Z = 0) P1=0$
- ❖ 出口處： $(Z = L) P2=0$
- ❖ 風道壁面、轉子爲無滑動(no slip)條件

四、數值方法

4.1 有限差分法

在數值方法求解上，本專題採用Patankar的有限體積法 (Finite Volume Method)，配合混合法則 (Hybird Scheme)，於交錯式格點安排下，將上述複合體系之偏微分方程式離散成電腦可計算之差分方程式。

$$\phi_P = \frac{a_N^\phi \phi_N + a_S^\phi \phi_S + a_W^\phi \phi_W + a_E^\phi \phi_E + \left[\frac{\rho \nabla}{\Delta t_f} \right]_p \phi_p^*}{a_N^\phi \phi_N + a_S^\phi + a_W^\phi + a_E^\phi + \left[\frac{\rho \nabla}{\Delta t_f} \right]_p}$$



4.2 程式之準確性分析

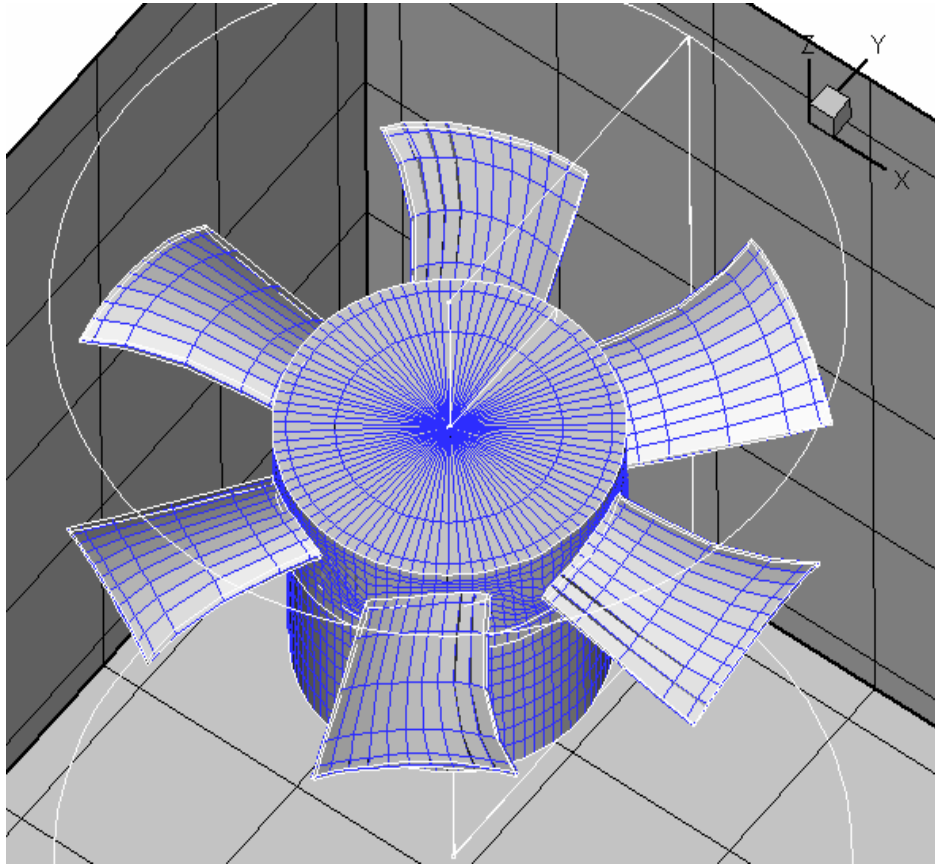
在進行研究之探討分析之前，首先討論本文所使用方程式做測試，以驗證此數值系統準確性與可靠度，此部分包括：

- (a) 網格獨立及
- (b) 數值驗證兩部分。



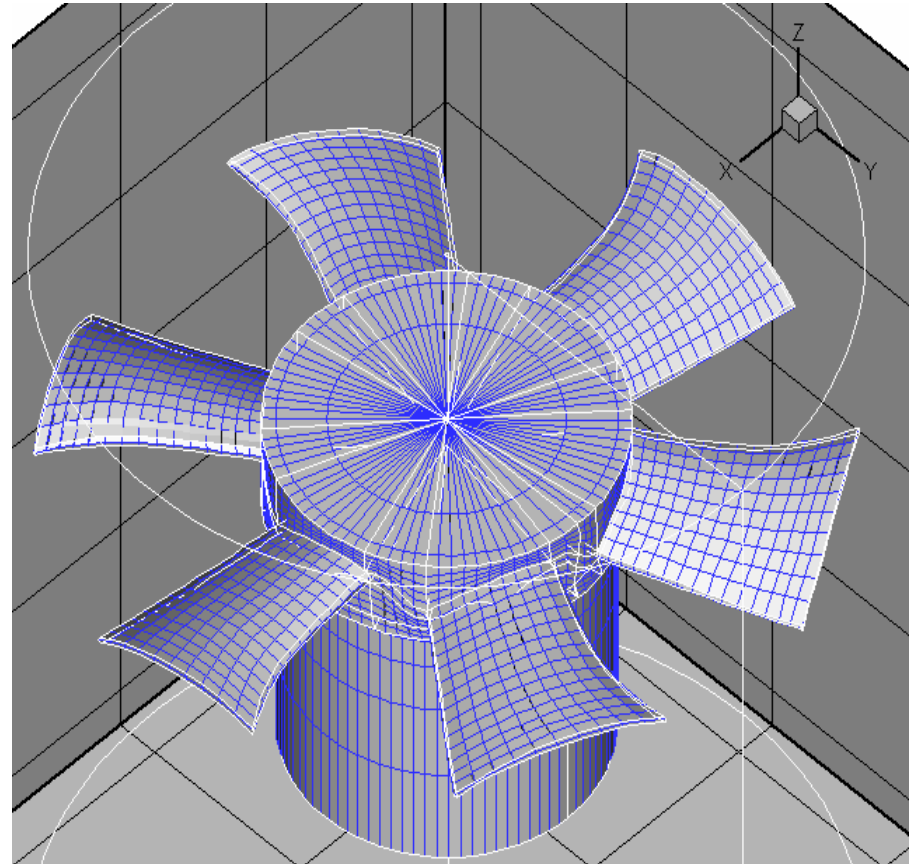
(a) 網格獨立

在網格獨立評估中，採用 $90 \times 10 \times 41$ 、 $90 \times 20 \times 27$ 等兩組網格系統進行測試，在參數設定為轉速 N 為 860rpm ，經數值計算結果後，發現其揚程-流量曲線幾乎完全相同，故採用第一組格點數較少之圖形作為各個數值計算來用於網格系統作為求解的基礎。



網格較少之模型

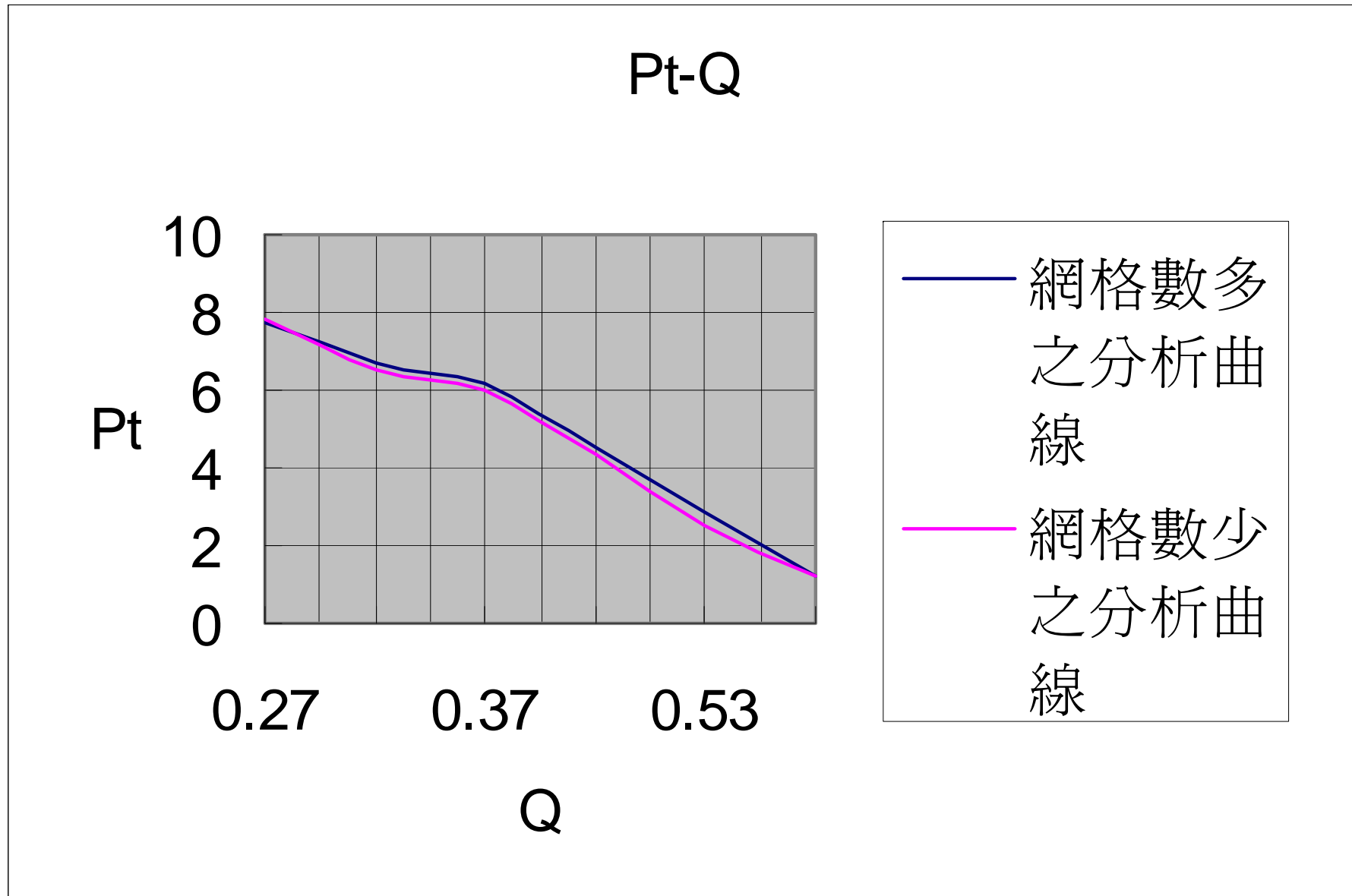
90×10×41



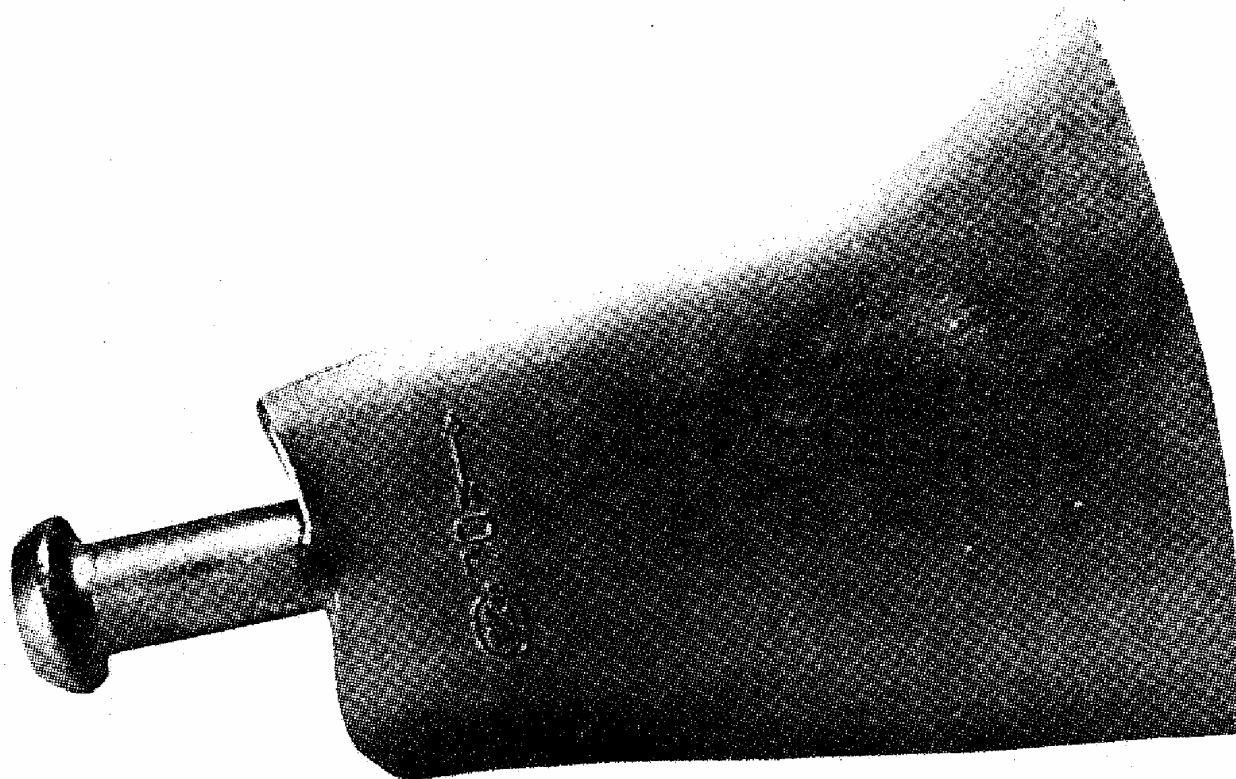
網格較多之模型


90×20×27

網格比較圖



斧頭葉片

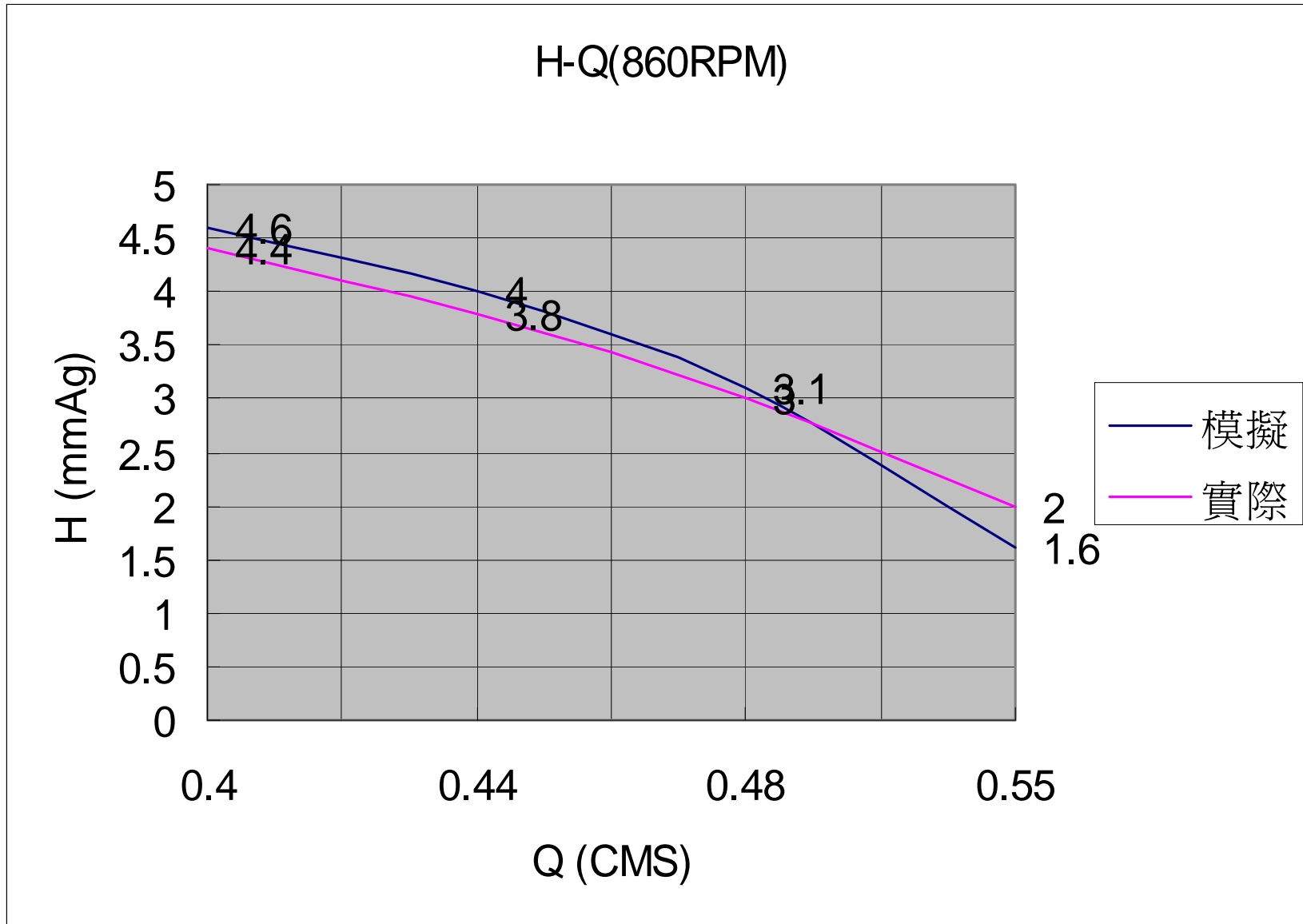
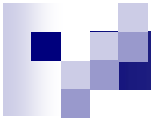




(b)數值驗證

❖以電腦模擬風道長度為一倍風扇的直徑為40cm，風扇則為外徑40cm內徑18cm、葉片數為六片之斧頭形風扇在860RPM的轉速下求得揚程-流量特性曲線圖，並與實際的實驗結果比較

❖數值計算結果比較發現實際及模擬的流量-揚程曲線趨勢相似，誤差大致在10%~12%，由此可知此數值模式尚適合作風扇之流場分析。



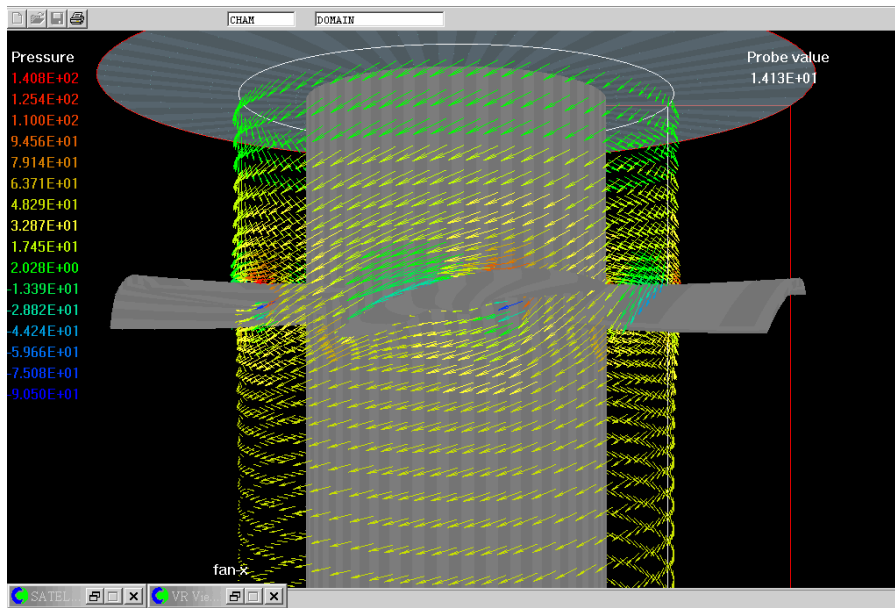


五、結果分析與討論

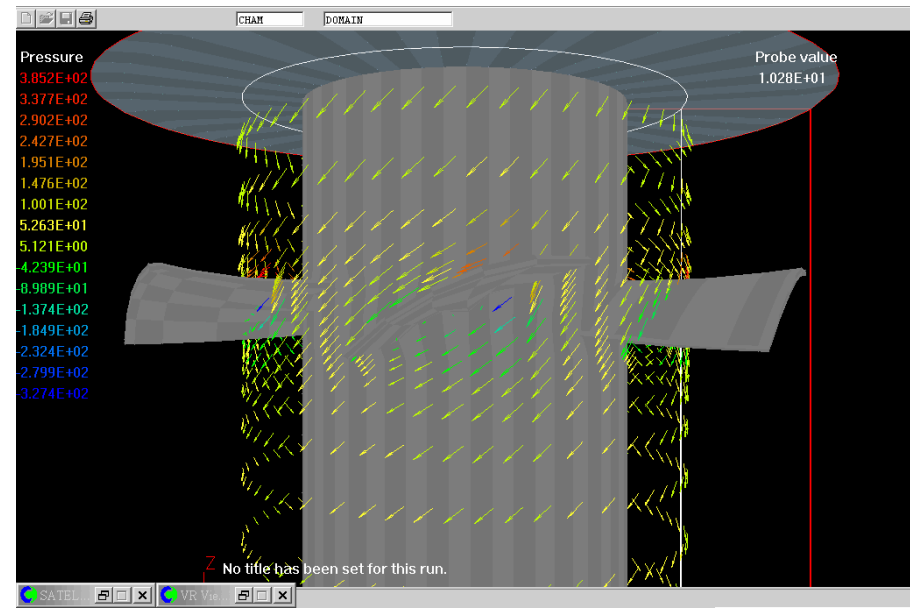
本研究針對下列各個不同風扇之安裝角及不同轉速對軸流風機性能的影響做一分析，並加以討論其流場、流線及靜壓分佈情形做一探討

5.1 不同安裝角對軸流風機性能的影響

下圖為安裝角17度及27度在轉速皆為860rpm下之流場變化

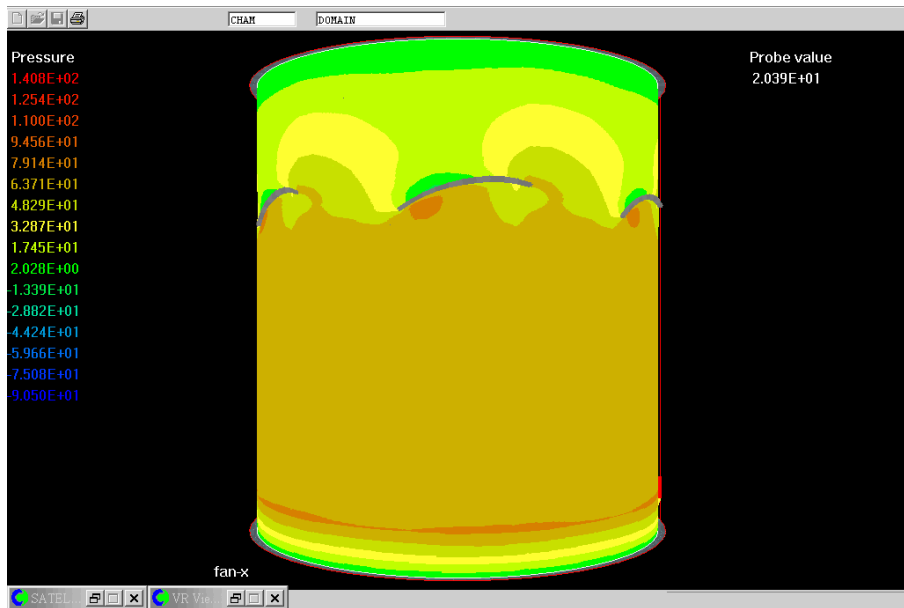


安裝角17度

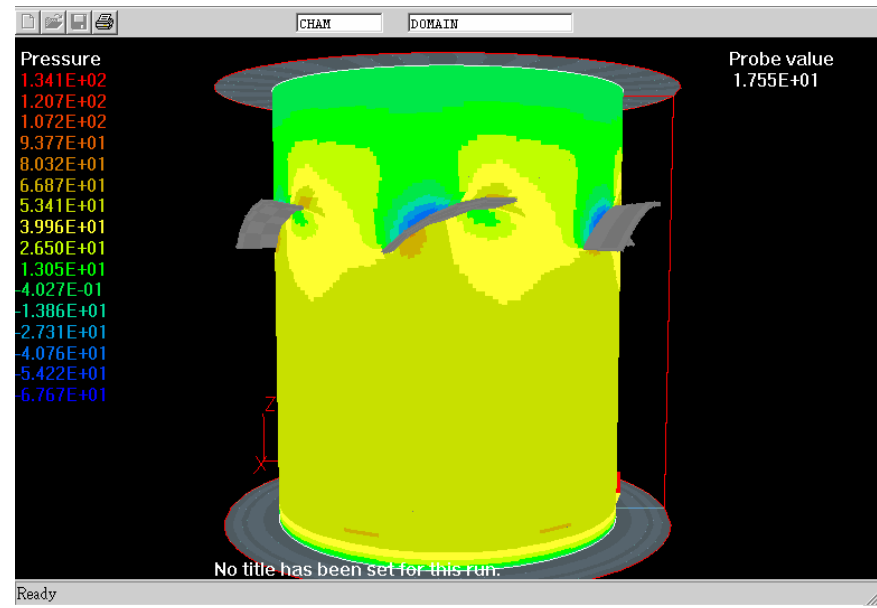


安裝角27度

下圖為轉速為860rpm在安裝角17度及27度下之靜壓分佈

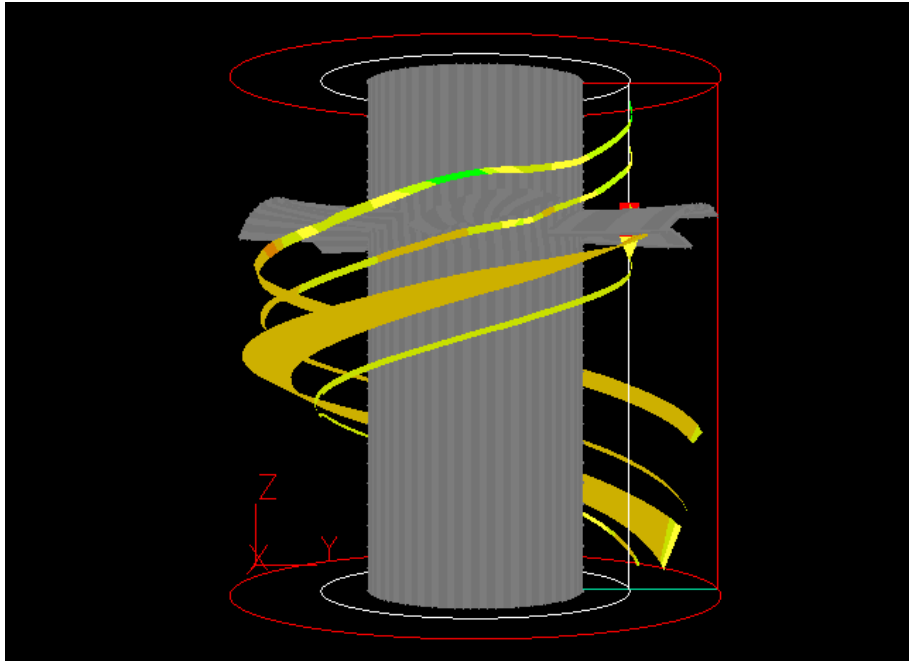


安裝角17度

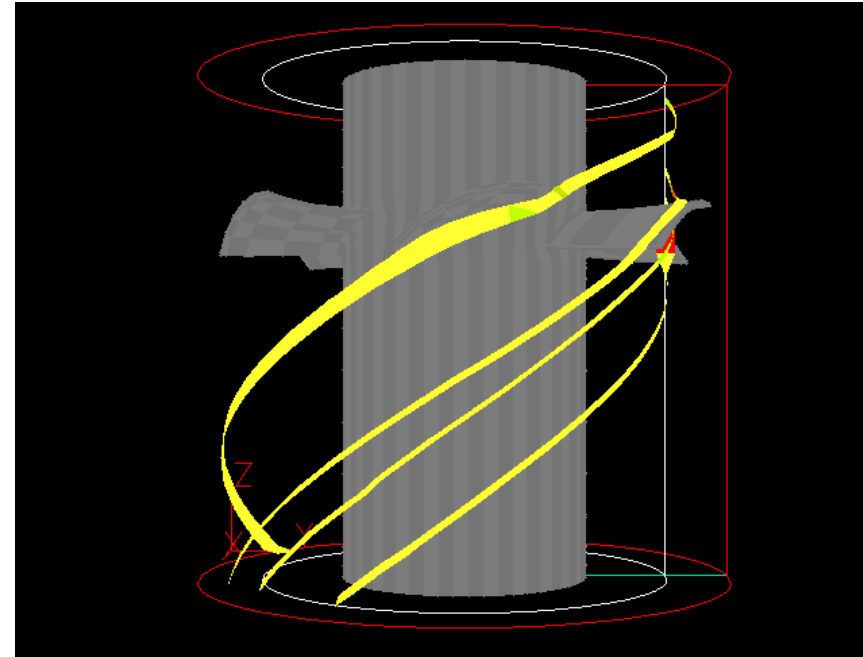


安裝角27度

下圖為安裝角17度及27度在轉速皆為860rpm下之流線分佈



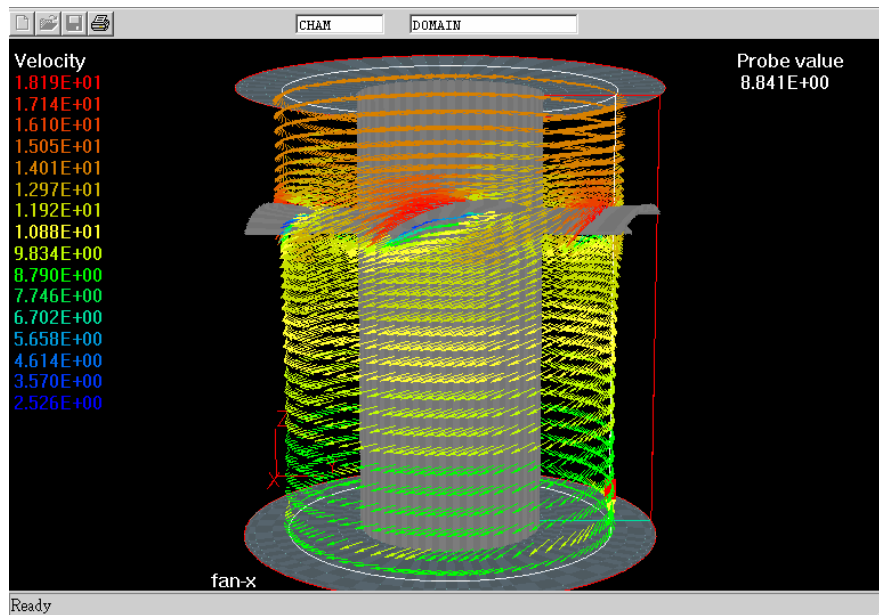
安裝角17度



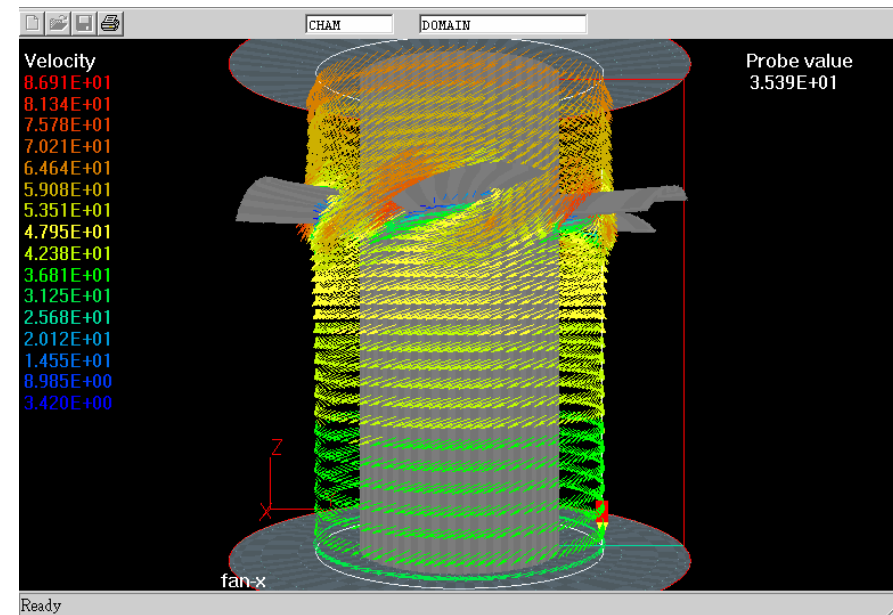
安裝角27度

5.2 不同轉速對軸流風機性能的影響

下圖為安裝角17度在轉速為860rpm及3240rpm下之流場變化

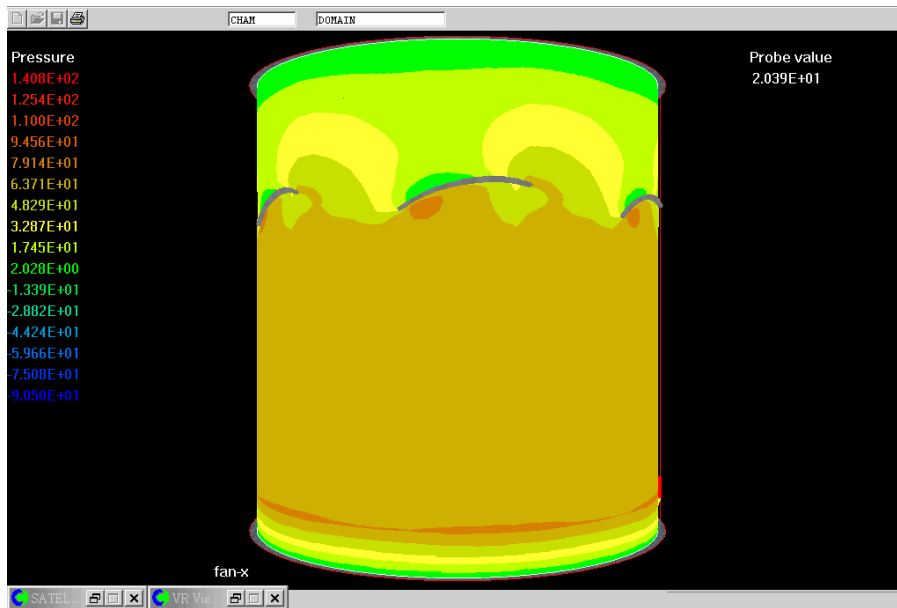


860rpm

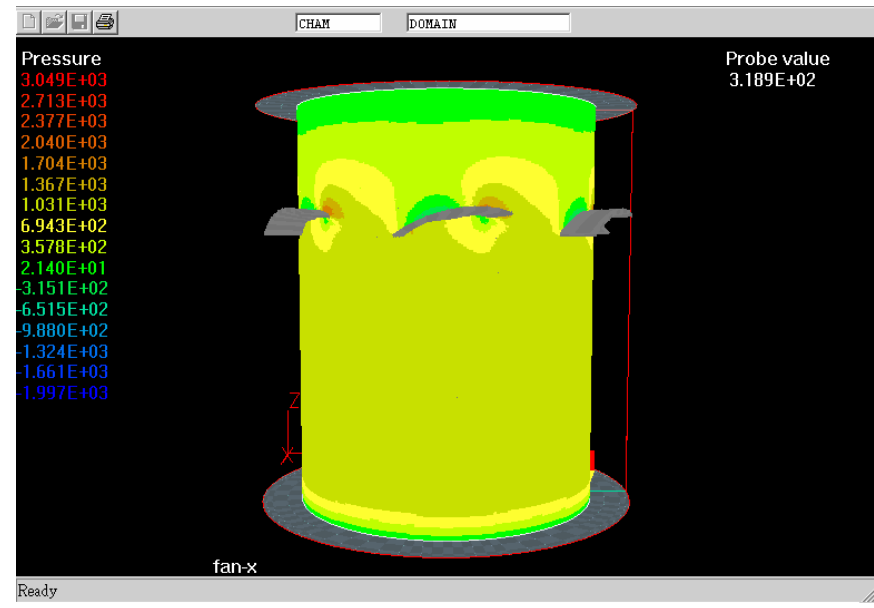


3240rpm

下圖為安裝角17度在轉速為860rpm及3240rpm下之靜壓分佈

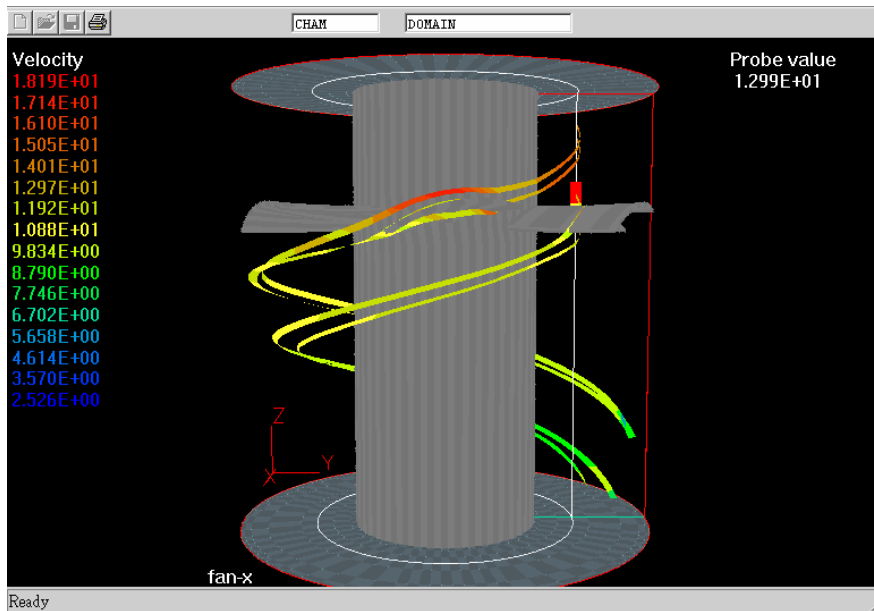


860rpm

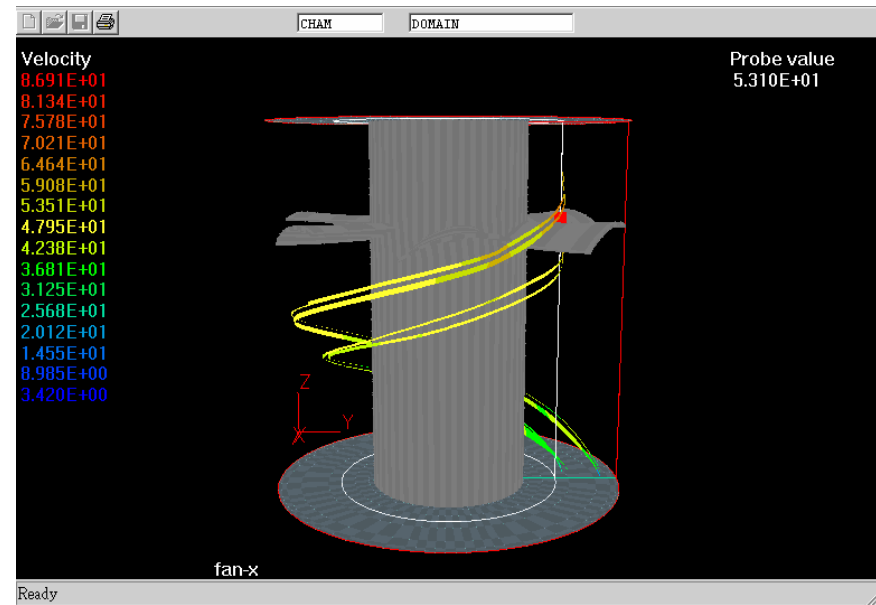


3240rpm

下圖為安裝角17度在轉速為860rpm及3240rpm下之流線分佈



860rpm

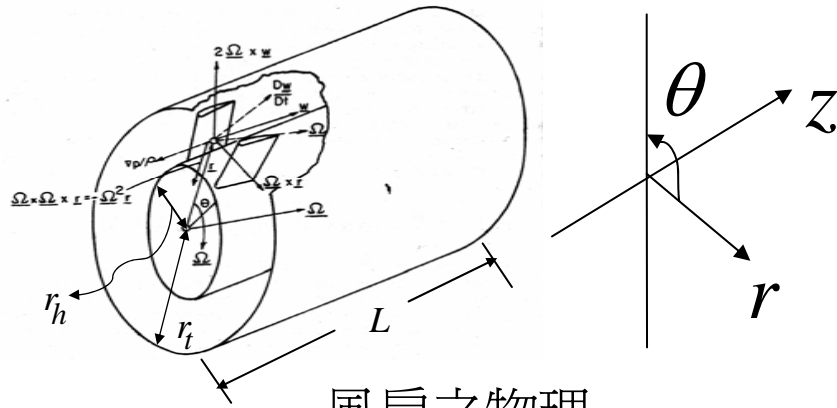
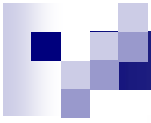


3240rpm



六、結論

- ❖ 本研究已建立了冷凍空調用軸流式風扇之電腦輔助設計及分析的模式
- ❖ 藉用電腦輔助設計(CAD)的功能加上計算流體力學(CFD)的性能分析特性，可以大大的降低傳統風機設計的時程及成本
- ❖ 在不改變風機的尺寸、大小情況之下，我們可藉由改變轉速、安裝角來達到風機的性能分析



風扇之物理模型

